2004 Condensed Phase and Interfacial Molecular Science Research Meeting

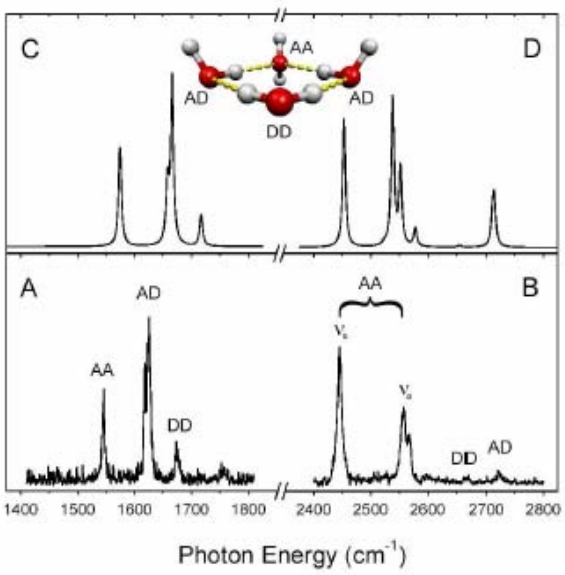

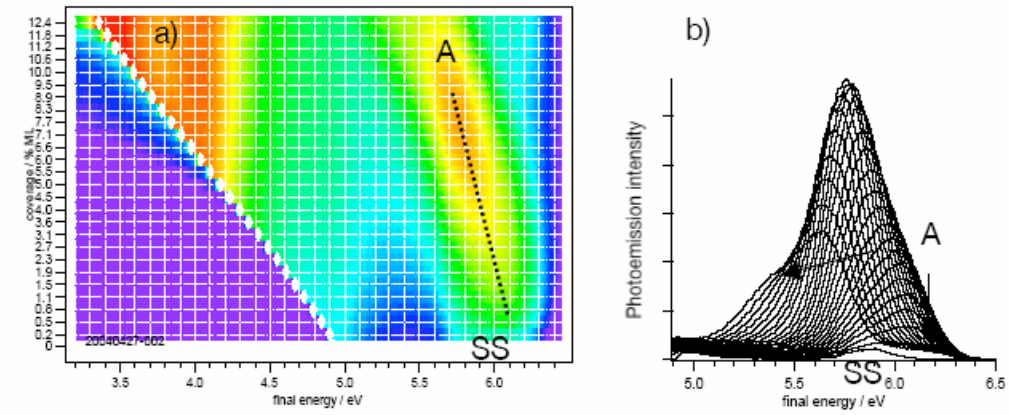

Airlie Conference Center
Warrenton, Virginia
October 24-27, 2004

Office of Basic Energy Sciences

Chemical Sciences, Geosciences & Biosciences Division

Cover

Top

Structure and Dynamics of Chemical Processes in Water Clusters

K. D. Jordan Dept. of Chemistry, University of Pittsburgh, Pittsburgh, PA. 15260
and M. A. Johnson, Dept. of Chemistry, Yale University, New Haven CT 06520

Comparison of the experimental (lower) and theoretical (upper) spectra for the water tetramer anion. Spectra A and C refer to $(H_2O)_4^-$ in the water bending region, while B and D correspond to the $(D_2O)_4^-$ isotopomer in the OD stretching region.

Bottom

Optical Manipulation of Ultrafast Electron and Nuclear Motion on Metal Surfaces

Hrvoje Petek, Department of Physics and Astronomy, University of Pittsburgh, Pittsburgh, PA 15260

a) 3D plot of 2 photon photoemission spectra of Cs/Cu(111) at 300 K as a function of Cs coverage. The dotted line indicates approximate shift in the energy of the antibonding state A with coverage. b) detail of the photoemission spectra in a) showing the tuning of A through the resonance with surface state.

Foreword

This volume summarizes the scientific content of the 2004 Research Meeting on Condensed Phase and Interfacial Molecular Science (CPIMS) sponsored by the U. S. Department of Energy (DOE), Office of Basic Energy Sciences (BES). This meeting marks the initiation of a new BES Contractor's Research meeting that will focus on the molecular-level understanding of complex physical and chemical processes in condensed phases and at interfaces. The meeting features the participation of 71 principal investigators from the following core research activities and nanoscale science initiative programs: Chemical Physics Program (36), Photochemical and Radiation Sciences Program (21), Atomic, Molecular and Optical Sciences Program (3), Nanoscale Science, Engineering and Technology/Theory, Modeling and Simulation in Nanoscience (11). The research described here is supported by the Chemical Sciences, Geosciences and Biosciences Division of BES, through the Fundamental Interactions Team, with an approximate annual funding level of $16.6 M.

The agenda reflects some of the research topics covered within the broad CPIMS theme, including: structure and dynamics of liquid water, chemistry of metal clusters, physical and chemical processes induced by low-energy electrons in aqueous solutions, dynamics and reactions on surfaces, optical and electronic responses in nanoscale materials, and probing or manipulation of single molecules at interfaces. Theory and experiment is well integrated throughout, indicative of the need for both in understanding these complex systems.

Contractor Research meetings are intended to facilitate an understanding of BES programmatic goals, enhance the alignment of fundamental research efforts with those goals, and foster new ideas and collaborations among the participants. The three Contractors' meetings currently sponsored by our Team (Combustion, AMOS and Solar Photochemistry) are passing the quarter-century mark in longevity and are very highly regarded by their participants. I sincerely hope that CPIMS will become another successful Contractors' meeting in our long-standing tradition. CPIMS differs in one important respect from the others in that it includes participation from all of the core research areas within our Team. Thus, it does not coincide with a single box on our organizational chart. However, from the PIs' perspective, a "program" is defined more by the annual Contractors' Meeting than by boxes on a BES organizational chart. I urge the participants to provide feedback to us on how well CPIMS has succeeded (or failed) in this regard and on ways it can be improved in future years.

I am delighted that the program managers from our Team, Mary Gress, Frank Tully and Dick Hilderbrandt, and our Division director, Walt Stevens, will be attending the meeting. I gratefully acknowledge the contributions of this year's speakers for their investment of time and for their willingness to share their ideas with the meeting participants. Thanks also go to Dick Hilderbrandt for assembling the book of abstracts, and to Diane Marceau from BES, Sophia Kitts and Kellye Sliger from Oak Ridge Institute of Science and Education, and the staff of the Airlie Conference Center for taking care of the logistical aspects of the meeting.

Eric Rohlfing
Team Leader, Fundamental Interactions
Chemical Sciences, Geosciences and Biosciences Division
Office of Basic Energy Sciences
September 2004

Agenda

U. S. Department of Energy
Office of Basic Energy Sciences
2004 Meeting on Condensed Phase and Interfacial Molecular Sciences

Sunday, October 24

3:00-6:00 pm	**** Registration ****
6:00 pm	**** Reception (No Host) ****
7:00 pm	**** Dinner ****

Monday, October 25

7:00 am	**** Breakfast ****
8:00 am	*Introductory Remarks* **Walter Stevens** and **Eric Rohlfing**, BES/DOE
Session I	Chair: **Eric Rohlfing**
8:30 am	*Dynamics of Nanoscopic Water:* *Ultrafast Vibrational Echo Experiments on Reverse Micelles* **Michael Fayer**, Stanford University
9:00 am	*Probing Water Confined in Reverse Micelles through Quasielastic Neutron Scattering and Molecular Dynamics Simulations* **Nancy Levinger**, Colorado State University
9:30 am	*The Dynamics and Kinetics of Hydrogen Bonds in Water* **Andrei Tokmakoff**, MIT
10:00 am	**** Break ****
10:30 am	*Development of a New Polarizable, Flexible Interaction Potential for Water: From Clusters to Liquid Water and Ice* **Sotiris Xantheas**, PNNL
11:00 am	*Optical Spectroscopy at the Spatial Limit* **Wilson Ho**, UC Irvine
11:30 am	*Semiempirical Representations of Molecular Interaction for Statistical Mechanical Simulation* **Greg Schenter**, PNNL
12:00 pm	**** Lunch ****
5:00 pm	**** Reception (No Host) ****
6:00 pm	**** Dinner ****

Session II Chair: **Scott Anderson**

7:00 pm *Clusters: Unraveling Fundamental Oxygen-Transfer Reaction Mechanisms Effected by Heterogeneous Catalysts*
Will Castleman, Penn State

7:30 pm *Structure and Dynamics in Metal-Molecular Complexes via IR Spectroscopy*
Michael Duncan, University of Georgia

8:00 pm *Computational Electron Spectroscopy: A Powerful Tool for Studies of Size-, Structure-, Charge State-, and Composition-Specific Properties of Finite Systems*
Julius Jellinek, Argonne National Laboratory

8:30 pm *Gas-Phase Transition Metal Containing Molecules: Electronic Structure and Bonding*
Tim Steimle, Arizona State University

Tuesday, October 26

7:30 am **** Breakfast ****

Session III Chair: **Bruce Garrett**

8:30 am *Dynamics of Low Energy Electrons in Ion Radiolysis of Aqueous Systems*
Simon Pimblott, Notre Dame Radiation Laboratory

9:00 am *Electron-Driven Chemistry: The Challenge to Theory*
Bill McCurdy, LBNL

9:30 am *Low Energy Electron Interactions with Complex Targets*
Thom Orlando, Georgia Tech

10:00 am **** Break ****

10:30 am *Electron-Stimulated Reactions at the Interfaces of Thin Water Films*
Greg Kimmel, PNNL

11:00 am *Delocalized Charges and Excitations in Molecular Materials*
Paul Barbara, University of Texas

11:30 am *How Water Networks Accommodate an Excess Electron: Structure and Dynamics of the Binding Site through Cluster Spectroscopy*
Mark Johnson, Yale University and **Ken Jordan**, Univ. of Pittsburgh

12:10 pm **** Lunch ****

Session IV Chair: **Ian Harrison**

4:00 pm *Dynamics of Electrons at Interfaces on the Femtosecond Timescale*
Charles Harris, LBNL

4:30 pm *Eley-Rideal and Hot Atom Reactions between H Atoms on Metal and Graphite Surfaces*
Bret Jackson, University of Massachusetts

5:00 pm *Self-Organization and Oxidative Surface Reaction Dynamics of Condensed Phase Systems*
Steve Sibener, University of Chicago

5:30 pm *A Combined QM/MM and Kinetic Monte Carlo Approach to Surface Science*
Mark Gordon, Ames National Laboratory

6:00 pm **** Reception (No Host) ****

7:00 pm **** Dinner ****

Wednesday, October 27

7:00 am **** Breakfast ****

Session V Chair: **Frank Tully**

8:00 am *Recent Progress Understanding Slow Dynamics and Aging*
David Chandler, LBNL

8:30 am *Computational Nanophotonics*
Steve Gray, Argonne National Laboratory

9:00 am *Scalable Methods for Electronic Excitations and Optical Responses of Nanostructures*
Steven Louie, LBNL

9:30 am **** Break ****

10:00 am *Single Molecule Conformational and Enzymatic Dynamics*
Sunney Xie, Harvard University

10:30 am *Beakers Without Walls: Formation of Deeply-Supercooled Solutions from Nanoscale Amorphous Solid Films*
Bruce Kay, PNNL

11:00 am *Single-Molecule Spectroscopy and Dynamics of Nanoscale Interfacial Rate Processes*
Peter Lu, PNNL

11:30 pm *Closing Remarks*
Eric Rohlfing, BES/DOE

11:45 am **** Lunch ****
(Optional boxed lunches available)

Table of Contents

Invited Presentations (Ordered by Agenda)

Invited Presentations

(ordered by agenda)

Solvent Dynamics and Photoinduced Electron Transfer in Complex Molecular Systems

Michael D. Fayer
Department of Chemistry, Stanford University, Stanford, CA 94305
email: fayer@stanford.edu

This program has two interrelated aspects, the investigation of dynamics of liquids in confined environments that influence solvent dynamics and the investigation of photoinduced electron transfer and geminate recombination in complex systems particularly those with confined or topologically complex structures. For photoinduced electron transfer to be useful in solar energy conversion it is necessary for both the forward electron transfer to be efficient and for the radicals that are formed to be able to avoid geminate recombination. Changing the topology of a system may influence electron transfer in two ways. First, the topology can modify the spatial relationship among donors and acceptors, and second the structure of the environment can influence the solvent dynamics in a manner that can change electron transfer dynamics. This program is using experiments and theory to develop an understanding of both components of this problem. Examining geminate recombination kinetics following forward transfer is a difficult problem both experimentally and theoretically that increases with difficulty as the system topology becomes more complex. Directly studying the dynamics of common solvents, e.g. water, in confined or topologically complex structures, such as reverse micelles, is in its infancy. Considerable progress is being made on both fronts. As can be seen by the list of publications, over the last several years we have been pursuing both directions and developing the necessary equipment, techniques, and theory to continue our push into uncharted territory.

In the following because of space limitations, only the first direct experiments that examine the dynamics of nanoscopic water, as a function of the size of the water nanopool in reverse micelles, will be discussed. A great deal of effort has also gone into the development of instrumentation to be able to make measurements of photoinduced electron transfer and geminate recombination with unprecedented accuracy and detail. Initial experiments have been carried out in solution, a liquid of donors in a pure acceptor solvent, and experiments on micelles. These experiments have been analyzed with detailed theory that includes the solvent structure (radial distribution function), transport, and in the case of micelles, the spatially non-uniform structure of the medium in which the donors and acceptors are embedded. Future experiments will examine photoinduced electron transfer in reverse micelles and other structurally confined systems. These experiments will be combined with the results of the ultrafast vibrational echo experiments that directly examine water or other solvents in confined media to understand the influence on electron transfer of solvent dynamics modified by nanoscopic confinement.

Water plays a major role in a multitude of physical and biological systems. The key feature of liquid water is its formation of dynamic hydrogen bond networks that are responsible for water's unique properties. Hydrogen bonds are constantly being formed and broken, and long (weak) hydrogen bonds become short (strong) bonds and vice versa. Hydrogen bond network dynamics occur over a range of time scales from tens of fs to ps. In many processes, water does not exist in its bulk form, but rather in nanoscopically confined environments. Nanoscopic water is important in biology, geology, and chemistry, and material processing.

Reverse micelles are widely used as model systems for studying water in nanoscopic environments. Reverse micelles can be formed in a mixture of water, surfactant, and organic solvent. The water molecules are trapped in nanometer size cavities (one to tens of nm) created

by the surfactant molecules oriented so that their ionic or polar head groups point inward toward the aqueous phase. Sodium bis(2-ethylhexyl) sulfosuccinate (AOT) is a common surfactant used to make reverse micelles. Time dependent experiments on probe molecules in AOT reverse micelles have provided a great deal of important information on nanoscopic water properties but only indirect information on dynamics. Difficulties in interpreting such experiments arise from the uncertainties in the location of the probe molecules in the reverse micelle and the complexity of deciphering the influence of the water dynamics on the observable associated with the probe molecule.

We have applied ultrafast infrared spectrally resolved stimulated vibrational echo spectroscopy and spectrally resolved vibrational echo peak shift measurements to directly examine the dynamics of nanoscopic water in AOT reverse micelles. Recent vibrational echo experiments on bulk water and comparisons to molecular dynamics simulations have provided substantial insights into bulk water dynamics. The vibrational echo experiments are being used to study the dynamics in water nanopools as a function of their size, and the results are compared to those obtained on bulk water. Using 50 fs IR pulses, the experiments measure the vibrational dephasing of the OD hydroxyl stretch of dilute HOD in the water nanopools. Vibrational dephasing, which is caused by the frequency evolution of the hydroxyl stretch oscillator, is sensitive to hydrogen bond network dynamics because the hydroxyl stretch frequency is strongly dependent on the strength and number of hydrogen bonds. The frequency is shifted to lower frequency for stronger hydrogen bonds and an increased number of hydrogen bonds. By tracking the evolution of the stretch frequency, one can observe the dynamical change of the hydrogen bond network. The dilute OD hydroxyl stretch is investigated to eliminate vibrational excitation transport, and to assure that the absorption of the sample is not too high. Detailed simulations of water show that the observables associated with vibrational echo experiments are the same whether an OD or OH stretch is monitored. Therefore, measurements on the OD stretch provide an accurate picture of water dynamics.

The ensemble-averaged measure of the vibrational frequency evolution is characterized by the frequency-frequency correlation function (FFCF), $C(t) = \langle \delta\omega(t)\delta\omega(0) \rangle$. The FFCF for bulk water has been determined using vibrational echo experiments and compared to FFCFs obtained from molecular dynamics simulations of water. Recent simulations produce results that are in near quantitative agreement with the experiments. The simulations provide qualitative insights into the nature of the hydrogen bond dynamics on different time scales.

Monodispersed AOT reverse micelles were prepared in CCl_4 solvent, with $w_0 = [H_2O]/[AOT]$ = 10, 5, and 2. The size of the nanoscopic water pool at the center of the micelle can be assigned from w_0. The w_0 studied nanopool sizes of approximately 4.0 nm, 2.6 nm, and 1.7 nm, and the number of water molecules in the nanopools are estimated to be ~1000, ~300, and ~50, respectively. Experiments were also performed in the identical manner on bulk water as well as on a 6M NaCl solution.

Transform limited, 50 fs long ~4 μm tunable pulses were produced using a Ti:Sapphire regenerative amplifier pumped optical parametric amplifier system. The OPA was tuned to match the peak of the absorption spectrum of the sample under investigation. The laser pulse is split into three separate beams and focused into the sample cell. The inter-pulse delays between the first-second and second-third pulses are τ and T_w, respectively. The resultant vibrational echo signal was passed through a monochromator prior to detection. The frequency resolved vibrational echo signal was measured at the absorption peak frequency of each sample for the the

experiments described here, but some frequency dependent results have been obtained. Frequency resolution avoids the ambiguity introduced when signals from both the 0-1and 1-2 vibrational transitions are observed simultaneously in a non-frequency resolved experiment. In addition, the presence or lack of a detectable wavelength dependence provides insights into the nature of the results. Vibrational echo traces were collected as a function of τ for a series of T_ws. IR pump-probe experiments at the magic angle were used to obtain the vibrational lifetime, T_1, and were used in the data analysis.

The background subtracted FT-IR spectra of the OD stretching mode in reverse micelles and bulk water show substantial changes with micelle size. The peak positions for bulk water and w_0 = 10, 5, 2 are 2506 cm^{-1}, 2539 cm^{-1}, 2558 cm^{-1}, and 2566 cm^{-1}, respectively. The spectral changes demonstrate that there are structural changes that increase as the water nanopools become smaller. Vibrational echo decays (τ scans) for a single T_w show a very pronounce slowing of the decay as the reverse micelle nanopool gets smaller. The vibrational echo decay curves for many T_ws for each sample were fit using diagrammatic perturbation theory calculations with a tri-exponential FFCF, which is the form that was found appropriate for water. The fitting showed that all of the components of the FFCF changed relative to bulk water as the nanopools became smaller, but the largest changes were in the slowest component of the FFCF. Another experimental observable that was measured in these experiments and can be calculated from the FFCF is the vibrational echo peak shift. Peak shift data provide a convenient method for comparing the micelle results to those of bulk water, to test one possible explanation for the differences between bulk water and the reverse micelle nanoscopic water, and to assess the validity of the FFCF obtained from fitting the T_w dependent decay curves. The peak shift data on 6 M NaCl water solution were only slightly different from those for bulk water while even the w_0 = 10 micelle data show a difference from bulk water data that are many times greater. This demonstrates that the differences in dynamics of the reverse micelle nanopools compared to bulk water do not arise from the ionic strength of the nanopools. Furthermore, the peak shifts calculated with no adjustable parameters using the FFCF obtained by fitting the echo decay curves were in good agreement with the peak shift data. This supports the validity of the fits.

As mentioned above, the larges differences between bulk water and the nanopools were in the longest time scale dynamics. For bulk water, and w_0 = 10, 5, 2 (4 nm, 2.4 nm, 1.7 nm), the slowest decay components are 1.5 ps, 13 ps, 21 ps, and 70 ps, respectively. In analogy to water, the substantial slowing demonstrates that the rate of hydrogen bond breaking and making decrease dramatically as the nanopools become smaller. Because chemical processes can depend on the water's structural rearrangement, the reduction in the rate of hydrogen bond making and breaking in nanoscopic water will have major impact on chemical dynamics.

Many additional experiments are in progress to study nanoscopic water dynamics, e.g., the wavelength dependence of the vibrational echo dynamics and orientational relaxation of the water molecules. Photoinduced electron transfer experiments in reverse micelles will be conducted in the near future. Additional confined environments, such as nanotubes and zeolites are on the drawing board.

Publication Supported by DOE 2002 – 2004

"Hydrogen Bond Dissociation and Reformation in Methanol Oligomers Following Hydroxyl Stretch Relaxation," K. J. Gaffney, Paul H. Davis, I. R. Piletic, Nancy E. Levinger, and M. D. Fayer, J. Phys. Chem. A 106, 12012-12023 (2002).

"Influence of Diffusion on the Kinetics of Donor-Acceptor Electron Transfer Monitored by the Quenching of Donor Fluorescence," V. S. Gladkikh, A. I. Burshtein, H. L. Tavernier, and M. D. Fayer, J. Phys. Chem. A 106, 6982-6990 (2002).

"Hydrogen Bond Breaking and Reformation in Alcohol Oligomers Following Vibrational Relaxation of a Non-hydrogen Bond Donating Hydroxyl Stretch," K. J. Gaffney, I. R. Piletic, and M. D. Fayer, J. Phys. Chem. A 106, 9428-9435 (2002).

"Orientational Relaxation and Vibrational Excitation Transfer in Methanol - Carbon Tetrachloride Solutions," K. J. Gaffney, I. R. Piletic, and M. D. Fayer, J. Chem. Phys., 118, 2270-2278 (2003).

"Structural Dynamics of Hydrogen Bonded Methanol Oligomers: Vibrational Transient Hole Burning Studies of Spectral Diffusion," I. R. Piletic, K. J. Gaffney, and M. D. Fayer, J. Chem. Phys. 119, 423-434 (2003).

"Ultrafast Heterodyne Detected Infrared Multidimensional Vibrational Stimulated Echo Studies of Hydrogen Bond Dynamics," John B. Asbury, Tobias Steinel, C. Stromberg, K. J. Gaffney, I. R. Piletic, Alexi Goun, and M. D. Fayer, Chem. Phys. Lett. 374, 362-371 (2003).

"Hydrogen Bond Dynamics Probed with Ultrafast Infrared Heterodyne Detected Multidimensional Vibrational Stimulated Echoes," John B. Asbury, Tobias Steinel, C. Stromberg, K. J. Gaffney, I. R. Piletic, Alexi Goun, and M. D. Fayer, Phys. Rev. Lett. 91, 237402-1 – 237402-4 (2003).

"Hydrogen Bond Breaking Probed with Multidimensional Stimulated Vibrational Echo Correlation Spectroscopy," John B. Asbury, Tobias Steinel, C. Stromberg, K. J. Gaffney, I. R. Piletic, and M. D. Fayer, J. Chem. Phys. 119, 12981-12997 (2003).

"Hydrogen Bond Networks: Structure and Evolution After Hydrogen Bond Breaking," John B. Asbury, Tobias Steinel, and M. D. Fayer, J. Physical Chemistry B 108, 6544-6554 (2004).

"Vibrational Echo Correlation Spectroscopy Probes of Hydrogen Bond Dynamics in Water and Methanol," John B. Asbury, Tobias Steinel, and M. D. Fayer, J. Lumin. 107, 271-286 (2004).

"Photoinduced Electron Transfer and Geminate Recombination for Photoexcited Acceptors in a Pure Donor Solvent," V. O. Saik, A. A. Goun and M. D. Fayer, J. Chem. Phys. 120, 9601-9611 (2004).

"Photoinduced Intermolecular Electron Transfer in Liquid Solutions," V. O. Saik, A. A. Goun, J. Nanda, Koichiro Shirota, H. L. Tavernier, and M. D. Fayer, J. Phys. Chem. 108**,** 6696-6703 (2004).

"Vibrational Echo Correlation Spectroscopy: a New Probe of Hydrogen Bond Dynamics in Water and Methanol," John B. Asbury, Tobias Steinel, and M. D. Fayer, in Femtosecond Laser Spectroscopy: Progress in Lasers, Ed. P. Hannaford, Kluwer, Brussells, 2004.

"Photoinduced Electron Transfer in the Head Group Region of Sodium Dodecyl Sulfate Micelles," J. Nanda, P. K. Behera, H. L. Tavernier and M. D. Fayer, J. Lumin. submitted (2004).

"Nanoscopic Water: Dynamics in Reverse Micelles Measured with Ultrafast Infrared Vibrational Echo Spectroscopy," Howe-Siang Tan, Ivan R. Piletic, Ruth E. Riter, Nancy E. Levinger and M. D. Fayer, Phys. Rev. Lett. submitted (2004).

"Fundamental Properties of Solvent Pools of Reverse Micelles Used in Nanoparticle Synthesis"

Nancy E. Levinger and Branka M. Ladanyi, Principal Investigators
Department of Chemistry, Colorado State University, Fort Collins, CO 80523-1872
Email: Nancy.Levinger@ColoState.edu, Branka.Ladanyi@ColoState.edu

With funding from this grant, we are investigating fundamental properties of the solvent pool in reverse micelles that could be used as templates for nanoparticle synthesis. The program utilizes a two pronged approach, both experimental and theoretical, to explore basic structure and dynamics of water inside the nanoconfines of reverse micelles. Reverse micelles are nanostructured macromolecular assemblies that form in ternary or higher order mixtures of polar, nonpolar and amphiphilic molecules. When the reverse micelle is spherical, the diameter is proportional to $w_0 = [H_2O]/[\text{surfactant}]$. To date, our studies have focused on the dynamics within the water pool of Aerosol OT (sodium di-2-ethylhexyl sulfosuccinate, AOT) reverse micelles.

Experimentally, we have used quasielastic neutron scattering (QENS) to explore water motion inside the reverse micelles. Because the incoherent scattering cross section is much larger for H than for other nuclei, QENS is a powerful technique for investigating the dynamics of hydrogen-containing species. Selective deuteration of the sample can enhance signals from the interior of the reverse micelles. In the experiments reported here, we have used perdeuterated nonpolar solvents, isooctane or cyclohexane, and, when possible, AOT with deuterated alkyl tails. The experiments were performed using the QENS spectrometer at the Intense Pulsed Neutron Source (IPNS) at Argonne National Laboratory and using the disk chopper spectrometer at NIST. Experiments for which we have the most complete analysis were performed at IPNS with an 85 μeV energy resolution over the momentum transfer (Q) range of 0.36 to 2.53 $Å^{-1}$ at room-temperature with reverse micelle samples at water contents $w_0 = [H_2O]/[\text{AOT}]$ of 1, 2.5 and 5.

We have investigated the motion of water molecules in AOT reverse micelles with water content w_0 ranging from 1 to 5 on samples in which the nonpolar phase (isooctane) and the AOT alkyl chains were deuterated, thereby suppressing their contribution to the QENS signal. QENS results were analyzed via the jump diffusion/isotropic rotation model, which fits the results reasonably well despite the fact that confinement effects are not explicitly taken into account. This analysis indicates that in reverse micelles with low water content (w_0 = 1 and 2.5) the

translational diffusion rate is too slow to be detected, while for $w_0 = 5$, the diffusion coefficient is much smaller than for bulk water. Rotational diffusion coefficients obtained from this analysis increase with w_0 but remain smaller than for bulk water. However, rotational mobility is less drastically reduced than translational mobility.

In parallel to QENS experiments, we have simulated the reverse micelles and the QENS response from the reverse micelles using molecular dynamics (MD) simulations. Using the Faeder/Ladanyi model (*J. Phys. Chem. B* **104**, 1033 (2000)) of reverse micellar interior, MD simulations were performed to calculate the self-intermediate scattering function, $F_S(\mathbf{Q},t)$ for water hydrogens. Comparison of the time Fourier transform of this $F_S(\mathbf{Q},t)$ with the QENS dynamic structure factor, $S(\mathbf{Q},\omega)$, shows good agreement between the model and experiment. Separate intermediate scattering functions $F_S^{CM}(\mathbf{Q},t)$ and $F_S^R(\mathbf{Q},t)$ were determined for translational and rotational motion. Consistent with the decoupling approximation used in the analysis of the experimental QENS data, the product of $F_S^{CM}(\mathbf{Q},t)$ and $F_S^R(\mathbf{Q},t)$ is a good approximation of the total $F_S^{CM}(\mathbf{Q},t)$. We find that the decay of $F_S(\mathbf{Q},t)$ is nonexponential and our analysis of the MD data indicates that this behavior is due to lower water mobility close to the interface and to confinement-induced restrictions on the range of translational displacements. Rotational relaxation also exhibits nonexponential decay. However, rotational mobility of O-H bond vectors in the interfacial region remains fairly high due to the lower density of water-water hydrogen bonds in the vicinity of the interface. These experimental and simulation results have recently been accepted for publication.[1]

Recently, we have explored the impact of changing the counterion on the dynamics of water motion in AOT reverse micelles. We know from our previous studies that the nature of the water in the reverse micelles depends on micelle size and shape as well as the counterion associated with the surfactant headgroup. To probe the impact of counterion, we have exchanged the AOT standard Na^+ counterion for K^+, Ca^{2+}, and Cu^{2+}. While the K and Ca exchanged reverse micelles are reported to retain a spherical form, the Cu exchanged reverse micelles possess an ellipsoidal form. We have performed QENS experiments on these ion exchanged reverse micelles both at IPNS and at NIST. We are also simulating the effect of exchanging the counterion. Our preliminary analysis shows that the water dynamics depends on the counterion charge, size and type.

Future studies include QENS experiments and simulations on other various reverse micellar systems. For example, we will explore the role played by the long chain alcohol cosurfactant in quaternary reverse micelles specifically focusing on the dynamics of alkyl tail and its impact on water dynamics. We are also working to develop an atomistic model for reverse micelles. To this end, we have simulated planar interfaces with and without surfactant present.

[1] M. R. Harpham, B. M. Ladanyi, N. E. Levinger and K. W. Herwig, "Water Motion in Reverse Micelles Studied through Quasielastic Neutron Scattering and Molecular Dynamics Simulations", *J. Chem. Phys.* in press.

Structural Dynamics in Complex Liquids Studied with Multidimensional Vibrational Spectroscopy

Andrei Tokmakoff, Joel D. Eaves, Christopher J. Fecko, Phillip L. Geissler,*
Joseph J. Loparo and Sean T. Roberts

Department of Chemistry, Massachusetts Institute of Technology, Cambridge, MA 02139
E-mail: tokmakof@MIT.edu

**Department of Chemistry, University of California, Berkeley, CA 94720*

Our study of the collective structure and molecular dynamics of liquids has focused on the experimental and theoretical study of hydrogen bond rearrangements in water, as viewed through infrared spectroscopy. The physical and chemical properties of water are dictated by hydrogen bond interactions and the reconfiguration of the structure of water during the breaking and forming of hydrogen bonds. Hydrogen bond dynamics and collective reorganization in water also play crucial roles in aqueous chemical and biochemical reaction dynamics, particular where transport of electrons and protons is involved. Water is a remarkably structured liquid, considering that at any instant it has 80-90% of the hydrogen bonds found in the tetrahedral structure of ice. But the structure imposed by these highly directional hydrogen bonds evolves very quickly, with large scale fluctuations on femtosecond time scales and subsequent more permanent hydrogen bond breaking and forming on roughly 1 ps time scales. Presently, our understanding of hydrogen bond dynamics draws largely from classical molecular dynamics computer simulations, but ultrafast infrared spectroscopy is rapidly opening new windows into the evolution of intermolecular structure in water.

We have investigated the hydrogen bond dynamics of water with a combined experimental and theoretical study of the OH stretch spectroscopy of HOD in D_2O. This widely studied model system can be used to characterize the vibrational dynamics of an isolated OH stretch vibration within D_2O molecules, whose hydrogen bond dynamics closely mirror those of H_2O. The OH stretch frequency ω is particularly sensitive to the hydrogen bonding environment leading to a broad absorption line in the mid-infrared (3 μm). Femtosecond infrared spectroscopy

can be used to characterize spectral diffusion within the OH absorption line, which in turn is determined by the hydrogen bond dynamics and kinetics. To ensure that dynamics on all possible time-scales are observed, we use 45 fs pulses with enough bandwidth to span the entire absorption line. Infrared vibrational echo peak shift measurements were performed to characterize spectral diffusion through the OH frequency correlation function. When combined with polarization-selective femtosecond pump-probe measurements, we are able to reveal the structural fluctuations of individual hydrogen bonds that precede the reorganization of water's hydrogen bond network. These include the vibrations of hydrogen bonds and hindered rotational fluctuations within relatively fixed environments, prior to a reconfiguration of the many-body liquid structure on picosecond time scales.

A model for the OH frequency shifts for HOD in D_2O, which accounts for intermolecular interactions using classical molecular dynamics simulations, has been used to investigate the relationship between vibrational frequency and hydrogen bonding configurations about the HOD molecule. We use a model in which the quantum mechanical OH coordinate, represented with a gas phase Morse potential, is perturbed by the time-dependent interactions experienced by an OH coordinate in a molecular dynamics simulation of one HOD molecule in 107 D_2O molecules. The OH frequency distribution taken from static configurations is 260 cm^{-1} wide, with strongly hydrogen bound species on the red side of the line and weak or broken hydrogen bonds on the blue side of the line. The model predicts a reasonably strong correlation between OH frequency and the OH···O hydrogen bond length to the nearest neighbor (ρ=0.77), and a weaker correlation with hydrogen bonding angle (ρ=0.49). Poor correlation exists between OH frequency and the tetrahedrality of the first solvent shell. We find that no simple structural or geometric order parameter captures all of the observed dynamics. However, the OH frequency correlates strongly (ρ=0.99) with the molecular electric field experienced by the OH coordinate due to the changing configurations of all D_2O molecules. The OH frequency shift is therefore essentially a Stark effect induced by the hydrogen bond acceptor and other water molecules.

Our two-dimensional infrared experiments answer questions about the 10% of broken hydrogen bonds in water. Broken hydrogen bonds are often treated as free, energetically stabilized species in equilibrium with the hydrogen bonded state. We find evidence for an alternative explanation. Instead, each water molecule in the liquid experiences large fluctuations about a preferential tetrahedral hydrogen-bonded structure, and broken hydrogen bonds only

exist transiently during the frequent exchange of hydrogen bonding partners. This information is obtained from 2D IR experiments, which distinguish between broken and intact hydrogen bonds by their absorption frequency and then watch their evolution in time. 2D IR spectroscopy correlates how molecules initially at one frequency (ω_1) evolve to a final frequency (ω_3) during the course of a waiting period (τ_2). Analysis of 2D IR line shapes shows that broken hydrogen bonds return to a bonded geometry on the time scale of water's fastest intermolecular motions (≤150 fs).

DOE Supported Publications (2002-2004)

1. "Coherent 2D IR Spectroscopy: Molecular structure and dynamics in solution," M. Khalil, N. Demirdöven and A. Tokmakoff, *Journal of Physical Chemistry A*, **107** (2003) 5258.
2. "Ultrafast hydrogen bond dynamics in the infrared spectroscopy of water," C. J. Fecko, J. D. Eaves, J. J. Loparo, A. Tokmakoff and P. G. Geissler, *Science*, **301** (2003) 1698.
3. "Dynamics of hydrogen bonds in water: Vibrational echoes and two-dimensional infrared spectroscopy," C. J. Fecko, J. D. Eaves, J. J. Loparo, S. T. Roberts, A. Tokmakoff and P. L. Geissler, in *Ultrafast Phenomena XIV*, ed. by T. Kobayashi, T. Okada, T. Kobayashi, K. A. Nelson, S. DeSilvestri (Springer-Verlag, Berlin) accepted.
4. "A unified analysis of ultrafast vibrational and orientational dynamics of HOD in D_2O," J. J. Loparo, C. J. Fecko, J. D. Eaves, S. T. Roberts and A. Tokmakoff, in *Ultrafast Phenomena XIV*, ed. by T. Kobayashi, T. Okada, T. Kobayashi, K. A. Nelson, S. DeSilvestri (Springer-Verlag, Berlin) accepted.
5. "Solvation dynamics of N-methylacetamide in D_2O, $CDCl_3$ and DMSO-d_6," M. F. DeCamp, L. P. DeFlores, J. M. McCracken, and A. Tokmakoff, in *Ultrafast Phenomena XIV*, εδ. βψ Τ. Κοβαψασηι, Τ. Οκαδα, Τ. Κοβαψασηι, Κ. Α. Νελσον, Σ. ΔεΣιλωεστρι (Σπρινγερ−ζερλαγ, Βερλιν) αχχεπτεδ.
6. Γενερατιον οφ 45 φεμτοσεχονδ πυλσεσ ατ 3 μm with a $KNbO_3$ optical parametric amplifier," C. J. Fecko, J. J. Loparo and A. Tokmakoff, *Optics Communications*, in press.

Molecular Theory & Modeling

Development of a new polarizable, flexible interaction potential for water: From clusters to liquid water and ice

Sotiris S. Xantheas
Chemical Sciences Division
Pacific Northwest National Laboratory
902 Battelle Blvd.
Mail Stop K1-83
Richland, WA 99352
sotiris.xantheas@pnl.gov

The objective of this research effort is to develop a comprehensive understanding of the collective phenomena associated with aqueous solvation. It is of particular interest to investigate the interplay between molecular level information and macroscopic observables. We focus the research effort on models of molecular interactions for water simulations because the description of aqueous systems is a major focus of the proposed work. Development of intermolecular potential models for computer simulations of aqueous systems has been an active field since the pioneering work of Rahman and Stillinger. A sampling of the literature over the last 30 years indicates that a very large number of water models have been introduced. As stated by Wallqvist and Berne in 1993, "a single model that satisfactorily captures all of the essential experimental features of water has yet to be found." The large number of water interaction potentials that have been developed so far attests to the fact that a single empirical water model that is appropriate for a wide range of properties and aqueous systems still remains a challenge. The majority of these models are empirically adjusted so that *classical* simulations reproduce selected experimental properties over specific ranges of physical conditions. These models are not generally applicable to other properties or to physical conditions outside those for which they are parameterized.

An alternative approach is to parameterize the relevant interactions based upon the results of *ab initio* calculations for clusters. Clusters offer the advantage of providing valuable information on the nature of intermolecular interactions and the magnitude of collective phenomena at the molecular level. They also can offer valuable insights into the flowing issues:

- the structure of the hydrogen bonded network and its relation to vibrational spectroscopy,
- how its dynamics and energetics are controlled by cooperative effects,
- the parts of the respective cluster PESs that are relevant for describing macroscopic properties, and
- the most effective way of incorporating this information into models that simulate condensed environments

Although the earliest attempts to develop water models using electronic structure calculations dates back nearly 30 years, it is only within the last few years that methodological developments in electronic structure software and their efficient implementation on supercomputers have made it feasible to increase the accuracy of the electronic structure methods for molecular systems. The use of electronic structure calculations in developing empirical interaction models has been advanced by the significant progress made in exploiting new approaches for recasting the many-body expansion for the binding energy U:

$$U = U_{1\text{-}body} + U_{2\text{-}body} + U_{3\text{-}body} + \ldots + U_{n\text{-}body}, \qquad (1)$$

where $U_{1\text{-}body}$ is the energy penalty for distorting the individual fragments from their gas phase geometries to the ones they assume in the whole system, $U_{2\text{-}body}$ is the energy of all pairs of fragments (dimers), $U_{3\text{-}body}$ the energy of all triplets (trimers) and so on. The $U_{2\text{-}body}$ represents the *pairwise-additive* term, while the sum of higher order terms represent the *non-additive* component of the total system. This relation provides insight into the connection between the cluster and condensed phase energetics and can furthermore assess the relevance of clusters in quantifying the magnitude of nonadditive terms in the above many-body energy expansion. Application of the energy decomposition for water clusters up to the hexamer suggests that the many-body energy expansion converges rapidly for the various networks found in the global and local minima of these clusters. For these systems, the sum of the two- plus three-body terms reproduces over 97% of the cluster energetics with the two-body term alone amounting to about 80%. This result implies that accurate interaction potentials for these networks can be constructed from the potential energy surfaces of just the dimer and trimer clusters.

We have relied on this finding in order to recast equation (1) into the following:

$$U = U_{1\text{-}body} + U_{2\text{-}body} + U_{\text{many-}body}, \qquad (2)$$

where the term $U_{\text{many-}body}$

- contains all-non additive terms to infinite order,
- is assumed to be caused exclusively by induction and
- is modeled using moments (dipole, quadrupole) that are determined iteratively via a self-consistent scheme.

The 1-body term is responsible for describing the intramolecular vibrations and the geometrical changes in the intramolecular geometry of water due to various environments. We have used the monomer potential energy (PES) and dipole moment (DMS) surfaces of Partridge and Schwenke, which were derived from high level electronic structure calculations and they reproduce the non-linear character of the DMS as previously suggested by experimental IR measurements.

Our previous work in understanding the correspondence between molecular level information and macroscopic properties, as well as recent developments of force fields similar to ours that are based upon utilizing our electronic structure results as benchmarks, have indicated that the water dimmer PES holds the key in the accurate description of cluster and condensed phase (liquid water / ice) energetics. This is consistent with the realization that the two-body energy in the many-body expansion (1) amounts to about 80% of the total interaction energy for clusters in the regime ($6 < n < 20$) as well as for proton ordered ice (ice XI). With the aid of electronic structure calculations, we have furthermore identified "chemically important" configurations of the water dimer PES and used the energetic and structural information from approximately 35 water dimer configurations in parametrizing the 2-body term in the rigid (TTM2-R) and flexible (TTM2-F) versions of our interaction potential. Given that the interaction energy of the water dimer has not yet been directly measured (let alone the energetics of larger clusters), the use of electronic structure methods represents an indispensable and currently irreplaceable approach in obtaining cluster energetics. The issue of accuracy is of utmost importance given that errors scale in proportion to the number of molecules in the clusters. We have used the available hardware and software (NWCHEM) at EMSL's Molecular Science Computing Facility (MSCF) in order to obtain accurate binding energies for the first few water clusters (n=2-6, 8, 17-21). These served as benchmarks to assess the accuracy of our newly developed model. Initially we have obtained the energetics of the water dimer PES at the MP2/aug-cc-pVTZ level of theory in order to develop the first version (TTM) of the water

potential. The TTM cluster energetics were associated with an (*rms*) error of 1.9 kcal/mol with respect to the MP2/CBS binding energies for the n=2-6 clusters. Consequent use of a new dimer PES *universally scaled* to the MP2/CBS limit for the dimer minimum configuration reduced that (*rms*) error to just 0.3 kcal/mol and – at the same time – produced accurate macroscopic properties for liquid water and ice such as the liquid radial distribution functions, density and diffusion coefficient and the energy of proton ordered ice. Furthermore, our flexible interaction potential is currently *the only one* among the flexible models that produces the correct increase of the water bend angle in water clusters, liquid water and ice Ih and XI, in contrast to all other flexible models which show a decrease in the bend angle.

The fact that our developed interaction potential (TTM2-F) is parameterized to the cluster energies (D_e) suggests that it is more appropriate to use it in conjunction with quantum path integral simulations which explicitly account for zero-point energy and finite temperature effects and at the same time can describe the variation of these effects across different environments.

Collaborators on this project include CJ Burnham, GS Fanourgakis. E Aprà, RJ Harrison.

References to publications of DOE sponsored research (2002-present)

1. C. J. Burnham and S. S. Xantheas, "Development of Transferable Interaction Potentials for Water: I. Prominent Features of the Water Dimer Potential Energy Surface", *Journal of Chemical Physics* **116**, 1479 (2002)
2. S. S. Xantheas, C. J. Burnham, R. J. Harrison, "Development of Transferable Interaction Potentials for Water: II. Accurate Energetics of the First Few Water Clusters from First Principles", *Journal of Chemical Physics* **116**, 1493 (2002)
3. C. J. Burnham and S. S. Xantheas, "Development of Transferable Interaction Potentials for Water: III. Re-parameterization of an All-Atom Polarizable Rigid Model (TTM2-R) from First Principles", *Journal of Chemical Physics* **116**, 1500 (2002)
4. C. J. Burnham and S. S. Xantheas, "Development of Transferable Interaction Potentials for Water: IV. A Flexible, All-atom Polarizable Potential (TTM2-F) based on Geometry Dependent Charges derived from an *ab-initio* Monomer Dipole Moment Surface", *Journal of Chemical Physics* **116**, 5115 (2002)
5. T. H. Dunning, Jr., R. J. Harrison, D. Feller, and S. S. Xantheas, "Promise and Challenge of High-performance Computing, with Examples from Molecular Modeling", special issue on "New Science from High Performance Computing" (invited) *Philosophical Transactions of the Royal Society of London, Series A, Mathematical and Physical Sciences* **360**, 1079 (2002)
6. C. J. Burnham and S. S. Xantheas, M. A. Miller, B. Applegate and R. E. Miller, "The Formation of Cyclic Water Complexes by Sequential Ring Insertion: Experiment and Theory", *Journal of Chemical Physics* **117**, 1109 (2002)
7. P. R. McCurdy, W. P. Hess and S. S. Xantheas, "Nitric Acid-Water Complexes: Theoretical Calculations and comparison with Experiment", G. Wilse Robinson Festschrift (invited) *Journal of Physical Chemistry A* **106**, 7628 (2002)
8. D. Tzeli and A. Mavridis, S. S. Xantheas, "A First Principles Examination of the Acetylene-Water clusters, HCCH-$(H_2O)_n$, n=2, 3 and 4", *Journal of Physical Chemistry A* **106**, 11327 (2002)
9. G. M. Chaban, S. S. Xantheas, R. B. Gerber, "Anharmonic Vibrational Spectroscopy of the F^- $(H_2O)_n$ complexes, n=1, 2" *Journal of Physical Chemistry A* **107**, 4952 (2003)

10. S. S. Xantheas, E. Aprà, "The binding energies of the D_{2d} and S_4 water octamer isomers: High-level electronic structure and empirical potential results", *Journal of Chemical Physics* **120**, 823 (2004)
11. J. M. Bowman, S. S. Xantheas, "*Morphing* of *ab initio*-based interaction potentials to spectroscopic accuracy: Application to $Cl^-(H_2O)$", *Pure and Applied Chemistry* **76**, 29 (2004)
12. C. J. Burnham and S. S. Xantheas, "On the importance of zero-point effects in molecular level classical simulations of water", *Journal of Molecular Liquids* **110**, 177 (2004)
13. S. S. Xantheas, "Intermolecular Interactions and Cooperative Effects from Electronic Structure Calculations: An Effective Means for Developing Interaction Potentials for Condensed Phase Simulations" in *Novel Approaches to the Structure and Dynamics of Liquids: Experiments, Theories and Simulations*, NATO Science Series II: Mathematics, Physics and Chemistry vol. 133 J. Samios and V. A. Duriv (Eds.), pp. 1-15, Kluver Academic Publishers, Dordrecht, The Netherlands (2004)
14. G. S. Fanourgakis, E. Aprà and S. S. Xantheas, "High-level *ab-initio* calculations for the four low-lying families of minima of $(H_2O)_{20}$: I. Estimates of MP2/CBS binding energies and comparison with empirical potentials", *Journal of Chemical Physics* **121**, 2655 (2004)

Optical Spectroscopy at the Spatial Limit

Wilson Ho

Department of Physics and Astronomy and Department of Chemistry
University of California, Irvine
Irvine, CA 92697-4575

E-mail: wilsonho@uci.edu

Program Scope

Our research program hinges on the use of low temperature scanning tunneling microscopes (STM) in ultrahigh vacuum to probe single atoms and molecules as well as nanostructures built from them. By fabricating different environments for them, we hope to reveal previously hidden properties and to gain a deeper understanding of their chemistry. Here, The detection of photons emitted from the junction of a scanning tunneling microscope taps into the combined strengths of the scanning tunneling microscope and optical spectroscopy. The theme of this program is reflected in three main thrusts: 1. photon emission stimulated by tunneling electrons; 2. tip enhanced Raman spectroscopy; 3. radio-frequency (RF) induced photon emission. These thrusts were chosen to set the experimental challenge of reaching the single molecule sensitivity in optical spectroscopy. These experiments would lead to an understanding of the inner machinery of single molecules that are difficult to obtain with other approaches. Results from these studies are expected to provide the scientific basis for the unusual properties, processes, and phenomena in chemical and physical systems at the nanoscale.

Recent Progress

During 2002-2004, our experiments were designed to find new applications of the STM in order to increase our understanding of the properties and phenomena associated with molecules, chemical bonding and reaction, and molecular nanostructures. The STM was used to manipulate and probe the bonding of one to four Xe atoms and single CO and benzene dithiol molecules to a single porphyrin molecule [2], the assembly of a metallic chain [7,8], and the construction of a metal-molecule-metal bridge [8]. Molecular fluorescence stimulated by tunneling electrons was observed [5] as well as light emission from Ag chains down to a single atom [7]. Detailed mechanisms were elucidated for the conformational changes in a single molecule. A new tunneling mechanism into the vibronic states of single molecules was demonstrated [11,12]. This period also saw the extension of the substrate from metals to thin oxides, allowing the observation of molecular fluorescence [5] and vibronic states [11,12].

The growth of a thin Al_2O_3 film (5.2 Å thick) on NiAl(110) also led to a new series of experiments with the discovery of bipolar electron transport for molecules adsorbed on the oxide surface. Electrons can tunnel through the same electronic state of the molecule at both positive and negative sample biases – a process that is not possible for molecules in a single tunneling barrier. This phenomenon arises from the formation of the double-barrier tunnel junction, consisting of the vacuum and the oxide barriers. The molecule is effectively isolated and

sandwiched between these two tunneling barriers. Furthermore, by tuning the tip-molecule separation, the ratio of tunneling rates through the two barriers is controlled. This results in dramatic changes in the relative intensities in individual conduction channels associated with different vibronic states of the molecule.

The double-barrier tunnel junction also led to the observation of field effect transport by charging of single impurities in a monolayer organic crystal. We use a scanning tunneling microscope to study charge transport in a doped monolayer of C_{60} molecules supported on a thin Al_2O_3 film grown on the NiAl(110) surface. The doping centers were formed by deposition of individual Ag atoms on the C_{60} monolayer. Differential conductance spectroscopy shows that charging of these impurities affects the conduction through C_{60} molecules located around the impurities. This effect is used to observe the electrostatic interaction of a pair of charged impurities. Charging of one impurity charge trap is found to shift the energy levels of the other, an analogue of the field-effect action.

Future Plans

Experiments in the future are designed to combine optical spectroscopy with the STM in the three areas described in the Program Scope section. To date, only one experiment has reported the observation of single molecule photon emission induced by tunneling electrons [5]. Extension to other molecules not only demonstrates the range of application of the technique but also the possibility to obtain new understanding of the molecular properties and the photon emission mechanisms. We will extend our initial experiment to include other molecules and insulating surfaces in addition to oxides, such as alkali halides. The second type of experiments is to demonstrate the feasibility of Raman spectroscopy down to the single molecule level. Here we rely on the phenomenon of surface enhanced Raman scattering by using Ag tip and Ag sample. In the Raman experiment, an external laser light irradiates the tunneling junction. This arrangement can be extended to the use of femtosecond lasers, thus providing an opportunity to reach the limits of both the spatial and temporal resolutions. The third optical experiment with the STM relies on the use of a radio frequency (RF) signal to drive the bias between the tip and the sample. This provides a way to induce HOMO-LUMO electronic transition in a single molecule that relaxes by photon emission. The highest spatial resolution is expected to come from the light emission induced by tunneling electrons, i.e. sub-Å. Single molecule resolution is achieved in the Raman and femtosecond experiments through low coverages of adsorbed molecules.

Publications

[1] T. Yamanaka, A. Hellman, S. Gao, and W. Ho, "*State-Resolved Femtosecond Two-Pulse Correlation Measurements of NO Photodesorption from Pt(111)*", Surf. Sci. **514**, 404-408 (2002)

[2] X. Qiu, G.V. Nazin, A. Hotzel, and W. Ho, "*Manipulation and Characterization of Xenon-Metalloporphyrin Complexation with a Scanning Tunneling Microscope*", J. Am. Chem. Soc. **124**, 14804-14809 (2002).

[3] N. Nilius, T.M. Wallis, and W. Ho, "*Vibrational Spectroscopy and Imaging of Single Molecules: Bonding of CO to Single Palladium Atoms on NiAl(110)*", J. Chem. Phys. **117**, 10947-10952 (2002).
[4] W. Ho, "*Single Molecule Chemistry*", an invited review paper, J. Chem. Phys. **117**, 11033-11061 (2002).
[5] X.H. Qiu, G.V. Nazin, and W. Ho, "*Vibrationally Resolved Fluorescence Excited with Submolecular Precision*", Science **299**, 542-546 (2003).
*** "*Lighting Up Single Molecules*", Physics World **16**, 3 (2003).
*** "*Imaging Fluorescence with Submolecular Precision*", Micro/Nano **8**, 6 (2003).
*** News Item, "*Tunneling Electrons Stimulate Individual Molecules*", D.S. Burgess, Photonics Spectra, March 2003, p. 34.
[6] N. Nilius, T.M. Wallis, and W. Ho, "*Influence of a Heterogeneous Al_2O_3 Surface on the Electronic Properties of Single Pd Atoms*", Phys. Rev. Lett. **90**, 046808 (2003).
*** Figure from paper appeared on cover of this issue of Phys. Rev. Lett.
[7] G.V. Nazin, X.H. Qiu, and W. Ho, "*Atomic Engineering of Photon Emission with a Scanning Tunneling Microscope*", Phys. Rev. Lett. **90**, 216110 (2003).
[8] G.V. Nazin, X.H. Qiu, and W. Ho, "*Visualization and Spectroscopy of a Metal-Molecule-Metal Bridge*", Science **302**, 77-81 (2003). Published online 4 September 2003; 10.1126/science.1088971.
*** Perspectives, "*How to Assemble a Molecular Junction*", A.C. Kummel, Science **302**, 69 (2003).
*** La Chronologie 2003 de La Recherche, "*Pont Moléculaire*", La Recherche, Janvier 2004, p. 40.
*** Nanoelectronics, "*Irvine Team Images Single-Molecule Junction*", R. Alexander, Business Communications Company Electronic Materials Update, October 2003.
*** News of the Week, "*Molecular Electronics, Seeing is Believing, STM technique lets single-molecule junction be prepared and imaged*", Mitch Jacoby, Chemical & Engineering News, September 8, 2003, p. 16.
[9] S. Gao, J.R. Hahn, and W. Ho, "*Adsorption Induced Hydrogen Bonding by CH Group*", J. Chem. Phys. **119**, 6232-6236 (2003).
[10] C. Silien, N.A. Pradhan, W. Ho, and P.A. Thiry, "*Influence of Adsorbate-Substrate Interaction on the Local Electronic Structure of C_{60} Studied by Low-Temperature STM*", Phys. Rev. B **69**, 115434 (2004).
[11] X.H. Qiu, G.V. Nazin, and W. Ho, "*Vibronic States in Single Molecule Electron Transport*", Phys. Rev. Lett. **92**, 206102 (2004).
[12] N. Liu, N.A. Pradhan, and W. Ho, *"Vibronic States in Single Molecules: C_{60} and C_{70} on Ultrathin Al_2O_3 Films"*, J. Chem. Phys. **120**, 11371-11375 (2004).

Molecular Theory & Modeling

Development of Statistical Mechanical Techniques for Complex Condensed-Phase Systems

Gregory K. Schenter
Chemical Sciences Division
Pacific Northwest National Laboratory
902 Battelle Blvd.
Mail Stop K1-83
Richland, WA 99352
greg.schenter@pnl.gov

The long-term objective of this project is to advance the understanding of the relation between detailed descriptions of molecular interaction and the prediction and characterization of macroscopic collective properties. To do this, we seek to better understand the relation between the form and representation of intermolecular interaction potentials and simulation techniques required for statistical mechanical determination of properties of interest. Molecular simulation has the promise to provide insight and predictive capability of complex physical and chemical processes in condensed phases and interfaces. For example, the transport and reactivity of species in aqueous solutions, at designed surfaces, in clusters and in nanostructured materials play significant roles in a wide variety of problems important to the Department of Energy.

We start from the premise that a detailed understanding of the intermolecular interactions of a small collection of molecules, through appropriate modeling and statistical analysis, will enable us to understand the collective behavior and response of a macroscopic system, thus allowing us to predict and characterize thermodynamic, kinetic, material, and electrical properties. Our goal is to improve understanding at the molecular level in order to address increasingly more complex systems ranging from homogeneous bulk systems to multiple phase or inhomogeneous ones, to systems with external constraints or forces. Accomplishing this goal requires understanding and characterization of the limitations and uncertainties in the results, thereby improving confidence in the ability to predict behavior as systems become more complex.

A specific focus of the current work is to take advantage of electronic structure methods of established reliability. We seek to establish efficient and practical representations of the Born-Oppenheimer (BO) potential energy as a function of atomic nuclear positions. Although this in itself is a challenging task and a useful intermediate result, it is often not practical for the simulation of thermodynamic and dynamic properties of collections of molecules since its use can require quantum statistical mechanical simulation using Feynman path integral methods. This becomes increasingly important in aqueous systems where high frequency anharmonic vibrations are strongly dependent on the collective system environment or when light masses such as hydrogen are involved. An ongoing challenge of the current effort is to establish a well-defined and systematically improvable relation between the Born-Oppenheimer atomic potential (flexible molecules) to be used in quantum statistical mechanical simulation and a simplified, rigid molecule representation of an effective potential to be used in classical statistical mechanical simulation. We require that the observables obtained from a full quantum statistical mechanical simulation of flexible molecules to be reproduced from classical statistical mechanical simulation of the effective rigid molecule potential.

A concrete example of the relation between an effective rigid classical potential and the Born-Oppenheimer potential, and the systematic characterization of quantum mechanical effects, was provided by an analysis of the second virial coefficient of water [2], which is well characterized by experiment. In this study, an effective potential was obtained such that classical simulation with the effective potential reproduced the quantum mechanical simulations on the BO potential. At a temperature of 300K, there is a 0.3 kcal/mol difference between the minima of the BO and the effective potentials. This difference between the BO and effective potentials was studied for clusters using rigid-body models and PES derived from electronic structure calculations.

In the Figure 1 we show the minimum energy, E_e, as a function of water cluster size, n, which shows a shift between the results for the Dang-Chang model, which was parameterized so that classical simulations reproduce experimental observables, and the TTM2-F model, which was fitted to the BO potential. Comparing the average energy of the clusters for the Dang Chang and TTM2-F models we see agreement when statistical mechanical estimates is used for the classically derived potential and quantum statistical mechanical estimates for the potential derived from electronic structure calculations. It is interesting that the TIP4P model, which is a classically derived potential, agrees better with the TTM2-F model for the minimum energies and that quantum simulation is needed to provide good agreement with the TTM2-F average energies. The current work is a preliminary harmonic analysis. In the future, we propose to carry out full anharmonic sampling to obtain relevant thermodynamic observable properties.

In developing interaction potentials, more direct information from experiment is desired. Towards these ends, we have studied the EXAFS spectra of dilute solutions of Ca^{2+} and Sr^{2+} in water and methanol [10]. Using classical MD techniques and polarizable potential models, we provided a detailed study of the solvation structure of dilute Ca^{2+} and Sr^{2+}-water solutions and also Ca^{2+}-methanol solution. Ca^{2+} and Sr^{2+} were chosen because of their important in many biological processes and environmental problems, respectively. We developed a set of polarizable ion-solvent interactions that accurately describes the hydration enthalpy, the coordination numbers and the peak locations of the ion-solvent radial distribution functions. Simulated MD EXAFS spectra were found to be in good agreement with corresponding

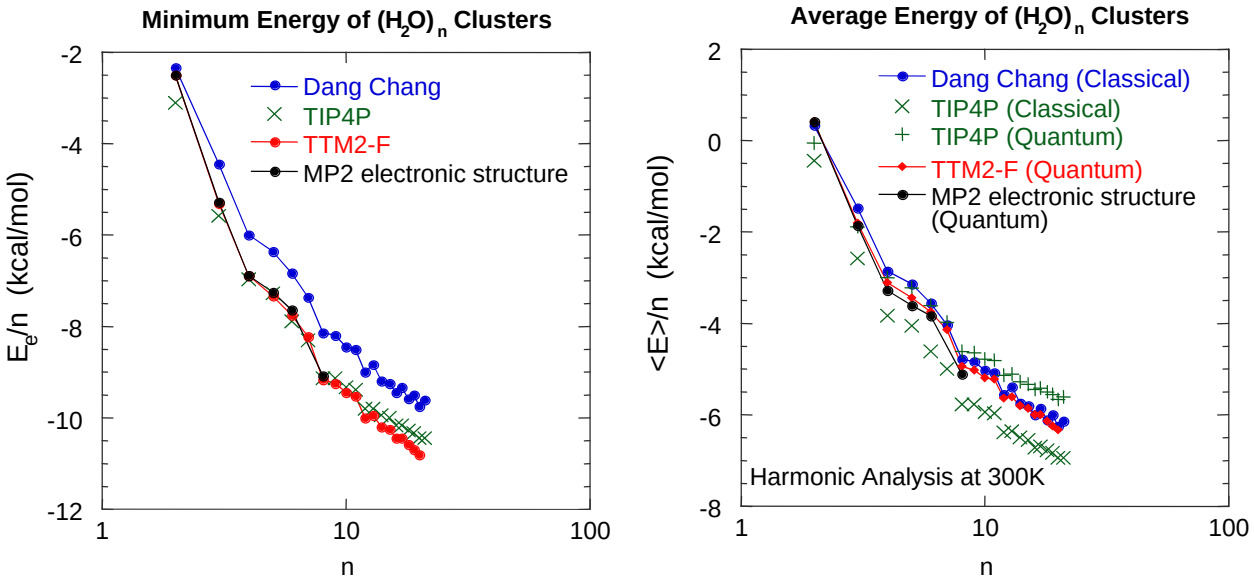

Figure 1. Comparison of the minimum energy and average energy as a function of cluster size.

experimental measurements. The use of a polarizable potential model in the MD simulations of EXAFS spectra is a significant advance over previous EXAFS simulations using pair potentials because the interactions between the ions and the media can be described more accurately and the solvent molecules can respond to the electric fields created by their environments in a very realistic way. Comparisons of results using pairwise additive and polarizable potentials show that polarization effects do not significantly alter the EXAFS spectra. However, these studies did show more subtle differences between the experimental and theoretical structure of the ion-water interactions in solution that present a challenge to current empirical models.

The free energy is a fundamental property of water clusters that is useful in understanding the population and rate of formation of various size clusters. We have developed a definition of cluster free energies that is consistent with gas-to-particle nucleation and have built systematic procedures that relate the details of molecular interaction to the nucleation rate [3,4,12,14]. This approach has been applied to water clusters to gain an understanding of the population of water clusters in the atmosphere [1,5] and to understand the dynamics of water nucleation. More significantly, we have characterized the sensitivity of the observed nucleation rate to the details of the interaction potential, which allows us to take into account the effects of impurities in the system on nucleation. The development of a consistent theory of the nucleation process based upon variational transition state theory for evaporation rates and building procedures for accounting for dynamical corrections was essential to accomplishing this connection between molecular interaction and the macroscopic process nucleation.

In an effort to develop more robust representations of intermolecular interaction, we are exploring the use of semiempirical self-consistent field (SCF) methods. Neglect of differential diatomic overlap (NDDO) methods that include such parameterizations as MNDO, AM1, and PM3, have the ability to treat the formation and breaking of chemical bonds, but have been found to poorly describe hydrogen bonding and weak electrostatic complexes. In contrast, most empirical potentials are not able to describe bond-breaking and formation, but have the ability to add missing elements of hydrogen bonding using classical electrostatic interactions. We have developed a new method that combines aspects of both NDDO-based SCF techniques and classical descriptions of polarization to describe the diffuse nature of the electronic wavefunction in a self-consistent manner. We have developed the self-consistent polarization NDDO (SCP-NDDO) theory with the additional description of molecular dispersion developed as a second-order perturbation theory expression. Initial efforts using this approach have allowed us to parameterize the model to reproduce the accurate MP2/CBS estimates of small water cluster binding energies of Xantheas *et al*, as well as the intramolecular frequency shifts as a function of cluster size. Initial steps have been made to parameterize protonated and hydroxide water clusters. Future efforts will extend the parameterization to aqueous solvation of more complex ions.

Collaborators on this project include B. C. Garrett, S. M. Kathmann, S. S. Xantheas, and L. X. Dang, and D. T. Chang.

References to publications of DOE sponsored research (2002-present)

1. G. K. Schenter, S. M. Kathmann, and B. C. Garrett, "Equilibrium Constant for Water Dimerization: Analysis of the Partition Function for a Weakly Bound System," *Journal of Physical Chemistry* A **106**, 1557-1566 (2002).
2. G. K. Schenter, "The development of effective classical potentials and the quantum statistical mechanical second virial coefficient of water," *Journal of Chemical Physics* **117**, 6573-6581 (2002).
3. S. M. Kathmann, G. K. Schenter, and B. C. Garrett, Understanding the Sensitivity of Nucleation Kinetics: A Case Study on Water," *Journal of Chemical Physics* **116**, 5046-5057 (2002).
4. G. K. Schenter, S. M. Kathmann, and B. C. Garrett, "Dynamical Benchmarks of the Nucleation Kinetics of Water," *Journal of Chemical Physics* **116**, 4275-4280 (2002).
5. B. C. Garrett, S. M. Kathmann, and G. K. Schenter, "Thermochemistry and Kinetics of Small Water Clusters," in Water in Confining Geometries, edited by V. Buch and J. P. Devlin, (Springer-Verlag, New York, 2003) p. 25.
6. Y. D. Suh, G. K. Schenter, L. Zhu, and H. P. Lu, "Probing nanoscale surface enhanced Raman-scattering fluctuation dynamics using correlated AFM and confocal ultramicroscopy," *Ultramicroscopy* **97**, 89-102 (2003).
7. L. Zhu, G. K. Schenter, M. Micic, Y. D. Suh, N. Klymyshyn, and H. P. Lu, "Nanosurface-enhanced Raman scattering fluctuation dynamics," in *Proceedings of SPIE,* **4962**, "Manipulation and Analysis of Biomolecules, Cells, and Tissues," edited by D. V. Nicolau, J. Enderlein, R. C. Leif, and D. L. Farkas, (SPIE, Bellingham, WA, 2003) p. 70.
8. M. Dupuis, G. K. Schenter, B. C. Garrett, and E. E. Arcia, "Potentials of mean force with ab initio mixed Hamiltonian models of solvation," *Journal of Molecular Structure (THEOCHEM)* **632**, 173 (2003).
9. G. K. Schenter, B. C. Garrett, and D. G. Truhlar, "Generalized transition state theory in terms of the potential of mean force," *Journal of Chemical Physics* **119**, 5828-5833 (2003).
10. L. X. Dang, G. K. Schenter and J. Fulton, "EXAFS spectra of the dilute solutions of Ca^{2+} and Sr^{2+} in water and methanol," *Journal of Physical Chemistry B* **107**, 14119 (2003).
11. M. P. Hodges, R. J. Wheatley, G. K. Schenter, and A. H. Harvey, "Intermolecular potential and second virial coefficient of the water-hydrogen complex," *Journal of Chemical Physics* **120**, 710 (2004).
12. S. M. Kathmann, G. K. Schenter, and B. C. Garrett, "Multicomponent dynamical nucleation theory and sensitivity analysis," *Journal of Chemical Physics* **120**, 9133-9141 (2004).
13. J. L. Daschbach, G. K. Schenter, P. Ayotte, R. S. Smith, and B. D. Kay, "Helium diffusion through H_2O and D_2O amorphous ice: Observation of a lattice inverse isotope effect," *Physical Review Letters* **92**, 198306 (2004).
14. S. M. Kathmann, G. K. Schenter, and B. C. Garrett, "Dynamical Nucleation Theory: Understanding the Role of Aqueous Contaminants," in Proceedings of the 16th International Conference on Nucleation and Atmospheric Aerosols, edited by M. Kulmala and M. Kasahara (Kyoto University Press, 2004), p. 243-246.

Clusters: Unraveling Fundamental Oxygen-Transfer Reaction Mechanisms Effected by Heterogeneous Catalysts

A. W. Castleman, Jr.
Penn State University
Departments of Chemistry and Physics
104 Chemistry Building
University Park, PA 16802
awc@psu.edu

Program Scope:

Catalysis functions as one of the cornerstones of industrial societies, and in the context of DOE interests, plays a major role in energy production and usage. The impact of being able to tailor the design of catalysts which possess high degrees of selectivity as well as large turnover rates for specifically chosen reactions cannot be over stated. Acquiring this capability is a long term goal. Our program is directed toward unraveling fundamental mechanisms of oxygen transfer reactions that involve materials known to function as viable heterogeneous catalysts at the bulk scale. The emphasis is on basic studies that serve to elucidate the influence of stoichiometry, oxidation and charge states, size, identify reactive sites that play an important role in effecting several classes of reactions. Particular attention is being focused on systems that are potentially significant for converting alternative fuels to more useful forms and identifying mechanisms of reactions that may serve in pollutant abatement.

The prospective use of nanoscale clusters as catalytic materials is arousing interest in the fields of chemistry and physics, prompted especially by findings that there are often significant differences in the reactivities of small particles compared to bulk catalysts of similar composition. It is recognized that comparing the chemistry of neutral and ionic clusters with reactions that occur on condensed phase catalysts is of great value in providing the basis for understanding this size dependent behavior. Valuable new information, including the identification of reaction sites for guidance in tailoring the design of catalysts, can be garnered from such comparisons. In this context, both transition metal oxides and noble metal particles are receiving increased attention as potentially useful catalysts in a wide range of applications and are the subjects of our investigations.

Recent Progress:

During the recent grant period, major attention has been devoted to studies of oxygen-transfer reactions involving several classes of molecules that are important in combustion, either as fuels, intermediates, or products whose abatement will reduce levels of pollution emanating from processes associated with energy production. Work has been undertaken on systems whose behavior in the condensed state has revealed promise as viable catalysts. In this regard, transition metal oxides comprised of vanadium, niobium, and tantalum, and initial studies of oxide clusters of gold have received particular attention.

Considerable progress has been made in identifying the mechanisms and determining the energetics of selected reactions as influenced by stoichiometry, oxidation and charge states, and size, providing an identification of reactive sites that play an important role in effecting selected classes of reactions. Reactivities of selected organic molecules used in

energy production including ones that show promise as alternative fuels, and on reactions of the products of combustion such as CO and SO_2, with studies directed to identifying mechanisms of reactions that may serve in pollutant abatement have been elucidated. Recent studies on *single metal* containing transition metal oxides comprised of vanadium, niobium, and tantalum, and beginning studies of oxide clusters of gold, have received particular attention. Findings from our laboratory have provided new insight into the role of stoichiometry for selected cationic systems, particularly for mechanisms including dehydration, dehydrogenation, oxygen-transfer, and cracking reactions involving cationic species. Work was also undertaken on related anionic species to elucidate the roles of the charge state and electronic characteristics on catalytic behavior and effectiveness. In general, except for the gold cluster systems, anions were found to be far less effective, a fact which along with other results points to the influence of electron density at the reaction site.

During the recent grant period we uncovered a number of examples demonstrating the connection between the study of cluster reactions in the gas phase and those which are operative in the case of conventional heterogeneous catalysis. In particular, in a number of cases we have found cluster size/stoichiometry specific reactions that are identical to those in industrial processes, and moreover we have been able to identify the important reactive centers responsible for the transfer reactions. In fact, in each case where evidence pointed to a particularly likely candidate from condensed phase measurements, the same sites and mechanisms have been revealed from the gas phase cluster investigations. For example, in related studies we have identified that the well-known conversion of ethylene to acetaldehyde over vanadium oxide catalysts occurs solely in reaction centers of V_2O_5 and V_4O_{10}, just as suspected from bulk phase catalytic investigations. In a similar manner, we have identified other reaction centers for phosgene production in the case of heterogeneous oxygen transfer reactions to CCl_4, and in the case of the formation of dimethyl ether and formaldehyde from methanol. Importantly, we have also noted differences between reactions effected by vanadium oxides compared to niobium and tantalum oxides, again in agreement with what has been observed in bulk catalytic systems. We are very encouraged by these findings in that they further establish the value of cluster studies in offering the possibility of investigating species of widely varying oxidation states, charge states, and stoichiometries that are difficult to individually assess on surfaces.

As a prelude to future experiments, we also devoted some effort to unraveling some aspects of the photochemistry of sulfur dioxide. In addition, we have given further attention to developing the Coulomb explosion technique which we devised as a unique method for arresting intermediates in fast reactions and for investigating the kinetics and mechanisms of fast reactions.

Future Plans:

The continuing program will focus on understanding the role of catalyst–support and binary catalyst interactions. Particular attention will be directed to unraveling the role of electronegativities and electronic density of states in affecting the process of oxygen transfer, which is so important in alternative fuel usage, pollution abatement, and general combustion chemistry. Such studies offer the prospect of gaining considerable new insights into the basis of catalytic activity. Numerous systems among transition metal oxides warrant study and we are engaged in investigations of both selected classes of transition metal oxides and several metal clusters to unravel the principles governing their catalytic effectiveness. The main focus is on using model catalytic systems to investigate reaction mechanisms and determine

the energetics and rates of individual steps involved in their interactions with molecules important in the field of combustion.

The continuing program is to be comprised of several phases; the first will entail investigations to provide quantitative data on the reaction rates, reaction cross sections, and bonding of important complexes and species identified in the work thus far. We intend to deduce the thermochemistry of product species bound to the clusters. In combination with mass analysis, collision induced dissociation experiments will also assist in product identification. In another phase of the proposed work, attention will be focused on identifying the role of binary catalytic systems, including the role of support materials, with the studies directed to the problem of pollution abatement, such as CO, SO_2, NO, and NO_2. In a similar way, the third phase of the program will be devoted to the study of oxidation mechanisms of molecules that find use as alternative sources of energy such as methanol, ethanol, and hydrogen. Quantitative measurements will be made of the kinetics of interaction of specifically chosen molecules with the selected cluster systems. Thereby, valuable information about reaction intermediates, reaction mechanisms, and the relationship between cluster structure and reactivity will be derived. These studies will encompass investigations of early transition metals such as vanadium, niobium, and tantalum oxide clusters, as well as those of nickel and molybdenum in various combinations with each other. To further unravel the role of electron density, additives such as Mg and Na will also be employed in the studies. Our work on oxidized gold clusters will comprise binary systems with Ag, Mg, and Na as compositional components. These studies will provide insight into the role of electronegativity differences of the composite clusters. The implementation of both the guided ion beam and fast flow reactor techniques will enable the quantification of the reaction kinetics, their energetics, and a detailed examination of the reaction products formed. Ultimately, comparison of these results with condensed phase reactions will lead to a better understanding of the interaction of reactant species with the active sites of catalytic surfaces.

References:

527. "Calculation to Determine the Mass of Daughter Ions in Metastable Decay," J. R. Stairs, T. E. Dermota, E. S. Wisniewski, and A. W. Castleman, Jr., *Int. J. Mass Spectrom*. **213**, 81 (2002).

530. "NH_3 Adsorption Around Ni_n ($n \leq 4$) Clusters," B. Chen, A. W. Castleman, Jr., C. Ashman, and S. N. Khanna, *Int. J. Mass Spectrom*. **220/2**, 171 (2002).

532. "Studies of Metal Oxide Clusters: Elucidating Reactive Sites Responsible for the Activity of Transition Metal Oxide Catalysts," (invited feature article) K. A. Zemski, D. R. Justes, and A. W. Castleman, Jr., *J. Phys. Chem. B* **106**, 6136 (2002).

534. "Dynamics of Gas Phase Clusters: Insights into Size and Solvation Effects on Electronic Relaxation and Hydrogen Transfer," E. S. Wisniewski, B. D. Leskiw, S. M. Hurley, T. E. Dermota, D. P. Hydutsky, K. L. Knappenberger, Jr., M. A. Hershberger, and A. W. Castleman, Jr., In *Femtochemistry and Femtobiology: Ultrafast Dynamics in Molecular Science* (A. Douhal and J. Santamaria, Eds.) World Scientific: Singapore, New Jersey, London, 21-41 (2002).

537. "Solvation Effects on Electronic Excited States of Methanol: A Study of Neat and Mixed Methanol/Water Clusters," E. S. Wisniewski, M. A. Hershberger, and A. W. Castleman, Jr., *J. Chem. Phys.* **116**, 5738 (2002).

538. "Cluster Dynamics: Influences of Solvation and Aggregation," Q. Zhong and A. W. Castleman, Jr., *Quantum Phenomena in Clusters and Nanostructures* (S. N. Khanna and A. W. Castleman, Jr., Eds.) Springer: Berlin, Heidelberg, New York, Hong Kong, London, Milan, Paris, Tokyo, (2003).

540. "Femtosecond Photodissociation Dynamics of Excited State SO_2," E. S. Wisniewski and A. W. Castleman, Jr., *J. Phys. Chem. A* (R. S. Berry Issue) **106**,10843 (2002).

544. "Comparison of Methyl and Hydroxyl Protons Generated in a Coulomb Explosion Event: Application of a Time-of-Flight Gating Technique to Methanol Clusters," E. S. Wisniewski and A. W. Castleman, Jr., special issue of *Int. J. Mass Spectrom.* devoted to Gaseous Ion Thermochemistry and Solvation **227**, 577 (2003).

551. "$V_2O_5^+$ Reactions with C_2H_4 and C_2H_6: Theoretical Considerations of Experimental Findings," D. R. Justes, A. W. Castleman, Jr., R. Mitrić, and V. Bonačić-Koutecký, *Eur. Phys. J. D* **24**, 331 (2003).

559. "Photodissociation of Sulfur Dioxide: The $\tilde{E}$ State Revisited," K. L. Knappenberger and A. W. Castleman, Jr., *J. Phys. Chem.A*, **108**, 9-14 (2004).

560. "Probing the Dynamics of Ionization Processes in Clusters", A. W. Castleman, Jr. and T. E. Dermota, Proceedings ISACC 2003 Conference, *World Scientif*ic (in press).

561. "Ultrafast dynamics in cluster systems", T. E. Dermota, Q. Zhong, and A. W. Castleman, Jr., *Chemical Reviews*, **104**, 1861-1886 (2004)

563. "Reactivity of Atomic Gold Anions Toward Oxygen and the Oxidation of CO: Experiment and Theory," M. L. Kimble, A. W. Castleman, Jr., R. Mitrić, C. Bürgel, and V. Bonačić-Koutecký, *J. Am. Chem. Soc.*, **126**, 2526-2535 (2004).

564. "Probing the Oxidation of Carbon Monoxide Utilizing Au_n^-," M. L. Kimble and A. W. Castleman, Jr., *Proceedings of Gold 2003: New Industrial Applications for Gold Conference* Vancouver, Canada, September 28 – October 1, 2003.

565. "Gas phase Studies of Au_n^+ for the Oxidation of Carbon Monoxide," M. L. Kimble and A. W. Castleman, Jr., Special Issue of the *Int. J. Mass Spectrom.*, in Honor of Professor Tilmann D. Märk. **233**, 99-101 (2004).

568. "Reactions of Vanadium and Niobium Oxides with Methanol," D. R. Justes, N. A. Moore, and A. W. Castleman, Jr., *J. Phys. Chem. B*, **108**, 3855-3862 (2004).

570. "Elucidating Mechanistic Details of Catalytic Reactions Utilizing Gas Phase Clusters," M. L. Kimble, D. R. Justes, N. A. Moore, and A. W. Castleman, Jr., *Proceedings of the International Symposium on Clusters and Nano-Assemblies: Physical and Biological Systems* Richmond, VA (2003) (in press).

572. "The Influence of Cluster Formation on the Photodissociation of Sulfur Dioxide: Excitation to the E State", K. L. Knappenberger, Jr., and A. W. Castleman, Jr., *J. Chem. Phys*., **121**, 3540-3549 (2004).

573. "A Kinetic Analysis of the Reaction between $(V_2O_5)n=1,2^+$ and Ethylene", D. R. Justes, R. Mitrić, N. A. Moore, V. Bonačić-Koutecký, and A. W. Castleman, Jr., *J. Chem. Phys*., (submitted).

575. "Joint Experimental and Theoretical Investigations of the Reactivity of $Au_2O_n^-$ and $Au_3O_n^-$ with Carbon Monoxide", Michele L. Kimble, A. Welford Castleman, Jr., Christian Bürgelb, Roland Mitrićb, and Vlasta Bonačić-Koutecký, *Journal of the American Chemical Society* (submitted).

Vibrational Spectroscopy at Metal Cluster Surfaces

DE-FG02-96ER14658

Michael A. Duncan

Department of Chemistry, University of Georgia, Athens, GA 30602-2556

maduncan@uga.edu

Program Scope

The focus of our research program is the study of gas phase metal clusters to evaluate their potential as models for the fundamental interactions present on heterogeneous catalytic surfaces. These clusters are molecular sized aggregates of metals or metal compounds (oxides, carbides). We focus specifically on the bonding exhibited by "physisorption" on cluster surfaces. Complexes containing one or more metal atoms bound to small molecules provide the models for physisorption. Infrared spectroscopy in various forms is employed to measure the vibrational spectroscopy of the metal clusters themselves and, in particular, the spectra of physisorbed molecules. These studies investigate the nature of the metal-adsorbate interaction and how it varies with metal composition and cluster size. The vibrational frequencies measured are compared with the predictions of theory to reveal the electronic state and geometric structure of the system. Neutral clusters are studied with infrared multiphoton ionization spectroscopy, while ionic clusters are studied with mass-selected infrared photodissociation spectroscopy.

Recent Progress

The main focus of our work over the last two years has been infrared spectroscopy of mass-selected cation-molecular complexes, e.g., $Fe^+(CO_2)_n$, $V^+(C_2H_2)_n$, $Ni^+(H_2O)_n$, $Nb^+(N_2)_n$. These species are produced by laser vaporization in a pulsed-nozzle cluster source, mass-selected with a specially designed reflectron time-of-flight mass spectrometer and studied with infrared photodissociation spectroscopy using an IR optical parametric oscillator laser system (IR-OPO; wavelength coverage: 2000-4500 cm^{-1}). We have studied the infrared spectroscopy of various transition metal ions in complexes with CO_2, acetylene, water and molecular nitrogen. In each system, we examine the shift in the frequency for selected vibrational modes in the adsorbate molecule that occur upon binding to the metal. The number and frequencies of IR-active modes in multi-ligand complexes reveals the structures of these systems, while sudden changes in vibrational spectra or IR dissociation yields are used to determine the coordination number for the metal ion in these complexes. In some systems, new vibrational bands are found beginning at a certain complex size that correspond to intra-cluster reaction products. In small complexes with strong bonding, we use the method of "rare gas tagging" with argon or neon to enhance dissociation yields. In all of these systems, we employ a close interaction with theory to investigate the details of the metal-molecular interactions that best explain the spectroscopy data obtained. We perform our own density functional theory (DFT) or MP2 calculations (using Gaussian 03W) and when higher level methods are required (e.g., CCSD), we collaborate with local theorists (P.v.R. Schleyer, H.F.

Schaefer). Our infrared data on these transition metal ion-molecule complexes is the first available, and it provides many examples of unanticipated structural and dynamic information.

Studies of metal-CO_2 clusters have investigated Fe^+, Ni^+ and V^+ metal ions with from one up to 10-14 CO_2 ligands attached. In all of these systems, the CO_2 asymmetric stretch (2349 cm^{-1} in the isolated molecule) is studied and found to shift 30-50 cm^{-1} to higher frequency when the ligand is attached directly to the metal. Ligands are found to bind in a linear configuration with the metal, i.e., M^+-OCO, with high symmetry configurations for multiple ligands. When external ligands are present, a second band is measured at 2350 cm^{-1}. Its proximity to the isolated molecule band establishes that this represents molecules bound externally on the surface of the cluster that experience only a small perturbation. In the iron system, the coordination number is not clearly evident from the onset of the surface band, but this appears gradually in the n=4-6 size range. For nickel and vanadium, however, the surface band appears sharply at a cluster size of n=5, and this is also the cluster size at which the overall dissociation yield abruptly increases. The coordination in these systems is therefore four ligands. In both vanadium and nickel clusters with CO_2, another new vibrational band strongly shifted further to the blue emerges at much larger cluster sizes in the n=8-10 size range. This is assigned as a CO_2 ligand bound to a metal *oxide* core ion of the form $MO^+(CO)$, i.e., an oxide carbonyl species that results from an intracluster oxidation reaction.

$M^+(C_2H_2)_n$ clusters have been studied for the metals nickel and cobalt in the region of the symmetric and asymmetric stretching modes of acetylene. Although the symmetric stretch is not IR active for the isolated molecule, distortion of the ligand in these complexes induces IR activity for this mode. The C-H stretches in these systems are shifted to the red by 30-50 cm^{-1} from the corresponding modes in the isolated acetylene molecule, consistent with predictions for π-complexes. Coordination numbers are established as four acetylenes for nickel and three for cobalt. New vibrational bands emerge that are shifted even further to the red, but these are only seen after the coordination is exceeded by one ligand. These bands are assigned to the presence of a cyclobutadiene ligand that results from an intracluster cyclization reaction. Prof. P.v.R. Schleyer has collaborated with us on the theory of these systems. Small complexes with acetylene have also been studied for vanadium and iron.

$M^+(H_2O)_n$ complexes and those tagged with argon have been studied for iron, nickel and vanadium complexes. In the vanadium system, partial rotationally resolved spectra have been obtained. In the iron system, complexes with one or two water molecules (argon tagged) exhibit isomeric structures for both argon and water binding sites. Nickel complexes have been studied for up to 30 water molecules, providing a detailed probe of the dynamics of solvation. Hydrogen bonded structures appear for the first time at a cluster size of n=4-5, and the free-OH symmetric stretch disappears at n=8 indicating that most external water molecules are bound within a hydrogen bonding network after this size. The IR signature that we have recently identified for clathrate structures in protonated water clusters, $H^+(H_2O)_n$, is a single peak for the free-OH asymmetric stretch, but this signature is not found for the $Ni^+(H_2O)_n$ complexes.

$M^+(N_2)_n$ complexes have been studied in the N-N stretch region for Fe^+, V^+ and Nb^+ complexes. Again, binding to metal makes this mode IR active even though it is forbidden in the isolated molecule. The N-N stretch is red shifted for these metals, and coordination numbers are usually six for these complexes. Theory shows that most metals prefer end-on binding configurations, but some (e.g., cobalt) prefer to bind side-on as in a π-complex.

Future Plans

Future plans for this work include the extension of these IR spectroscopy studies to more ligands, to complexes with multiple metal atoms and to a more extended region of the IR spectrum. In the vanadium-water system, we have already measured spectra in the water bending mode region for complexes containing up to 15 metal atoms, using a free electron laser. This work establishes the feasibility of studies on larger metal systems. We want to study more reactive metals with hydrocarbons such as ethylene or methane that might produce carbenes, vinylidene or ethylidyne species. These systems should exhibit characteristic IR spectra, and will allow us to make better contact with IR spectroscopy on metal surfaces. Studies of carbon monoxide have been limited so far because the tuning range of our present laser system only extends down to 2000 cm^{-1}. However, new crystals have just become available (silver-gallium-selenide) to extend the range of OPO systems like ours down to the 1000-2000 cm^{-1} range. We hope to obtain one of these crystals soon, which would then allow us to study ligands like CO and to probe other adsorbate molecules in additional vibrational modes (C-C stretch of acetylene, water bending mode, etc.).

In all of these studies, we have focused on the qualitative effects of metal-adsorbate interactions and trends for different transition metals interacting with the same ligand. Our collaboration with theory has revealed that density functional theory has serious limitations for these metal-ligand complexes that were not previously recognized. This is particularly evident in metals such as vanadium and iron, where two spin states of the metal lie at low energy. DFT has difficulty identifying the correct relative energies of these spin states. Further examinations of this issue are planned, as it has significant consequences for the applications of DFT.

Publications (2002-2004) for this Project

1. D. van Heijnsbergen, G. von Helden, G. Meijer and M.A. Duncan "IR-REMPI Spectroscopy of Magnesium Oxide Clusters," *J. Chem. Phys. A* **116**, 2400 (2002).

2. G. Gregoire and M.A. Duncan, "Infrared Spectroscopy to Probe Structure and Growth Dynamics in Fe^+-$(CO_2)_n$ Complexes," *J. Chem. Phys.* **117**, 2120 (2002).

3. R.S. Walters, T. Jaeger and M.A. Duncan, "Infrared Spectroscopy of Ni^+-$(C_2H_2)_n$ Complexes: Evidence for Intracluster Cyclization Reactions," *J. Phys. Chem. A* **106**, 10482 (2002).

4. M.A. Duncan, "Infrared Spectroscopy to Probe Structure and Dynamics in Metal Ion-Molecule Complexes," *Intl. Rev. Phys. Chem.* **22**, 407 (2003).

5. N.R. Walker, G.A. Grieves, R.S. Walters and M.A. Duncan, "The Metal Coordination in $Ni^+(CO_2)_n$ and $NiO_2^+(CO_2)_m$ Complexes," *Chem. Phys. Lett.* **380**, 230 (2003).

6. R.S. Walters, N.R. Walker, D. Pillai and M.A. Duncan, "Infrared Spectroscopy of $V^+(H_2O)$ and $V^+(D_2O)$ Complexes: Ligand Deformation and an Incipient Reaction," *J. Chem. Phys.* **119**, 10471 (2003).

7. N.R. Walker, R.S. Walters and M.A. Duncan, "Infrared Photodissociation Spectroscopy of $V^+(CO_2)_n$ and $V^+(CO_2)_nAr$ Complexes," *J. Chem. Phys.* **120**, 10037 (2004).

8. T.D. Jaeger, A. Fielicke, G. von Helden, G. Meijer and M.A. Duncan, "Infrared Spectroscopy of Water Adsorption on Vanadium Cluster Cations (V_x^+; x=3-15)," *Chem. Phys. Lett.* **392**, 409 (2004).

9. R.S. Walters and M.A. Duncan, "Infrared Spectroscopy of Solvation and Isomers in $Fe^+(H_2O)_{1,2}Ar_m$ Complexes," *Austr. J. Chem.*, in press.

10. N.R. Walker, G.A. Grieves, R.S. Walters and M.A. Duncan, "Growth Dynamics and Intracluster Reactions in $Ni^+(CO_2)_n$ Complexes via Infrared Spectroscopy," *J. Chem. Phys.*, in press.

Computational Electron Spectroscopy – A Powerful Tool for Studies of Size-, Structure-, Charge State-, and Composition-Specific Properties of Finite Systems

Julius Jellinek

Chemistry Division, Argonne National Laboratory, Argonne, Illinois, 60439
jellinek@anl.gov

Program Scope

Electronic characteristics, such as spectra of electron binding energies, are among the most fundamental properties of physical systems be they atoms, molecules, clusters, or extended systems. Accurate knowledge of the electronic energy levels and the electronic density of states is essential as they define many other physical and chemical properties. The goal of this program is to develop a new general, rigorous, accurate, and efficient theoretical/computational methodology for characterization of electronic energy spectra and to apply it to study fundamental properties of atomic clusters. The work involves conceptual developments and large-scale computations. The focus is on one- and multi-component atomic clusters of metallic elements. We study the correlation between the electronic properties and the size, structure, charge state, and composition of these systems. The analysis includes the role of the extra couplings between the different properties induced by the finiteness of size. We use the results of computations to extract, analyze, and explain the physical information embedded in the data generated in photoelectron spectroscopy experiments and to make prediction that will stimulate future experiments. Our broader goal is to achieve a degree of knowledge that will allow for use of clusters as building blocks in rational design and assembly of nanosystems with desired properties.

Recent Progress

New Scheme for Computation of Electron Binding Energies within Density Functional Theory. Because of its efficiency and successes, density functional theory (DFT) – we restrict our consideration to the traditional, time-independent DFT – became the tool of choice in theoretical/computational studies of many-electron systems. Atomic clusters of metallic elements are such systems. DFT has been used extensively to characterize their structures and energies, but the one-particle Kohn-Sham (KS) eigenenergies of DFT correspond to auxiliary quasiparticles rather than real electrons. Therefore, corrections are required to convert (the negatives) of these eigenenergies into electron binding energies (EBEs). A number of correction schemes have been considered in the past, but they suffer from various shortcomings and limitations. These include applicability only to a certain (e.g., local density) implementation of DFT, orbital insensitivity (as in the constant shift correction scheme), and use of quantities that are ill-defined in DFT as a ground state theory (e.g., in approaches that use holes or fractional occupation of orbitals). We have formulated a new correction scheme[1] that is free from all these limitations. Its merits can be summarized as follows: 1) It is general and applicable to any implementation of DFT; 2) It yields orbital-specific corrections; 3) It uses only ground state properties rigorously defined within DFT; and 4) It furnishes highly accurate spectra of EBEs. The main elements of the new scheme include the following. The correction $\Delta_i(i)$ that converts the negative of the KS eigenenergy $\varepsilon_i(i)$ of the most external i-th electron in an i-electron system into its binding energy $BE_i(i)$ is by definition

$$\Delta_i(i) = BE_i(i) - (-\varepsilon_i(i)) . \quad (1)$$

$BE_i(i)$ can be computed rigorously within DFT as

$$BE_i(i) = E(i-1) - E(i) , \quad (2)$$

where $E(i)$ is the ground state energy of the i-electron system. In a N-electron system the correction $\Delta_i(i)$ can be computed for any $i = N$, $N-1$, …, 1 by gradually removing one electron at a time from the top and using equations (1) and (2). If one is interested in the binding energies of the top j electrons, the

$\Delta_i(i)$ should be computed for $i = N$, $N-1$, …, $N-j+1$. The correction $\Delta_i(N)$, that converts the negative of an i-th KS eigenenergy $\varepsilon_i(N)$ of an N-electron system into the binding energy $BE_i(N)$ of the i-th electron,

$$BE_i(N) = -\varepsilon_i(N) + \Delta_i(N), \tag{3}$$

is then computed through recursive application of the interpolation

$$\Delta_i(k+1) = \Delta_i(k) + \alpha_i(k+1)[\Delta_{i+1}(k+1) - \Delta_i(k)], \tag{4}$$

where

$$\alpha_i(k+1) = \frac{\varepsilon_i(k+1) - \varepsilon_i(k)}{\varepsilon_{i+1}(k+1) - \varepsilon_i(k)} \tag{5}$$

and $k = i$, …, $N-1$. The schematic of the interpolation scheme is shown in Fig. 1. Further details are given in Ref. 1. We applied the new scheme to study the size, structure, charge state, and composition dependence of properties of metal clusters, in general, and the phenomenon of size-induced transition to metallicity, in particular.

Size-Induced Transition to Metallicity. This phenomenon is one of the most intriguing and important, yet least understood, aspects of the size-dependence of cluster properties. It is of central relevance to many nanotechnologies, e.g., in establishing the ultimate limits of miniaturization in nanoelectronics. Small metal clusters, or more precisely atomic clusters of elements that are metals in bulk quantities, may lack altogether properties usually associated with the metallic state. These properties then grow in as the clusters grow in size. Is the transition to metallicity monotonic or not? What is the size or size-range over which it takes place? Which property (or properties) is (are) the best indicators of the transition? Answers to these questions are largely unknown.

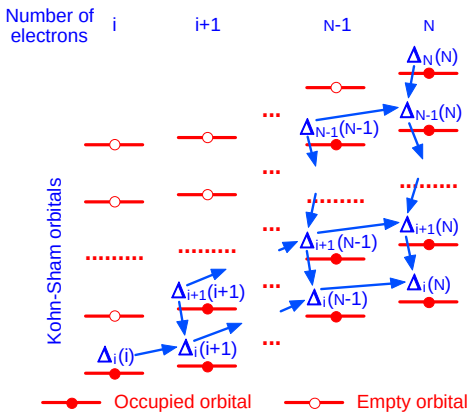

Figure 1. *Schematic of the interpolation scheme defined by Eqs. (4) and (5).*

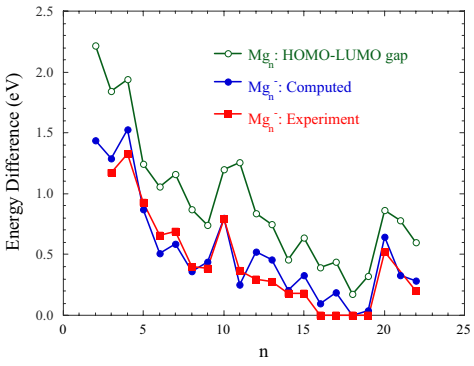

Figure 2. *The computed and measured difference in the binding energies of the two most external electrons in Mg_n^- and the HOMO-LUMO gap of Mg_n.*

One way to study the phenomenon of size-induced transition to metallicity is to analyze the HOMO-LUMO gap, which is a finite-size analog of the bulk band gap. Closure of this gap can be viewed as an indication of a metallic, or metal-like, state. It has been argued that experimentally the HOMO-LUMO gap can be obtained in photoelectron spectroscopy (PES) measurements on anionic species as the extra electron will occupy the LUMO of the neutrals. In Fig. 2 we present the computed[2-4] and measured[5] difference in the binding energies of the two most external electrons in Mg_n^-, n=2-22, clusters together with the computed HOMO-LUMO gap of their neutral Mg_n counterparts. The figure clearly shows that the values computed and measured for Mg_n^- are in an essentially quantitative agreement, and both are different from the HOMO-LUMO gap of the neutral Mg_n. The fundamental reason for the differences is that the energetically most stable structures of the anionic and neutral clusters may be, and for some sizes indeed are, different. This coupling between the charge state and the preferred structure is another finite-size effect that has to be taken into account in the analysis and interpretation of measured data. We considered also other features, such as consistency with the jellium model picture and the character of the valence charge distribution, as alternative indicators of the size-induced transition to metallicity. Our major results can be summarized as follows: 1) In agreement with the experiments, the computed difference in the binding energies of the two

most external electrons in Mg_n^- decreases as n increases and becomes zero at n=18. This is consistent with what can be viewed as an evolution towards a metallic state because the mentioned energy difference is the anionic counterpart of the HOMO-LUMO gap of the neutrals as the finite-size analog of the bulk band gap. The difference in the binding energies, however, decreases nonmonotonically, and it becomes nonzero again for n>18; 2) contrary to the commonly held view, PES experiments on anionic finite systems do not, in general, probe the properties of their neutral counterparts; the charge state may have a substantial effect on other, e.g., structural and consequently electronic, properties; 3) consistency with the jellium model picture may not be an adequate indicator of metallicity; 4) approach to the same value in the degree of s-p hybridization in anionic and neutral Mg_n clusters as their size increases is a better indicator of the transition to metallicity than the change in that degree considered separately in either anionic or neutral clusters. Detailed discussion of these findings is given in Refs. 2-4.

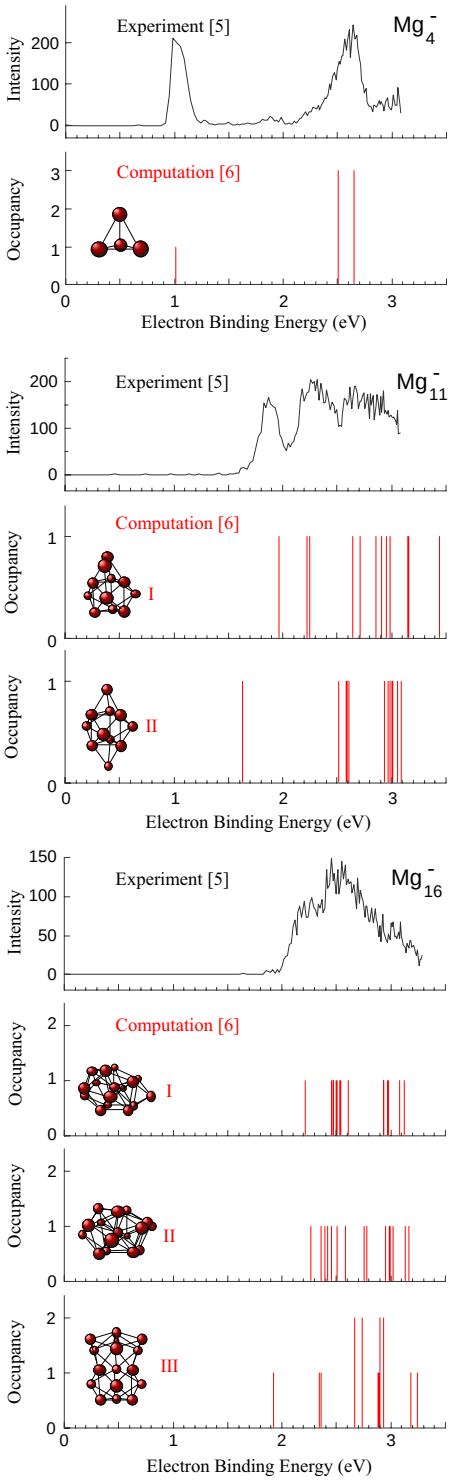

Figure 3. *Computed structure-specific and measured spectra of electron binding energies*

Role of Structure. We used our new correction scheme to compute the spectra of EBEs for different isomers of Mg_n^- clusters of different sizes[4,6]. These are shown for Mg_4^-, Mg_{11}^-, and Mg_{16}^- together with their measured spectra[5] in Fig. 3. The quality of the agreement between the computed and measured results can be gauged by the case of Mg_4^-, which forms only one isomeric form. In fact, the excellent agreement between the two is the experimental corroboration of the theoretically predicted tetrahedral structure. Examination of the results for Mg_{11}^- and Mg_{16}^- again reveals an excellent agreement between the features of the measured spectra and the pattern of EBEs computed for the most stable isomers of the clusters. Although the overall pattern of the EBEs computed for the second isomer of Mg_{16}^- is somewhat different, the computed spectrum is within the range of the measured spectrum and, therefore, this isomer may be a contributor to the measured spectrum. This is not the case for the second isomer of Mg_{11}^- and the third isomer of Mg_{16}^-. The binding energy of the most external electron of these isomers is not represented in the corresponding measured spectra and therefore one can eliminate them as contributors to these spectra. These results illustrate how high accuracy computations of structure-specific EBEs used in conjunction with measured PES allow for identification of and discrimination between the structural forms of clusters generated in a given experiment.

Role of Composition. We applied our scheme to compute and analyze spectra of EBEs of anionic Al_n and Al_nNi clusters. Experimental PES data are available for these systems[7] (also L.-S. Wang et al., to be published), and our computed results are in excellent agreement with these data. The case of bimetallic clusters is especially interesting. Can we understand and explain the changes in the spectrum caused by introducing an atom of a different type into a cluster (doping)? In Fig. 4 we show the spectra of the computed and measured EBEs for Al_{12}^-, Al_{13}^-, and $Al_{12}Ni^-$. The measured spectra are very different for the three clusters, and the computations reproduce these differences. We

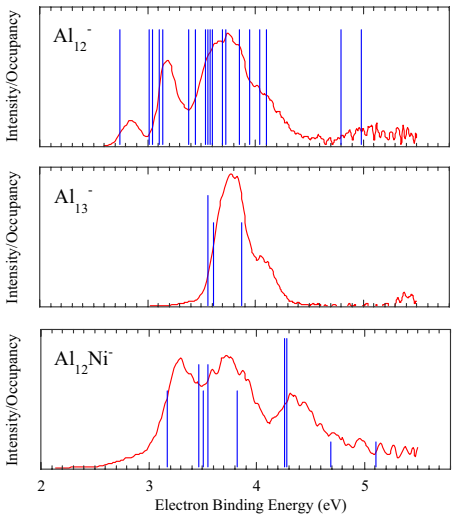

Figure 4. *Computed (bar graphs) and measured (line graphs) spectra of electron binding energies.*

formulated and performed a detailed analysis that allowed us to explain how the three-humped spectrum of Al_{12}^- evolves into a single-peaked (with a shoulder) spectrum of Al_{13}^-, when one adds an Al atom to Al_{12}^-, and into a shifted three-humped spectrum of $Al_{12}Ni^-$, when one adds a Ni atom to Al_{12}^-. This analysis identifies the separate roles of the changes in the structure/symmetry and the number of electrons caused by adding different atoms to a cluster. It is general and applicable to any finite system to characterize the changes in its EBE spectra as a function of its size and composition.

Future Plans

It is clear that exploration of the size-induced transition to metallicity in Mg_n clusters requires extension of the studies to larger sizes. The size-range n=2-22 is well within the nonscaling regime, where the properties change nonmonotonically with the size. Among the questions to be addressed and answered are: 1) Can one identify different stages in the size-evolution of electronic properties within the nonscaling regime? 2) If yes, what defines the number and nature of these stages? 3) At what size, or size-range, does the scaling (i.e., monotonic) evolution of electronic properties set in? 4) At what size does the dependence on the charge state become inessential? 5) What are the roles of doping and temperature in changing the degree of metallicity of finite systems? But the most complex and important task is to formulate a general conceptual framework that defines those features and attributes which can be viewed as the finite-size analog of the bulk metallic state and which evolve into the traditional metallic properties as the size of the systems increases. This framework will have to include the coupling between the different finite-size descriptors of metallicity and account for the possible differences in the rates of change of these descriptors as a function of size.

Future work will include a more comprehensive analysis of the contribution of different structural forms of a cluster (more generally, finite system) to its PES measured under different experimental conditions (e.g., temperature). This, of course, will require appropriate experimental data. Theoretically, evaluation of the branching ratio between the different isomeric forms contributing to a measured PES will involve evaluation of the entropic contribution (i.e., computation of the vibrational density of states). The task, therefore, calls for development of methods for computation of more realistic, anharmonic densities of states.

The studies of the composition-dependence of the EBE spectra of bimetallic clusters will be extended to analyze the systematic (but not necessarily monotonic) changes in these spectra as a function of the stoichiometric (i.e, percentile) composition. These will be performed for clusters of different sizes and different elemental composition. Later work will include ternary systems. The goal here is to identify and formulate general guiding criteria that will allow for rational design and assembly of heterogeneous clusters and cluster-based systems with desired electronic and other properties.

References

1. J. Jellinek and P. H. Acioli, J. Chem. Phys. 118, 7783 (2003).
2. P. H. Acioli and J. Jellinek, Phys. Rev. Lett. 89, 213402 (2002).
3. J. Jellinek and P. H. Acioli, J. Phys. Chem. A 106, 10919 (2002); 107,1670 (2003).
4. J. Jellinek and P. H. Acioli, in *Metal-Ligand Interactions in Molecular-, Nano-, Micro-, and Macro-Systems in Complex Environments,* N. Russo, D. R. Salahub, and M. Witko, Eds., Kluwer Academic Publishers, Dordrecht, 2003, p. 121.
5. O. C. Thomas, W. Zheng, S. Xu, and K. H. Bowen, Phys. Rev. Lett. 89, 213403 (2002).
6. P. H. Acioli and J. Jellinek, Eur. Phys. J. D 24, 27 (2003).
7. X. Li, H. Wu, X. Wang, and L.-S. Wang, Phys. Rev. Lett. 81, 1909 (1998).

Generation, Detection and Characterization of Gas-Phase Transition Metal Containing Molecules

Timothy C. Steimle
Department of Chemistry and Biochemistry
Arizona State University
Tempe, Arizona 85287-1604
E-Mail: Tsteimle@asu.edu

I. Program scope

The reactions of a single metal atom, or possibly a metal dimer, with simple gaseous reagents are reasonable first order model systems for emulating metal cluster and molecular supported catalysis. Although the literature abounds with theoretical predictions for the reaction of naked metal atoms or metal clusters with simple hydrocarbons, hydrogen, and other gases, the gap between theoretical predictions and experimental observations is immense. The calculations typically predict structure and relative stability for the pre-reactive complex, insertion products, transition state complexes, and elimination products that occur along plausible reaction paths. The elimination products are small, transient, metal-containing radical molecules which are the focus of our studies. In our case, these molecules are generated in the reaction of a laser ablated metal vapor seeded in an Argon/reagent gas supersonic expansion. Highly quantifiable information about the geometric, and more importantly, electronic structure of these molecules is derived from the analysis of optical spectra recorded at the near natural linewidth limit. These simple molecules are also amenable to sophisticated electronic structure calculations, thereby creating the desired symbiosis between theory and experiment.

Experimental determination of the permanent electric dipole moments, μ, has been a major focus because dipole moments: are primarily dependent upon the chemically relevant valence electrons, are the most fundamental electrostatic property, and enter into the description of numerous phenomena. The observed large variation in μ even amongst simple, similar molecules (*e.g.* MoC ($X^3\Sigma^-$) μ = 9.4 D (unpublished results) *vs.* PtC($X^1\Sigma^+$) μ = 1.08D[1]) illustrates its sensitivity to the nature of the chemical bond. A comparison of predicted μ values with experimentally determined values is the primary criteria for assessing the effectiveness of various computational methodologies. This is particularly important for evaluating post-Hartree-Fock treatments, which are essential for obtaining quantitative predictions. A stringent test of computational methods [3,4] is the comparison of predicted values of μ obtained by both a finite field calculation, where $\mu = \left.\frac{\partial \text{Energy}}{\partial \vec{E}}\right|_{\vec{E}\to 0}$, and the expectation value approach, where $\mu = \left\langle \Psi^{el} \left| \sum_i er_i \right| \Psi^{el} \right\rangle$. The two approaches are related by [2]:

$$\left.\frac{\partial \text{Energy}}{\partial \vec{E}}\right|_{\vec{E}\to 0} = \left\langle \Psi^{el} \left| \sum_i er_i \right| \Psi^{el} \right\rangle + 2\left\langle \frac{\partial(\Psi^{el})}{\partial \vec{E}} \left| \hat{H}^{el} \right| \Psi^{el} \right\rangle \qquad 1)$$

where $\vec{E}$ is the applied electric field. According to the Hellman-Feynman theorem, the finite field and expectation value prediction will be identical (*i.e.* the 2nd term of Eq. 1 = 0) when Ψ^{el} is either the exact eigenfunction of the Hamiltonian or a predicted wave function that has been fully optimized in the variational sense. For transition metal containing molecules, *ab initio* generated wave functions require extensive treatment of electron correlation and are not fully optimized in the variational sense. Therefore, if the predicted wavefunction, Ψ^{el}, is an accurate approximation to the true wavefuntion, then the expectation value prediction and the finite field predicted value will agree with the experimentally derived value.

II. Recent accomplishments

a. Dipole moment measurements.

This presentation will focus on unpublished results for tungsten nitride, WN, and rhenium nitride, ReN and make a comparison with isovalent chromium nitride, CrN [5] and molybdenum nitride, MoN [6]. The optical Stark laser induced fluorescence (LIF) spectrum of the $R_{ee}(0.5)$ branch feature of WN and the associated energy level pattern are presented in Figure 1. The molecules were generated in the reaction of laser ablated tungsten with an ammonia/argon supersonic expansion.

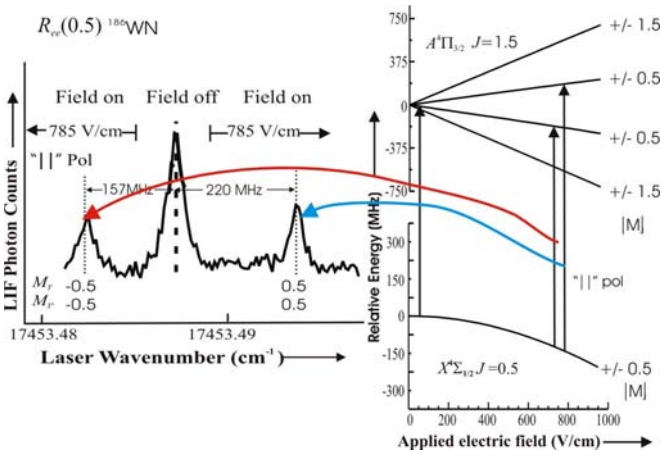

Figure 1. The $R_{ee}(0.5)$ branch feature of the (0,0) $A^4\Pi_{3/2} - X^4\Sigma_{1/2}$ band system of ^{186}WN recorded in the presence of a 785 V/cm static electric field. The field was switched off across the middle portion of the scan, and then back on as a means of simultaneously recording the field free and Stark shifted features. The linewidths of the spectral features are approximately 50 MHz.

Spectra of similar quality were recorded for the (0,0) $[26.0]0^+ - X0^+$ band system of ^{187}ReN. The determined values for μ and the reduced dipole moment (≡ μ/bond distance) are collected in Table I. Trends in these values will be rationalized using a molecular orbital correlation diagram and they will be compared with theoretical predictions.

Table I. Dipole moments for CrN, MoN, WN and ReN.

Parameter	^{186}WN		^{187}ReN		CrN	MoN
	$X^4\Sigma$	$A^4\Pi_{3/2}$	$X0^+$	$[26.0]0^+$	$X^4\Sigma$	$X^4\Sigma$
μ (Debye)	3.77(18)	2.45(3)	1.96(8)	3.53(4)	2.31(4) [b]	2.44(5)[c]
μ/R_e (D/Å)	2.26	1.45	1.20	2.12	1.47	1.48

[a] The numbers in parentheses represent a 2σ error estimate. [b] Ref. 5; [c] Ref. 6

b. Identification of new metal containing molecules

A primary objective of this project is the identification of new transition metal containing polyatomic molecules. Amongst the new polyatomic molecules that we have observed are platinum imide, PtNH (**Figure 2)** and scandium cyanide, ScCN (or ScNC)(**Figure 3)**. Interestingly, there was no evidence of ScC_2 in the ablated scandium/CH_4 reaction products even though YC_2 (Publication #1) is efficiently made in these sources.

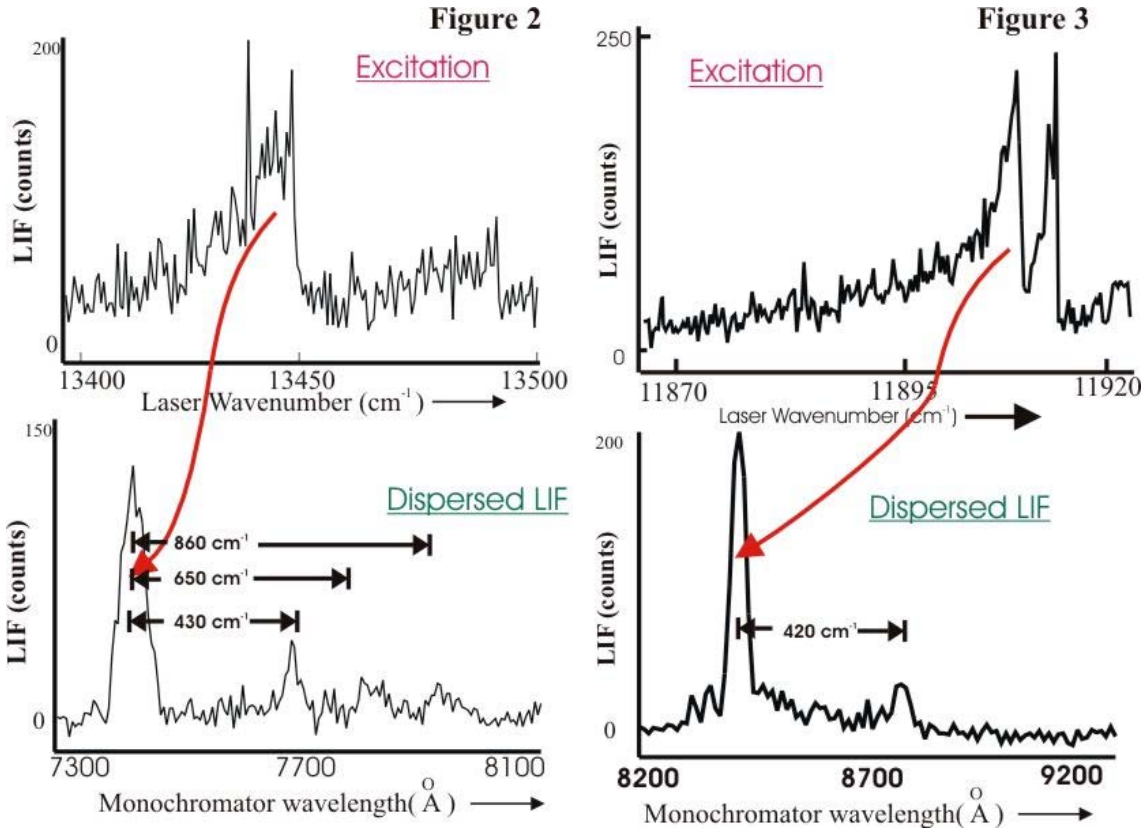

III. Future directions

a. Discharge sources as an alternative method for molecular production.

The number of polyatomic molecules that we have detected and characterized are far fewer than the number of diatomic molecules. Our current laser ablation/reaction production scheme may favor generation of diatomic fragments because of the associated energetic ablation plasma. In the future, we will also use a dc-discharge supersonic expansion source with volatile organometallic precursors similar to what we used in the study of SiCH [7] and GeCH [8]. Initial studies will use trimethyl(methycyclopetadienyl) platinum, $(CH_3)_3(CH_3C_5H_4)Pt$, seeded in an argon carrier gas.

b. Mid-infrared spectroscopy

The metal imides, MNH, amides, MNH_2, hydroxides, MOH, carbenes, MCH_2, and methylidines, MCH, have been, and will continue to be, targets for our high-resolution spectroscopic studies. Many of these molecules are observed in our TOF mass spectra, but detecting them via LIF spectroscopy has been challenging. While extremely sensitive and informative for many molecules, electronic spectroscopy with LIF detection has certain drawbacks which include: a) long spectral searches required, b) the excited

electronic states may be heavily perturbed making analysis difficult, and c) the excited state may be weakly fluorescent due to pre-dissociation or internal relaxation. Searching problems in the mid-IR are much reduced because all C-H, N-H and O-H stretching frequencies are in the range of 2900 cm^{-1} -3100 cm^{-1}, 3200 cm^{-1} -3500 cm^{-1}, 3750 cm^{-1} - 3900 cm^{-1}, respectively. Furthermore, it is likely that pre-dissociation or internal relaxation effects are much reduced in the mid-IR due to the lower density of states.

We plan to construct a difference frequency generation (DFG) spectroscopic source similar to that currently used by the Rice University group [9,10]. This system incorporates two recent technological advances that greatly facilitate DFG. In this scheme the traditional Ar^+ laser is replaced by a powerful compact and low-noise, single frequency, cw, diode-pumped Nd:YAG laser operating at 1064 nm and the mixing media is a periodically poled lithium niobate (PPLB) crystal. The periodic-polling facilitates phase matching eliminating the need for accurate temperature control.

References

1. S. A. Beaton and T.C. Steimle*, J. Chem. Phys*. 111, **24**, 10876-10882 (1999).
2. *Introduction to Computational Chemistry* F. Jensen (John Wiley & Sons, 1999).
3. M. Medved, M. Urban, and J. Noga, *Theor. Chem. Acc*. 98, 75 (1997).
4. C. W. Bauschlicher, Jr. S. R. Langhoff, A. Komornicki, *Theor. Chim. Acta* **77** (4), 263 (1990).
5. T.C. Steimle, J. S. Robinson and D. Goodridge, *J. Chem. Phys.* **110**, 881 (1999).
6. D.A. Flecther, K.Y. Jung, and T.C. Steimle, *J. Chem. Phys*. **99**, 901, (1993); *ibid* , J. Chem. Phys. **108**, 10327, (1998).
7. T.C. Smith, D.J. Clouthier and T.C. Steimle, *J. Chem. Phys*. 115, 817 (2001).
8. T.C. Smith, D.J. Clouthier and T.C. Steimle, *J. Chem. Phys*.,115, 5047 (2001).
9. Yu. G. Utkin, Jia-Xiang Han, Fuge Sun, Hong-Bing Chen, Graham Scott, and R.F Curl, *J. Chem. Phys* 118(23), 10470 (2003).
10. Jia-xiang Han, Yu. G Utkin, Hong-bing Chen, L. A.Burns and R. F Curl, *J. Chem. Phys* 117(14) 6538 (2002).

Publications (2002-2004)

1. "Rotational Analysis of the A^2A_1-X^2A_1 Band System of Yttrium Dicarbide:YC_2"T.C. Steimle, R.R. Bousquet, K-I Namiki and A.J. Merer J. Mol. Spectroscopy 215, 10-28, (2002).
2. "The permanent electric dipole moments of iron monocarbide, FeC" T.C. Steimle, W. Virgo and David Hostutler, J. Chem. Phys. 117, 1511 (2002).
3. "The permanent electric dipole moments of ruthenium monocarbide, RuC" T.C. Steimle, W. Virgo and J. M. Brown , J. Chem. Phys. 118, 2620-2625 (2003).
4. "The permanent electric dipole moments and magnetic hyperfine interactions of ruthenium mononitride, RuN. Timothy C. Steimle and Wilton Virgo J. Chem. Phys. 118, 12965 (2003).
5. "The permanent electric dipole moments of Ruthenium Monocarbide in the $^3\Pi$ and $^3\Delta$ states" Wilton L. Virgo, Timothy C. Steimle, Laura E. Aucoin and J.M. Brown. (Chem. Phys. Lett. **391**,75-80, 2004)

Dynamics of Low Energy Electrons in Ion Radiolysis of Aqueous Systems

Simon M. Pimblott, Jay A. LaVerne, and Daniel M. Chipman
pimblott.1@nd.edu, laverne.1@nd.edu, chipman.1@nd.edu
Radiation Laboratory, University of Notre Dame, Notre Dame, IN 46556

Program Scope

Deposition of high-energy radiation in a condensed phase leads to a cascade of low-energy electrons that produces a nonhomogeneous spatial distribution of molecular ionizations, excitations, dissociative electron attachment processes, and dissociative electron recombination reactions. These fundamental processes are investigated using a multi-facetted approach employing experiments in conjunction with Monte Carlo kinetic modeling and electronic structure calculations. The goal is to address the role of low-energy electrons in determining mechanisms, kinetics, and yields in the radiolysis of aqueous and hydrocarbon solutions. The interest in these issues is fundamental nature, but the chemical systems are found throughout the DOE portfolio in nuclear technology and in radioactive waste remediation and management, as well as in other technological challenges involving radiation.

One feature that distinguishes radiolysis from photolysis is the clustering of damage. This clustering of molecular fragments defines the track and gives the chemistry its characteristic transient (ps-ns timescale) kinetics. The transient chemistry is nearly diffusion controlled, and it depends critically on both the identities of the reactive particles and their spatial locations. The structure of the radiation track is controlled almost entirely by low-energy secondary electrons produced by the inelastic encounters of the primary irradiating particle with medium molecules. These electrons typically have energies below 100 eV. [1]

Although low-energy electrons are of central importance in the origin of the clustering within a radiation track, and the nature of their interactions controls the initial yields of the chemically reactive species, there is very little quantitative information available in the solid phase, and virtually none in the liquid phase. [2] Qualitatively, the secondary electron travels a short distance from its parent event and ionizes or excites a second molecule, sometimes producing another electron with even lower energy. In addition, low-energy electrons can undergo dissociative electron attachment processes, [3] which may also lead to the dissociation of a molecule. The daughter events are produced close to the primary event, and this leads to the clustering of the fragments in spurs. [4]

Recent Progress

Data on the effects of radiations such as alpha particles and accelerated light and heavy ions are scarce, and the only system investigated thoroughly is the dependence of the Fricke dosimeter on radiation type and energy. [5] Comparison of stochastic independent reaction times (IRT) simulations for track segments with experimentally determined differential yields shows excellent agreement for energetic electrons, and for non-relativistic ions, including ^{1}H, ^{4}He, ^{12}C, and ^{20}Ne. [6] The results reveal a significant effect of particle type and energy, which reflects the competition between intra-track reaction of the radiation-induced radicals, diffusion, and scavenging. Examination of the underlying Monte Carlo track structure simulations shows that the radial energy loss profiles are similar for ions with the same velocity/charge ratio. About ~ 40% of the

energy is deposited initially within a water diameter of the track axis, with the remainder transported away by secondary electrons.

Preliminary Monte Carlo simulations of the degradation of low-energy electrons in ice have been performed [7] and the simulation method has been validated by comparison with the experimental EELS spectrum of ice. [8] The simulations have been analyzed with specific reference to the range of the electrons (spur width), and the number and nature of the secondary events (spur content). The predicted ranges of low-energy electrons in ice are relatively long. For most energies in the interval studied, 0 to 25 eV, the range is greater than 10 nm. Secondary low-energy electrons are generated with a spectrum of energies, which can be calculated from a full track structure simulation. The mean penetration distance averaged over the energy distribution for a 1 MeV fast electron gives a track mean of 8.4 nm. Radiation chemical studies have generally assumed that the low-energy electron thermalization distribution is Gaussian, independent of energy, and centered on the event in which the low-energy electron is generated. A Gaussian of standard deviation 5.2 nm and mean 8.3 nm is required to fit the observed hydrated electron decay kinetics for fast electron pulse radiolysis. [9] The agreement between the two distances, obtained in entirely different ways, is remarkable, given the approximations still inherent in both methods. However, the Gaussian electron distribution used to model track chemistry bears no resemblance to the simulated distribution of the thermalization distance.

Extensive experimental and modeling studies on γ and fast electron radiolysis of aqueous solutions have been performed, and have provided considerable information about the kinetics and reactions of radiation-induced radicals and molecular products, and about their long-time yields. [10] This program is complementing these studies by examining the radiolysis of water and aqueous solutions with heavy ions. The present experimental and modeling studies are focusing on the kinetics and yields of the transient radical species, e_{aq}^- and OH, which are ultimately responsible for much of the observed radiation damage.

Future Plans

a. Non-homogeneous track chemistry in aqueous solutions.

The effects of radiation type and energy on radiation chemical kinetics provides the most direct insight into the non-homogeneous diffusion and reaction processes occurring in a radiation track. A major thrust of this program is a systematic experimental determination of the effects of ion type and energy on the radiolysis of aqueous solutions to enable the construction of a database of the yields and kinetics of e_{aq}^- and OH radicals in heavy ion radiolysis of water. The database of information obtained from the experimental studies will be analyzed using stochastic IRT kinetic techniques [11] incorporating track structures simulated using a collision-to-collision approach and employing interaction cross-sections appropriate for liquid water, [12] with the goal that the combination of experiment with modeling will provide a realistic description of the diffusion-reaction processes underlying the kinetics. Modeling of the track chemistry of a heavy ion necessitates the simulation of track segments for ions of different energy, followed by integration, as track segment yields are very different from the track average yield except at high ion energies. Stochastic calculations will complement the experimental component of this program, examining the dependence of the yields of scavenger systems to probe the decay kinetics of e_{aq}^- and OH and of the production of the

molecular products, H_2 and H_2O_2. The simulations provide a direct picture of the energy transfer from the radiation to the medium, of the physical consequences of the energy transfer events, and of the roles of the reactions comprising the radiation chemical reaction mechanism. Examination of the underlying radiation track structure and the details of the simulated reaction kinetics will provide insight into the effects of the competing physical, physico-chemical and chemical processes on the experimentally observed chemistry.

b. Local track structure in water.

Monte Carlo track-structure type simulations of the degradation of low-energy electrons in density-normalized gaseous and ice water will be performed to investigate how condensation affects the interactions of low-energy ionizing radiation with water, and to elucidate the effects of phase on local track (spur) structure in water. Absolute cross-sections for amorphous ice, [13] which is structurally similar to liquid water, are markedly different from the corresponding gas phase cross-sections: most notably the elastic cross section is dominated by the long-range charge-dipole interaction in the gas phase and is 30 times smaller in ice. The simulations will be analyzed for the range of the electrons (radiation chemical spur width), and the distances between adjacent events. Stochastic track structure simulations for γ, and heavy ion, radiolysis of liquid water predict that the yield of electrons with energy in the range ~ 0 to 25 eV is ~ 4.0 per 100 eV of transferred energy, and that the mean energy of these low-energy electrons is about 9.7 eV. Monte Carlo simulations will provide the number, nature and relative positions of the electronic excitation, dissociative electron attachment and recombination events of the low-energy electrons as a function of the electrons initial energy. This data is particularly important for elucidation of the clustering of the damage sites.

c. Dissociative electron attachment reactions.

A dissociative electron recombination reaction, speculated to produce H_2O^* or perhaps H_3O^*, has been identified as the dominant source of sub-picosecond H_2 in heavy ion radiolysis of water; [14] however, other mechanisms such as dissociative electron attachment to water cannot be discounted as contributing pathways in γ and fast electron radiolysis. The ultra-short lived species produced by dissociative electron attachment processes, which may involve resonance states of a transient molecular anion, $(H_2O)_n^-$ (as distinct from the hydrated electron) or fragment anions, H^-, O^- and OH^-, are not characterized in the liquid phase. Theoretical studies to characterize the transient products of dissociative electron attachment will provide input and understanding for the description of low-energy electron chemistry. These studies will involve electronic structure calculations on the energetics of $(H_2O)_n^-$ as well as Monte Carlo simulations investigating the role of DEA in the production of radiation induced radicals and ions.

References

1. S.M. Pimblott, J.A. LaVerne, A. Mozumder & N.J.B. Green, *J. Phys. Chem.* **1990**, *94*, 488-95.
2. S.M. Pimblott & N.J.B. Green, "Recent advances in the kinetics of radiolytic processes", in "Research in Chemical Kinetics", Eds. R.G. Compton & G. Hancock, Elsevier, Amsterdam, Vol. 3, p. 117-74, **1995**.

3. W.C. Simpson, M.T. Sieger, T.M. Orlando, L. Parenteau, K. Nagesha & L. Sanche *J. Chem. Phys.* **1997**, *107*, 8668-77; (b) W.C. Simpson, T.M. Orlando, L. Parenteau, K. Nagesha & L. Sanche *J. Chem. Phys.* **1998**, *108*, 5027-34.
4. Mozumder & J.L. Magee *J. Chem. Phys.* **1966**, *45*, 3332-41.
5. J.A. LaVerne & R.H. Schuler, *J. Phys. Chem.* **1987**, *91*, 5770-6.
6. S. M. Pimblott & J. A. LaVerne, *J. Phys. Chem. A* **2002**, *106*, 9420-9427.
7. N.J.B. Green & S.M. Pimblott, *Res. Chem. Intermed.* **2001**, 27, 529-38.
8. M. Michaud, P. Cloutier & L. Sanche, *Phys. Rev. A* **1991**, *44*, 5624-7.
9. S.M. Pimblott & A. Mozumder, "Modelling of physicochemical and chemical processes in the interaction of fast charged particles with matter" in *Charged Particle Interactions with Matter*, eds. A. Mozumder and Y. Hatano, Marcell-Dekker Inc., **2003**, pp75-101.
10. J.A. LaVerne & S.M. Pimblott, *J. Phys. Chem.* **1991**, *95*, 3196-206 and references within.
11. (a) S.M. Pimblott & J.A. LaVerne, *J. Phys. Chem. A*, **1997**, *101*, 5828-38: (b) S.M. Pimblott & J.A. LaVerne, *J. Phys. Chem. A*, **1998**, *102*, 2967-75.
12. (a) S.M. Pimblott, J.A. LaVerne, A. Mozumder & N.J.B. Green, *J. Phys. Chem.* **1990**, *94*, 488-95; (b) S.M. Pimblott, J.A. LaVerne & A. Mozumder, *J. Phys. Chem.*, **1996**, *100*, 8595-8606.
13. M. Michaud, A. Wen & L. Sanche *Radiat. Res.* **2003,** *159*, 3-22.
14. (a) B. Pastina, S.M. Pimblott, & J.A. LaVerne, *J. Phys. Chem. A* **1999**, *103*, 5841-6; (b) J. A. LaVerne & S. M. Pimblott, *J. Phys. Chem. A* **2000**, *104*, 9820-2.

DOE Sponsored Publications in 2002-2004

1. A. Alba García, L.D.A. Siebbeles, H. Schut, A. van Veen & S.M. Pimblott, "Positronium formation polyethylene: a computer simulation study", *Radiat. Phys. Chem.*, **2003**, *68*, 623-25.
2. S.M. Pimblott & J.A. LaVerne, "Effects of Track Structure on the Ion Radiolysis of the Fricke Dosimeter", *J. Phys. Chem. A*, **2002**, *106*, 9420-7.
3. A. Hiroki, S.M. Pimblott & J.A. LaVerne, "Hydrogen Peroxide Production in the Radiolysis of Water with High Radical Scavenger Concentrations", *J. Phys. Chem. A*, **2002**, *106*, 9352-8.
4. R.E. Harris & S.M. Pimblott, "On ^{3}H β Particle and ^{60}Co γ Irradiation of Aqueous Systems", *Radiat. Res.* **2002**, *158*, 493-504.
5. S.M. Pimblott & L.D.A. Siebbeles, "Energy loss by non-relativistic electrons and positrons in liquid water", *Nucl. Inst. Meth. B*, **2002**, *194*, 237-50.
6. E. Abadjieva, H. Schut, A. Alba Garcia, R. Escobar Galindo, A. van Veen, S.M. Pimblott, "The design of an electrostatic variable energy positron beam for studies of defects in ceramic coatings and polymer films", *Appl. Surf. Sci.*, **2002**, **194**, 47-51.
7. M. Běgusová & S.M. Pimblott, "Stochastic simulation of γ radiolysis of acidic ferrous sulfate solution at elevated temperatures", *Radiat. Prot. Dosim.*, **2002**, *99*, 73-6.
8. A. Alba García, S.M. Pimblott, H. Schut, A. van Veen & L.D.A. Siebbeles, "Positronium formation dynamics in radiolytic tracks: a computer simulation study", *J. Phys. Chem. B*, **2002**, *106*, 1124-30.

Electron-Atom and Electron-Molecule Collision Processes

C. W. McCurdy and T. N. Rescigno
Chemical Sciences, Lawrence Berkeley National Laboratory, Berkeley, CA 94720
cwmccurdy@lbl.gov, tnrescigno@lbl.gov

Program Scope: This project seeks to develop theoretical and computational methods for treating electron collision processes that are currently beyond the grasp of first principles methods, either because of the complexity of the targets or the intrinsic complexity of the processes themselves. We are developing methods for treating low energy electron collisions with polyatomic molecules, complex molecular clusters and molecules bound to surfaces and interfaces, for studying electron-atom and electron-molecule collisions at energies above that required to ionize the target and for calculating detailed electron impact ionization and double photoionization probabilities for simple atoms and molecules.

Recent Progress and Future Plans: We report progress in three distinct areas covered under this project, namely electron-polyatomic molecule collisions, electron impact ionization and double photoionization.

1. Electron-Molecule Collisions

We have completed the first phase of a major study of dissociative electron attachment (DEA) to water. Low-energy dissociative attachment in water proceeds via Feshbach resonances corresponding to the formation of metastable negative ion states. Using the Complex Kohn Variational method, augmented with large-scale configuration-interaction studies, we constructed a complete, three-dimensional complex energy surface for the lowest ($^2B_1$) resonance and then carried out time-dependent wavepacket studies of the dissociation dynamics in full dimensionality using the Multi-Configuration Time-Dependent Hartree method in collaboration with H-D. Meyer (Heidelberg University). The results of this study, which represent the first ever fully *ab initio* calculation of dissociative electron attachment to a polyatomic target, were found to be in substantial agreement with experiment and were published in two papers in Physical Review A. We plan to extend these studies to the two higher ($^2A_1$ and $^2B_2$) resonance states, thereby providing a complete first-principles treatment of DEA in this important system, including cross sections and branching ratios between the H^- + OH and O^- + H_2 product arrangements .

The Complex Kohn method continues to serve as our principal tool for studying electron-molecule scattering. In collaboration with A. E. Orel (UC Davis), we have used this method to study low-energy electron scattering by ethylene and tetrafluoroethene , which are both important in low-temperature plasma technology. We also completed an initial study of the dynamics of resonant vibrational excitation of NO, using the complex Kohn method to characterize the resonance curves along with a local complex potential model for the nuclear dynamics. Our plans are to explore the importance of non-local

effects in the excitation dynamics of this molecule and to predict cross sections for dissociative electron attachment to NO. Experimental studies on dissociative attachment to NO are also underway at LBNL.

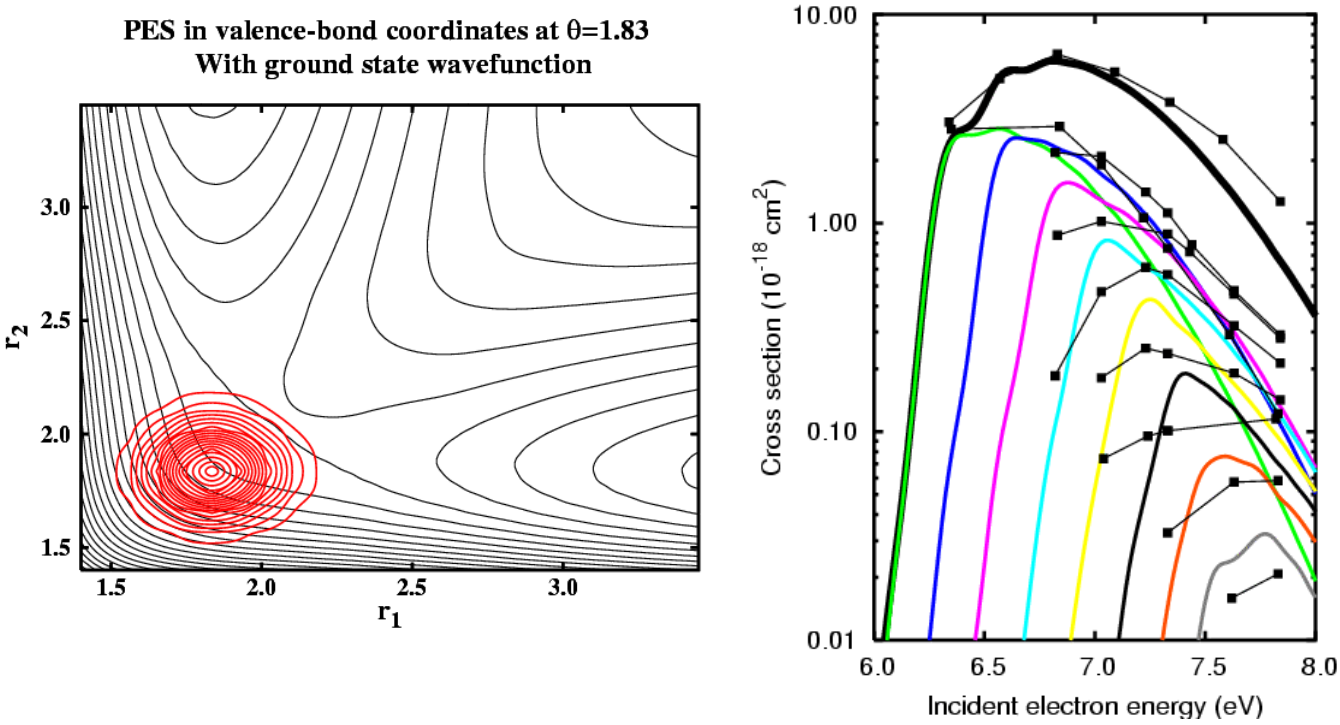

Left Panel: Initial wave packet shown on a cut of the 3D potential surface for the $^2B_1$ resonant state of H_2O. **Right Panel:** Comparison of calculated and measured (lines with squares) cross sections for production of OH in vibrational states v = 0 to v=7 in dissociative electron attachment to water. Thick line: total cross section.

2. Electron-Impact Ionization

Our studies of electron impact ionization are based on the e*xterior complex scaling* (ECS) method - an approach that has provided the only *complete* solution to the quantum mechanical three-body Coulomb problem at low collision energies to date. Using a time-dependent version of the basic ECS approach, we have successfully extended our studies to treat ionization of an atomic target with two active electrons. We have completed a study of electron-impact ionization of helium in the S-wave model, providing the first ever calculation of single differential ionization cross sections for a target with two active electrons. The results have been submitted to Physical Review A. We also plan to extend these studies to look at excitation-ionization and its signature on the differential ionization cross section.

3. Double Photoionization

We have continued with a theoretical effort, initiated in FY03, directed at studying double photoionization (one photon in, two electrons out) of atoms and molecules using the exterior complex scaling approach. The viability of the approach was successfully demonstrated this year with an extensive study of differential cross sections for double photoionization of helium which was published in Physical Review A along with a second paper on complex ionization amplitudes recently submitted for publication. We have also made substantial progress in extending these studies to a molecular target and have obtained preliminary results for double photoionization of H_2. All of this work has been carried out using an implementation of ECS with B-splines in collaboration with F. Martín (Autonomous University of Madrid). We are planning a further modification of our current approach that will replace the B-splines with a more efficient Discrete Variable Representation. We are also working on a hybrid approach that combines the use of molecular Gaussian basis sets with the Discrete Variable Representation and ECS. Such an approach avoids the use of single-center expansions, simplifies the computation of two-electron integrals and will pave the way for studies of double photoionization of more complex molecules.

Publications (2002-2004):

1. T. N. Rescigno, W. A. Isaacs, A. E. Orel, H.-D. Meyer and C. W. McCurdy, "Theoretical Studies of Excitation in Low-Energy Electron-Polyatomic Molecule Collisions", in *Photonic, Electronic and Atomic Collisions, Invited Papers*, *Proceedings of the XXII International Conference on Photonic, Electronic and Atomic Collisions,* Santa Fe, NM 2001 (Rinton Press, Princeton 2002).
2. C. W. McCurdy, M. Baertschy, W. A. Isaacs and T. N. Rescigno, "Reducing Collisional Breakup of a System of Charged Particles to Practical Computation: Electron-Impact Ionization of Hydrogen", in *Photonic, Electronic and Atomic Collisions, Invited Papers*, *Proceedings of the XXII International Conference on Photonic, Electronic and Atomic Collisions,* Santa Fe, NM 2001 (Rinton Press, Princeton 2002).
3. T. N. Rescigno, W. A. Isaacs, A. E. Orel, H.-D. Meyer and C. W. McCurdy, "Theoretical Study of Resonant Vibrational Excitation of CO_2 by Electron Impact", *Phys. Rev. A* **65**, 032716 (2002).
4. C. W. McCurdy, D. A. Horner and T. N. Rescigno, "Time-dependent approach to collisional ionization using exterior complex scaling", *Phys. Rev. A* **65**, 042714 (2002).
5. W. Vanroose, C. W. McCurdy and T. N. Rescigno, "On the Interpretation of Low Energy Electron-CO_2 Scattering", *Phys. Rev. A* **66**, 032720 (2002).
6. T. N. Rescigno and C. W. McCurdy, "Collisional Breakup in Coulomb Systems", in *Many-Particle Quantum Dynamics in Atoms and Molecules*, edited by V. Shevelko and J. Ullrich (Springer-Verlag, Heidelberg, 2003).

7. C. W. McCurdy, W. A. Isaacs, H.-D. Meyer and T. N. Rescigno, "Resonant Vibrational Excitation of CO_2 by Electron Impact: Nuclear Dynamics on the Coupled Components of the $^2\Pi_u$ resonance", *Phys. Rev. A* **67**, 042708 (2003).
8. T. N. Rescigno, M. Baertschy and C. W. McCurdy, "Resolution of phase ambiguities in electron-impact ionization amplitudes", *Phys. Rev. A* **68**, 020701 (R) (2003).
9. C. Trevisan, A. E. Orel and T. N. Rescigno , "Ab Initio Study of Low-Energy Electron Collisions with Ethylene", *Phys. Rev. A* **68**, 062707 (2003)
10. W. Vanroose , C. W. McCurdy and T. N. Rescigno, "Scattering of Slow Electrons by Polar Molecules: Application of Effective-Range Potential Theory to HCl", *Phys. Rev. A* **68**, 052713 (2003).
11. W. Vanroose, Z. Zhang , C. W. McCurdyand T. N. Rescigno, "Threshold Vibrational Excitation of CO_2 by Slow Electrons", *Phys. Rev. Letts*. **92**, 053201 (2004).
12. C. W. McCurdy and F. Martin, ""Implementation of Exterior Complex Scaling in B-Splines to Solve Atomic and Molecular Collision Problems", J. Phys. B **37**, 917 (2004).
13. C. W. McCurdy, D. A. Horner, T. N. Rescigno and F. Martin, "Theoretical Treatment of Double Photoionization of Helium Using a B-spline Implementation of Exterior Complex Scaling", *Phys. Rev. A* **69**, 032707 (2004).
14. Z. Zhang, W. Vanroose, C. W. McCurdy, A. E. Orel and T. N. Rescigno , "Low-energy Electron Scattering by NO: Ab Initio Analysis of the $^3\Sigma^-$, $^1\Delta$ and $^1\Sigma^+$ shape resonances in the local complex potential model", *Phys. Rev. A* **69**, 062711 (2004).
15. D. J. Haxton, Z. Zhang, C. W. McCurdy and T. N. Rescigno, "Complex Potential Surface for the $^2B_1$ Metastable State of the Water Anion", *Phys. Rev. A* **69**, 062713 (2004).
16. D. J. Haxton, Z. Zhang , H.-D. Meyer , T. N. Rescigno and C. W. McCurdy, "Dynamics of Dissociative Attachment of Electrons to Water Through the $^2B_1$ Metastable State of the Anion", *Phys. Rev. A* **69**, 062714 (2004).
17. C. S. Trevisan , A. E. Orel and T. N. Rescigno, "Ab initio study of Low-Energy Electron Collisions with tetrafluoroethene, C_2F_4" , *Phys. Rev. A* **70**, 012704 (2004).
18. C. W. McCurdy, M. Baertschy and T. N. Rescigno, "Solving the Three-Body Coulomb Breakup Problem Using Exterior Complex Scaling", *J. Phys. B* (topical review) (accepted).

"Low-Energy Electron Interactions with Complex Targets"

Thomas M. Orlando, *School of Chemistry and Biochemistry and School of Physics, Georgia Institute of Technology, Atlanta, GA 30332-0400*
Thomas.Orlando@chemistry.gatech.edu

Objectives: The primary objectives of this program are to investigate the fundamental physics and chemistry involved in low-energy (1-100 eV) electron scattering with molecular solids, surfaces and interfaces. The program is primarily experimental and concentrates on the important questions concerning how gas-phase concepts have to be modified when trying to understand electron collisions with complex condensed-phase targets.

Progress: This is the second year of the program which began in July 2002. We have focused on three main tasks that are being carried out in the Electron- and Photon-Induced Chemistry on Surfaces (EPICS) Laboratory at the Georgia Institute of Technology (GIT).

Task 1. ***The temperature dependence of low-energy (5 –250 eV) electron stimulated desorption of H^+, H_2^+, and $H^+(H_2O)_n$ and the uptake and autoionization of HCl on low-temperature water ice.*** We have used low-energy electron stimulated desorption (ESD) to study the production of H^+, H_2^+, and protonated water clusters ($H^+(H_2O)_n$) from pure non-porous amorphous solid water (ASW) and crystalline (CI) water ice films [1-4]. We observe a threshold energy of 22 ± 1 eV for the ESD of H^+ and H_2^+. H^+ ESD has a secondary threshold above ~ 40 eV and dominates the cation yields from both ASW and CI. A small yield of protonated clusters $H^+(H_2O)_n$, where n=1-8, is also observed for incident electron energies above ~ 40 eV, and the yield for $H^+(H_2O)_{n=1-8}$ increases significantly at ~ 70 eV. The $H^+(H_2O)_{n=1-8}$ yields are higher from ASW relative to CI and decrease with temperature, whereas the proton and H_2^+ yields show the opposite trend, increasing with temperature. All of these cation desorption channels involve localized two-hole states containing a_1 character. Since a_1 levels are involved in hydrogen bonding and are perturbed via nearest neighbor coupling, the ESD cation yields are very sensitive to the local potential and disorder in the terminal layer of the ice. The changes in the yields with phase and temperature are associated with structural and physical changes in the adsorbed water and longer lifetimes of excited state configurations containing a_1 character. This is shown below in Figure 1. Also shown is the thermal desorption data of 0.05 ML of HCl adsorbed on ASW.

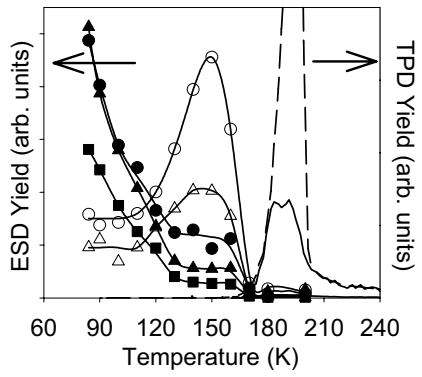

Figure 1. Temperature dependence of electron stimulated cation yields (left axis) compared to thermal desorption data (right axis). The H^+ (-○-) and H_2^+ (-Δ-) yields increase as a function of temperature, whereas the cluster ion yields (i.e. H_3O^+ (-•-), $H^+(H_2O)_2$ (-▲-) and $H^+(H_2O)_3$ (-■-) decrease. These changes occur prior to any appreciable thermal desorption of H_2O (dashed line) and molecular HCl (solid line). Note the HCl and H_2O desorption processes are correlated.

We have utilized the dependence of the ESD cation yields on the local potential to examine the details of HCl interactions on low-temperature (80- 140 K) water ice surfaces. This experiment relies upon the results of the previous task which examined the ESD of protons and

protonated clusters $(H^+)(H_2O)_n$, where n=1-8. As discussed above, these cation desorption channels involve localized two-hole states and the yields are very sensitive to the local disorder in the terminal layer of the ice. We have observed an enormous reduction of the proton signal and a concomitant increase in the protonated cluster signals due to the presence of sub-monolayer quantities of HCl. This occurs at temperatures as low as 80 K and indicates rapid uptake and non-activated autoionization of HCl. This forms ion-pair states that lead to disorder, reduced numbers of dangling bonds and increased hole-localization. These results clearly demonstrate the utility of ESD to probe the interactions of acidic molecules with low-temperature ice surfaces.

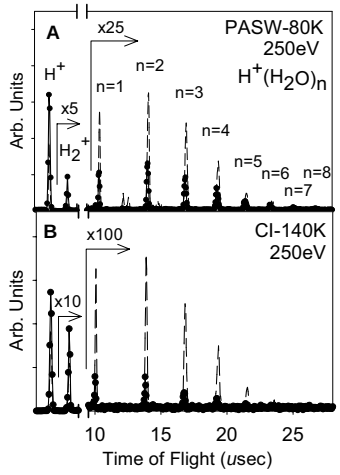

Figure 2. The time-of-flight distribution of cations produced and desorbed during pulsed 250 eV electron beam irradiation of PASW (A) and CI (B). The filled circles represent data obtained from pristine ice whereas the dashed line indicates the ion yield after the addition of 0.06 ML of HCl. The HCl ionizes causing a large reduction in H^+ and H_2^+ and an increase in $H^+(H_2O)_n$ yields.

Task 2. ***A theoretical description and experimental demonstration of diffraction in electron stimulated desorption (DESD).*** The role of diffraction in electron-stimulated desorption (DESD) is demonstrated and described theoretically [5,6]. Specifically, initial state effects in DESD of Cl^+ from Si(111)-(1×1):Cl is examined and the theory is expanded to encompass spherical-wave and multiple scattering effects of low-energy incident electrons by introducing a separable propagator method. The scattering amplitude is calculated and compared with a plane-wave approximation, which can be applied to reduce the calculation time of DESD. Qualitative analysis of Cl^+ desorption shows that the initial excitation occurring on the Si(111)-(1×1):Cl surface primarily involves the Si. Two desorption mechanisms are proposed, i) ionization of the Si(3s) level followed by Auger cascading from the σ-bonding surface state and shake-up of an electron in the non-bonding π-level and ii) direct ionization of the Si-Cl σ-bonding state. Temperature effects on DESD rates are also analyzed and modeled. The feasibility and potential utility of DESD for holographic imaging is also discussed.

Task 3. ***Low-energy electron-induced damage of DNA: Neutral fragments yields.*** We have utilized a VUV source using third-harmonic generation in rare gases to detect the neutral fragments produced during the low-energy electron beam induced damage of DNA plasmids physisorbed on graphite substrates. We are also monitoring the DNA damage using *in situ* Fourier transform infrared spectroscopy and post-irradiation gel-electrophoresis. The data indicates that negative ion-resonances of the interfacial water and substrate interactions contribute to the damage of DNA.

Future Plans:

Task 1. The role of co-adsorbates on ESD and DEA processes. We will continue our studies of low-energy electron stimulated desorption from low-temperature ice surfaces and interfaces containing co-adsorbed species. In particular, we will examine physisorbed O_2 and Cl_2 on multilayer ice. We will also examine interface structure, dynamics and electron scattering resonances associated with the presence of ions typically found in environmental and biological systems.

Task 2. Vacuum ultraviolet photo-induced processes in water films: The competition between ionization and dissociation. We plan to continue VUV based photo-ionization mass spectrometry techniques to examine the low-energy electron-induced damage of DNA plasmids and DNA strands. This work will involve very careful control (i.e. removal) of substrate effects. In addition, it will play close attention to the role intrinsic water plays in DNA damage initiated by low-energy electrons.

Task 3. Theoretical description of electron-molecule scattering with DNA and other complex organic molecules. We have used the theory developed to describe DESD from well-ordered Cl-terminated Si surfaces [5,6] to look at interference effects during the elastic and inelastic scattering of electrons with a model helical collision system constructed from of Ar scattering centers. The geometrical arrangement has been chosen to represent the B-DNA. We will continue this work by applying it to a collision system representative of the A form of DNA. We will also incorporate more realistic scattering potentials into the calculation.

References (Publications from this program)

1.) T. M. Orlando and M. T. Sieger, "The Role of Electron-stimluated production of O_2 from water ice and the radiation processing outer solar system surfaces" *Surf. Sci.* **528**, 1-7 (2003).
2.) J. Herring, A. Alexandrov, and T. M. Orlando**,** "The stimulated desorption of cations from pristine and acidic low-temperature ice surfaces" *Phys. Rev. Lett.* 92, 187602-1, (2004).
3.) J. Herring and A. Alexandrov,and T. M. Orlando "Electron-stimulated desorption of H^+, H_2^+ and $H^+(H_2O)_n$ from nanoscale water thin-films", *(accepted)*, *Phys. Rev. B.*. (2004).
4.) J. Herring, A. Alexandrov, and T. M. Orlando "Probing the interaction of hydrogen chloride on low-temperature water ice surfaces using electron stimulated desorption", (*submitted)*, *J. Chem. Phys.*
5.) T. M. Orlando**,** D. Oh, M. T. Sieger, and C. Lane, "Electron collisions with complex targets: diffraction effects in stimulated desorption", *Physica Scripta*, T110, 256, (2004).
6.) D. Oh, M. T. Sieger and T. M. Orlando, "A theoretical description of diffraction effects in electron-stimulated desorption"*(accepted), Phys. Rev. B.* (2004).

Chemical Kinetics and Dynamics at Interfaces

Non-Thermal Reactions at Surfaces and Interfaces

Greg A. Kimmel (PI) and Nikolay G. Petrik
Fundamental Science Directorate
Pacific Northwest National Laboratory
P.O. Box 999, Mail Stop K8-88
Richland, WA 99352
gregory.kimmel@pnl.gov

Program Scope

The objective of this program is to investigate non-thermal reactions at surfaces and interfaces using ultra-high vacuum, surface science techniques. The fundamental mechanisms of radiation damage to molecules in the condensed phase are of considerable interest to a number of scientific fields ranging from radiation biology to astrophysics. In nuclear reactor design, waste processing, radiation therapy, and many other situations, the non-thermal reactions in aqueous systems are of particular interest. Since the interaction of high-energy radiation (gamma-rays, alpha particles, etc.) with water produces copious amounts of low-energy secondary electrons, the subsequent reactions of these low-energy electrons are particularly important. The general mechanisms of electron-driven processes in homogeneous, dilute aqueous systems have been characterized in research over the last several decades. More recently, the structure of condensed water and its interactions with electrons, photons, and ions have been extensively studied and a variety of non-thermal reaction mechanisms identified. However, the complexity of the electron-driven processes, which occur over multiple length and time scales, has made it difficult to develop a detailed molecular-level understanding of the relevant physical and chemical processes.

We are focusing on low-energy, electron-stimulated reactions in thin water films. Our approach is to use a molecular beam dosing system to create precisely controlled thin films of amorphous solid water (ASW) and crystalline ice. Using isotopically layered films of D_2O and H_2O allows us to explore the spatial relationship between where the incident electrons deposit energy and where the electron-stimulated reactions subsequently occur within the films. Furthermore, working with thin films (0-10 monolayers [ML]) allows us to explore the role of the substrate in the various electron-stimulated reactions.

Recent Progress and Future Directions:

Electron-stimulated reactions at the interfaces of amorphous solid water films on Pt(111)
It has long been known that molecular hydrogen and oxygen are the two main reaction products from the radiolysis of water. Both products are thought to arise primarily from the diffusion-controlled chemical reactions between precursors created by energetic particles. However, in thin ASW films, which are often used as models for other aqueous systems, a somewhat different picture has emerged. We have investigated the electron-stimulated production of molecular hydrogen from thin films of ASW and crystalline ice grown on Pt(111) as a function of the thickness of the films. Using isotopically labeled films of D_2O and H_2O, we find that molecular hydrogen is produced almost entirely at the ASW/Pt and ASW/vacuum interfaces of the films:

Figure 1 shows the D_2 electron-stimulated desorption (ESD) produced during the irradiation of 30 ML thick ASW films. For these films, an H_2O cap or spacer layer was deposited on top of or beneath a D_2O layer keeping the total coverage constant. In each case, as the coverage of the cap or spacer layer increases, the D_2 production from the corresponding interface decreases exponentially. Also, when a thin layer of D_2O (e.g. 2-3 ML) is deposited on top of an H_2O layer and subsequently capped to with more H_2O to create an "$H_2O/D_2O/H_2O$ sandwich" very little D_2 is produced (data not shown).

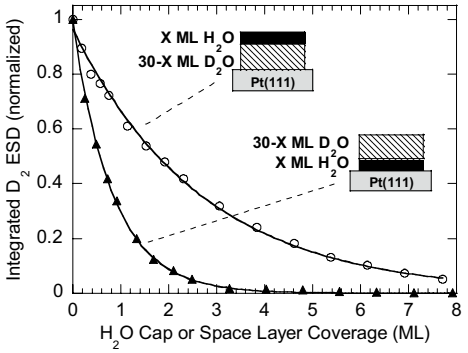

Figure 1. D_2 ESD yields from isotopically layered 30 ML thick ASW films versus the coverage of an H_2O cap (circles) or spacer (triangles) layer. The films were irradiated with 87 eV electrons at 100 K.

While the reactions leading to D_2 occur at the interfaces of the film, the energy that drives these reactions is absorbed within the penetration depth of the incident electrons in the film. Through a variety of electronic excitations, the incident electrons deposit the energy in the ASW film that drives the reactions at the interfaces. Insight into the spatial distribution of the initial excitations and the transport of energy to the interfaces can be gained by examining how the hydrogen ESD depends on the thickness of the water film. Figure 2 shows the electron-stimulated production of D_2 from 2 ML of D_2O deposited on top of an H_2O spacer layer (circles) or beneath an H_2O cap layer (triangles) versus the coverage of the H_2O cap or spacer layer. For the 2 ML of D_2O deposited on top of H_2O, the D_2 ESD yield increases monotonically with H_2O coverage and saturates for θ_{H2O} > approximately 25 ML. For just 2 ML of D_2O on the Pt(111), the D_2 ESD yield is small. However, the *D_2 ESD yield* increases substantially as the *H_2O cap layer coverage* increases. The results clearly demonstrate that the electron-stimulated production of hydrogen at the interfaces of the ASW films is not due to the diffusion of atomic or molecular species to the interfaces. Instead, electronic excitations produced by the incident electrons subsequently migrate to either interface prior to reacting. Future work will examine the role of the substrate in these electron-stimulated reactions by using different substrates such as Ru(0001) and ZrO_2.

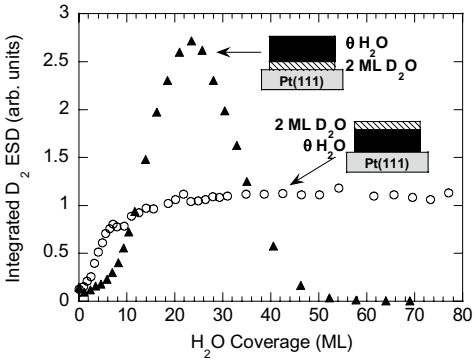

Figure 2. D_2 ESD yield from 2 ML of D_2O versus the coverage of an H_2O cap (circles) or spacer (triangle) layer. The peak in the D_2 ESD yield from the water/Pt interface at ~25 ML demonstrates the transfer of energy to that interface.

Electron-Stimulated Reactions in Thin D_2O Films on Pt(111) Mediated by Electron Trapping

To understand the role of the Pt substrate in more detail, we investigated the electron-stimulated reactions in very thin (0-10 ML) D_2O films. The results show that the electron-stimulated reactions in thick water films are qualitatively different from those for thinner films. For $1\ ML \leq \theta < \sim 2\ ML$, no reactions at the water/Pt(111) interface are observed, while for larger coverages electron irradiation leads to dissociation of water molecules *at the interface*. Figure 3 shows a series of D_2O temperature programmed desorption (TPD) spectra from D_2O films deposited on Pt(111) after the films have been irradiated at 100 K for several different fluences. For films where the $\theta < \sim 2.3$ ML, the TPD intensity decreases due to electron-stimulated sputtering of the film, but no other changes in the TPD spectra are evident. For $\theta > \sim 2.5$ ML, a new, high-temperature feature appears in the TPD spectra. Several tests clearly demonstrate that this new peak is due to D_2O interacting with D atoms adsorbed on the Pt(111). Other processes such as the electron-stimulated desorption of molecular hydrogen and oxygen, and electron-stimulated sputtering also undergo distinct changes at ~2 – 2.5 ML (data not shown).

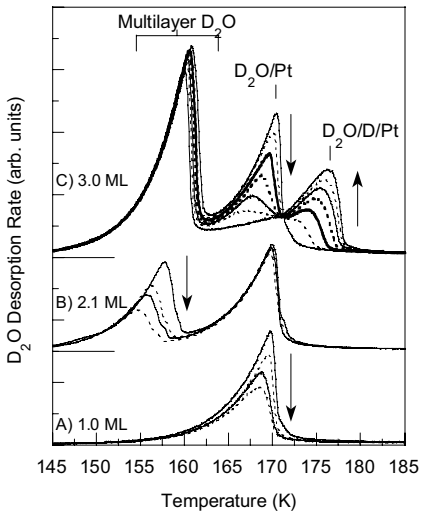

Figure 3. Post-irradiation D_2O TPD's for films with initial D_2O coverages of A) 1.0 ML, B) 2.1 ML and C) 3.0 ML. The 1 and 2 ML films are sputtered when irradiated with 87 eV electrons. For coverages greater than ~2.5 ML, electron-stimulated reactions lead to D atoms accumulation on the Pt(111).

The Pt substrate might be expected to efficiently quench electronically excited molecules adsorbed on the surface. The reaction yields would then increase in thicker films since reactions farther from the substrate are no longer quenched. However, the data show that some reactions occur within ~2 ML of the water/Pt interface but only when the water coverage is greater than 2 ML. Therefore, quenching of the electronically excited species involved in the reactions by the substrate is not the correct explanation. Furthermore, since the electronic structure of condensed water is nearly independent of coverage and only slightly perturbed from the gas phase, the cross sections for ionization, excitation, and electron attachment are not expected to change qualitatively with thickness, especially for $\theta > 1$ ML. In contrast, the trapping of low-energy electrons at surfaces and in thin films is known to depend sensitively on the properties of the surface. Since ions (H_2O^+ and H_3O^+) react preferentially with "trapped" electrons, the electron-ion recombination step is the link between the electron-stimulated reactions and the electron trapping characteristics of water films: For thin films ($\theta < 2$ ML), the electron trapping probability is low and leads to electrons localized at the vacuum interface. As a result, few electronically excited molecules are formed by electron-ion recombination. For $\theta > 3$ ML, the electron trapping probability increases and trapping now occurs in the interior of the film. The electronic excitations resulting from electron-ion recombination can subsequently migrate to *either* the ASW/Pt or ASW/vacuum interface where they drive reactions or desorption. In the future, we plan to use Fourier transform infrared spectroscopy to better characterize the reaction products in the thin films, and to investigate these processes at lower electron energies (i.e. closer to the ionization threshold for water).

References to publications of DOE sponsored research (FY 2002 – present)

1. R. S Smith, Z. Dohnálek, G. A. Kimmel, K. P. Stevenson, and B. D. Kay, "The Relationship between the Self-diffusivity of Supercooled and Amorphous Solid Water," in ACS symposium series 820, *Liquid Dynamics: Experiment, Simulation, and Theory* (2002*)*

2. Z. Dohnálek, G. A. Kimmel, D. E. McCready, J. S. Young , A. Dohnálkova, R. S. Smith, and B. D. Kay, "Structural and Chemical Characterization of Aligned Nanoporous MgO Films Grown via Reactive Ballistic Deposition," *J. Phys. Chem. B.,* **106**, 3526-3529 (2002).

3. P. Ayotte, R. S. Smith, G. Teeter, Z. Dohnálek, G. A. Kimmel, and B. D. Kay, "A Beaker without Walls: Formation of Deeply-Supercooled Binary Liquid Solutions of Alchohols from Nanoscale Amorphous Solid Films," *Phys. Rev. Lett.,* **88**, 245505 (2002).

4. Z. Dohnálek, Greg A. Kimmel, Patrick Ayotte, R. Scott Smith, and Bruce D. Kay, "The deposition angle-dependent density of amorphous solid water films," *J. Chem. Phys.* **118**, 364 (2003).

5. Nikolay G. Petrik and Greg A. Kimmel, "Electron-Stimulated Reactions at the Interfaces of Amorphous Solid Water Films Driven by Long-Range Energy Transfer from the Bulk," *Phys. Rev. Lett.,* **90**, 166102 (2003).

6. Greg A. Kimmel, Mats Persson, Z. Dohnálek, and Bruce D. Kay, "Temperature independent physisorption kinetics and adsorbate layer compression for Ar adsorbed on Pt(111)," *J. Chem. Phys.* **119**, 6776 (2003).

7. R. S. Smith, Z. Dohnálek, G.A. Kimmel, G. Teeter, P. Ayotte, J. Daschbach and B. D. Kay. 2003. "Molecular Beam Studies of Nanoscale Films of Amorphous Solid Water". Water in Confining Geometries. V Buch and J P Devlin. Springer. 337.

8. Nikolay G. Petrik and Greg A. Kimmel, "Electron-stimulated reactions in thin D_2O films on Pt(111) mediated by electron trapping," *J. Chem. Phys.* **121**, 3727 (2004).

9. Nikolay G. Petrik and Greg A. Kimmel, "Electron-stimulated production of molecular hydrogen at the interfaces of amorphous solid water films on Pt(111)," *J. Chem. Phys.* **121**, 3736 (2004).

Title: *"New Multipulse Femtosecond Techniques for the Investigation of Chemistry and Physics of the Conduction Band of Water",* Paul F. Barbara, Center for Nano and Molecular Science and Technology, 1 University Station A5300, Austin, TX 78712. p.barbara@mail.utexas.edu

PROGRAM SCOPE: This research project is focused on the investigation of delocalized charges in molecular materials. We used ultrafast spectroscopy to obtain new insights on the structure and dynamics of highly delocalized excess electron in neat liquids, micelles, and reverse micelles. Recently we have begun the investigation of highly delocalized excitonic and polaronic states in nanostructured hybrid materials and devices - which is relevant to many promising strategies for solar energy conversion. In order to deal with the tremendous heterogeneity of such materials we have turned to a new single molecule spectroscopy (SMS) technique that is a "functional equivalents" for photo-electro-chemistry and ultrafast spectroscopy.

RECENT PROGRESS: Our research has focused on the understanding of highly delocalized "conduction-band-like" excited states of solvated electrons in bulk water, in water trapped in the core of reverse micelles, and in alkane solvents. We have strived in this work to probe conduction-band-like states by a variety of novel ultrafast spectroscopy techniques. We have recorded the *optical spectrum* of the conduction band of the hydrated electron for the first time. This was accomplished by applying a photo-detrapping technique that we had developed in a previous funding cycle, but had not yet been applied to characterize the actual spectrum. In the cases of reverse micelles, we have been investigating the potential role of conduction bands in the electron attachment process and the photoinduced detrapping, and have published two papers on this topic. Finally, we have been exploring solvated electrons in isooctane from various perspectives.

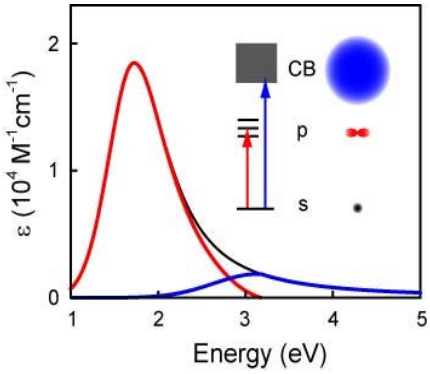

Figure 1. The optical absorption spectrum of e_{aq}^- has been decomposed into s→p (red) and s→CB (blue) components. See text for details.

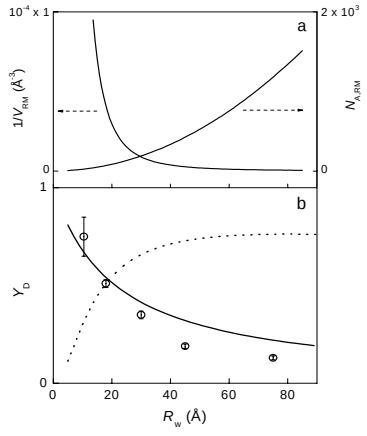

Figure 2. See text for details.

RM water pools offer a unique environment to study the effect of spatial confinement on the energetics, chemical reactions, and relaxation processes of the hydrated electron. The spectroscopy of the hydrated electron, e_{aq}, in the interior of RM have been extensively investigated by both experiment and theory. Reverse micelles have a water pool surrounded by a surfactant layer, and typically are comprised of a water/surfactant/nonpolar-solvent mixture, such as the well known water/AOT/alkane system. Solutions of well structured RM can be made reliably with a water pool radius, R_w, in the range of 10–90 Å. We used ultrafast spectroscopy to investigate the excited state dynamics and photochemistry of the hydrated electron in the water pool of a RM comprised of water and the surfactant AOT, dissolved in an isooctane solution. Solvated electrons were generated in the isooctane solvent by photoionization (3 photons of 400 nm). The isooctane solvated electrons were observed to rapidly attach to the reverse micelle and relax in the

water pool within 1 picosecond. A second 400 nm excitation pulse was employed to excite the equilibrated hydrated electron in the RM water, inducing an electron transfer ET reaction with the surfactant molecules. The ultrafast data as a function of RM size offer new insights into spatial confinement effects in the chemistry and relaxation dynamics of excess electrons in nanometer sized water pools. As shown in Figure 2 the electron transfer, ET, yield (Y_D) and ET rate monotonically decrease with an increasing water pool radius and reveal a strong dependence of the e_{CB} ET yield on R_w. As in the case of e_{CB} reactions in bulk solutions, we assume that the ET yield reflects a competition of the e_{CB} ET rate and the e_{CB} relaxation rate to the lower p and s states. A simple quantitative model for the RM ET reaction can be constructed using elements from our published treatment of ET between *hydrated electron states* and electron acceptors in bulk solution. The bulk solution model was based on the ET rates being proportional to two independent factors: (i) the electron density of the highly delocalized *hydrated electron state* at the position of the highly localized acceptor orbitals, and (ii) the number of acceptor molecules located within the effective radius of the e_{CB}.

Applying this model to the RM water pools leads to the following picture. Photo-excitation of the e_{aq} (~3 Å) located randomly in the water pool induces the ET reaction by preparing a highly delocalized e_{CB} state (>30 Å) that is electronically overlapped with the AOT acceptors at the RM edge. A simple expression for the ET rate k_{ET} within the confinement model can be simply adopted from the Kee et al. treatment of hydrated electron ET reactions in bulk water. In the Kee et al. model, the electron transfer rate per acceptor between any form of the hydrated electron and a "good" electron acceptor fits a "universal curve" as follows,

$$k_{ET,A}(r_x) = \frac{k^s_{ET,A} r^3_{e_{aq}}}{r^3_x} \qquad (1)$$

where r_x is the radius of the state in question. $k^s_{ET,A}$ is an experimentally determined constant assigned to the static electron transfer rate constant for e_{aq} using only the previously determined mean values for NO_3^-, Cd^{2+}, and SeO_4^{2-} in aqueous solutions. Using previous estimates for the CB lifetime, and as a simple expression for the yield, a prediction (Eqn. 2) for the Y_D as a function of R_w is derived with no adjustable parameters.

$$Y_D(R_w) = \frac{k_{ET}(R_w)}{k_{ET}(R_w) + 1/\tau_{CB}} \qquad (2)$$

The agreement between Eqn. 3PR (sold line) and the experiential data is excellent (see Figure 11b). This implies a spatial confinement effect may indeed be very important for the e_{CB} ET reaction in the water pool of RM.

We published a different paper on the kinetics of the attachment of isooctane solvated electrons to the water pools of the reverse micelles (water/AOT/isooctane) has been studied by ultrafast time-resolved spectroscopy. The electrons generated in isooctane by photoionization (3 photons of 400 nm) are observed to rapidly attach to reverse micelles, resulting in hydrated electrons in the water pools of the reverse micelles. **The *yield (and implied rate) of electron attachment* shows a surprisingly large dependence on R_w that is well-fit by a cubic curve.** The measured electron attachment rates (inferred from attachment yields) show a greater dependence on reverse micelle size than that predicted by a diffusion-controlled reaction model strongly suggesting that the excess conduction band like states of the RMs are the precursor to electron attachment.

Finally, we have explored the electron–cation geminate recombination mechanism of isooctane (induced by photoionization) with two and three pulse femtosecond time-resolved absorption spectroscopy. The geminate recombination kinetics are well-fit by a single exponential decay

with a time constant of 400 fs over a large photoionization pulse energy range. When the electrons in the form of the contact ion pairs are pumped by an electron pump pulse, the excited electrons return to form the relaxed contact ion pair within 30 fs and only a short delay of the neutralization process was observed. The geminate recombination rate is not affected either by varying the incident intensity of the ionization pulse or by exciting the recombining electrons with a high power near infrared pulse during the recombination process. These surprising observations strongly suggest that the geminate recombination rate is not limited by diffusive motion of the ion to form a contact ion pair (as previously believed), but rather by the electron transfer reaction rate between the ions in a Wannier-like contact ion pair.

All of these results strongly support the conclusion that optically accessible, highly delocalized electronic states exist in these various media. Indeed, this ultrafast research has partially inspired our present interest in delocalized electronic states in the context of nanomaterials, which we hope to pursue in the proposal presently being reviewed form our laboratory on **FV-TR-SMS**. Many of the most promising strategies for solar energy conversion involve charge separation of an exciton in a photovoltaic device comprised of a nanostructured composite of various types. Our groups uses novel *single molecule (particle) modulation spectroscopy techniques* to investigate photoinduced charge separation and charge transfer reactions in model photovoltaic solar energy devices based on nanoparticles. Single molecule electron transfer rate constants k_{et} and other aspects of the kinetics and dynamics are being studied using coordinated and simultaneous single molecule spectroscopy and device modulation (E-field, excitation intensity, etc). This approach is a new single molecule spectroscopy (SMS) "functional equivalents" for photo-electro-chemistry and ultrafast spectroscopy. Preliminary FV-TR-SMS results on nanoparticles in model photovoltaic devices demonstrate that these methods are well suited to study the kinetics of photoinduced charge separation and transfer at the molecular level, and will allow us investigate in the proposed research critical unresolved issues regarding how charge separation and charge transfer processes depend upon chemical structure, morphology and the physical state (e.g. charging) of the layers and interfaces.

FUTURE PLANS: We propose to use novel *single molecule (particle) modulation spectroscopy techniques* to investigate charge separation and charge transfer reactions in model photovoltaic solar energy devices. Single molecule electron transfer rate constants k_{et} and other aspects of the kinetics and dynamics will be studied using **coordinated and simultaneous single molecule spectroscopy and device modulation** (E-field, excitation intensity, etc). **We believe that this general strategy will ultimately lead to new tools that are SMS "functional equivalents" for electro-chemistry, and ultrafast spectros-copy.** These novel SMS experimental techniques have enormous potential for solar energy research offering, in principle, unprecedented time and spatially resolved information on the "local" structure and dynamics of nanostructured materials and devices.

The first SMS modulation technique for charge transfer research was recently developed in the PI's laboratory, namely fluorescence voltage single molecule spectroscopy (**FV-SMS**) (see Figure 3). In **FV-SMS** the single molecule spectroscopy of nanoparticles imbedded in an electronic device is measured as a function of electrical bias which controls the concentrations of charges in the device. **FV-SMS** gives electrochemistry like information on nanoparticles, and is particularly well suited for studying the "blinking" of nanoparticles induced by photochemistry, e.g. photooixidation. Figure 3 is a simple example of a **FV-SMS** device. Here insulators are used in the bottom layers to restrict the device to top electrode injection (hole polarons only) for simplicity, which aids in the analysis.

This DOE proposal takes a new and distinct direction by combining FV-SMS with *light intensity modulation and/or pulsed lasers* to create a set of time resolved spectroscopic techniques, i.e. Fluorescence Voltage-Time Resolved-Single Molecule Spectroscopy (FV-TR-SMS). Preliminary FV-TR-SMS results demonstrate that these new methods are well suited to study the kinetics of photoinduced charge separation and transfer at the molecular level. We are particularly interested in elucidating how electron delocalization can influence the rates and mechanism of reaction occurring within a single nanoparticle and across an *imbedded interface* of a nanoparticle with donor or acceptor layers. Materials under investigation will include various nanoparticle materials (conjugated polymers, molecular nanocrystals of conjugated organics, and inorganic/ conjugated polymer nanoparticle composites) imbedded in model photovoltaic multilayer devices with hole and electron transport layers. The devices will be analogous to that shown in Figure 1 but will often involve both hole and electron transport layers.

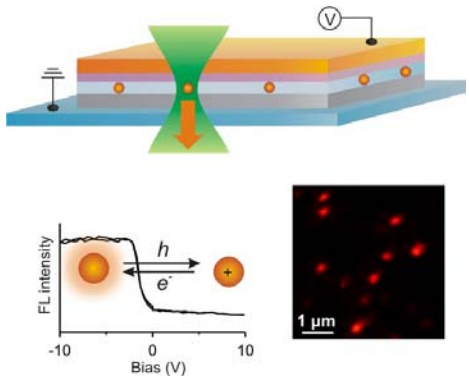

Figure 3. Configuration of a typical **FV-SMS** setup and **FV-SMS** data for prototypical conjugated polymer nanoparticles. The purple layer is a hole transport layer (TPD).

Recent Publications Resulting from this Research:

"Conduction Band Spectrum of the Hydrated Electron", Tak W. Kee, Young Jong Lee" and Paul F. Barbara, Science, *submitted* (final revision requested from editor).

"The Mechanism of Electron–Cation Geminate Recombination of Liquid Isooctane", Tieqiao Zhang, Young Jong Lee, Tak W. Kee, and Paul F. Barbara, Chem. Phys. Lett., (final revision requested from editor).

"Kinetics of Electron Attachment to Reverse Micelles" , Young Jong Lee, Tieqiao Zhang and Paul F. Barbara, J. Phys. Chem. B (Letter), 108, 5175 (2004)..

"Pump-Probe Spectroscopy of the Hydrated Electron in Reverse Micelles", Young Jong Lee, Tak W. Kee, Tieqiao Zhang and Paul F. Barbara, J. Phys. Chem. B, 108, 3474(2004).

"Solvation dynamics of the hydrated electron depends on its initial degree of electron delocalization", Patanjali Kambhampati, Dong Hee Son, Tak W. Kee, and Paul F. Barbara, J. Phys. Chem. A, 106, 2374(2002).

Structure and Dynamics of Chemical Processes in Water Clusters – DE-FG02-00ER15066

K. D. Jordan Dept. of Chemistry, University of Pittsburgh, Pittsburgh, PA. 15260
and M. A. Johnson, Dept. of Chemistry, Yale University, New Haven CT 06520

Our joint program exploits size-selected cluster spectroscopy and electronic structure theory to reveal the molecular level details of transient aqueous molecular ions and radicals as well as the hydrated electron. We are particularly interested in those species, such as $H^+ \cdot (H_2O)_n$ and $OH^- \cdot (H_2O)_n$, that are intrinsic to proton transport through water. Articles describing our results on both of these cluster systems have been published in *Science*[1,2] each of which appeared along with an accompanying *Perspective* article.[3,4] Our recent vibrational spectroscopic work on the hydrated electron clusters has provided the breakthroughs needed to (finally!) determine the network structures of the water molecules that bind an electron.[5-7] This information, in turn, guided a theoretical analyses of the formation pathways.[8,9] We focus this overview on these recent results, where the manuscripts have been submitted but are presently still out for review.

How water networks accommodate an excess electron

It is well established that the anions of water clusters with sizes n = 2,6,7 and ≥ 11 are much easier to form than those with n = 3-5, 8-10. However, even for the easily formed anions, it has proven surprisingly difficult to establish the morphologies of the associated water networks. Early spectroscopic work in the OH stretching region (2400 – 4400 cm^{-1}) demonstrated that the spectra of the anions were dramatically different from those of the analogous neutral clusters, with the anions being dominated by an intense doublet strongly red-shifted from the free OH stretch and persisting over the range n = 5-11.[10,11] Most effort was concentrated on the hexamer anion, with the structures advanced by various groups depicted in Fig. 1.

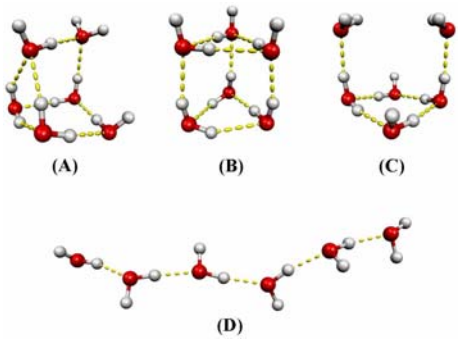

FIG. 1. Various geometries for the water hexamer anion proposed in the literature.

Two years ago, we set out to unambiguously establish the vibrational motions that were responsible for the strong doublet and to determine the structures of the anions. This effort consisted of three parts. First, a new experiment was designed to determine which isomer of the neutral hexamer was responsible for anion formation.[7] Armed with this information, we were able to establish theoretically that there is a pathway with no net barrier starting from the neutral precursor to the global minimum of the anion.[8] Second, we extended the wavelength range of our infrared spectrometer to much lower energy (800 – 1800 cm^{-1}), enabling us to measure the patterns of intramolecular bending transitions.[5] These bands provide complementary information to that contained in the pattern of OH stretching transitions determined previously. Moreover, the bending patterns are intrinsically simpler to interpret because there is only one bending transition for each water molecule. And third, we developed synthetic methodologies to efficiently prepare the smaller "missing" clusters, with special emphasis on the tetramer anion.[6] By working with smaller, and hence simpler systems, we are able to much better confine the possible structures since far fewer isomers are available to the system.

To identify the neutral precursor that attaches an electron to form the "magic" n = 6 anion, we modified our instrument so that slow electrons were injected into the beam after the cluster formation step was complete. This arrangement allowed us to introduce a laser pulse prior

to electron attachment and photodissociate most of the argon-solvated neutral clusters with resonant absorptions at a particular wavelength:

$$(H_2O)_n \cdot Ar_m + h\nu \rightarrow (H_2O)_n \cdot Ar_p + (m\text{-}p)Ar. \quad (1)$$

When this photodepleted $(H_2O)_n \cdot Ar_m$ cluster is a precursor for the formation of the anion:

$$(H_2O)_n \cdot Ar_m + e^- \rightarrow (H_2O)_n^- \cdot Ar_q + (m\text{-}q)Ar \quad (2)$$

there is an accompanying depletion of the product $(H_2O)_n^- \cdot Ar_q$ ion, which is detected after mass-selection. Thus, by tuning the mass spectrometer to monitor this peak intensity and scanning the laser, we obtain a spectrum of the neutral cluster responsible for anion formation. Because we detect a cluster anion with argon atoms attached, and argon atoms are much more weakly bound than a water molecule, the resulting spectrum of the neutral water cluster is also size-selected (*i.e.*, without contamination by fragmentation). The observed spectrum for the hexamer is displayed in Fig. 2. Theoretical analysis carried out by the Jordan group establishes that this is a so-called "book" form of the neutral, which had not been previously reported experimentally.[8] Having established that the book isomer is the key species leading to the anion, it is unlikely that the anion formed is the chain species proposed earlier (Fig. 1D), leaving the other, more compact isomers as the more plausible structural candidates.

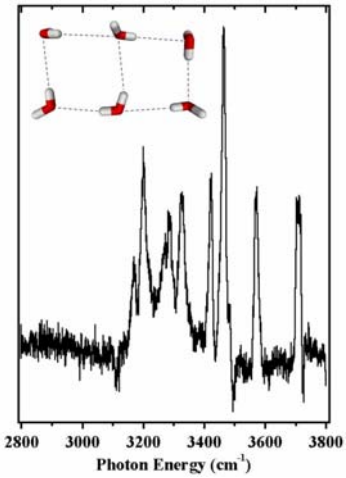

FIG. 2: Mid – infrared spectrum of the neutral precursor to the water hexamer anion. Analysis of the spectrum confirms that the book isomer (inset) is the key species.

Even with the positive identification of the neutral precursor, the OH stretching spectra are still too complicated to yield a unique structural assignment for the hexamer anion. We therefore extended our study to include the smaller anions. The tetramer anion had not been studied earlier because it is usually reported as "missing" in the cluster distribution. We succeeded in generating this (and other) species efficiently (and rationally) through the use of argon cluster-mediated association of water molecules to the dimer anion[6]:

$$(H_2O)_2^- \cdot Ar_p + mH_2O \rightarrow (H_2O)^-_{(m+2)} \cdot Ar_k + (p\text{-}k)Ar. \quad (3)$$

This approach overcomes the previous synthetic bottleneck that the electron affinities of the bare clusters are so small that addition of a water molecule simply causes the electron to evaporate, destroying the cluster anion. In our method, rapid evaporation of argon atoms dominates this destructive loss mechanism and thus preserves the cluster anions.

The crucial spectral data that lead to a structural identification for the larger clusters was obtained from the tetramer anion. This is the smallest system observed to yield sharp spectra, and therefore was also the simplest system in which to establish the structures responsible for the various spectral motifs. Even in this smallest regime, however, unambiguous structural identification required correlating the intramolecular bending and the OH stretching bands. To acquire the critical bending band patterns, we had to first modify our IR laser with an additional non-linear mixing stage based on parametric conversion in the delicate $AgGaSe_2$ crystal.

Determination of the bending and stretching band patterns had to be performed with isotopic labeling schemes to avoid severe line broadening that occurs when the stretching vibrations lie above the low-lying direct electron detachment continua of the small cluster anions. Thus, the OD stretching bands could be observed in the lower energy deuterium analogues, $(D_2O)_4^- \cdot Ar_m$. However, we then had to switch to the $(H_2O)_4^- \cdot Ar_m$ species in order to recover the bending pattern because the D_2O bending frequencies were out of the spectrometer's energy range. The resulting spectra are displayed in Fig. 3A and 3B, along with calculated patterns for the structure indicated in Fig. 3C and 3D.

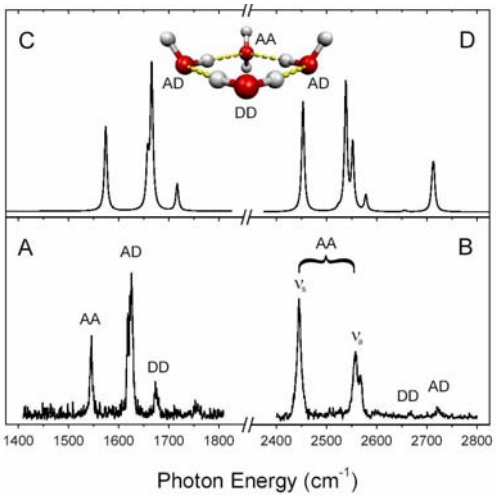

FIG. 3: Comparison of the experimental (lower) and theoretical (upper) spectra for the water tetramer anion. Spectra A and C refer to $(H_2O)_4^-$ in the water bending region, while B and D correspond to the $(D_2O)_4^-$ isotopomer in the OD stretching region.

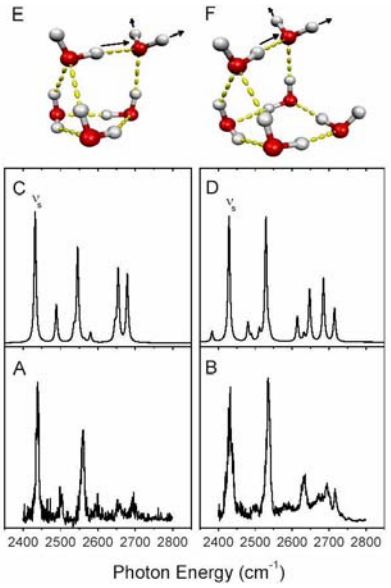

FIG. 4: Experimental spectra for the water pentamer (A) and hexamer (B) anions in the OD stretching region, along with the calculated spectra (C and D) for the structures indicated in the upper panel. The displacement vectors associated with the dominant low-energy symmetric stretches, υ_s, are included in the structures.

Most importantly, the strong doublet observed in the OH stretching spectra of the larger (n = 5-11) clusters is also found in the tetramer spectrum, where it is assigned to the symmetric and asymmetric stretching vibrations of a single water molecule bound to the cyclic framework with double acceptor (AA) motif. This arrangement allows both of its hydrogen atoms to point directly into the electron cloud. It is remarkable that the diffuse electron can induce such a significant red-shift in these otherwise "free" OH groups, a circumstance that lead to some of the earlier confusion. With this assignment in hand, we also carried out combined HOH bend/DOD stretch spectra for n = 5 and 6, and in each case we were able to extract unique structures with the results shown in Fig. 4. All of these structures feature a unique AA water molecule that is oriented directly at the electron cloud, and the vibrational motions of its hydrogen atoms largely account for the observed strong doublet. Thus, the binding site appears to be conserved with increasing cluster size, with the additional water molecules adding to the backside of the cluster, away from the diffuse electron. The structural identifications for the n = 4-6 cluster anions are important, as the binding site is now revealed. This opens a number of interesting avenues for further study.

References (published and accepted papers acknowledging DOE support are denoted by *):

*1. J.-W. Shin, N. I. Hammer, E. G. Diken, M. A. Johnson, R. S. Walters, T. D. Jaeger, M. A. Duncan, R. A. Christie, and K. D. Jordan, "Infrared signature of structures associated with the $H^+(H_2O)_n$, n = 6-27, clusters", *Science*, 304, 1137 (2004).

*2. W. H. Robertson, E. G. Diken, E. A. Price, J.-W. Shin, M. A. Johnson, "Spectroscopic determination of the OH^- solvation shell in the $OH^- \cdot (H_2O)_n$ clusters", *Science*, 299, 1367 (2003).

*3. W. H. Robertson, E. G. Diken, M. A. Johnson, "Snapshots of water at work", *Science*, 301, 320 (2003).

4. T. Z. Zwier, "Enhanced: The Structure of Protonated Water Clusters", *Science*, 304, 1119 (2004).

5. N. I. Hammer, J.-W. Shin, J. Headrick, E. G. Diken, G. H. Weddle, and M. A. Johnson "How water networks accommodate an excess electron: Structure and dynamics of the binding site", *Science*, submitted (2004).

6. J.-W. Shin, N. I. Hammer, J. M. Headrick, and M. A. Johnson, "Preparation and photoelectron spectrum of the "missing" $(H_2O)_4^-$ cluster", *Chem. Phys. Lett.*, submitted (2004).

*7. E. G. Diken, W. H. Robertson, and M. A. Johnson, "The vibrational spectrum of the neutral $(H_2O)_6$ precursor to the "magic" $(H_2O)_6^-$ cluster anion by argon-mediated, population-modulated electron attachment spectroscopy", *J. Phys. Chem. A*, 108, 64 (2004).

*8. E. M. Myshakin, K. Diri, and K. D. Jordan, "Theoretical investigation of the neutral precursor of $(H_2O)_6^-$", *J. Phys. Chem. A.*, in press.

9. E. M. Myshakin and K. D. Jordan, "Comments on the mechanism of formation of the $(H_2O)_n^-$, n = 3-8, ions", in preparation.

10. P. Ayotte, G. H. Weddle, C. G. Bailey, M. A. Johnson, F. Vila, and K. D. Jordan, "Infrared spectroscopy of negatively charged water clusters: Evidence for a linear network", *J. Chem. Phys*. 110, 6268 (1999).

11. P. Ayotte, C. G. Bailey, J. Kim, and M. Johnson, "Vibrational predissociation spectroscopy of the $(H_2O)_6^- \cdot Ar_n$, $n > 6$, clusters", *J. Chem. Phys*. 108, 444 (1998).

*12. E.M. Myshakin, K.D. Jordan W.H. Robertson, G.H. Weddle, and M.A. Johnson, "Dominant Structural Motifs of $NO^-(H_2O)_n$ complexes: Infrared spectroscopic and ab initio studies", J. Chem. Phys., **118**, 4945-4953 (2003).

*13. E. M. Myshakin, K. D. Jordan, E. L. Sibert, III, and M. A. Johnson, "Large Anharmonic Effects in the Infrared Spectra of the Symmetrical $CH_3NO_2^-(H_2O)$ and $CH_3CO_2^-(H_2O)$ Complexes", J. Chem. Phys., **119**, 10138 (2003).

*14. F. Wang and K. D. Jordan, "Theory of Dipole-Bound Anions", Annual Reviews of Physical Chemistry, **54**, 367 (2003).

*15. W.H. Robertson, K. Karapetian, P. Ayotte, K.D. Jordan, and M.A. Johnson, "Infrared Predissociation Spectroscopy of $I^-(CH_3OH)_n$, Cooperativity in Asymmetric Solvation", J. Chem. Phys., **116**, 4853 (2002).

*16. W. H. Robertson, M. A. Johnson, Y. M. Myshaken, and K. D. Jordan, "Evaluation of the Charge-Transfer component of the Anionic H-bond via Spin Suppression of the Intra-Cluster Proton Transfer Reaction in the NO^--H_2O Entrance Channel Complex", J. Phys. Chem., **106**, 10010 (2002).

*17. W.H. Robertson and M. A. Johnson, "Molecular Aspects of Halide Ion Hydration: The Cluster Approach," Annual Reviews of Physical Chemistry, **54**, 173-213 (2003).

*18. J.A. Kelley, G. H. Weddle, W. H. Robertson, and M. A. Johnson, "Linking the photoelectron and infrared spectroscopies of the $(H_2O)_6^-$ isomers." *J. Chem. Phys*., **116**, 1201-1203 (2002).

Dynamics of Electrons at Molecular Interfaces on the Femtosecond Timescale

Charles B. Harris, P.I.
Chemical Sciences Division,
Lawrence Berkeley National Lab
1 Cyclotron Road, Mail Stop Latimer,
Berkeley, CA 94720
CBHarris@lbl.gov

Program scope

This is a comprehensive program to study the properties of electrons at molecule/metal interfaces on the femtosecond timescale and the nanometer lengthscale. We examine a broad variety of systems (examples include atomic adsorbates, polymer oligomers, and model solvents) and phenomena (electron solvation and localization, the band structure of interfaces, and the electronic coupling of adsorbates to a metal substrate) with both experiment and theory.

Our primary experimental technique is angle-resolved two-photon photoemission (2PPE). Briefly, a femtosecond laser pulse excites electrons from the valence band of a Ag(111) substrate to the interface with an adsorbed molecular film (typically 1–3 monolayers thick). Some delay time later, Δt, a second laser pulse photoemits the electron, sending it to a time-of-flight detector. From the kinetic energy of the electron and the photon energy of the probe pulse, we can deduce the binding energy of the electronic state. The wavelength dependence of the photoemission spectrum tells whether the state is initially occupied, unoccupied, or a final state resonance.

This technique also gives us access to a wealth of information about the electron's dynamics. The kinetics of population decay and dynamical energy shifts (two-dimensional electron solvation) are determined with < 35 meV energy resolution and ~ 100 fs time resolution. An additional experimental degree of freedom is the angle between the surface normal and the detector. Only electrons with a specific amount of momentum parallel to the surface will reach the detector. The energy versus parallel momentum (the dispersion) gives the effective mass of the electron, m^*. For localized electrons ($m^* \gg 1$) the amplitude of the signal versus parallel momentum can give an estimate of the spatial extent of localization in two dimensions.

Two-photon photoemission accesses both electronic states of the molecular film, such as the highest occupied molecular orbital (HOMO) and the lowest unoccupied molecular orbital (LUMO), as well as states intrinsic to the surface. Image-potential states (IPS) are an important example of the latter. The IPS electrons are bound a few angstroms from the metal surface, making them sensitive probes of the electronic structure and dynamics of monolayer adsorbate films. In the direction parallel to the surface, however, the IPS electrons are free-electron-like, in most cases. Interactions with any disorder of the surface or with the dynamic motions of adsorbates can localize the electron in the plane of the surface.

Recent progress

Self-assembeled monolayers—Methylthiolate/Ag(111) : Dimethyldisulfide dissociatively chemisorbs on Ag(111), causing the S–S bond to break and two Ag–S chemical bonds to form. Monochromatic 2PPE is able to access the HOMO and the LUMO of this chemical bond and probe their properties as a function of the surface density. The Ag–S LUMO is very sensitive to the structure of the thiolate film. This sensitivity shows not in the binding energies of the states, but, rather, their dispersions. At low coverages, approximately 1 langmuir exposure, the Ag–S LUMO has a very large effective mass, indicating that the

state is localized. At intermediate coverages, (2.5 langmuirs exposure), the localized electrons are accompanied by delocalized electrons which have an effective mass $m^* = 0.5\ m_e$. Finally, at a saturated monolayer (4 langmuirs), there are only delocalized electrons. This can be understood using the phase diagram and self-assembly phase transition of the thiolate covered surfaces. At low surface densities, the methylthiolates lie mostly flat to the surface where they are a mobile "lattice gas". Here, each S–Ag bond is isolated from the others, and the states are highly localized. As the surface density increases, the nearest-neighbor distance between molecules decreases. When this distance becomes approximately the size of a molecule (the surface is saturated) then the molecules self-assemble into a compressed "standing up" phase which reduces the distance between the neighboring S–Ag bonds. When the overlap between neighboring sulfur atoms increases sufficiently, the LUMO is able to form a delocalized band.

Electron solvation and localization at interfaces : Electrons photoexcited to the metal surface can interact with the permanent dipole of adsorbate molecules. The interfacial electron perturbs the equilibrium geometry of the adsorbate molecules, which then reorganize to accomodate and energetically stabilize the new charge distribution. Essentially, this is a two-dimensional analogue of electron solvation in liquids. We have studied both polar and nonpolar adsorbates, and we have observed a wide variety of behaviors ranging from local workfunction changes (in butanol, for example) to electron solvation concomittant with localization (in nitriles). Observing the interplay of solvation and localization in two dimensions is an exciting experimental breakthrough (Figure 1).

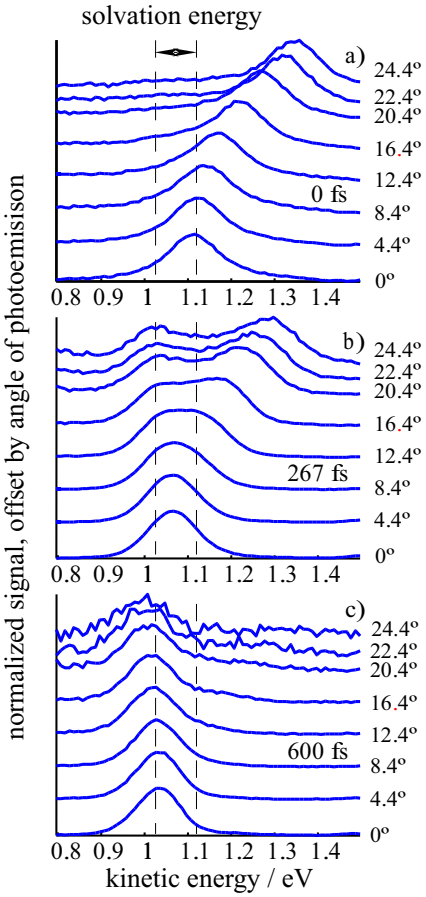

Figure 1: In 2 monolayers of butyronitrile/Ag(111), the $n = 1$ IPS is a) initially delocalized; b) the delocalized state begins to solvate as a localized feature appears; c) only a localized state remains.

We have examined thin films of alcohols on Ag(111) as models of protic solvents on metal electrodes. Notably the first monolayer of alcohol films solvates the electron very little, while thicker films solvate more. To further elucidate the molecular mechanisms for the timescales of the interfacial electron solvation, we have performed molecular dynamics simulations that treat the molecules classically and the electron quantum mechanically. Simulations of a model methanol/Pt(100) interface show that the equilibrium solvation dynamics differ from the bulk due to differences in the solvent cavity in the interfacial environment. The first monolayer is rigidly bound to the the Pt surface, while subsequent layers are more free to respond to the electron, creating a solvent cavity that is larger than the bulk.

Nitriles are archetypal aprotic solvents. Electron solvation dynamics at nitrile/Ag(111) interfaces are influenced critically by both the length of the nitrile's alkyl chain and the thickness of the overlayer. Inhomogeneity in the film leads to a spread in the binding energies of the IPS electrons, which is strongly correlated with a distribution of electron spatial extents. Disorder of the film can also dominate the dynamics, in some circumstances, and create electrons which are localized

at $\Delta t = 0$, while in other cases the electrons are intially delocalized and dynamically localize over several hundreds of femtoseconds. The initial condition on the electron (localized or delocalized) seems to have a pronounced effect on the subsequent solvation dynamics. Namely, the intially localized electrons have a larger total relaxation energy and relax at a higher rate. We are just beginning to unravel some of the many themes that contribute to the richness of interfacial solvation dynamics.

Spatial extent of localized electrons : If an electron localizes, the natural question is, "How big is it?" We have shown that the amplitude of the 2PPE signal as a function of parallel momentum can give an estimate of the spatial extent of the localized electron (rigorously, a lower bound). This is essentially Heisenberg's Uncertainty Principle, where a wavefunction's spread in momentum space is related to its spread in real space by a Fourier transform (Figure 2). Illustrative calculations that propagate a wavepacket in the presence of a localizing potential have shown that the width of the wavepacket in momentum space is not significantly perturbed by scattering effects as it departs from the surface if the well is not too deep. Thus, the localization estimate is reasonably accurate in our experiments.

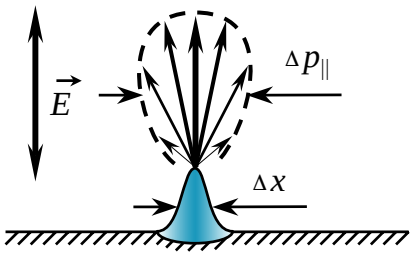

Figure 2: The 2PPE signal as a function of angle gives an estimate of the spatial extent of a localized IPS. The more tightly localized a state is, Δx, the broader its momentum distribution, $\Delta p_{\|}$, will be upon photoemission.

Fullerenes/Ag(111)—two-color 2PPE : Two-color experiments of C_{60}/Ag(111) probe the mechanism of photoexcitation and photoemission and the nature of the excited electronic states of these films. The states have been previously interpreted as being solely due to intramolecular excitations (Frenkel excitons). Our recent results, however, show that metal-to-molecule excitations can be significant. This is an important issue in understanding the properties of related interfaces used in molecular electronic devices.

Future work

Molecular electronics—PTCDA and fluorene oligomers : PTCDA is a model system for the burgeoning field of molecular electronics. It has a truly epitaxial growth on Ag(111), and the occupied electronic structure is fairly well understood. The unoccupied electronic structure and, especially, the dynamics, on the other hand, have not been explored. 2PPE may shed light on the the mechanism(s) of optical excitation (intramolecular or metal-to-molecule) and the nature of the molecular excited states of these films as a function of the layer thickness.

Polyfluorenes are blue-emitting polymers for organic light emitting diodes (OLEDs), but the nature of charge injection from the cathode into these systems is somewhat mysterious. 2PPE of films of fluorene oligomers as a function of oligomer chain length and the side-group functionalization may give details of optical charge injection in this promising technological system.

DMSO/Ag(111) : Our solvation results for nitriles can be extended by comparing them with DMSO. Acetonitrile and DMSO have very similar dipole moments and dielectric constants, yet they behave very differently as electrochemical solvents. Preliminary 2PPE results of one monolayer of DMSO/Ag(111) show that the DMSO monolayer does not solvate the IPS electrons, but the multilayer solvates a great deal and dynamically localizes the electrons. This is an important contrast to nitriles, which solvate and localize IPS electrons at all coverages. This is a direct, molecular scale probe of the contrasting differential capacitance of these two molecules as measured in electrochemistry.

Intraband relaxation : Intraband relaxation of delocalized IPS electrons is omnipresent in 2PPE. The kinetics of population decay as a function of parallel momentum show that electrons quickly relax to the bottom of the IPS band in many different adsorbate systems. Nevertheless, the process is not well understood. The simplest organizing principle to understand these many observations is friction. We are developing the theory to extract friction constants from the 2PPE results and the theory to describe the cause of the friction. Finally, these methods will be extended to further elucidate the mechanism of electron localization, which may be concomittant with intraband relaxation or even provide a channel for it.

H_2O/MgO/Ag(111) : MgO/Ag(100) provides an excellent model system to study oxide/metal interfaces with electron spectroscopies like 2PPE because of its epitaxial growth ($\sim 2.9\%$ lattice mismatch) and controllable stoichiometry. The water/MgO/Ag(100) system also serves as an interesting environment to explore interfacial adsorbate dynamics. Two ordered monolayer phases, each distinct from the ice-like bilayer that forms on Pt(111) and with different densities, can be prepared on MgO(100). 2PPE can probe this interface, supported by the silver substrate, in a manner similar to previous electron solvation experiments. The substrate–adsorbate interaction can be strengthened even further by varying the oxide thickness to modify its reactivity. The combination of controlled, ultrahigh vacuum surface science with ultrafast laser spectroscopy is thus capable of examining surface properites and dynamics on a system relevant to photochemistry, electrochemistry, and heterogeneous catalysis.

Articles supported by DOE funding 2002–2004

[1] I. Bezel, K. J. Gaffney, S. Garrett-Roe, S. H. Liu, A. D. Miller, P. Szymanski, and C. B. Harris. "Measurement and dynamics of the spatial distribution of an electron localized at a metal–dielectric interface." *J. Chem. Phys.*, **120**, 845 (2004).

[2] P. Szymanski, S. Garrett-Roe, and C. B. Harris. "Time- and angle-resolved two-photon photoemission studies of electron localization and solvation at interfaces." *Prog. Surf. Sci.*, **accepted** (2004).

[3] C. B. Harris, P. Szymanski, S. Garrett-Roe, A. D. Miller, K. J. Gaffney, S. H. Liu, and I. Bezel. "Electron solvation and localization at interfaces." In "Proc. SPIE," volume 5223, pages 159–168 (2003).

[4] P. T. Snee, S. Garrett-Roe, and C. B. Harris. "Dynamics of an excess electron at metal/polar interfaces." *J. Phys. Chem. B*, **107**, 13608 (2003).

[5] I. Bezel, K. J. Gaffney, S. Garrett-Roe, S. Liu, A. D. Miller, P. Szymanski, and C. B. Harris. "The size of a localized electron at a metal/adsorbate interface." In "Thirteenth International Conference on Ultrafast Phenomena," volume 72, pages 430–431. Opt. Soc. America (2002).

[6] S. H. Liu, A. D. Miller, K. J. Gaffney, P. Szymanski, S. Garrett-Roe, I. Bezel, and C. B. Harris. "Direct observation of two-dimensional electron solvation at alcohol/Ag(111) interfaces." *J. Phys. Chem. B*, **106**, 12908 (2002).

[7] A. D. Miller, I. Bezel, K. J. Gaffney, S. Garrett-Roe, S. H. Liu, P. Szymanski, and C. B. Harris. "Electron solvation in two dimensions." *Science*, **297**, 1163 (2002).

[8] A. D. Miller, K. J. Gaffney, S. H. Liu, P. Szymanski, S. Garrett-Roe, C. M. Wong, and C. B. Harris. "Evolution of a two-dimensional band structure at a self-assembling interface." *J. Phys. Chem. A*, **106**, 7636 (2002).

THEORY OF THE REACTION DYNAMICS OF SMALL MOLECULES ON METAL SURFACES

Bret E. Jackson

Department of Chemistry
University of Massachusetts
Amherst, MA 01003
jackson@chem.umass.edu

Program Scope

Our objective is to develop realistic theoretical models for molecule-metal interactions important in catalysis and other surface processes. The dissociative adsorption of diatomics on metals, Eley-Rideal and Langmuir-Hinshelwood reactions, recombinative desorption and sticking on surfaces are all of interest. To help elucidate the UHV-molecular beam experiments that study these processes, we examine how they depend upon the nature of the molecule-metal interaction, and experimental variables such as substrate temperature, beam energy, angle of impact, and the internal states of the molecules. Electronic structure methods based on Density Functional Theory are used to compute the molecule-metal interaction potentials. Both time-dependent quantum scattering techniques and quasi-classical methods are used to examine the reaction dynamics. Some effort is directed towards developing improved quantum scattering methods that can adequately describe reactions on surfaces, as well as include the effects of temperature (lattice vibration) in quantum dynamical studies.

Recent Progress

Much of our recent work has focused on Eley-Rideal (ER) and hot atom reactions. In an ER reaction, a gas-phase particle combines directly with another particle adsorbed onto a substrate. These reactions are often very exothermic. Following extensive studies of H atom reactions on metal surfaces we began to explore the H(g) + H/graphite ER reaction. This reaction is believed to play an important role in the formation of molecular Hydrogen on graphitic dust grains in interstellar space, as well as the etching of the graphite walls of fusion reactors. Using electronic structure methods, we demonstrated that an H atom could chemisorb onto a graphite surface, with the bonding C atom puckering out of the surface plane by several tenths of an Å [1]. We also computed the potential energy surface for the ER reaction of an incident H atom with this chemisorbed H atom, and showed that the reaction cross sections were very large – on the order of 10 $Å^2$ [1,3]. Motivated by our studies, the group of Küppers (Bayreuth) demonstrated experimentally that H could indeed chemisorb, and that the lattice did pucker [6]. We computed adsorbate vibrational frequencies and (recombinative) thermal desorption temperatures, and these were found to be in excellent agreement with experiment [6]. Küppers and co-workers then measured the cross sections for the H(g) + D/graphite ER reaction to form HD(g), while we computed the same. Again, theory and experiment were in excellent agreement [7]. We demonstrated that the H_2 formed in these ER reactions should be very highly excited, vibrationally. It has been suggested that vibrationally excited H_2 might be responsible for some of the unique chemistry that occurs in interstellar clouds.

We continued our studies of ER and hot atom reactions between H atoms on metals. In a hot atom (HA) reaction the incident particle traps onto the surface without reacting, forming a mobile precursor which may react with an adsorbate at a later time. If such a reaction occurs before the mobile precursor has fully relaxed, the products can be "hot," as

in the more direct ER reactions. In a study of H atom recombination on Ni(100), we allowed the lattice atoms to move, which required that we construct a potential energy surface based upon the instantaneous positions of the lattice atoms and the adsorbates [5]. We avoided the usual problems associated with pairwise potentials by using a potential based upon ideas from embedded atom and effective medium theory, but instead of using the isolated atom electron densities, we fit the one and two-body terms to reproduce the results of our high-level electronic structure calculations. Quasiclassical simulations of gas phase H (or D) reacting with adsorbed D (or H) were implemented. These were the first theoretical studies to look at the variation in ER and HA reactivity with respect to changes in the surface coverage, and they helped to construct the kinetics model described in the following paragraph. Our potential form also allowed for H atoms to penetrate into, and/or re-emerge from, the substrate before reacting or trapping. The reactions were mostly of the HA variety, and comparison with experiment was good.

Most of the experiments which examine these ER and HA reactions on metals are kinetics studies, exposing H or D-covered surfaces to H or D atomic beams, and measuring the rate of H_2, HD and D_2 formation as the surface coverage changes over seconds or minutes. In order to understand these experiments, we developed a kinetic model for ER and HA reactions that relates our (picosecond time scale) reactive scattering studies with the long time kinetics [2]. The model is based on a few simple ideas extracted from our classical and quantum calculations, such as the reaction probability or energy transfer per HA-adsorbate encounter. We were able to derive analytic expressions for reaction rates, saturation coverages, and product yields as a function of surface coverage. Agreement with the kinetics experiments was good [2].

We have implemented electronic structure and transition state theory studies of the resurfacing of H atoms from the bulk of Ni onto the Ni(111) surface [4]. These atoms are energetically "hot" and can engage in unique chemistry with adsorbates on the surface. Our computed resurfacing temperature is in excellent agreement with that observed by experiment. We have more recently discovered (ms in preparation) that the barriers to the resurfacing of H atoms from the bulk are strongly dependent on the surface H coverage. We have also computed the potential energy surfaces for reactions between these hot resurfacing atoms and surface-adsorbed H, as a function of surface coverage. We are considering quasiclassical trajectory studies in order to understand some very interesting experimental studies from the Hodgson group (Liverpool).

We have been studying the H(g) + Cl/Au(111) reaction, motivated primarily by two detailed experimental studies of this system. One of our findings is that the ER reaction cross section is much larger than for H(g) + H/metal reactions due to a steering mechanism [8,9]. This is related to the relatively large distance of the adsorbed Cl above the metal; i.e., the incoming H atom is strongly attracted to both the Cl and the metal, but it encounters the layer of adsorbed Cl atoms first. There are also some interesting variations with the Cl vibrational state, and an exchange pathway is observed. More than two years have been spent using quasi-classical trajectories to study this reaction for the case of large Cl coverage (ms submitted). The ER and HA reaction pathways for HCl formation are a bit more complicated than for H atom recombination. We find that HA reactions dominate the formation of HCl, and that there is evidence for significant energy loss into the substrate excitations.

A textbook chapter summarizing my DOE-funded ER and HA studies has appeared in "The Chemical Physics of Solid Surfaces" [10].

During the past year, both our efforts and the efforts of the experimental groups looking at H atom reactions on graphite have been focused on graphite edges. Real graphite surfaces are rough in the sense that a sizable fraction of the exposed carbon atoms can be on the edges of graphite planes, as opposed to the terraces. We have performed total energy electronic structure calculations to examine how H atoms react with edge vs terrace carbons. We found that the hydrogenation of an edge carbon proceeded with no barrier, and that the barrier for addition of a second hydrogen to the edge carbons was small [11]. Our studies of graphite are also relevant to a sizable body of work examining molecular hydrogen adsorption in and on carbon nano-tubes and nano-crystalline graphite. We have examined how molecular hydrogen can chemisorb onto such structures, and have found two low energy pathways where H_2 dissociatively adsorbs over one or two edge carbons, resulting in a doubly-hydrogenated edge carbon, or two neighboring singly-hydrogenated edge carbons, respectively [11]. The doubly-hydrogenated structure should give rise to a peak that has been observed (but not explained) in the radial distribution functions extracted from neutron scattering studies of graphitic nanostructures exposed to H_2.

Future Plans

The experiments of the Küppers group have shown that the sticking probabilities of H on the graphite terrace are large. Given the significant lattice distortion required for chemisorption, this is surprising, and not well understood. We have used electronic structure methods to map out the H-graphite interaction as a function of the position of the bonding carbon. We find a barrier to chemisorption of about 0.2 eV, in excellent agreement with the experiments. We have used these studies to construct a potential energy surface for trapping and sticking, and have implemented a collinear study of the trapping process (ms submitted). We find that the bonding carbon can reconstruct in 50 fs, and that trapping probabilities can be 5-20%. Our results suggest that sticking proceeds via a trapping resonance, which relaxes by dissipating energy into the substrate over several ps. We are currently mapping out the full three-dimensional potential, and will use the methods we have developed for ER reactions to compute quantum mechanical trapping cross sections. As in our collinear study, some additional lattice degrees of freedom will be included to help carry energy away from the newly formed bond.

We are continuing our studies of H atom reactions at graphite edge sites, since much of the current experimental work is focusing on these sites. It is possible that the formation of molecular hydrogen on interstellar dust grains occurs at these edge sites, since the barrier to H adsorption on the terrace carbons is relatively large. We are examining the pathways and computing the barriers to H(g) reacting with H atoms adsorbed on the edges. It is possible that while singly-hydrogentaed edge carbons are relatively unreactive with respect to ER abstraction, doubly-hydrogenated structures are more reactive. We are also examining barriers to and the dynamics of H atom diffusion and recombinative desorption.

We are interested in the dissociative adsorption of methane on metals, and have been computing barriers to methane dissociation at several sites on Ni and Pt surfaces. In an attempt to understand how methane reactivity varies with the temperature of the metal, we are now examining how these barriers change due to lattice distortion. This information will be used in quantum models of methane reactions on vibrating metal lattices.

References

[1]. X. Sha and B. Jackson,"First-principles study of the structural and energetic properties of H atoms on a graphite (0001) surface," Surf. Sci. 496, 318-330 (2002).

[2]. B. Jackson, X. Sha and Z. B. Guvenc, "Kinetic model for Eley-Rideal and hot atom reactions between H atoms on metal surfaces," J. Chem. Phys. 116, 2599-2608 (2002).

[3]. X. Sha, B. Jackson and D. Lemoine,"Quantum studies of Eley-Rideal reactions between H atoms on a graphite surface," J. Chem. Phys. 116, 7158-7169 (2002).

[4]. X. Sha and B. Jackson,"Ab initio and transition state theory studies of the energetics of H atom resurfacing on Ni(111)," Chem. Phys. Lett. 357, 389-396 (2002).

[5]. Z. B. Guvenc, X. Sha and B. Jackson, "The effects of lattice motion on Eley-Rideal and hot atom reactions: Quasiclassical studies of Hydrogen recombination on Ni(100)," J. Phys. Chem. B 106, 8342-8348 (2002).

[6]. Th. Zecho, A. Güttler, X. Sha, B. Jackson, and J. Küppers, Adsorption of Hydrogen and Deuterium atoms on the (0001) graphite surface," J. Chem. Phys. 117, 8486-8492 (2002).

[7]. Th. Zecho, A. Güttler, X. Sha, D. Lemoine, B. Jackson, and J. Küppers, Abstraction of D chemisorbed on graphite (0001) with gaseous H atoms," Chem. Phys. Lett. 366, 188-195 (2002).

[8]. D. Lemoine, J. Quattrucci, and B. Jackson, "Efficient Eley-Rideal reactions of H atoms with single Cl adsorbates on Au(111), Phys. Rev. Lett. 89, 268302-1-4 (2002).

[9]. J. Quattrucci, B. Jackson, and D. Lemoine "Eley-Rideal reactions of H atoms with Cl adsorbed on Au(111): Quantum and quasiclassical studies, J. Chem. Phys. 118, 2357-2366 (2003).

[10]. B. Jackson, "Eley-Rideal and hot atom reactions between H atoms on metal and graphite surfaces," in "The Chemical Physics of Solid Surfaces," vol. 11, D. P. Woodruff, ed., pp 51-77, Elsevier Science B. V. (2003).

[11]. X. Sha and B. Jackson,"The Location of Adsorbed Hydrogen in Graphite Nanostructures," J. Am. Chem. Soc. (in press).

Molecular Beam and Surface Science Studies of Heterogeneous Reaction Kinetics Including Combustion Dynamics

Steven J. Sibener
The James Franck Institute and Department of Chemistry
The University of Chicago, 5640 South Ellis Avenue
Chicago, IL 60637 s-sibener@uchicago.edu

I. Program Scope

This research program seeks to examine the heterogeneous reaction kinetics and reaction dynamics of surface chemical processes that are of direct relevance to efficient energy production, condensed phase reactions, and materials growth including nanoscience objectives. Illustrative highlights include: (1) a combined scanning probe and atomic beam scattering study of how the presence of self-assembling organic overlayers interact with metallic support substrates – this work has led to revision of the currently held view of how such adsorbates reconfigure surface structure at the atomic level, (2) an inelastic He atom scattering study in which we examined the effect of chain length on the low-energy vibrations of alkanethiol striped phase self-assembled monolayers on Au(111), yielding information on the forces that govern interfacial self-assembly, (3) a demonstration that one can utilize supersonic molecular beams to efficiently produce synthesis gas (SynGas) at relatively low Rh(111) catalyst temperatures, (4) examined the oxidative processes by which atomic oxygen reacts with condensed phase unsaturated hydrocarbons, (5) a combined experimental and theoretical examination of the fundamental atomic-level rules which govern defect minimization during the formation of self-organizing stepped nanostructures, (6) demonstrated that relatively defect-free stepped surfaces can be used as nano-templates for growing silicon nanowires having atomically-dimensioned widths, and (7) elucidated kinetic and photochemical details of NO/Ni surface chemistry, important for environmental NO_x control. Other activities are examining $O(^3P)$/SAM reactions, and O interactions with catalytic gold substrates. Innovative scanning probe and molecular beam instrumentation has been constructed to enable this relatively new experimental program.

II. Recent Progress

1. Coexistence of the (23 x √3) Au(111) Reconstruction and a Striped Phase Self-Assembled Monolayer: Self-assembled monolayers (SAMs) based on a sulfur head group have been widely studied, inspired by both fundamental studies of self-organization and potential technological applications. Despite this extensive scrutiny, the structure of the adsorbed species and the details of the interfacial region are still a topic of controversy. We have studied the effect of adsorption of a low-density alkanethiol monolayer on the state of the Au(111) reconstruction. It is commonly believed that the substrate deconstructs following formation of a thiolate self-assembled monolayer, but our results suggest this is not always the case. He diffraction from 1-decanethiol and 1-octanethiol striped phase monolayers is exploited to establish the surface nearest-neighbor spacing and to illustrate a unit cell corresponding to the long dimension of the (23x√3) reconstruction. Using our observed 0.198 $Å^{-1}$ peak spacing and the (11.5x√3) unit cell reported in the literature, we measure a substrate nearest-neighbor spacing of 2.76 Å along the $[1\bar{1}0]$ direction, which represents the atomic spacing of the uniaxially-compressed, reconstructed gold surface. Moreover, 1/2-order peaks in the diffraction from decanethiol/Au(111) demonstrate a distinction between neighboring thiolate dimers. These peaks are not observed for the

octanethiol/Au(111) system. Therefore, the 1/2-order peaks are not an inherent characteristic of alkanethiol SAMs. The most likely explanation for these peaks is a reconstructed substrate. Complementary STM data have shown persistence of the reconstruction during growth of a decanethiol striped phase monolayer and no evidence for vacancy islands typically associated with deconstruction. Our model involving a still-reconstructed substrate is consistent with all of the available data, while alternative models fail to explain the results from our laboratory.

2. Surface Vibrations in Alkanethiol Self-Assembled Monolayers of Varying Chain Length: Alkanethiol SAMs have been studied as a model system for self-assembly, with two basic phases seen to be prevalent, a high-density c(4×2) phase and a low-density (p×√3) phase. To better understand the self-assembly process it is necessary to delve deeper into the molecular interactions. In order to achieve this goal, we have performed a series of single-phonon inelastic He atom scattering experiments, complemented by appropriate numerical simulations, to delineate the forces driving the self-assembly, including inter-chain and chain-substrate interactions. The striped phases of 1-decanethiol, 1-octanethiol, and 1-hexanethiol exhibit FT_z phonons at 8.0, 7.3, and 7.3 meV, respectively. The interactions responsible for these phonons are driven by the van der Waals forces between the methylene/methyl groups and the Au substrate atoms. Our findings suggest that the modestly increased energy of the C10 mode with respect to C8 and C6 comes from increased binding due to the commensurate structure that C10 has with respect to the Au(111) reconstruction. This work represents a step forward in understanding the forces that govern interfacial self-assembly.

3. Molecular Beam Studies of Enhanced Routes to SynGas Production Using Methane: Methane is an abundant natural resource for making larger hydrocarbons through the Fischer-Tropsch process. To do this, it is necessary to partially oxidize CH_4 to synthesis gas (hereafter SynGas), CO and H_2, ideally in a 1:2 ratio. One method for accomplishing this is the direct partial oxidation of methane, $CH_4+1/2\ O_2 \rightarrow CO+2H_2$. We have explored, using our multiple-molecular beam reactive scattering techniques, detailed aspects of this reaction on Rh(111). We find that this reaction initially proceeds with the activated direct dissociative chemisorption of methane followed by subsequent oxidative chemistry to yield $CO+2H_2$ from the partial oxidation of CH_4. Concurrent molecular beams of O_2 and CH_4 were used, with both beams having narrow kinetic energy distributions. The reaction is highly activated, with the fraction of CH_4 converted being strongly dependent on normal translational energy, approaching unity for energies greater than ~1.3 eV. No CO_2 was detected under the conditions used, a key observation for reaction efficiency and minimization of greenhouse gases.

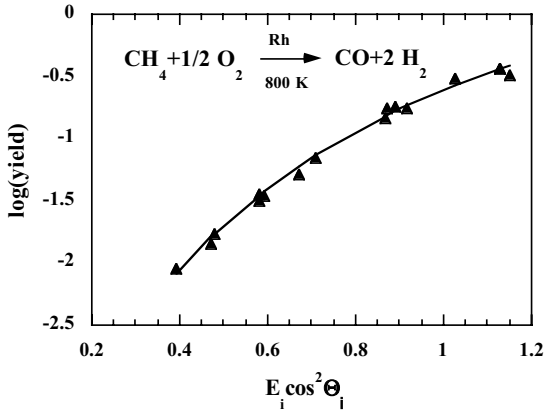

4. Condensed Phase Oxidative Reactions: We have examined (i) the reaction of $O(^3P)$ with condensed arenes and (ii) reactions of 1- and 2-Butene with $O(^3P)$ on the surface of Rh and ice. These investigations have emphasized that

significant differences occur in condensed phase reactions as compared to related gas phase oxidative reactions. For low gas pressures, the products of vapor phase reactions result from fragmentation and rearrangement, consistent with the need for an efficient energy disposal channel to open in order to form addition products. Our observations indicate that heterogeneous interfaces provide a mechanism for channeling away excess energy, therefore leading to adduct stabilization. These experiments provide kinetic data that are needed for the accurate modeling and design of advanced combustion and catalytic reforming systems.

5. In Search of Nano-Perfection: Experiment and Monte Carlo Simulation of Nucleation-Controlled Step Doubling: The atomic and nanoscale structure of surfaces, and the transformations between competing structures, depends upon the delicate balance of surface free energy terms that govern interfacial stability. Time-lapse elevated temperature STM measurements have recently allowed us to probe, precisely, the mechanistic details of interface formation and transformation. Such images reveal the existence of regions of relative structural perfection as well as regions that contain structural defects. Structural imperfections occur as a natural consequence of competing dynamical processes, such as nucleation kinetics and interface mobility. It is the purpose of this project to assess why such imperfections form, and to offer general routes to minimize their occurrence. We have employed oxygen-induced step doubling of vicinal Ni(977) surfaces as our physical system, using STM and Monte Carlo simulations to extract the desired details of interface evolution. Two topological defect features were observed on the surface after doubling reached its asymptotic limit: (i) "frustrated ends," which form when two counter-propagating step-doubling events that have a single step in common intersect, and (ii) residual "isolated single steps," which form when a single step is unable to partner with an adjacent step due to the presence of previously doubled structures. Simulations indicate that control of the competing interplay of nucleation kinetics and 2-dimensional growth kinetics is key to the formation of more perfect interfaces. Such optimized interfaces can act as templates for guiding the assembly of nanowires and other nanoscale molecular assemblies.

6. Reactive Deposition of Silicon Nanowires Templated on a Stepped Nickel Surface:
The controlled fabrication of nanoscale structures on surfaces represents a tremendous challenge, and has attracted much scientific and technological interest. Given our ability to generate unusually high-quality nano-templates consisting of stepped Ni(977) interfaces (see Sec. 5 above), we decided to explore the initial stages of Si nanowire growth by reactive deposition of disilane (Si_2H_6) on this substrate. At low dosing exposures, Si_2H_6 decomposes on the stepped surface and forms oriented nanoscale wires that decorate the substrate's step edges. The length distribution of Si nanowires varies as a function of total exposure and dosing rate. This method of gas-phase reactive deposition on a stepped metal surface, with the substrate acting as both catalyst and nano-template with easily tunable width (by varying the vicinal miscut angle) is a fruitful approach to creating massively-parallel nanoscale arrays of highly aligned structures.

7. Activated Chemistry and Photochemistry of NO on NiO/Ni:
These activities are exploring the mechanistic details of NO chemistry with NiO(111)/Ni(111). Intense and kinetic energy tunable molecular beams have led to the formation of unusual surface adsorbate structures exhibiting higher density (new bonding configurations); vibrational and photochemical studies have been performed on these new bonding arrangements. These studies

are improving our fundamental understanding of heterogeneous processes that are relevant to controlling NO_x in the environment.

Instrumentation Development: We have completed a major upgrade of the molecular beam-line used in many of our reaction dynamics and heterogeneous reactivity activities. We have specifically implemented a new beam chamber with much higher pumping speed than was present before; this new chamber/diffusion pump beam expansion chamber is allowing us to generate more intense and more monochromatic neutral beams with wider energy ranges than was possible with our prior arrangement. Higher performance beams of atomic oxygen are being developed at this time to take advantage of this new beam-line. We have also completed the assembly of a new cryogenically cooled STM ($LiqN_2$ or LiqHe can be used). Cryogenic images of semiconductors and SAMs have been achieved with temperatures as low as 30K. This new facility will give crucial support to our effort in SAM reactivity.

III. Future Plans: In the future we intend to examine several aspects of condensed phase reaction dynamics, including partial oxidation reactions. Some of these studies will pursue opacity-restricted reactions where precise control of the initial collision geometry will be accomplished using SAMs having specific end-group termination and surface geometry. Other studies will examine how condensed phase reactivity and dynamics differ from isolated molecule behavior. Reactions involving highly reactive reagents such as atomic oxygen will continue, while new systems focusing on nanoparticle reaction dynamics may also be explored.

IV. Publications:

In Search of Nano-Perfection: Experiment and Monte Carlo Simulation of Nucleation-Controlled Step Doubling, Yi Wang, T. P. Pearl, S. B. Darling, J. L. Gimmell, and S. J. Sibener, J. Applied Physics, 91 (12): 10081-10087 (2002).

Reactive Deposition of Silicon Nanowires Templated on a Stepped Nickel Surface, Yi Wang and S. J. Sibener, J. Phys. Chem. B 106, 12856-12859 (2002).

Coexistence of the (23×√3) Au(111) Reconstruction and a Striped Phase Self-Assembled Monolayer, S.B. Darling, A.W. Rosenbaum, Yi Wang, and S.J. Sibener, Langmuir 18, 7462-7468 (2002).

Surface Vibrations in Alkanethiol Self-Assembled Monolayers of Varying Chain Length, A.W. Rosenbaum, M.A. Freedman, S.B. Darling, I. Popova, and S.J. Sibener, J. Chem. Phys. 120, 3880-3886 (2004).

Applied Reaction Dynamics: Efficient Single Collision Partial Oxidation of Methane to CO on Rh(111), K.D. Gibson, M. Viste, and S. J. Sibener, submitted.

The Reaction of $O(^3P)$ with Condensed Arenes, K.D. Gibson and S. J. Sibener, to be published.

The Reaction of 1- and 2-Butene with $O(^3P)$ on the Surface of Rh and Ice, K.D. Gibson and S. J. Sibener, to be published.

O-atom Induced Reconstruction of Au(111), K. D. Gibson, and S. J. Sibener, to be published.

Beam Induced Changes in Adsorption Behavior of NO on NiO(111)/Ni(111), B. D. Zion and S. J. Sibener, to be published.

UV-photodesorption of Novel, Beam-Induced NO Layers, B. D. Zion and S. J. Sibener, to be published.

Title: Ames Laboratory Chemical Physics Program
Names of PIs: James W. Evans, Mark S. Gordon
Mailing address: Ames Laboratory, Iowa State University
Ames, IA 50011
Phone numbers: 515-294-1638, 515-294-0452
Fax number: 515-294-0266
e-mail addresses: evans@ameslab.gov mark@si.fi.ameslab.gov

PROGRAM SCOPE:

The theoretical Chemical Physics Program at Ames Laboratory supports integrated efforts in ***electronic structure theory and non-equilibrium statistical mechanics***. The primary focus is on the development and application of methods that enable the study of **semiconductor surface phenomena, heterogeneous catalysis, clusters related to surface science, and other reaction mechanisms** (e.g., in organometallic chemistry).

Electronic structure theory efforts integrate development of fundamental theory by expanding the capability for accurate treatment of large or complex systems of interest to DOE, with optimal strategies for computational implementation within GAMESS. One component of the effort involves the development and application of QM/MM methods (specifically a Surface Integrated Molecular Orbital - Molecular Mechanics or SIMOMM approach), designed to treat adsorption and reaction phenomena on semiconductor surfaces such as Si(100). Another component, in collaboration with the Ames Lab Condensed Matter Physics program, is providing a rigorous basis for tight-binding (TB) methods which are extremely useful for studies of extended surface and materials systems. As indicated above, a general feature of our program involves interfacing of *electronic structure and non-equilibrium statistical mechanical studies* of surface phenomena. The latter include Kinetic Monte Carlo (KMC) simulation and other multi-scale modeling methods. One aspect of this effort focuses on systems and processes relevant for nanoscale science and technology which are based on semiconductor surfaces (e.g., deposition or growth, etching and oxidation, functionalization). Another aspect relates to heterogeneous catalysis on transition metal surfaces, where we consider both reactions on extended single crystal surfaces (connecting atomistic to mesoscale behavior) as well as nanoscale catalyst systems (exploring the role of fluctuations).

RECENT PROGRESS:

DEVELOPMENT OF ELECTRONIC STRUCTURE THEORY

(i) Rigorous basis for Tight-Binding Theory. We developed molecule-deformed minimal atomic basis sets capable of reproducing full-valence space CASSCF wavefunctions. This was applied to analyze bonding of Si_4H_6, and Si_2-Si_{10}, and band structure in crystals [22-24].

(ii) Reducing the cost of high-level calculations. A configurational analysis, based on cluster considerations and proximities of localized orbitals, achieved considerable computational reduction in CASSSCF type MCSCF calculations, thus increasing applicability to larger systems [30]. Related work developed a procedure for generating CI wave functions void of configurational "deadwood".

(iii) Grid-free Density Functional Theory (DFT). In order to provide an alternative to the common numerical grid-based approach to solving the DFT equations, we have developed a purely analytic approach that relies on the resolution of the identity.

(iv) Relativistic effects; precise electronic structure calculations for small cations. We have developed a hierarchy of methods for treating spin-orbit and other relativistic effects. These methods range from one-electron semi-empirical methods to the full Breit Pauli to Douglas-Kroll through third order, as well as the RESC and NESC methods.

SEMICONDUCTOR SURFACE CHEMISTRY AND SURFACE SCIENCE

(i) Competitive etching and oxidation of perfect Si(100) surfaces. We have performed integrated QM/MM and non-equilibrium lattice-gas modeling studies to characterize both the key reaction energetics and the development of complex mesoscale surface morphologies during exposure of Si(100) to oxygen. The former characterized the oxygen adsorption pathway, conversion between strongly bound adsorbed states, and the barrier for etching Si + O(ads) $\rightarrow$ SiO(gas) + vacancy [1]. Etching dominates at ~600C, but there is competitive oxide island formation [mediated by diffusion of O(ads)] which protects the underlying Si from etching. Thus, prolonged etching produces oxide covered Si nanoprotrusions, around which etching proceeds. Initial KMC modeling, simplifying treatment of the Si surface dynamics, describes quantitatively these complex morphologies [17].

(ii) Hydrocarbon adsorption on Si(100). Adsorption of acetylene was studied via SIMOMM using a MCSCF+MRMP2 wavefunction and shown to be significantly multiconfigurational over large sections of the potential energy surface [21].

(iii) SiC clusters. Such clusters are the building blocks for silicon carbide. Thus, we performed a careful study of Si_2C_2 and SiC_3 demonstrating their multiconfigurational nature.

HETROGENEOUS CATALYSIS

(i) Non-equilibrium reactant ordering and critical phenomena. Non-equilibrium ordering of chemisorbed reactants occurs during reaction, somewhat analogous to in equilibrium. We have characterized such non-equilibrium order-disorder transitions [3]. CO-oxidation reactions display bistability which disappears above some critical temperature, analogous to equilibrium critical phenomena. We also provided a full analysis of such non-equilibrium critical phenomema [10,20].

(ii) Connecting-the-length-scales from atomistic ordering to mesoscale patterns. The interplay between local ordering and reaction kinetics in catalytic reactions and rapid diffusion of species such as CO produces mesoscale pattern formation. We have developed a multiscale modeling strategy, Heterogeneous Coupled Lattice-Gas (HCLG) simulation, to treat this problem [3,25,26]. This included precise analysis of "percolative" chemical diffusion in mixed reactant adlayers. The success of HCLG was confirmed for both simple benchmark models and for realistic models. For the latter, we provided the first detailed atomistic modeling of the CO+O reaction on Pd(100) [18,19,25].

(iii) Fluctuations in nanoscale reaction systems: Studies of CO-oxidation on Field Emitter Tips provide rare insight into fluctuation-induced transitions in a bistable reaction system. We have analyzed such experiments in detail, focusing on non-equilibrium critical behavior [2,10,20].

FUTURE PLANS:

DEVELOPMENT OF ELECTRONIC STRUCTURE THEORY

(i) Rigorous basis for semi-empirical approaches. Our recent work showed that bonding-related energy changes are typically dominated by the zeroth-order parts of molecular wavefunctions, and that the latter can be represented and analyzed in terms of "quasiatomic" orbitals, i.e. *minimal basis set atomic orbitals that are deformed by their molecular environments*. This approach will be extended and a variety of applications pursued for surface processes and materials systems.

(ii) Extending the QM/MM method (SIMOMM). The SIMOMM method has so far been applied to silcon, diamond, and silicon carbide surfaces. We will now develop, implement and test extensions of the SIMOMM methodology to important catalytic oxide surfaces. Of immediate interest are silica and alumina. We also plan to develop an interface between SIMOMM and our effective fragment potential (EFP) method in order to develop robust theoretical models for the surface-liquid interface.

(iii) Reliable computations on heavier elements. Electronic structure calculations on molecules containing heavy elements are traditionally performed with effective core potentials (ECP), since these potentials contain the essential scalar relativistic effects implicitly. However, the typical ECP valence orbitals do not have the correct nodal characteristics. This can cause serious problems, especially when one is interested in spectral properties. We will therefore develop model core potentials (MCP) and their energy derivatives, and implement these into GAMESS. Unlike ECPs, MCPs have the correct nodal behavior.

SEMICONDUCTOR SURFACE CHEMISTRY AND SURFACE SCIENCE

(i) Etching, oxidation, and other reactions on vicinal Si(100) surfaces. Our atomistic lattice-gas modeling is being refined to incorporate a realistic description of step, island, and pit structure on the Si(100) surface. This will enable detailed modeling of etching and reaction on imperfect surfaces, or on vicinal surfaces, better reflecting experimental systems. QM/MM will be applied to provide more detailed information on key energetics as input to such modeling. Processes of interest will include etching by oxygen and oxidation, etching via halogens, and film growth via CVD.

(ii) Nanostructure formation and functionalization via deposition on Si(100). We have initiated studies of the deposition of group III metals on Si(100), motivated by the observed self-organization of "atomic wires" by Al, Ga, As, etc. QM/MM is being used to assess key diffusion and interaction energies, and KMC to model anisotropic nucleation & growth of wires to compare with experiment. Other projects more related to functionalization will consider both energetic issues and modeling of spatial ordering or self-organization (which is important for effective device applications).

HETEROGENEOUS CATALYSIS

(i) CO-oxidation and related reactions on Pd(100), Pd(111), etc. We will develop further realistic atomistic models for catalytic reactions on various metal surfaces. We analyze reaction behavior via KMC simulation both on extended surfaces and in nanoscale systems (e.g., supported clusters). Efforts will explore high-pressure catalysis and associated oxide formation processes. Increasingly our modeling will incorporate input from electronic structure studies.

(ii) Multiscale modeling of pattern formation in surface reactions. We will continue to develop efficient multiscale algorithms including implementation parallel KMC simulation as part of the HCLG approach, development of efficient algorithms for on-the-fly analysis of chemical diffusion.

DOE-SPONSORED PUBLICATIONS 2002-2004: (*indicates partial SciDAC support)

[1] *Passive and Active Oxidation of Si(100) by Atomic Oxygen: Theoretical Study of Possible Reaction Mechanisms*, C.H. Choi, D.-J. Liu, J.W. Evans, M.S. Gordon, JACS **124**, 8730 (2002).
[2] *Catalytic CO Oxidation on Nanoscale Pt Facets: Inter-facet CO Diffusion… and Fluctuation Behavior*, N. Pavlenko, J.W. Evans, D.-J. Liu, R. Imbihl, Phys. Rev. E **65**, 016121 (2002).
[3] *From Atomistic Lattice-Gas Models for Surface Reactions to Hydrodynamic Reaction-Diffusion Equations*, J.W. Evans, D.-J. Liu, M. Tammaro, Chaos **12**,131 (2002).
[4] *Fluctuations and Bistability in a Hybrid Atomistic Model for CO Oxidation on Nanofacets: An Effective Potential Analysis*, D.-J. Liu, J.W. Evans, J. Chem. Phys. **117**, 7319 (2002).
[5] *Speeding Up Spin-Orbit Calculations*, D. G. Fedorov, M. S. Gordon, ACS Symposium Series 828, *Low-Lying Potential Energy Surfaces*, M. R. Hoffmann, K. G. Dyall, Ed., Oxford, 2002.
[6] *The Distributed Data SCF*, Y. Alexeev, R. A. Kendall, M. S. Gordon, *Computer Physics Commun.,* **143**, 69 (2002).
[7] *Study of Isomers of C36 Fullerene using Single & Multireference MP2 Pert. Theory*, S. A. Varganov, P. V. Avramov, S. G. Ovchinnikov, M. S. Gordon, *Chem. Phys. Lett.,* **362**, 380 (2002).

[8] *Deadwood in Configuration Spaces. II. SD and SDTQ Spaces*, Joseph Ivanic, Klaus Ruedenberg, Theor. Chem. Accounts, **107**, 220-228 (2002)
[9] *Electron Pairs, Localized Orbitals and Electron Correlation*, Laimutis Bytautas, Klaus Ruedenberg, Molecular Physics, **100**, 757 (2002)
[10] Critical Behavior in an Atomistic Surface Reaction Model exhibiting Bistability: CO-Oxidation, N. Pavlenko, R. Imbihl, J.W. Evans, Da-Jiang Liu, Phys. Rev. E **68**, 016212 (2003).
[11] *The Parallel Implementation of a Full CI Program*, Z. Gan, Y. Alexeev, R.A. Kendall, M.S. Gordon, J. Chem. Phys., **119**, 47 (2003).
[12] *Are both symmetric and buckled dimers on Si(100) minima?...,* Y. Jung, Y. Shao, M.S. Gordon, D.J. Doren, M. Head-Gordon, J. Chem. Phys. **119**, 10917 (2003).*
[13] *Structures and Fragmentations of Small Silicon Oxide Clusters by ab initio…* W.C. Lu, C.Z. Wang, V. Nguyen, M.W. Schmidt, M.S. Gordon, K.M. Ho, J. Phys. Chem. A **107**, 6936 (2003).
[14] *MCSCF Method for Ground and Excited States Based on Full Optimizations of Successive Jacobi Rotations*, Joseph Ivanic, Klaus Ruedenberg, J. Comp. Chemistry **24**, 1250 (2003).
[15] *Split-Localized Orbitals Can Yield Stronger Configuration Interaction Convergence than Natural Orbitals*, L. Bytautas, J. Ivanic, K. Ruedenberg, J. Chem. Phys. **119**, 8217 (2003).
[16] *Spin-orbit Coupling in molecules: chemistry beyond the adiabatic approximation*, D.G. Federov, S. Koseki, M.W. Schmidt, M.S. Gordon, Int. Rev. Phys. Chem. **22**, 551 (2003).
[17] *Atomistic Modeling of Morphological Evolution during Simultaneous Etching and Oxidation of Si(100),* M. Albao, D.-J. Liu, C. H. Choi, M.S. Gordon, J.W. Evans, Surf. Sci. **555**, 51 (2004)*
[18] *Lattice-Gas Modeling of CO Adlayers on Pd(100),* D.-J. Liu, J. Chem. Phys. **121**, 4352 (2004).
[19] *Lattice-Gas Modeling of the Formation and Ordering of Oxygen Adlayers on Pd(100),* D.-J. Liu, J.W. Evans, Surface Science, **563**, 13-26 (2004)
[20] *Crossover between Mean-Field and Ising Critical Behavior in a Lattice-Gas Reaction-Diffusion Model*, Da-Jiang Liu, N. Pavlenko, and J.W. Evans, J. Stat. Phys., **114**, 101 (2004).
[21] *Adsorption of Acetylene on Si(100)-(2x1)*, J.M. Rintelman, M.S. Gordon, J. Phys. Chem., **120**, xxxx (2004).
[22] *Molecule Intrinsic Minimal Basis Sets. I Ab-Initio Optimized Molecular Orbitals*, W. C. Lu, C. Wang, M. Schmidt, L. Bytautas, K. M. Ho, K. Ruedenberg, J. Chem. Phys., **120**, 2629 (2004)
[23] *Molecule Intrinsic Minimal Basis Sets. II. Bonding… for Si_4H_6 and Si_2 to Si_{10}*, W. C. Lu, C. Z.Wang, M. Schmidt, L. Bytautas, K. M. Ho, K. Ruedenberg, J. Chem. Phys., **120**, 2638 (2004).
[24] *Electronic Structures in Crystals…Highly Localized Quasiatomic Minimal Basis Orbitals*, W. C. Lu, C. Z. Wang, T.L. Chan, K. Ruedenberg, K. M. Ho, Phys. Rev. B **70**, 041101 (2004).
[25] *From Atomic Scale Reactant Ordering to Mesoscale Reaction Front Propagation: CO Oxidation on Pd(100)*, D.-J. Liu, J.W. Evans, Phys. Rev. B, **70**, in press (2004)
[26] *Connecting-the-Length-Scales from Atomistic Ordering to Mesoscale Spatial Patterns in Surface Reactions: HCLG Algorithm*, D.-J. Liu, J.W. Evans, SIAM Multiscale Modeling (2004).*
[27] *Kinetic Monte Carlo Simulation of Non-Equilibrium Lattice-Gas Models*, J.W. Evans, Handbook of Materials Modeling, edited by H. Metiu, S. Yip (Kluwer, Dordrecht, 2004).*
[28] *Spin-orbit coupling methods and applications to chemistry*, D.G. Federov, M.W. Schmidt, S. Koseki, M.S. Gordon, "Recent Advances in Relativistic Molecular Theory", Vol. 5, K. Hirao and Y. Ishikawa, Eds., World Scientific, Singapore, pp. 107-136, 2004.
[29] *Economical Description of Electron Correlation*, L. Bytautas, K. Ruedenberg, *Symp. Recent Advances in Electron Correlation Methodology* (A. K. Wilson, K. A. Peterson Ed.s, ACS, 2004).
[30] *Dissociation Potential Curves of Low-Lying States in Transitions Metals. II. Hydrides of Groups 3 & 5*, S. Koseki, Y. Ishihara, D.G. Fedorov, M.W. Schmidt, M.S. Gordon,, J. Phys. Chem., in press (2004).

Theory of Dynamics in Complex Systems

David Chandler

Chemical Sciences Division
Lawrence Berkeley National Laboratory
And
Department of Chemistry
University of California, Berkeley
Berkeley, California 94720

Email: chandler@cchem.berkeley.edu

My DOE sponsored research is devoted to developing and applying theoretical treatments of complex systems. The specific systems currently under investigation are disordered dielectrics, and super-cooled liquids and glasses. To treat the phenomena exhibited by such materials, my coworkers and I have considered models based upon a coarse grained picture of space and time [1]. We have shown that these models can be used to interpret thermal properties, such as the precipitous growth of relaxation times as temperature is lowered towards a glass transition, and we have uncovered an unsuspected crossover, where the relaxation of a glass former evolves from hierarchical dynamics at low temperatures to diffusive dynamics at yet lower temperatures [2]. We have also succeeded in explaining "decoupling" phenomena, where viscosity growth, for example, is not proportional to a diffusion constant inverse [3,4].

Decoupling is a fluctuation effect, and when such effects are present, one expects the presence of growing length scales as with a phase transition, and also non-linear response. In our work, we have demonstrated that growing length scales are found in d+1 dimensions, where d is the physical dimension, and 1 refers to time [1,5]. Dynamical arrest of glass formers is an order-disorder phenomenon in space-time, namely an entropy crisis in trajectory space. Others before us have ventured the view that the dynamical arrest of glass formers is related to an entropy crisis, but in state space rather than trajectory space. In state space, the picture has physical inconsistencies. These problems, however, are removed with our trajectory space picture.

My most recent work on this topic has focused on non-linear effects. Two illustrations are noteworthy. First, on applying a dc force field, the resulting drag velocity of a probe molecule in a super-cooled material is less per unit force at high force strength than it is at low force strength. As such, the response to a sufficiently strong ac field will cause amplification, akin to the action of a ratchet. Second, a super cooled material under shear will produce a shear banding of mobility. In the presence of this banding, the macroscopic mobility of a probe molecule will vanish in directions transverse to the shear. Therefore, the action of shear leads to a dynamic switch. Namely, motion is halted by shaking. While not yet observed experimentally, the theoretical principals from

which we have found these effects seem entirely sound, and I believe experimental verification will soon follow.

In future work, I hope to develop systematic methods for deriving coarse grained models from atomistic models. If successful, these developments will enable the use of molecular dynamics and transition path sampling in situations of relevance to multi scale modeling. Our recent study of nucleation in a super-cooled lattice gas hints at the possible future for such developments [6].

References

1. Garrahan, J.P. and D. Chandler, "Geometrical explanation and scaling of dynamical heterogeneities in glass forming systems," Phys. Rev. Lett., **89**, 035704.1-035704.4 (2002).

2. Garrahan, J.P and D. Chandler, "Coarse Grained Microscopic Model for Glass Formers, Proceedings of the National Academy of Sciences, **100**, 9710-9714 (2003).

3. Jung, Y., J.P. Garrahan and D. Chandler. "Excitation lines and the breakdown of Stokes-Einstein relations in super-cooled liquids," Phys. Rev. E, **69**, 061205.1-061205.7 (2004).

4. Berthier, L., J. P. Garrahan and DC, Europhys. Lett, submitted (2004)

5. Marroli, M., J. P. Garrahan and DC, in preparation (2004).

6. Pan, A. and D. Chandler. "Dynamics of Nucleation in the Ising Model," J. Phys. Chem. B, in press (2004).

COMPUTATIONAL NANOPHOTONICS: MODELING OPTICAL INTERACTIONS AND TRANSPORT IN TAILORED NANOSYSTEM ARCHITECTURES

Stephen K. Gray (gray@tcg.anl.gov),[1] Julius Jellinek (jellinek@anl.gov),[1] George C. Schatz (schatz@chem.northwestern.edu),[2] Mark S. Ratner (ratner@chem.northwestern.edu),[2] Mark I. Stockman (mstockman@gsu.edu),[3] Koblar A. Jackson (jackson@phy.cmich.edu),[4] Serdar Ogut (ogut@uic.edu)[5]

[1]Chemistry Division, Argonne National Laboratory, Argonne, IL 60439; [2]Department of Chemistry, Northwestern University, Evanston, IL 60208; [3]Department of Physics and Astronomy, Georgia State University, Atlanta, GA 30303; [4]Department of Physics, Central Michigan University, Mt. Pleasant, MI 48859; [5]Department of Physics, University of Illinois at Chicago, Chicago, IL 60607

PROGRAM SCOPE

Nanophotonics concerns confinement and manipulation of light in nanosystems, with exciting new possibilities in, e.g., nanoscale optoelectronics and chemical and biomedical sensing. We carry out theory, modeling and simulations of light interacting with nanosystems composed of metal nanoparticles (MNPs), nanoholes in thin films, and hybrid systems including nonlinear materials and quantum dots. This work requires a broad range of theoretical and computational methods. Thus, a key component of our program involves developing and assembling a comprehensive suite of nanophotonics simulation tools. We also work with applied mathematicians and computer scientists in the development of optimal algorithms and software with high-performance capabilities. Our work involves microscopic studies of relevant electronic, structural and optical properties, and electrodynamics studies of light interacting with nanosystems. We envision the complete, reliable simulation of nanophotonics phenomena from first principles.

At the microscopic level, a goal is to understand the mechanisms that underlie assembly of atoms into clusters and clusters into larger nanosystems. Understanding these mechanisms and the key parameters they depend on is indispensable for the rational design and synthesis of cluster-based nanoarchitectures with desired properties. The atomic-level mechanisms governing particle growth are ultimately defined by the interatomic interactions. An accurate description of these interactions is needed to uncover correct mechanisms. The potentials that describe the interatomic interactions also have to be computationally efficient as the number of atoms in the systems of interest is large (~10^4-10^5) and computational simulations of the assembly processes require long runs. Another goal of our microscopic work is to provide optical information, e.g. static and dynamic polarizabilities, which can be used to estimate size-dependent dielectric constants for clusters or small nanoparticles of relevance to our electrodynamics work.

The dynamics of light interacting with many of the nanosystems we are interested in is governed by Maxwell's equations, assuming certain frequency-dependent dielectric constants describe metallic regions of space. We use computational electrodynamics methods to solve numerically Maxwell's equations in order to develop an understanding of the physical phenomena that can take place. A goal of this work is to learn how to manipulate surface plasmon (SP) excitations. SPs are collective electronic excitations localized near the surfaces of metallic structures that can be excited by light. This localization occurs on length scales less than optical wavelengths, which suggests it might be possible to manipulate SPs to design, for example, new classes of nanoscale optoelectronics devices where photons take the place of electrons.

RECENT PROGRESS

Microscopic Studies of Electronic, Structural and Optical Properties

The construction of accurate interatomic potentials for metal cluster formation requires addressing three issues: 1) Choice of the functional form and the number of adjustable parameters, 2) Choice of the set of fitting properties, and 3) Choice of the fitting procedure (which also affects the resulting values of the parameters). Based on an extensive analysis, we chose to use the functional form of the so-called Gupta-like potential, the genesis of which is in the second-moment approximation to the tight-binding model. For fitting we used our previously developed minimal maximum error fitting procedure. To arrive at a set of parameters that is adequate also for finite systems we use as fitting properties not only bulk attributes but also those of the diatomic molecule (equilibrium bond length, bond energy, and force constant). The central new element in our approach is that we converted the effectively four-parameter Gupta-like potential into a truly five-parameter potential. It is the extra flexibility due to the fifth parameter that makes the new potential more accurate. So far we performed the fits for nickel and silver. The current work focuses on rigorous evaluation of the new potentials as gauged by structural and thermal properties and data obtained in electronic structure computations.

Given interaction potentials, finding possible system structures is also a challenge. We developed an unbiased method for searching cluster energy surfaces to find ground state cluster structures. A key element is the use of highly compressed random geometries as starting points for gradient-based structure relaxations. From these initial geometries, the effective catchment basin of the global minimum is greatly enhanced, making the minimum easier to find. The method was applied to Lennard-Jones clusters as a test case, and to the problem of the shape transition in silicon clusters [1].

With structural information as provided, for example, by the methods above, one can then consider estimating polarizabilities and optical properties of relevance to nanophotonics. We used density functional theory (DFT) to compute dipole static polarizabilities, α, for Si_n and Cu_n. For silicon clusters, we used ground state structures for n=2-28 and additional structures for n = 50 to investigate the dependence of α on cluster size and shape. The results show prolate clusters to be more polarizable than compact, quasi-spherical structures. More interestingly, the size trends for compact and

prolate structures show very different behavior. In both cases, the trends can be fit to the results of jellium-based models of the polarizability, indicating a metallic response of these clusters to external fields. For Cu_n, we computed α for a large number of structural isomers for n = 2-10, exploring the effect of changes in methodology (including basis sets and level of theory) on the results. The results indicate that the theoretical values of α are much smaller than recent measured values [M. B. Knickelbein, J. Chem. Phys. **22**, 10450 (2004)]. We conclude that the differences cannot be due to the choice of method. Instead, they may be due to the effect of permanent cluster dipole moments.

The static polarizabilities above provide zero-frequency (long wavelength) information. Also of interest are frequency-dependent (dynamic) polarizabilities, which require excited electronic state properties and present additional computational challenges. Time-dependent density functional theory within the adiabatic local density approximation (TDLDA) is a promising approach for calculating excited state properties of confined systems. As a starting point, we calculated the absorption spectra of Ag_n clusters (n =2-8) using TDLDA with a real space *ab initio* pseudopotential method. The absorption spectra show sharp features around 3 to 5 eV especially for clusters with even number of atoms as well as Ag_7, in agreement with experiment and related calculations. We also formulated a new way of calculating the full (wavevector and frequency dependent) dielectric function $\varepsilon(r_1, r_2, \omega)$ and its inverse from first principles within a TDLDA framework, and applied it to hydrogenated Si clusters. Our results hint that while the spatial dependence of the dielectric function is drastically altered compared to bulk (which is expected due to quantum confinement and finite size effects), the frequency dependence of the imaginary part of the dielectric function (especially the position of the plasmon-like peak) is very much reminiscent of the bulk spectrum.

In collaboration with Klimov (Los Alamos National Laboratory), we developed a microscopic theory of enhanced relaxation of a semiconductor quantum dot at a nanoscale proximity of a metal surface based on Random Phase Approximation (RPA) [2]. This theory predicts a giant enhancement of radiativeless relaxation when a quantum dot is closer than 2 nm to the surface due to the effect of Landau damping. This phenomenon and the theoretical approach developed for its description will be useful in the future studies of nanostructured systems with a few-nm features where the macroscopic electrodynamics is inapplicable.

Electrodynamics Studies

Our electrodynamics work yields electric and magnetic fields, and thus intensities or energy densities associated with light interacting with nanostructures. Ideally, dielectric or related information from our microscopic work could serve as input to these calculations. However, the nanosystems we have considered so far in our electrodynamics work are sufficiently "large" that bulk dielectric constant information is adequate. Previous work has shown how the finite-difference time-domain (FDTD) method can be used to treat the electrodynamics of metallic nanosystems [S. K. Gray and T. Kupka, Phys. Rev. B **88**, 045415 (2003)]. In a joint experimental-theoretical paper, we used the FDTD method to study how total internal reflection (TIR) light can be used

to excite the SP resonance in silver and gold nanowire systems [3]. In the calculations, 50 nm diameter metal nanowires are placed on top of a glass surface and evanescent TIR waves moving along the glass-air interface are used to excite the SP resonances. We showed how enhanced low angle scattering into the air resulted when the light was tuned to the SP resonance, in agreement with experimental observations of related MNPs. We also showed how the scattering angle can be further reduced if chains of metal nanowires are used, which is a promising indicator for propagation of SP excitations along such chains.

Nanoscale holes in thin metal films can also display SP excitations, and represent a rough complement to MNPs. Furthermore, traveling surface plasmon polaritons (SPPs) can emanate from the holes and move on the surface of the film. In another joint experimental-theoretical paper [4], we showed how isolated 200 nm diameter holes in 100 nm thick gold film can act as point sources of SPPs. We also showed that the observation of the SPPs is facilitated by an interference effect between directly penetrating waves and the SPPs. A strength of the FDTD method is that very complicated configurations can be considered. In some calculations we actually included a realistic description of the experimental probe, a near-field optical microscope probe. These calculations, which required a parallel implementation of the FDTD method and utilized Argonne's Jazz computing facility, showed that the information garnered from the probe is not the total near-field but more reflective of the contribution to the near-field intensity from the polarization direction associated with the incident laser field.

Based on the analytical-numerical Green's function method in quasistatic approximation, we developed a theory of coherent control of ultrafast energy localization in nanosystems [5]. We showed that the phase degrees of freedom of ultrashort laser pulses are effective "knobs" that allow one to control the linear and nonlinear energy distribution on the femtosecond-nanometer spatio-temporal scale. This predicted effect of coherent control has recently been observed experimentally by Petek and co-workers (University of Pittsburgh). The significance of this work is that this effect represents the only method that allows ultrafast control of the nanoscale optical fields because the spatial focusing of optical radiation on the nanoscale is impossible.

We proposed a "nanolens" that enhances the intensity of local optical fields by a factor of million [6], the highest value up to date. The corresponding analytical-numerical theory is based on the multi-center multipole expansion of the quasistatic Green's function. The nanolens involves arrays of nanoparticles. In related work we showed how simple dimer array SP resonances can be viewed as bonding and antibonding combinations of isolated SPs [7]. Whereas the nanolens concentrates localized SP energies, it is also possible to concentrate (traveling) SPPs. We developed and applied an approximate (Eikonal) theory showing rapid adiabatic concentration of optical energy from SPPs in tapered nanoplasmonic waveguides [8]. This allows one to transfer a significant fraction of the laser radiation energy to the nanoscale.

In collaboration with several members of Argonne's Mathematics and Computer Science Division (B. Norris, P. Fischer, B. Smith) we have been working on new algorithms with

accuracy and scalability for high-performance computer applications. We are working with them on two projects, one concerning use of pseudospectral techniques and the other multi-scale grid-refinement methods. Both these projects will result in efficient, new and more accurate ways of treating our electrodynamics problems.

FUTURE PLANS

Our future work, while extending and expanding the efforts described above, will also bring the various components of our project closer, bridging the microscopic and continuum level descriptions of nanophotonics.

Future work will include fitting the potential parameters for various metals as well as bimetallic systems and performing large-scale dynamical simulations of cluster-based nanoassembly. The assembly mechanisms will be studied as a function of cluster size and composition. As means of guiding the assembly towards the desired photonic nanoarchitectures, we will study the role of patterned supports and temperature, as well as the conditions of deposition of the clusters on the supports such as the deposition energy and angle. An important issue that we will also explore is the thermal stability of both the cluster building blocks and the nanosystems assembled from them.

Regarding cluster electronic properties, we will explore methods for partitioning the static polarizability into pieces associated with individual atoms. We will use the dynamical polarizabilities and absorption spectra of small clusters to construct a complex model dielectric function $\varepsilon(\omega)$, which can be used as input in our electrodynamics simulations. We will approach this in two different ways, one from using a dielectric sphere model, and the other using our new formulation of the full dielectric matrix calculations. The latter will involve application of our new method of calculating $\varepsilon(r_1, r_2, \omega)$ to Ag clusters. Another future direction is calculation of optical spectra using the GW-Bethe Salpeter method for the two-particle Green's function. A comparison between TDLDA and GW-Bethe-Salpeter spectra will be rather instructive in terms of the predictive power of the two approaches. Extension to larger clusters, which will involve parallelization of the real space and TDLDA codes on the Argonne Jazz cluster, is the next step. We expect to achieve spectra for up to 50 Ag atoms, which corresponds to a cluster size slightly larger than 1 nm.

The microscopic optical information provided above will provide the basis for FDTD and related electrodynamics simulations of small nanoparticles. We will also extend our time-domain or FDTD electrodynamics simulations to the study of various MNPs and nanoholes in different media. FDTD simulations of various 1-D and 2-D arrays of nanoholes in thin metal films will be carried out in order to learn how to control SPPs with nanoscale devices in mind. Work on arrays of MNPs on glass and in polymer layers will also be initiated, with important implications for near-field imaging. Both the MNP array and hole array work will complement emerging experiments being carried out at Argonne and elsewhere.

A frequency-domain approach to complement our time-domain (FDTD) work is the discrete dipole approximation (DDA). We plan to add the DDA method to our suite of

nanophotonics codes and capabilities, and use it to study recently fabricated triangular prisms of gold that exhibit multiple plasmon resonance behavior that has not been seen previously. Also, we will develop an interface between classical electrodynamics based on DDA and quantum chemistry so that we can study the coupling of molecules to enhanced electromagnetic fields on metal particle surfaces.

Motivated by the earlier work on V-shaped nanostructures [5], we will explore how to control SP excitations on more general MNPs, and delve into potential uses of the effect in the encoding and decoding of information. We will also explore coherent control in nanostructures including various nonlinear phenomena. Full electrodynamic modeling of both the proposed nanolens [6] and tapered waveguide systems [8], based on FDTD and/or Green's function ideas, will be carried out. Realistic modeling of the tapered waveguide system is is a particularly formidable problem because in the process the SPP wavelength is reduced by two orders of magnitude. This will require multi-scale algorithms such as those being developed with Argonne's Mathematics and Computer Science Division.

PUBLICATIONS OF DOE SPONSORED RESEARCH (2003-2004)

[1] "Unraveling the shape transformation in silicon clusters," K. A. Jackson, M. Horoi, I. Chaudhuri, Th. Frauenheim and A. A. Shvartsburg, *Phys. Rev. Lett.* **93**, 013401 (2004).

[2] "Dipolar emitters at nanoscale proximity of metal surfaces: Giant enhancement of relaxation," I. A. Larkin, M. I. Stockman, M. Achermann, and V. I. Klimov, *Phys. Rev. B (Rapid Communications)* **69**, 121403(R) (2004).

[3] "Optical scattering from isolated metal nanoparticles and arrays," G. A. Wurtz, J. S. Im, S. K. Gray, and G. P. Wiederrecht, *J. Phys. Chem. B* **107**, 14191 (2003).

[4] "Surface plasmons at single nanoholes in Au-films," L. Yin, V. K. Vlasko-Vlasov, A. Rydh, J. Pearson, U. Welp, S.-H. Chang, S. K. Gray, G. C. Schatz, D. E. Brown, and C. W. Kimball, *Appl. Phys. Lett.* **85**, 467 (2004).

[5] "Coherent control of nanoscale localization of ultrafast optical excitation in nanosystems," M. I. Stockman, D. J. Bergman, and T. Kobayashi, *Phys. Rev. B* **69**, 054202 (2004).

[6] "Self-similar chain of metal nanospheres as an efficient nanolens," K. Li, M. I. Stockman, and D. J. Bergman, *Phys. Rev. Lett.* **91**, 227402 (2003).

[7]"Plasmon hybridization in nanoparticle dimers," P. Nordlander, C. Oubre, E. Prodan, K. Li, and M. I. Stockman, *Nano Letters* **4**, 899 (2004).

[8] "Nanofocusing of optical energy in tapered plasmonic waveguides," M. I. Stockman, *Phys. Rev. Lett.* **93***, in press* (2004).

Acknowledgment: Work at Argonne National Laboratory was supported by the U.S. Department of Energy, Office of Basic Energy Sciences, Division of Chemical Sciences, Geosciences, and Biosciences under DOE Contract No. W-31-109-ENG-38.

ELECTRONIC EXCITATIONS AND OPTICAL RESPONSE OF NANOSTRUCTURES

Steven G. Louie (sglouie@berkeley.edu),[1] Martin Head-Gordon (mhg@bastille.cchem.berkeley.edu),[2] James R. Chelikowsky (jrc@msi.umn.edu),[3] Emily A. Carter (eac@Princeton.edu),[4] Michel Van Hove (vanhove@lbl.gov)[5]

[1]Department of Physics, University of California, and Materials Sciences Division, Lawrence Berkeley National Laboratory, Berkeley, CA 94720; [2]Department of Chemistry, University of California, and Chemical Sciences Division, Lawrence Berkeley National Laboratory, Berkeley, CA 94720; [3]Department of Chemical Engineering and Materials Science, University of Minnesota, Minneapolis, MN 55455; [4]Department of Mechanical & Aerospace Engineering, Princeton University, Princeton, NJ 08544; [5]Materials Sciences Division and Advanced Light Source, Lawrence Berkeley National Laboratory, Berkeley, CA 94720 and Department of Physics, University of California, Davis, CA 95616

PROGRAM SCOPE

There has been much progress in the synthesis, characterization and theoretical studies of various nanostructures such as nanotubes, nanocrystals, atomic wires, organic and biological nanostructures, and molecular junctions. However, there remain immense challenges in both the basic and practical understanding of the properties of these structures and their interactions with external probes to realize their tremendous potential for application. Some of the exciting frontiers in nanoscience include molecular electronics, nanoscale opto-electronic devices, nanomechanics (nanomotors), light harvesting and emitting nanostructures. In all these areas, the electronic excited properties of the nanostructures and how they are coupled to the external stimulations/probes are crucial issues.

The electronic excitations and optical response in nanostructures are therefore of fundamental and technological importance. However, these processes can be significantly different from those in the regimes of the bulk or atomic/molecular limits. Quantum confinement effects and many-electron interaction effects are known to be important in reduced dimensional systems and are sensitive to the exact geometric structure owing to symmetry constraints and/or the nature of the nanointerface. The present program focuses on the theory and modeling of the electronic excited-state and optical properties of various nanostructures, applying the methodology to targeted timely problems. The techniques we are working on range from many-electron Green's functions approach (such as the GW/Bethe-Salpeter equation method) to time-dependent density functional theory to many-body coupled cluster theory.

Since nanostructures are neither at the molecular nor the bulk limits, the calculations of the excited-state properties are subject to severe computational bottlenecks. Another important goal is to attack these bottlenecks in collaboration with computational scientists and applied mathematicians, by seeking novel reformulations of the underlying physical theories.

RECENT PROGRESS

This program started a little over one year ago. Significant progress has been made in several areas.

Optical response of carbon nanotubes

Carbon nanotubes possess novel properties that are of fundamental scientific interest and significant technological potential. For example, their unique electronic and optical properties make them promising candidates as nanoscale opto-electronic devices. However, quantum many-electron effects often dramatically modify the properties of reduced dimensional systems. Employing a many-electron Green's

function approach (the GW/BSE method), we have performed first-principles calculations to investigate the quasiparticle self-energy and electron-hole interaction (excitonic) effects on the optical spectra of single-walled carbon nanotubes. We discovered that excitonic effects are orders of magnitude larger in the nanotubes than in bulk carbon materials and they qualitatively alter the optical response of both semiconducting and metallic tubes.[1,2] For example, as illustrated in Fig. 1, the exciton binding energies in the semiconducting nanotubes can be as large as 1 eV. These large many-electron effects elucidate recent experimental findings and explain the discrepancies between previous theories and experiments.

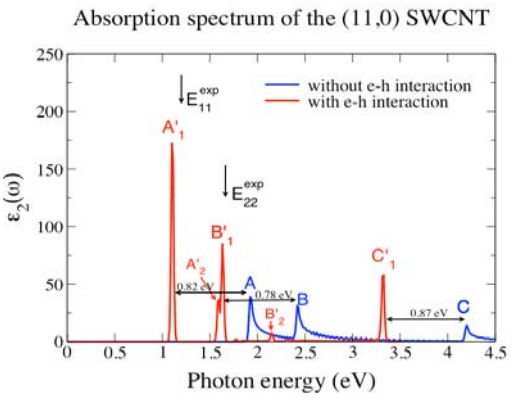

Fig. 1 Calculated optical absorption of a (11,0) single-walled carbon nanotube with (red) and without electron-hole interaction effects.

Temperature dependence of the band gap of semiconducting carbon nanotubes

The temperature dependence of the band gap, $E_g(T)$, is one of the fundamental signatures of a semiconductor, providing important insights into the nature and strength of electron-phonon interactions. The first measurements of $E_g(T)$ dated from the dawn of the semiconductor era. Calculations of such quantity are challenging, and so far have only been limited to bulk, inorganic semiconductors. Information on $E_g(T)$ for carbon nanotubes would be extremely valuable, since chiral indices (n,m) assignments are usually performed by comparing measurements of the optical gap at 300 K with zero temperature electronic structure calculations. We have calculated the temperature dependence of the band gap of semiconducting single-wall carbon nanotubes (SWNTs) by direct evaluation of electron-phonon couplings within a ``frozen-phonon'' scheme.[3] An interesting diameter and chirality dependence of $E_g(T)$ is obtained, including non-monotonic behavior for certain tubes and distinct ``family'' behavior (see Fig. 2). These results are traced to a strong and complex coupling between band-edge states and the lowest-energy optical phonon modes in SWNTs. The $E_g(T)$ curves are modeled by an analytic function with diameter and chirality dependent parameters; these provide a valuable guide for systematic estimates of $E_g(T)$ for any given SWNT.

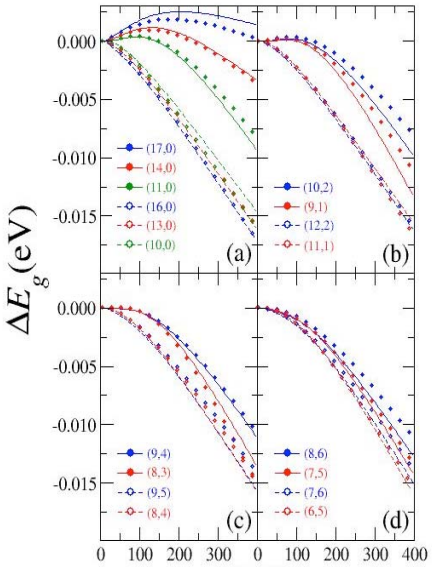

Fig. 2 Calculated and analytical $\Delta E_g(T) = E_g(T) - E_g(0)$ for a variety of SWNTs of different diameters and chiralities.

Doping quantum dots

In nanocrystals, one expects that both electronic and optical properties will be strongly affected by quantum confinement. For example, in bulk semiconductors, shallow donors (or acceptors) are crucial in determining the transport properties required to construct electronic devices. However, these properties will be significantly altered in highly confined systems such as quantum dots, i.e., nano-scale fragments of semiconductor crystals, which have been electronically passivated. Important questions arise concerning the nature of dopants in these systems. For example, at what length scale will dopants cease

to play a role similar to that in bulk semiconductors? To answer such questions, we examined a hydrogenated silicon quantum dot doped with a single phosphorous atom [4]. Here we summarize one of the most interesting results: the behavior of the hyperfine splittings (HFS) as a function of size. The HFS have only recently been measured. Given the charge distribution of the dopant electron, one can evaluate the isotropic hyperfine parameter and the corresponding hyperfine splitting in Fig. 3. At small sizes, the HFS is very large owing to strong localization of the electron around impurity. As the radius increases, the value of the splitting decreases. The measured values of the HFS fall on the best fit to calculated results.

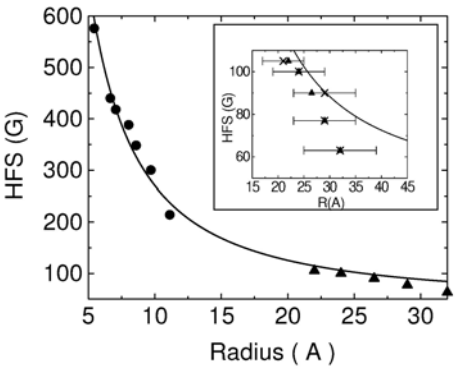

Fig. 3 Calculated (dots) and experimental (triangles) hyperfine splitting (HFS). The line is the best fit to calculations. Inset shows experimental data together with the fit to theory.

Optical excitations in Si and Ge dots

One of the most striking and best studied effects in semiconductor quantum dots is the quantum size effect: an inverse correlation between the optical gap and the quantum dot size. This effect has been used to tune the color of CdSe semiconductor nanocrystals across the entire visible spectrum. Here we contrast quantum dots of Si with Ge. The band gap of bulk Ge (0.68 eV) is significantly smaller than the gap of Si (1.1 eV). There has been a longstanding debate in the literature whether, below certain critical diameter, the bandgap of a Ge quantum dot would become bigger than that of a Si quantum dot. Previous studies, which are mostly semi-empirical in nature relying on parameters coming from fitting (measured or computed) properties of bulk Ge, have yield conflicting results. Fig. 4 compares our time dependent local density approximation (TDLDA) results [5] for both Si and Ge with previous calculations. We do not find a well defined "cross-over" between the Si and Ge optical gap curves for any crystallite size.

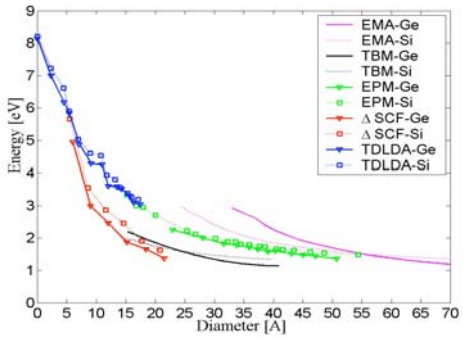

Fig. 4 Optical gap of Ge (solid lines, triangles) and Si (dotted lines, squares) nanocrystals, computed using TDLDA (blue, our work), effective mass approximation (magenta), tight binding (black), empirical pseudopotentials (green), and ΔSCF (red).

Localized molecular orbitals

Any scaleable method for efficiently evaluating the electron correlation energy of a molecule will be framed in terms of localized orbitals. Despite this fact, little attention has been paid to developing fast methods for the determination of localized orbitals. Localized orbitals extremize a measure of spatial locality, such as the second moment of the orbitals, or the self-interaction energy associated with the orbitals. We have developed a new approach to this problem, based on a surrogate function which has a single extremum (with a closed form), and whose first derivative matches that of the true function.[6] This defines an iterative step. The convergence of a sequence of such steps is then accelerated using the direct inversion in the iterative subspace (DIIS) method. The cost of evaluating the basic iterative step can be made to scale linearly with molecular size, by exploiting the spatial locality of the orbitals themselves. We have demonstrated linear scaling for this problem for the first time.

Electron correlation methods

We aim to develop novel scaleable methods for treating matter on the nanoscale based on proven many-body methods that accurately treat molecules. This requires new algorithms with reduced scaling, and possibly also modifications to the basic theories that synergize with this goal. We have begun by examining the simplest many-body theory, second order perturbation theory (MP2). The MP2 energy has contributions from opposite spin (OS) correlations and same spin (SS) correlations. Numerically, the OS terms are larger by typically a factor of 3, reflecting the fact that SS correlations are partly accounted for in mean field by Fermi statistics. Computationally the SS terms are most problematical due to the exchange operator. In a potentially exciting development, we have shown that the SS terms can be very effectively mimicked by a simple scaling of the OS terms, leading to a method we term SOS-MP2.[7] In an extensive series of chemical tests we have shown that SOS-MP2 is in fact superior to MP2 theory for atomization and reaction energies, and very similar for reaction barriers. Furthermore, we can evaluate the SOS-MP2 energy in time that scales 4^{th} order with molecular size (full MP2 is 5^{th} order), which we have demonstrated.

Orbital-free density functional theory (OF-DFT)

Algorithm/code development projects are carried out to advance the theory and applications of the orbital-free density functional theory (OF-DFT), the only linear scaling DFT algorithm for metallic systems. It is found that a previous algorithm for energy minimization, involving the square root of the density as the basic variational parameter, suffered from convergence problems when highly defective materials were examined (such as Al with a high vacancy concentration or large amounts of vacuum in the unit cell when studying surfaces). In the new code, the electronic density itself is employ as the variational parameter. The only problem this poses is that the minimization now must be done by applying mixed equality-inequality constraints, which require the use of the Active-Set method for constrained minimization, introducing additional algorithmic complexity. This new approach seems to be more stable. The new code now can optimize the size and shape of periodic unit cells by minimizing the stress tensor, for a variety of kinetic energy functionals. It also includes both the LDA and GGA-PBE exchange-correlation functionals. Moreover, the code has been written to be compatible with the commercial Kohn-Sham DFT code CASTEP, in terms of input files, so that one can seamlessly go between the two codes for comparison.

Embedding approach to Kondo resonances

Employing the embedding theory, calculations are planned with the goal toward an *ab initio* description of the Kondo resonance that occurs for magnetic transition metal atoms adsorbed or embedded in a nonmagnetic metal host. Conventional DFT studies for Co on Cu(111) have been completed, a system verified experimentally by STM to exhibit this resonance. Shown in Fig. 5 is a partial density of states (PDOS) for the Co atom on a Cu surface within DFT. This is expected to change qualitatively once a PDOS is constructed from an embedding theory calculation that explicitly accounts for the open-shell singlet excited state character of the Kondo resonance. In preparation for those calculations, the embedding theory code is re-coded into a more versatile quantum chemistry package, namely, MOL-CAS, where all matrix elements involving the embedding potential are now evaluated using Gaussian basis sets combined with an atom-centered real-space grid. In

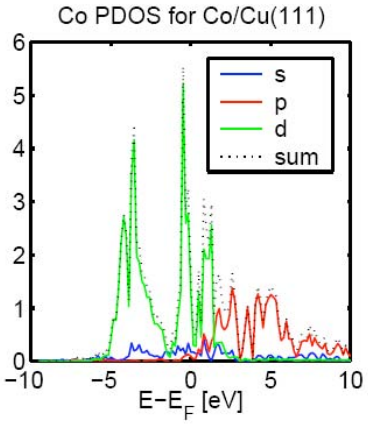

Fig. 5 Calculated partial density of states of Co on Cu(111) surface.

another advance, while the previous embedding theory relied on norm-conserving pseudopotentials mapped onto quantum chemistry effective core potentials, ultrasoft pseudopotentials are employed in the DFT calculations that are carried out prior to the embedding calculations. Especially for transition metals, this results in a huge computer time savings. This was achieved by developing a scheme for mapping the ultrasoft pseudopotential onto a norm-conserving pseudopotential representation, which in turn can then be mapped onto the quantum chemistry effective core potential representation for use in the embedding theory.

Interface to experiments

Development of methods also offers an interface to experiments that study nanostructures, for example, at the Advanced Light Source and in the Molecular Foundry. Such nanoscale experiments often require advanced theory to extract the important structural, electronic, optical, magnetic, chemical and other information that lead to fundamental understanding and prediction. Major experiments include photoelectron diffraction, x-ray absorption spectroscopy, scanning tunneling microscopy, and related techniques such as low-energy electron diffraction, all of which must be simulated theoretically. This "theory of the experiment" will rely on first-principles results of electronic structure and excitation calculations. Mathematical methods to be enhanced or developed include optimization (for example to find the globally optimum theoretical parameters that explain the experimental observations), and inversion of very large matrices in the solution of systems of linear equations (typically to calculate multiple scattering paths of electrons at surfaces and interfaces).

FUTURE PLANS

We will continue and expand on both work on the fundamental understanding of electron excitations and optical response of nanostructures and on methodology developments.

Future work will include continued efforts to understand quantum confinement and electron correlations effects in the optical properties of carbon nanotubes using the first-principles many-electron Green's function approach based on the GW/BSE method. In particular, we will examine those effects which may be probed in photoluminescence excitation and femtosecond pump-probe experiments. A project on computing the radiative lifetime of excitons in the semiconducting nanotubes will be initiated. Recent time-resolved fluorescence data suggest that the radiative lifetime of excited SWCNT has an upper limit of ~ 100 ns. Various mechanisms which may affect the lifetime will be explored. Studies of this kind will also be extended to other nanostructures such as the Si nanowires and the BN nanotubes.

Expanding on a first-principles method for the static dielectric properties in finite systems composed of 10-100 atoms, we plan to consider dynamic screening, aiming at two major goals: (1) Obtain a more complete understanding of how dielectric screening is affected by quantum confinement. (2) Assess the accuracy of semi-empirical models used in studies of optical excitations in molecules and small clusters. Also, a real-space implementation of Green's functions methods, namely the GW and Bethe-Salpeter equation (BSE) approaches for electronic and optical excitations, for finite systems will also be done. In finite systems, one can express the dielectric function in terms of single-electron optical transitions, with significant reduction in numerical complexity. We are currently finalizing the development of GW-BS codes that explicitly use the single-electron transition approach. The current implementation enables us to study electronic and optical excitations in systems with up to 100 atoms or more with the same accuracy as previous GW-BSE calculations, performed in systems with up to a few dozen atoms.

Molecular electronics, i.e., electron transport through single molecules, has generated much excitements and controversies in recent years. We have developed a first-principles scattering-state approach to calculating the nonlinear I-V characteristics of nanostructures, including self-consistently the effects of

finite bias voltage and induced current and the influence of the atomistic arrangement of the molecular junction. This approach, which is based on density functional theory and local orbital basis, will be applied to explore the transport properties of molecules, atomic wires, and nanotubes. We are also currently exploring the possibility of applying real space methods (i.e., on a grid) to predict the electronic transport properties of molecular species.

In the development of local orbitals for order N methods, we are examining whether it is possible to formulate new criteria that define localized orbitals that are not only local in space, but also in a sense optimal for the description of electron correlations. This is our main planned application for localized orbitals. In treating electron correlations with scalable methods, we are investigating more sophisticated forms of the scaling (discussed above), because the optimal factor appears to be distance-dependent. Long-range correlations require a scale factor of 2 (electron spin does not matter once overlap vanishes), while short-range correlations require a scale factor of about 1.3. Simple scaling works well because the short-range terms are numerically far larger. However there are problems like physisorption, cluster condensation and self-assembly that depend strongly on long-range correlations. The second main thrust is the development of reduced scaling methods to evaluate the MP2 and SOS-MP2 energies, with the ultimate objective of linear scaling.

In order to use the OF-DFT approach to study, e.g., nanowires and nanoparticles, it is critical that the algorithms used allow the study of aperiodic systems. The OFDFT code described above relies, as do most condensed matter codes, on the use of 3D periodic boundary conditions so as to utilize Fast Fourier Transforms (keeping the scaling as NlnN). To study aperiodic nanosystems, it will be necessary to work in real space and to utilize an algorithm that retains at least NlnN scaling. As a result, exploratory study is performed to see if the OFDFT energy and potential can be re-expressed profitably in real space using the multigrid technique. The multigrid technique, a linear iterative solver, will replace the currently-used conjugate-gradient (CG) algorithm for electronic minimization. We plan to eliminate the use of FFTs entirely, using a discretized representation of gradients and Laplacians, via use of this O(N) multigrid technique. The multigrid technique will make it much easier for the code to be parallelized. It is expected to be faster than CG minimization. Lastly, multigrid can be used with a variety of boundary conditions, including periodic, Dirichlet, and Newmann, all of which will be useful in applications.

PUBLICATIONS OF DOE SPONSORED RESEARCH (2004)

[1] "Excitonic Effects and Optical Spectra of Single Walled Carbon Nanotubes," C. D. Spataru, S. Ismail-Beigi, L. X. Benedict, and S. G. Louie, Phys. Rev. Lett. **92**, 077402 (2004).

[2] "Quasiparticle Energies, Excitonic Effects and Optical Absorption Spectra of Small-diameter Single-walled Carbon Nanotubes," C. D. Spataru, S. Ismail-Beigi, L. X. Benedict, and S. G. Louie, Appl. Phys. A **78**, 1129 (2004).

[3] "Temperature dependence of the band gap of semiconducting carbon nanotubes," R. B. Capaz, C. D. Spataru, P. Tangney, M. L. Cohen, and S. G. Louie, submitted to Phys. Rev. Lett. (2004).

[4] "Quantum confinement in phosphorus-doped silicon nanocrystals," D. V. Melnikov and J. R. Chelikowsky, Phys. Rev. Lett. **92**, 046802 (2004).

[5] "*Ab initio* absorption spectra of Ge nanocrystals" G. Nesher, L. Kronik and J. R. Chelikowsky, Phys. Rev. B (in press).

[6] "An efficient method for calculating maximally self-interacting localized orbitals", J. E. Subotnik, Y. Shao, W. Liang and M. Head-Gordon, J. Chem. Phys. (in press, 2004).

[7] "Scaled opposite spin second order correlation energy: An economical electronic structure method", Y. Jung, R. Lochan, A. D. Dutoi, and M. Head-Gordon, J. Chem. Phys. (in press, 2004).

Experimental and Theoretical Investigation of Dispersed Kinetics of Proteins and Quantum Dots

PI: Sunney Xie
Harvard University, Department of Chemistry and Chemical Biology
12 Oxford Street, Cambridge, Massachusetts 02138
xie@chemistry.harvard.edu

Program Scope

We investigate the phenomenon of dynamic disorder and conformational fluctuation within proteins by conducting single-molecule electron-transfer experiments Our findings lead to a new theory that accounts for subdiffusion and dispersed kinetics of an enzyme molecule. The power law kinetics of photoinduced electron transfer in quantum dots is also investigated.

Recent Progress

1. Conformational fluctuation within a single protein molecule *(Wei Min and Guobin Luo, graduate students, Professor Binny Cherayil, on sabbatical from The Indian Institute of Science)*

The rate of electron transfer (ET) is sensitive to the donor-acceptor distance, which can serve as a probe to monitor protein motion with angstrom resolution. We have investigated the equilibrium conformational fluctuation of the donor–acceptor distance within a single protein molecule. Through the standard biotin-streptavidin linkage, fluorescein molecules were immobilized onto a quartz surface. A highly specific monoclonal anti-fluorescein antibody binds to the fluorescein moiety and quenches the fluorescence of fluorescein via excited state electron transfer from a nearby tyrosine residue (Figure 1a). [PC1] The

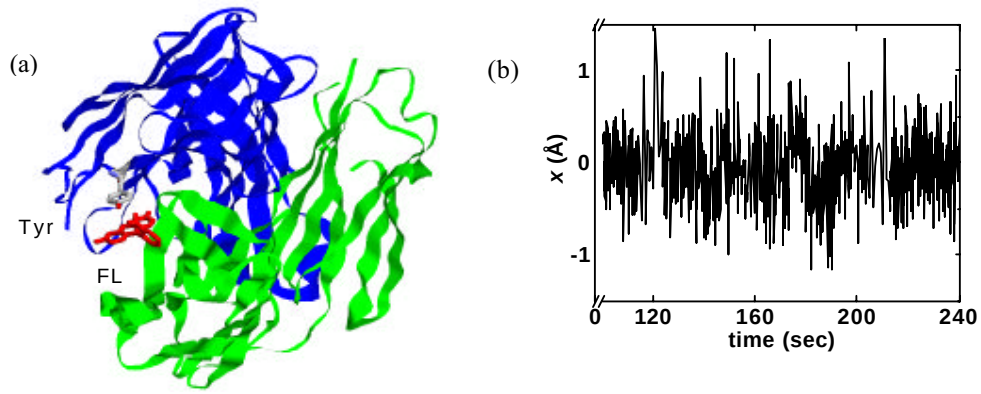

Fig. 1. (a) Schematics of the structure of the FL and anti-FL complex. The tyrosine donor (Tyr) and fluorescein acceptor (FL) for the photo-induced electron transfer reaction are highlighted. (b) An experimental trajectory of the donor acceptor distance, *x*, for a single FL and anti-FL complex.

fluorescence lifetime (i.e. electron transfer time) of a single fluorescein anti-fluorescein complex was monitored as a function of time (Figure 1b). The autocorrelation function of the

donor-acceptor distance, x(t) is deduced (Figure 2b), which decays over a broad range of time scales from milliseconds to hundreds of seconds. The result is similar to our previous observation on a different system. [Yang et al, Science 302, 262 (2003)].

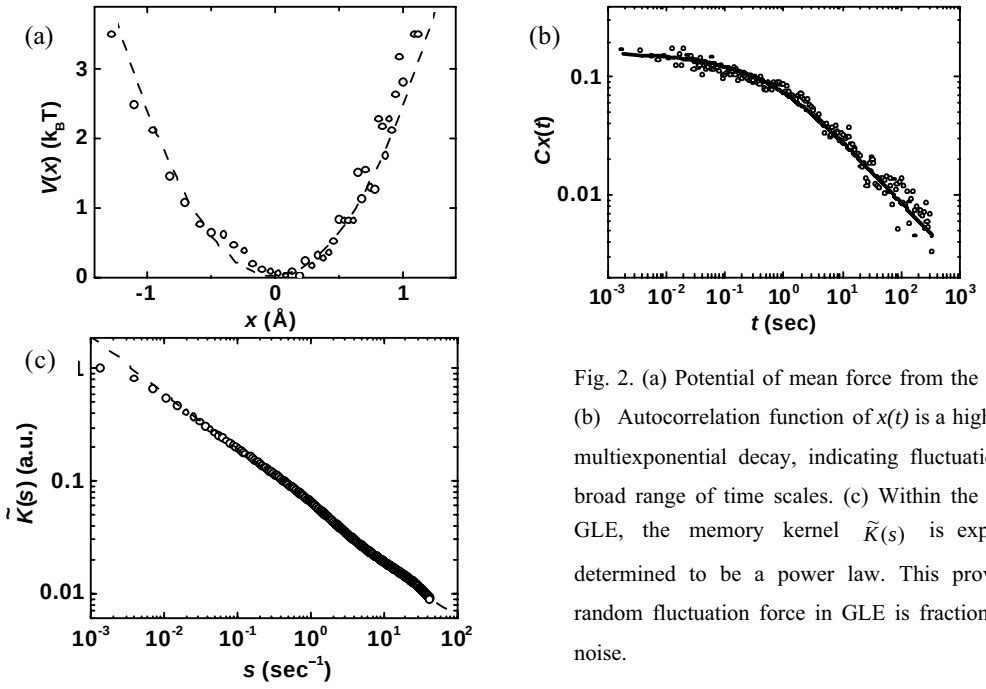

Fig. 2. (a) Potential of mean force from the x trajectory. (b) Autocorrelation function of *x(t)* is a highly stretched multiexponential decay, indicating fluctuations over a broad range of time scales. (c) Within the frame work GLE, the memory kernel $\tilde{K}(s)$ is experimentally determined to be a power law. This proves that the random fluctuation force in GLE is fractional Gaussian noise.

We model $x(t)$ as the coordinate of a fictitious particle diffusing in a harmonic potential. The generalized Langevin equation (GLE) governs its dynamical evolution:

$$m\frac{dv(t)}{dt} = -\zeta\int_0^t d\tau K(t,\tau)v(\tau) - \frac{dV(x)}{dx} + F(t)$$

where m is the mass of the particle, $dx(t)/dt = v(t)$ is its velocity, $V(x)$ is the potential, ? is the friction coefficient, and F(t) is the random fluctuation force with a certain spectrum. K(t,t) is the memory function, which is related to F(t) by the fluctuation-dissipation theorem,

$$K(t,\tau) = \frac{1}{\zeta k_B T}\langle F(t)F(\tau)\rangle$$

Recently, Kou and Xie put forward a model assuming F(t) to fractional Gaussian noise (fGn). It follows that K(t,τ) is a power law function, given by

$$K(t,\tau) = 2H(2H-1)|t-\tau|^{2H-2},$$

where H is a constant between ½ and 1. When H=1/2, the GLE describes Brownian diffusion in the harmonic potential whereas ½<H<1 describes subdiffusion. F(t) being fGn, x(t) becomes a Gaussian Non-Markovian process, which is mathematically tractable. Our experimental results prove the fGn nature of the random fluctuation force and its characteristic power law memory kernel.

2. A unified theory for rates of chemical reaction by applying the combination of GLE with fGn to the celebrated Kramers problem *(Professor Sam Kou, collaborator at Harvard's Statistics Department; Wei Min, graduate student)*

If subdiffusion with long memory exists for the distance between any two points within a protein molecule, it must also exist for a reaction coordination of a chemical reaction. We have developed a new theory based on the solution of the Kramers problem using GLE with fGn noise. Stochastic simulation of GLE with fGn was performed by the circulant matrix method. Analytical results have also been obtained.

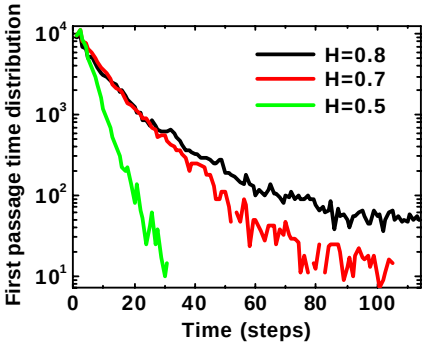

Figure3. Stochastic simulation of the first passage time distribution for a particle undergoing subdiffusion and escaping a barrier under three different conditions, with H being a measure of the ruggedness of the potential. When H=0.5, the least rugged case, the decay is single exponential, as described by Kramers. For high ruggedness, the decays become stretched exponential.

Figure 3 shows the first passage time distributions of chemical reactions for three different H values. We have obtained the stretched exponential decays of the first passage time distributions for H>1/2. This work provides a unified theory for condensed phase chemical reaction kinetics, dynamic disorder in particular, with simple and reasonable assumptions. It can be reduced back to Kramers' theory and Grote-Hynes' theory under limiting conditions. Our new theory can readily account for the dispersed kinetics of CO binding to myoglobin observed by Frauenfelder et al, as well as our recent single-molecule experiments on fluctuating rate constants of single enzyme molecules.

3. Mechanism of dispersed kinetics of electron transfer in quantum dots *(Peng Chen and Kangtaek Lee, postdoctoral fellows)*

Quantum dots (QDs) are a new generation of fluorescent markers for biological labeling with exceptional optical properties. However, the fluorescent blinking of QDs in solution complicates their application in single particle tracking. In Figure 4, we show that the QD blinking is largely suppressed inside living cells and in cell lysate. We identified two cell lysate components, cysteine and histidine. Each of them in buffer can suppress QD blinking. The QD blinking behavior results from a photoinduced excited state electron transfer process to QD surface electron traps. This leaves a positive charge in the core and generates a charge separated state and thus a dark QD. Realizing both cysteine and histidine are common biological ligands for Zn^{II} sites in metalloproteins, we provided a mechanism for the blinking suppression: cysteine, histidine and other small molecules act as ligands binding to the Zn^{II} trap sites on the surface of the CdSe/ZnS core/shell QDs. This ligand binding raises the energy of the charge separated state and reduces the rate of the photoinduced electron transfer

process, thus suppressing the blinking. Power law distributions of the on and off time have been studied under different conditions. We have developed a model to explain the dispersed kinetics in this system.

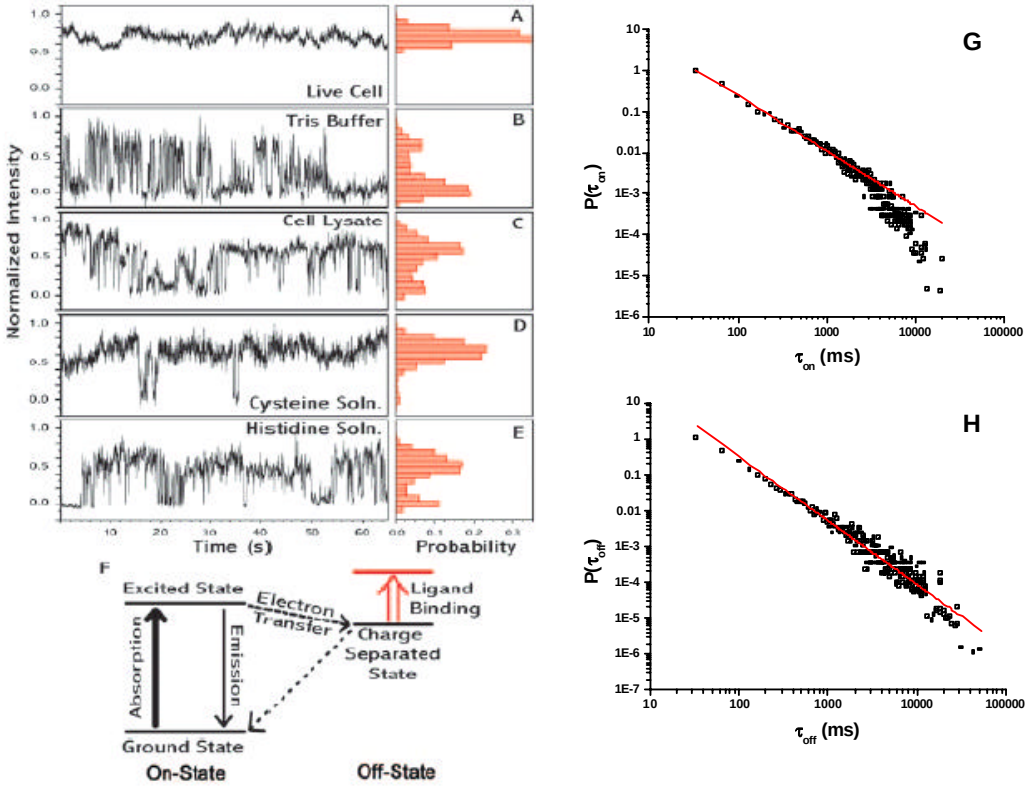

Figure 4. (A)-(E) Fluorescence intensity traces of single QDs in live cells, tris buffer, cell lysate, cysteine and histidine solutions. (F) The blinking of QDs is suppressed in live cells because ligand binding to the defect sites raised the energy of the charge separated state and thus the activation barrier for the electron transfer reaction. (G) Power law on-time distribution of a single QD. (H) Power law off-time distribution of a single QD.

Publications

Krug, John T. II; Sánchez, Erik J.; Xie, X. Sunney "Design of near-field probes with optimal field enhancement by finite difference time domain electromagnetic simulation," *J. Chem. Phys.* 116, 10895 (2002).

Sánchez, Eric J.; Krug, John T. II; Xie, X. Sunney "Ion and Electron Beam Assisted Growth of Nanometeric Si_mO_n Structures for Near-Field Microscopy," *Rev. Sci. Instr.* 73, 3901 (2002).

Yang, Haw; Luo, Guobin; Karnchanaphanurach, Pallop; Louie, Tai-Man; Rech, Ivan; Cova, Sergio; Xun, Luying; Xie, X. Sunney "Protein conformational dynamics probed by single-molecule electron transfer", *Science* 302, 262 (2003)

Kou, S. C. and Xie, X. Sunney "Generalized Langevin Equation with Fractional Gaussian Noise: Subdiffusion of a Single Protein Molecule", *Phys. Rev. Lett.* in press.

Chemical Kinetics and Dynamics at Interfaces

Structure and Reactivity of Ices, Oxides, and Amorphous Materials

Bruce D. Kay (PI), R. Scott Smith, Zdenek Dohnalek and John L. Daschbach
Chemical Sciences Division
Pacific Northwest National Laboratory
P.O. Box 999, Mail Stop K8-88
Richland, Washington 99354
bruce.kay@pnl.gov

Additional collaborators on these projects include G. K. Schenter, G. A. Kimmel, P. Ayotte, J. Kim, and G. Teeter.

Program Scope

The objective of this program is to examine physiochemical phenomena occurring at the surface and within the bulk of ices, oxides, and amorphous materials. The microscopic details of physisorption, chemisorption, and reactivity of these materials are important to unravel the kinetics and dynamic mechanisms involved in heterogeneous (i.e., gas/liquid) processes. This fundamental research is relevant to solvation and liquid solutions, glasses and deeply supercooled liquids, heterogeneous catalysis, environmental chemistry, and astrochemistry. Our research provides a quantitative understanding of elementary kinetic processes in these complex systems. For example, the reactivity and solvation of polar molecules on ice surfaces play an important role in complicated reaction processes that occur in the environment. These same molecular processes are germane to understanding dissolution, precipitation, and crystallization kinetics in multiphase, multicomponent, complex systems. Amorphous solid water (ASW) is of special importance for many reasons, including the open question over its applicability as a model for liquid water, and fundamental interest in the properties of glassy materials. In addition to the properties of ASW itself, understanding the intermolecular interactions between ASW and an adsorbate is important in such diverse areas as solvation in aqueous solutions, cryobiology, and desorption phenomena in cometary and interstellar ices. Metal oxides are often used as catalysts or as supports for catalysts, making the interaction of adsorbates with their surfaces of much interest. Additionally, oxide interfaces are important in the subsurface environment; specifically, molecular-level interactions at mineral surfaces are responsible for the transport and reactivity of subsurface contaminants. Thus, detailed molecular-level studies are germane to DOE programs in environmental restoration, waste processing, and contaminant fate and transport.

Our approach is to use molecular beams to synthesize “chemically tailored” nanoscale films as model systems to study ices, amorphous materials, supercooled liquids, and metal oxides. In addition to their utility as a synthetic tool, molecular beams are ideally suited for investigating the heterogeneous chemical properties of these novel films. Modulated molecular beam techniques enable us to determine the adsorption, diffusion, sequestration, reaction, and desorption kinetics in real-time. In support of the experimental studies, kinetic modeling and Monte Carlo simulation techniques are used to analyze and interpret the experimental data.

Recent Progress and Future Directions

Helium Diffusion Through H_2O and D_2O Amorphous Ice: The First Observation of a Lattice Inverse Isotope Effect. Isotopic substitution has long been an invaluable tool in the experimentalist's arsenal to determine the details of a chemical reaction or diffusion mechanism. In general, if a heavier isotope is substituted for an atom directly involved in a process, the rate for that process is usually slower. For example, in a reaction that involves the breaking of a bond containing a hydrogen atom, the substitution of deuterium will normally result in a decrease in the reaction rate. Thus, through a series of selective isotopic substitutions one can learn about the microscopic details of a chemical reaction. The decrease in the rate is the result of a lower zero-point energy in the reactant well of the heavier isotope. A lowering of the zero-point energy means a larger energy barrier to reach the transition state and thus a lower rate.

We have found that the diffusion rate of helium through amorphous solid water (ASW) is strongly dependent on the isotopic composition of the ASW lattice (see Figure 1). Further, the lattice isotope effect is the "inverse" of a normal isotope effect, in that diffusion is faster in the heavier (D_2O) isotope lattice. This is the first observation of an isotope effect for diffusion in a solid where the isotopic mass change occurs in the nominally static lattice. The explanation for this inverse isotope effect comes from transition state theory used to calculate the diffusion rate of helium between the ice-like cages. While the He/D_2O system lattice does have a lower zero-point energy in the reactant well (helium in an ice-like cage), there is a greater lowering of the zero-point energy at the transition state (helium in a hexagonal water ring), and the net result is an overall lower barrier for helium diffusion in D_2O than in H_2O. This effect, termed a "tight" transition state, is well known for the inverse primary isotope effect observed in H/D diffusion in Pd and in crystalline ice. In both of these cases, the isotope effect is due to changes in mass of the diffusing species. In the present case, the isotope effect arises predominantly from vibrational zero-point energy differences associated with the frustrated rotational modes of the H_2O (D_2O) molecules composing the water lattice. The magnitude of the secondary isotope effect is a sensitive probe of angular anisotropies in the He–water interaction potential. Current efforts are aimed at using the experimental data to test of the accuracy of various water/water and helium/water potentials.

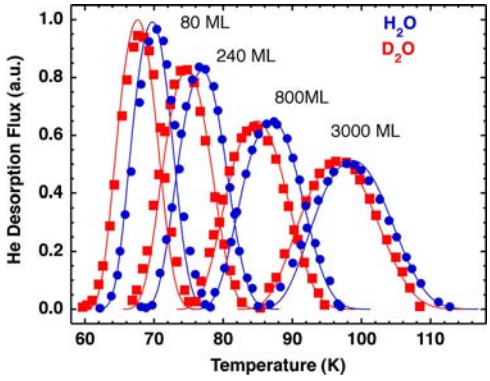

Figure 1. The Temperature programmed desorption (TPD) of He implanted ASW (H_2O (circles) and D_2O (squares)) capped with 80, 240, 800, and 2400 ML of ASW. The lines are Arrhenius fits using a kinetic hopping model. The data clearly show that helium diffuses more rapidly through D_2O than H_2O.

Creating "Beakers without Walls": Deeply Supercooled Binary Liquid Solutions from Nanoscale Amorphous Films. Supercooled liquids are thermodynamically metastable which makes studies of this fundamentally important regime difficult. One challenge in the study of the physiochemical properties of liquid in a supercooled state is the difficulty in preventing crystallization. We have recently demonstrated an alternate approach to create and study these elusive liquids which we call "beakers without walls." Through the use of use of molecular beams and nanoscale amorphous solid films, we are able to produce deeply supercooled liquid solutions and study their transport properties. Our approach is to heat an amorphous solid above its glass transition temperature, Tg, where upon it transforms into a supercooled liquid prior to crystallization.

For pure substances, these supercooled liquids rapidly freeze into the thermodynamically stable crystalline solid. The FTIR spectra show that pure species rapidly crystallize whereas crystallization is inhibited in the mixtures. This is shown in Figure 2, where amorphous deposits of pure methanol and ethanol readily crystallize upon heating above their glass transition temperature. However, a compositionally tailored nanoscale film (20 nm thick) comprised of methanol deposited on top of ethanol undergoes extensive diffusive intermixing upon heating above the glass transition. This intermixing produces a deeply supercooled binary solution that resists crystallization. The diffusion coefficient in this mixture is over a million-fold smaller than that room temperature! Furthermore, this supercooled solution is "ideal" and the desorption from this solution is perfectly described by a kinetic model based on Raoult's Law. The lifetime of the supercooled liquid is determined by the kinetics of phase separation and crystallization, which ultimately lead to the formation of the thermodynamically stable phase(s). This study opens up possibilities to answer questions regarding the spatial homogeneity and kinetic stability in the metastable regime of deeply supercooled liquid solutions in unprecedented detail. Future directions are aimed at extending these studies to aqueous solutions of alcohols, acids, bases, and salts.

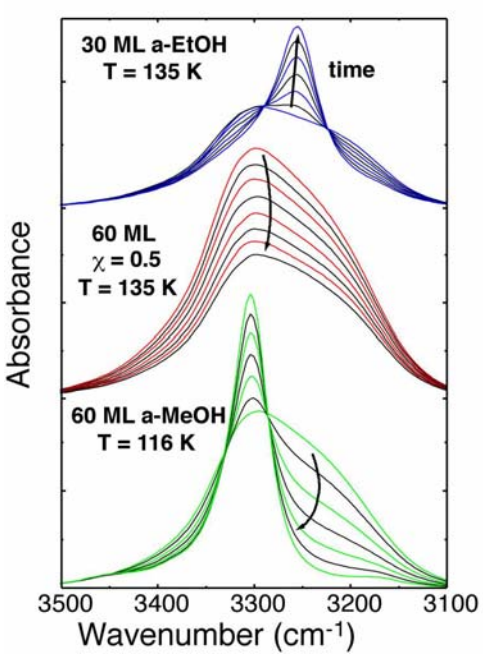

Figure 2. A time series of FTIR spectra for initially amorphous thin films of ethanol (top), ethanol and methanol (middle), and methanol (bottom). The spectra show that the pure films crystallize whereas the mixed film does not.

Synthesis, Characterization, and Reactivity of Nanoporous Thin Films. In order to make a useful catalytic material, the chemical composition of the nanoporous material must also be controlled. For these materials, the transport of reagents through the pores and the catalytic reactions are intimately coupled. The interaction of gases and fluids with these nanoporous films forms the basis for a variety of the useful applications of porous materials. For example, the rates of uptake, sequestration, reaction, and release of gases in these materials often determine their performance characteristics in devices such as catalysts and chemical sensors. Understanding these processes is essential for the rational design and synthesis of materials for particular applications.

We have previously shown that morphology of vapor deposited amorphous solid water films in ASW films is strongly dependent on the incident growth angle. Films with structures from non-porous to highly porous were grown by increasing the angle of incidence of the impinging molecules. A simple physical mechanism, ballistic deposition, can be used to understand the dependence of morphology on the growth angle. The basic premise of ballistic deposition is that molecules incident from the gas phase stick at the first site they encounter at the surface of the solid without subsequent diffusion. Ballistic deposition at or near normal incidence results in rough surfaces due to the stochastic nature of the deposition process. At grazing incidence, deposition can not occur in regions behind high points on the surface due to simple shadowing, resulting in the formation of columnar, porous materials.

Based on ballistic deposition and shadowing concepts, we have developed a new technique, reactive ballistic deposition (RBD), to grow compositionally and structurally tailored metal oxides with extremely high porosities and surface areas. Figure 3 shows an electron micrograph for a 1 micron thick,

nanoporous MgO film. The film consists of an array of highly oriented, predominantly independent, columnar filaments tethered to the underlying substrate. These thin films have been characterized by N_2 adsorption and electron microscopy and have surface areas as high exceeding 1000 m^2/g. The films are thermally robust, retaining their surface area up to 1200 K. We speculate that the largely independent filaments are responsible for the observed high-temperature stability and will give rise to facile transport of reagents within the film.

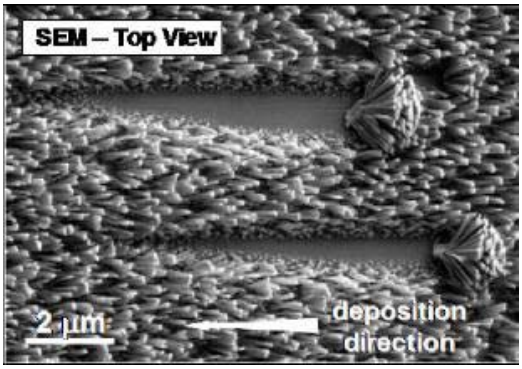

Figure 3. Thin film of MgO grown at a molecular beam growth angle of 85°.

We are currently applying these same techniques and concepts to grow highly porous metallic films (Au, Pd). Future research in this area will focus on characterizing the chemical reactivity and reaction kinetics and dynamics in these novel materials.

References to Publications of DOE sponsored Research (FY 2002- present)

1. "The Effect of Porosity on the Adsorption, Desorption, Trapping and Release of Volatile Gases by Amorphous Solid Water", P Ayotte, RS Smith, KP Stevenson, Z Dohnálek, GA Kimmel, and BD Kay, *J. of Geophysical Research – Planets* **106**, 33387-33392 (2001).
2. "Structural and Chemical Characterization of Aligned Crystalline Nanoporous MgO Films Grown via Reactive Ballistic Deposition", Z Dohnálek, GA Kimmel, DE McCready, JS Young, A Dohnálková, RS Smith, and BD Kay , *J. Phys. Chem. B* **106**, 3526-3529, 2002.
3. "The Continuity between ASW and Supercooled Liquid Water", R. Scott Smith, Zdenek Dohnálek, Greg A. Kimmel, K. P. Stevenson, and Bruce D. Kay, (**Invited** Book Chapter in *ACS Symposium Series 820: Liquid Dynamics, Experiment, Simulation and Theory*, (ed. J. T. Fourkas) 198-211 (American Chemical Society, Washington, DC, 2002).
4. "A Beaker without Walls: Formation of Deeply Supercooled Binary Liquid Solutions of Alcohols from Nanoscale Amorphous Solid Films", P Ayotte, RS Smith, Z Dohnálek, GA Kimmel, and BD Kay, *Phys. Rev. Lett.* **88**, 245505-1-245505-4, 2002.
5. "Adsorption Dynamics and Desorption Kinetics of Argon and Methane on MgO(100)", Z Dohnálek, RS Smith, and BD Kay, *J. Phys. Chem. B* **106**, 8360-8366, 2002.
6. "The deposition angle-dependent density of amorphous solid water film", Z Dohnalek, GA Kimmel, P Ayotte, RS Smith and BD Kay. *J. Chem. Phys.,* **118**, 364 (2003).
7. "Molecular Beam Studies of Nanoscale Films of Amorphous Solid Water", RS Smith, Z Dohnalek, GA Kimmel, G Teeter, P Ayotte, J Daschbach and BD Kay. in *Water in Confining Geometries* (eds. V. Buch and J. P. Devlin) 337 (Springer, 2003).
8. "Temperature independent physisorption kinetics and adsorbate layer compression for Ar adsorbed on Pt(111)", GA Kimmel, M Persson, Z Dohnalek & BD Kay, Journal of Chemical Physics **119**, 6776-6783, 2003.
9. "Adsorption, desorption, and clustering of H_2O on Pt(111)", J. L. Daschbach, B. M. Peden, R. S. Smith and B. D. Kay, Journal of Chemical Physics **120**, 1516-1523, 2004.
10. "Helium diffusion through H_2O and D_2O amorphous ice: Observation of a lattice inverse isotope effect", J. L. Daschbach, G. K. Schenter, P. Ayotte, R. S. Smith and B. D. Kay**,** Physical Review Letters **92**, 198306, 2004.
11. "Reactive Growth of Nanoscale MgO Films by Mg Atom Deposition onto O_2 Multilayers", J Kim, Z Dohnálek, JM White, and BD Kay, J. Phys. Chem. B, **108**, 11666, 2004.

Single-Molecule Kinetics and Dynamics in the Condensed Phase and at Interfaces

Single-Molecule Interfacial Dynamics and Single-Protein Conformational Dynamics[1]

H. Peter Lu
Chemical Sciences Division
Pacific Northwest National Laboratory
P.O.Box 999, MSIN K8-88
Richland, WA 99352
Peter.lu@pnl.gov

Program Scope

Our research is focused on the use of single-molecule techniques to understand molecular dynamics in condensed phase and at interfaces. Single-molecule approaches are unique for heterogeneous and complex systems because the static and dynamic inhomogeneities can be identified, characterized, and/or removed by studying one molecule at a time. Single-molecule spectroscopy reveals statistical distributions correlated with microscopic parameters and their fluctuations, which are often hidden in ensemble-averaged measurements. Single molecules (and molecular complexes) are observed in real time as they traverse a range of energy states, and the effect of this ever-changing "system configuration" on chemical reactions and other dynamical processes can be mapped. We selected two system classes for our molecular dynamics research: 1) electron transfer reactions on solid surfaces (interfaces) and 2) reactions and dynamics in proteins and protein complexes. The selection of biomolecules in studying condensed-phase chemical dynamics reflects both relevance and advantages. The proteins have been engineered by years of evolution to perform interesting dynamics (large-scale conformational motion, cooperativity, selective chemistry, etc.). Many of them have been studied at length by other methods at ensemble level providing a sound basis for interpretation of new data that are not obtainable in ensemble-averaged experiments. And, there is a wide public interest in the findings.

Single-molecule photon stamping spectroscopy, time-resolved single-molecule anisotropy, single-molecule fluctuation and fluorescence resonance energy transfer (FRET) spectroscopy, near-field and atomic force microscopy-enhanced confocal imaging microscopes, and surface enhanced Raman spectroscopy have been applied to the study of single-protein conformation and reaction dynamics and interfacial electron transfer dynamics.

Recent Progress and Future Plans

Intermittent Single-Molecule Interfacial Electron Transfer Dynamics. Interfacial electron transfer (ET) dynamics is important for environmental and catalytic reaction systems. Extensive ensemble-averaged studies of the electron transfer kinetics in the dye-sensitized TiO_2 nanoparticle (NP) systems at different time scales had been reported. Their results show large discrepancies in the observed rates of electron transfer dynamics, which indicates broad inhomogeneity of kinetics of interfacial redox reaction dynamics. To examine interfacial electron transfer inhomogeneity, we have studied the dynamics of the single-molecule interfacial electron transfer process of cresyl violet and coumarin 343 adsorbed at the surface of TiO_2 NPs. Conducting single-molecule spectroscopy experiments can avoid molecular aggregation, multiple electron injection to a single particle, and multiple electron-cation recombination at a single particle. Fluorescence intensity trajectories of individual dye molecules adsorbed on a TiO_2 NP surface

[1] Collaborators on these projects include D. Hu, G. K. Schenter, and E. R. Vorpagel from PNNL

showed fluorescence fluctuations and blinking, with time constants distributed from milliseconds to seconds. The fluorescence fluctuation dynamics were found to be inhomogeneous from molecule to molecule and from time to time, showing significant static and dynamic disorders in the interfacial ET reaction dynamics. Based on a series of control experiments, we attribute fluorescence fluctuations to the interfacial ET reaction rate fluctuations, associating redox reactivity intermittency with the fluctuations of molecule-TiO_2 electronic and Franck-Condon coupling. Intermittent interfacial ET dynamics of individual molecules could be characteristic of a surface chemical reaction strongly involved with and regulated by molecule-surface interactions. The intermittent interfacial reaction dynamics that likely occur among single molecules in other interfacial and surface chemical processes can typically be observed by single-molecule studies, but not by conventional ensemble-averaged experiments. Currently, combining site-specific Raman spectroscopy, time-dependent wave packet scattering spectral analyses, and single-molecule fluorescence spectroscopy, we have been working on characterizing the molecular properties that control the ET processes, including donor-acceptor electronic coupling, the redox reaction driving force, the Franck-Condon factor, and nuclear relaxation energies. The long-term goal of this project is to develop a noninvasive, vibration-selective, and single-molecule sensitive spectroscopic methodology to study single-molecule dynamics and energetics in chemical and environmental reaction systems.

Inhomogeneous single-molecule protein conformational dynamics under enzymatic reactions: Although enzymatic reactions are traditionally studied at the ensemble level, the inhomogeneities of the reaction rate, the correlated enzyme conformational motions, and the non-synchronized nature of these multiple-step reactions make it extremely difficult to obtain stepwise mechanistic and dynamic information from such studies. We have been studying single-molecule enzymatic reactions, focusing on the enzyme active-site conformational dynamics, under physiological conditions in recent years. The static and dynamic disorder of single-molecule enzymatic reaction dynamics and associated protein conformational changes have been observed by measuring single-molecule protein domain motions, monitoring co-enzyme redox state turnovers in real-time, and recording enzymatic reaction product formation in real-time. Applying single-molecule spectroscopy, we have been able to probe protein conformational motions of a single enzyme (T4 lysozyme, an 18.6-kDa, single-subunit, and a 164-amino acid enzyme comprising two domains connected by an α-helix) during hydrolysis of the polysaccharide walls of *Escherichia coli B* cells. By attaching a donor-acceptor (tetramethylrhodamine-Texas Red; or Alexa 488-Alexa560) pair of dye molecules site-specifically to non-interfering sites on the enzyme, we measured the dynamics of the hinge-bending motions of the enzyme under enzymatic turnovers by monitoring the donor-acceptor emission intensity changes due to single-pair FRET (spFRET). The overall enzymatic reaction rate constants were found to vary widely from molecule to molecule. The enzyme's searching for reactive sites in the substrate was thought to account for most of this inhomogeneity. By applying a molecular dynamics (MD) simulation and a random-walk model to analyze the enzyme-substrate complex formation dynamics, we have revealed multiple intermediate conformational states in the chemical reaction process. This approach provides information on the microscopic conformational change mean drifting velocity, diffusion coefficient, friction coefficient, energy consumed by friction along the reaction coordinate, and the energy landscape for a complex condensed-phase chemical reaction. Our future direction of this project is to investigate the local-environmental and spatially confinement on the protein conformational motion dynamics and enzymatic reaction dynamics. Spatially confined enzyme molecules, such as tethered enzyme proteins on solid surfaces, have been reported to have an enhanced longevity of the enzymatic activities. However, the spatial and temporal inhomogeneities of the non-synchronizable stochastic protein rotational and conformational motions are extremely difficult to characterize with ensemble-averaged measurements. The long-term goal of this project is to extend our molecule-level understanding of protein conformational fluctuation and relaxation dynamics and their impact on enzymatic reaction dynamics. Non-Arrhenius and non-Markovian dynamics, hysteresis, cooperativity, and memory effects of enzymatic reactions are widely observed but are poorly understood due to the nature of the inhomogeneity in an ensemble-averaged measurement. These inhomogeneities, on the other hand, can be effectively removed and unambiguously identified by single-molecule approaches.

Single-molecule DNA-protein interaction dynamics in DNA damage recognitions: Protein-protein and protein-DNA interactions play critical roles in biological systems, and these interactions often involve complex mechanisms and inhomogeneous dynamics. Our single-molecule spectroscopy study reveals dynamics of fluctuating molecular noncovalent interactions within single excision repair protein (XPA)-DNA complexes that involve the DNA damage recognition processes. These results facilitate a molecule-level understanding for the dynamics and mechanisms of the damage-recognition process in DNA repair. We observed fluorescence intensity fluctuations in single XPA-DNA complexes at millisecond time scales. Control experiments have demonstrated that the fluctuations are due to XPA-DNA interactive and spontaneous conformational changes. The slow conformational coordinates are associated with interactive motions of the DNA-XPA complex at the binding site. Slow and large-amplitude conformational motions of DNA-XPA complexes have not been reported previously and this finding is consistent with XPA's ability to recognize a wide variety of DNA lesions. An approximately 10-fold variation occurs in the rates of the slow interactive conformational motions among the individual complexes. This inhomogeniety is most likely associated with the existence of different subsets of protein conformations seeking an induced fit to a conformationaly fluctuating DNA lesion. The fluctuation dynamics of XPA-DNA interactions was further evaluated by calculating the higher order correlation functions of the single-molecule trajectories, which suggests the interaction dynamics may be essentially fit to a two-state model. We have formed a working model of a "fly fishing" protein-protein interaction mechanism based on existing theories of conformational dimensionality reduction, fly-casting driven by induced-fit, water, and ion exclusion. These trapped and slow-fluctuating interactions could be crucial in XPA-DNA interaction dynamics and intrinsically pertinent to the protein-DNA complexes in other DNA damage recognition processes. Proteins rarely act alone, often involving protein-protein interactions as protein complexes. Our future effort in this work will involve studying protein-protein interaction conformational fluctuation dynamics. Our experiments will further substantiate that the slow and large-amplitude conformational fluctuations of the protein complex are important in controlling the recognition interactions, and large inhomogeneous rates were often existed in these dynamic processes.

Site-specific Atomic Force Microscopy-tip enhanced Raman spectroscopy: To identify and characterize the inhomogeneous interfacial chemical reaction dynamics, it is highly advantageous to obtain both topographic and spectroscopic characterization of surfaces and interfacial systems. For example, the site-to-site variations in the geometries and interactions at the molecule-surface interface result in an inhomogeneous distribution of electron transfer rates that can be effectively evaluated with single molecule methods. Vibrational-mode resolved single-molecule dynamics should be highly informative and powerful to decipher inhomogeneous chemical dynamics at interfaces and in condesed phase. In recent years, there have been tremendous advances in applying SERS to study nanoparticles and nanostructures at high sensitivity of the single-molecule level. To carry on the study of vibrational-mode resolved single-molecule dynamics, we have set up an atomic force microscopy coupled Raman microscope system capable of simultaneously measuring topographic and spectroscopic information at nanometer scale. In a site-specific Raman spectroscopic measurement, it has been typically observed that the Raman peak intensities, peak/peak intensity ratios, and peak positions show fluctuating behaviors. Our laser intensity dependent experimental results suggest that the fluctuations can even exist in multiple-dye-adsorbated NPs at high laser excitation intensity and that the fluctuations are predominately photoinduced. In contrast, we also see spontaneous fluctuations at low laser excitation intensity ($< 10^3$ W/cm^2). The overall Raman intensity fluctuation is dictated by the change of the interaction of the molecules with the local electric field of an NP, for example, the rotational and translational motions of the adsorbed molecules under the near-field and gradient-field of the NPs. Currently, we have focused on site-specific Raman spectroscopy applications on studying interfacial electron transfer dynamics. To reveal the physical nature of the reactivity inhomogeneity, we have been and will correlating topographical information with the electron transfer dynamics. Furthermore, we will apply site-specific Raman spectroscopy to obtain vibration-mode specified (Franck-Condon) description of electron transfer dynamics. The combined use of fluorescence, enhanced

Raman spectroscopy, and topographical mapping is expected to provide new insights required to understand interfacial electron transfer rate processes that involve site-dependent internal and external vibrational relaxations, solvent relaxation, and other factors controlled by the electronic and geometric properties of the reaction site. Detailed microscopic pictures of interfacial electron transfer dynamics are expected to emerge from these new experimental approaches.

References to publications of DOE sponsored research (FY2002–present)

1. V. Biju, Miodrag Micic, Dehong Hu, and H. Peter Lu, "Intermittent Single-Molecule Interfacial Electron Transfer Dynamics," *J. Am. Chem. Soc.* **126**, 9374-9381 (2004).

2. H. Peter Lu, "Single-Molecule Study of Protein-Protein and Protein-DNA Interaction Dynamics," an invited book chapter in Protein-Ligand Interactions, edited by Uli Nienhaus, The Humana Press Inc., in press (2004).

3. H. Peter Lu, invited review, "Single-molecule spectroscopy studies of conformational change dynamics in enzymatic reactions," a special issue of *Curr Pharm Biotech* (The way down from single genes, and proteins to single molecules.), **5**, 261-269 (2004).

4. Dehong Hu, H. Peter Lu, "Single Molecule Implanting of T4 Lysozyme on Bacterial Cell Surface: Towards Study Single Molecule Enzymatic Reaction in Living Cells," *Biophys. J.,* **87**, 656-661 (2004).

5. D. Hu, M. Micic, N. Klymyshyn, Y. D. Suh, H. Peter Lu, "Correlated topographic and spectroscopic imaging by combined atomic force microscopy and optical microscopy," *J. Luminescence*, **107**, 4-12 (2004).

6. Miodrag Micic, Nicholas Klymyshyn, H. Peter Lu, "Finite Element Method Simulations of the Near-Field Enhancement at the vicinity of Fractal Rough Metallic Surfaces," *J. Phys. Chem. B.,* **108**, 2939 (2004).

7. Dehong Hu, Miodrag Micic, Nicholas Klymyshyn, Yung Doug Suh, and H. Peter Lu "Correlated Topographic and Spectroscopic Imaging Beyond Diffraction Limit by Atomic Force Microscopy Metallic Tip-Enhanced Near-Field Fluorescence Lifetime Microscopy," *Rev. Sci. Inst.*, **74**, 3347 (2003).

8. Yu Chen, Dehong Hu, Erich R. Vorpagel, and H. Peter Lu, "Probing Single-Molecule T4 Lysozyme Conformational Dynamics by Intramolecular Fluorescence Energy Transfer," *J. Phys. Chem. B,* **107**, 7947 (2003).

9. Dehong Hu and H. Peter Lu, "Single-Molecule Nanosecond Anisotropy Dynamics of Tethered Protein Motions," *J. Phys. Chem. B*, **107**, 618 (2003).

10. Yung Doug Suh, Gregory K. Schenter, Leyun Zhu, and H. Peter Lu, "Probing Nano-Surface Enhanced Raman Scattering Fluctuation Dynamics using Correlated AFM and Confocal Ultramicroscopy," *Ultramicroscopy*, **97**, 89 (2003).

11. Miodrag Micic, Nicholas Klymyshyn, Yung Doug Suh, H. Peter Lu, "Finite Element Method Simulation of the Field Distribution for AFM Tip-Enhanced Surface Enhanced Raman Scanning Microscopy," *J. Phys. Chem. B*, **107**, 1574 (2003).

12. Leyun Zhu, Gregory K. Schenter, Miodrag Micic, Yung Doug Suh, Nicholas Klymyshyn, H. Peter Lu, "Nano-Surface Enhanced Raman Scattering Fluctuation Dynamics," *Proceedings of SPIE*, **4962**, 70 (2003).

Research Summaries

(Alphabetically by First PI)

Cluster Deposition Studies of the Effects of Cluster Size and Support Defect on Model Catalysts

Scott L. Anderson
Chemistry Department
University of Utah
315 S. 1400 E. Rm 2020
Salt Lake City, UT 84112
email: anderson@chem.utah.edu

Program Scope:

This program is aimed at improving our understanding of supported catalysts. Size- and energy-selected metal cluster ions are deposited on single crystal or thin film oxide supports and the physical and chemical behavior is studied. Sample temperature is varied over a wide range to examine diffusion and sintering effects on the size and binding site distributions, along with associated effects on the catalytic behavior. In addition, the oxide preparation method is varied to change the density of defects in the support, allowing study of defect effects on physical and catalytic properties.

Recent Progress:

Our effort early in the reporting period focused on the Ni/TiO_2 and Ir/TiO_2 systems, as described in the first two publications listed below. This report will describe more recent work on supported gold catalysts – catalysts that have been the focus of intense scrutiny since the discovery by Haruta and co-workers[1,2] of unique catalytic activity for supported nano-scale gold. As with many groups, we chose the CO oxidation reaction as a simple but relevant test system. Before presenting our results, it is worth briefly outlining related results in the literature.

Taking Au/TiO_2 as the best studied system, early Haruta studies determined that CO oxidation activity peaked quite sharply for average cluster size around 2 nm, as determined by TEM. Work in the Goodman[3] and Campbell[4] groups suggested that the thickness of the gold particles was the determining factor, with peak activity for two layer particles, which also had diameters in the few nanometer range. Recently Goodman and co-workers have shown CO oxidation activity for continuous overlayers of Au on TiO_2 films grown on Mo(112), with bilayer structures being significantly more active.[5] In contrast to this work indicating that rather large nanostructures are responsible for catalyst activity, several studies have shown non-negligible activity for much smaller Au species, at least in related systems. For example, size-selected cluster deposition of Au_n on MgO by Heiz and co-workers[6] showed onset of CO oxidation activity at Au_8 – a size unlikely to form bilayer structures. A provocative experiment in this context was reported by Fu et al.[7] who studied the water gas shift reaction on Au/CeO_2 and Pt/CeO_2 catalysts. They found that activity was identical for as-prepared catalysts with nanometer scale metal particles, and catalysts where the TEM-visible metal particles had been etched away, leaving only molecular scale metal-support complexes. The results below are the first direct probing of activity for size-selected Au_n on TiO_2 and Al_2O_3.

Au/TiO_2 model catalysts were prepared by deposition of Au_n^+ on room temperature single crystal rutile $TiO_2(110)$, at an impact energy of 1 eV/atom. The CO oxidation activity was probed by first exposing the samples to 600 L of $^{18}O_2$, in order to create a population of active oxygen on the surface. O_2 is known to bind and dissociate at oxygen vacancies on the TiO_2 surface, and atomic oxygen exposure has been shown to result in O binding to gold.[4] In our experiments, ion scattering spectroscopy (ISS) shows ^{18}O on the surface, and also some attenuation of Au ISS signal, consistent with oxygen bound at Au sites, and also at vacancy sites on the TiO_2. The CO oxidation reaction was then carried out by exposing the oxygen pre-loaded surface to pulses of CO, each lasting ~150 msec and amounting to an integrated dose of ~0.2 L/pulse. $C^{18}O^{16}O$ product desorbing from the surface was monitored by a differentially-pumped mass spectrometer. Fig. 1 shows a typical pulse sequence for clean TiO_2 and for TiO_2 with Au_1 - Au_4 deposited. Note that some CO oxidation occurs on the oxygen-dosed TiO_2, attributed to reaction with active oxygen species bound at vacancy sites.

For Au_1, the reaction is almost completely suppressed, indicating that: (a) CO oxidation does not

occur on Au/TiO_2, and (b), the presence of Au blocks reaction at the vacancy sites. We infer that Au binds at vacancy sites at room temperature, blocking them. The density of Au deposited is close to the vacancy density, thus we expect a large fraction of the vacancies to be Au-filled, accounting for the low reactivity of Au_1/TiO_2. For Au_2 deposition, the activity is higher, but still below that of clean TiO_2. We infer that Au_2 is also binding at defects, and is unreactive. In this case, however, the number density of Au_2 is ~half the vacancy density, thus we attribute the CO oxidation activity to reaction at unblocked vacancy sites. For Au_3 deposition, the activity is substantially higher than that of clean TiO_2, indicating that the gold sites are reactive. As shown in Fig. 2, activity decreases slightly for Au_4, then increases substantially for Au_7.

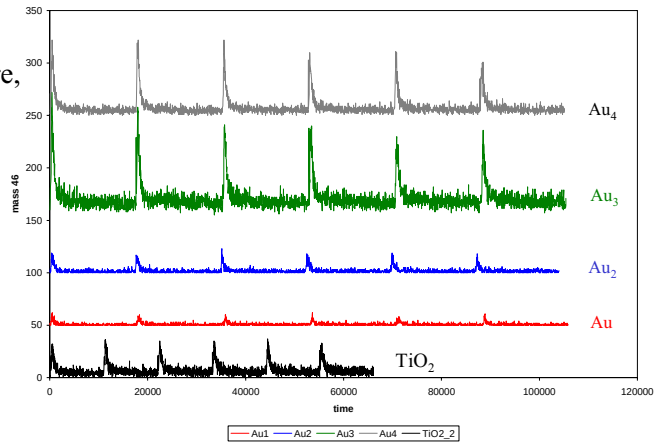

Figure 1. Time dependence of CO_2 evolution for TiO_2 and Au_n/TiO_2

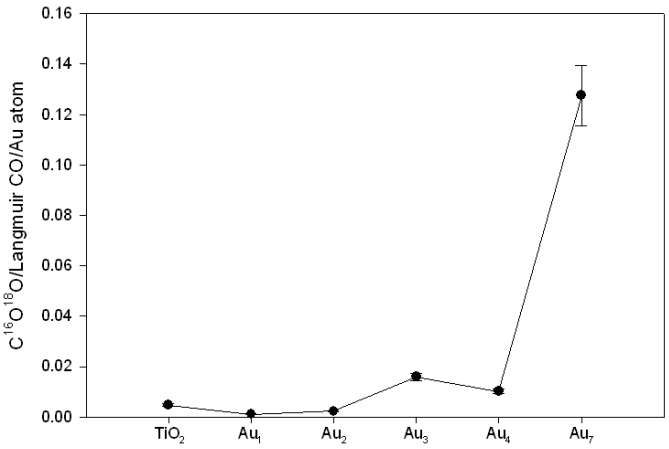

Figure 2. CO oxidation activity for TiO_2 and several catalysts prepared by deposition of Au_n on TiO_2

Fig. 1 also shows that the activity decreases slowly during the sequence of CO pulses. Activity declines to half the initial value in ~50 CO pulses, corresponding to ~10 L exposure. We attribute the decline largely to depletion of the active surface oxygen by reaction with CO, rather than to sintering or other changes in the catalyst. This conclusion is supported by the observation that the activity is ~80% restored when the inactive catalyst is re-exposed to O_2.

These results show several things. First, the sharp and strong size dependence indicates that Au_n^+ deposition at 1 eV/atom does not lead to substantial fragmentation or sintering of the clusters. In fact, the size-dependent activity is quite persistent, holding up through several cycles of O_2 exposure and CO pulsing. We also infer that activity first turns on at Au_3, and is large for sizes that are still well below the nanometer/bilayer size structures shown to be active in previous model catalyst studies. To try to understand the origin of the size dependence, we studied the binding of O_2 and CO to the samples using ISS. Oxygen binding to gold, as well as to vacancy sites, is found for all cluster sizes. For the non-reactive Au and Au_2 samples, we find that CO exposure leads to strong attenuation of Au ISS signal, and no attenuation of Ti or O ISS signals, indicating that CO is binding exclusive to Au centers. In contrast, for Au_3 or larger, no CO-induced attenuation of Au ISS is observed. Instead, attenuation is seen of the Ti and O ISS signal, not seen in absence of gold deposition. This result indicates that Au is required for CO binding, but that the CO is not bound directly to the Au for the larger clusters. Binding might be at sites at the periphery of the Au clusters, for example. CO TPD experiments indicate that CO binding to larger clusters is substantially weaker, relative to binding to isolated Au atoms. These results suggest that Au and Au_2 are unreactive under our conditions because CO binds too tightly to react with surface oxygen at room temperature.

The conclusion that our Au_n^+ are depositing more-or-less intact at 300K is interesting in light of STM data from Wahlström *et al.*[8] who evaporated Au atoms onto TiO_2 (110) in varying doses and at varying temperatures, and determined the average Au cluster size that formed. Extrapolation of their

results to our Au dose level (0.1 of a close-packed Au monolayer), suggests that we should see an average cluster size of tens of atoms, grown by diffusion and sintering of the deposited gold. Such sintering is clearly inconsistent with the strong dependence of reactivity on deposited cluster size. The most obvious differences between our experiment and theirs are that we deposit pre-formed clusters at hyperthermal energies, rather than thermal atoms. Pre-formed clusters are expected to diffuse and sinter differently than atoms, because clusters are inherently more stable (hence the tendency to sinter). It is not clear, however, why deposition of Au^+ does not appear to grow a distribution of large (and therefore reactive) clusters in our experiments.

To address that question, we studied thermal effects on samples prepared by Au^+ deposition, probed by a combination of x-ray photoelectron spectroscopy (XPS), ISS, CO adsorption, and CO-oxidation. As expected from Fig. 2, it is possible to induce significant reactivity in a Au_1/TiO_2 sample by annealing to elevated temperatures, thereby activating cluster formation. Maximum activity is found for 600 K annealing, then activity decreases after annealing to higher temperatures.

XPS and ISS provide a ready interpretation for this result. The Au 4f XPS spectra show evidence for three different Au chemical shifts, indicative of Au in three distinct surface bonding environments. As shown in Fig. 3, for Au deposited at 115 K, and not annealed above 200 K, ~90% of the Au has a $4f_{7/2}$ binding energy of 85.8 eV, with ~10% in a bonding environment with $4f_{7/2}$ binding energy of 85.4 eV. Because mobility is expected to be minimal at low temperatures, we attribute the 85.8 eV binding energy to Au bound on TiO_2 terrace sites, and the 10% with lower binding energy to Au bound at oxygen vacancies. This assignment is consistent with experiments done on TiO_2 which was lightly bombarded with He^+, creating additional oxygen vacancies, along with other defects. Au^+ deposited on this vacancy-rich TiO_2 has a much larger fraction of the Au in a bonding environment with $4f_{7/2}$ binding energy of 85.4 eV, i.e., in the sites assigned as Au-vacancy complexes. Lower Au 4f binding energy for Au-vacancy complexes is expected because the electron-rich vacancy sites transfer electron density to the gold. Given that the density of vacancies on our vacuum-annealed TiO_2 is also ~10%, we concluded that Au^+ deposited at low temperatures simply binds near its landing point.

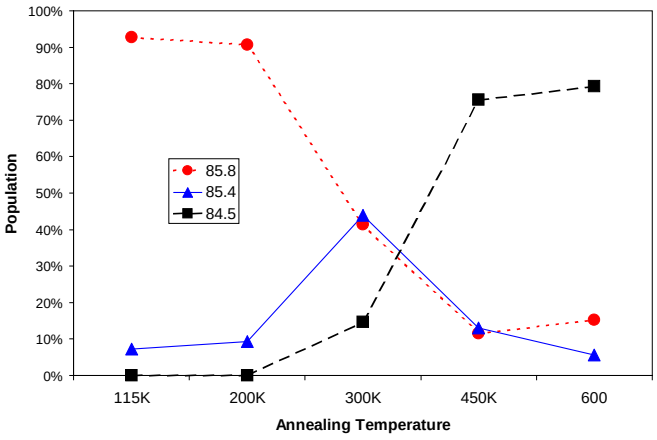

Figure 3. Populations of different Au-TiO_2 bonding environments as probed by XPS

When the sample is annealed to 300 K for 5 minutes, then re-cooled and examined by XPS, about 45% of the Au is still in the as-deposited state, 45% is in the state attributed to Au-vacancy binding, and ~10% is in a bonding environment characterized by new shoulder at even lower $4f_{7/2}$ binding energy - 84.5 eV. After annealing at 450 K or 600 K, the majority of the Au is in the state with 84.5 eV binding energy. This high temperature state is attributed to Au bound in small aggregates on the surface. ISS measurements are consistent with this picture. For annealing up to 300 K, there is no change in Au ISS intensity, indicating that the Au dispersion is not changing. This is just what would be expected if Au atoms were simply diffusing and binding at the nearest vacancy site. There is a small decrease in gold dispersion (i.e., a small Au ISS intensity decrease) at 450 K, consistent with aggregation into small one- or two-dimensional clusters, where most or all of the Au atoms are still exposed on the surface. The Au ISS continues to decrease at higher annealing temperatures, to about 60% of the initial intensity for T_{anneal} = 800K. Such a large ISS decrease suggests that 3-dimensional aggregates are starting to form, where some Au is no longer exposed on the surface. All these results, and the sharp size effects on activity, are consistent with sintering being insignificant at room temperature, but becoming important for

temperatures above 400 K.

For comparison, analogous experiments were performed for Au_n^+ deposited on epitaxial Al_2O_3 films grown on NiAl (110). No CO oxidation activity was observed for any cluster size studied. This result is consistent with the picture emerging in the Au/TiO_2 system, where activity is promoted by electron transfer from oxygen vacancies to Au_n. We also studied Au diffusion and sintering on the Al_2O_3 films. The Au XPS shows some shift to lower binding energies with increasing annealing temperature, but the shifts are small compared to those seen for TiO_2. On the other hand, the shifts in XPS binding energies with deposited cluster size are much larger for Au_n/Al_2O_3 than for Au_n/TiO_2. We interpret this as being a consequence of stronger, and more site-dependent bonding of Au to TiO_2. In that system, the dominant effects on Au chemical shifts come from the interaction of Au with TiO_2 and its surface oxygen vacancies. For Al_2O_3, the Au - surface binding is weaker and less site dependent, therefore the XPS is less dependent on binding site, and more dependent on Au aggregate size. ISS shows much more extensive sintering on Al_2O_3, compared to TiO_2. The Au ISS peak intensity is independent of T_{anneal} up to 300 K, but thereafter, the ISS declines rapidly, to only ~10% of the as-deposited intensity for T_{anneal} = 800 K. Such a large decrease suggests that Au readily sinters to three dimensional aggregates on Al_2O_3, and possibly desorbs or diffuses subsurface at the highest temperatures.

Future Plans:

Work is proceeding in several directions. Additional studies are planned for the Au/TiO_2 system, including infrared probing of CO binding sites for different size Au_n, where ISS suggests there should be a strong size dependence. We also will look at larger clusters and examine the effects of impact energies on sinter stability and chemical reactivity. Depending on how all this works out, we may look at thermal effects and reactions for Au/MgO, extending the earlier work of Heiz, where no characterization of the electronic or dispersion state of the deposited clusters was attempted. In parallel, we have begun some studies of Pd/TiO_2, and plan to compare physical and catalytic behavior with companion studies of Pd/SiO_2 and Pd/Al_2O_3.

References:

[1] H. Sakurai and M. Haruta, Appl. Catal., A **127** (1-2), 93 (1995).

[2] M. Haruta, Catal. Today **36** (1), 153 (1997).

[3] M. Valden, X. Lai, and D. W. Goodman, Science **281** (5383)), 1647 (1998).

[4] V. A. Bondzie, S. C. Parker, and C. T. Campbell, Catal. Lett. **63** (3-4), 143 (1999).

[5] M. S. Chen and D. W. Goodman, Science **article number 1102420** (2004).

[6] A. Sanchez, S. Abbet, U. Heiz, W.-D. Schneider, H. Häkkinen, R. N. Barnett, and U. Landman, J. Phys. Chem. A **103**, 9573 (1999).

[7] Q. Fu, H. Saltsburg, and M. Flytzani-Stephanopoulos, Science **301** (5635), 935 (2003).

[8] E. Wahlstrom, N. Lopez, R. Schaub, P. Thostrup, A. Ronnau, C. Africh, E. Laegsgaard, J. K. Norskov, and F. Besenbacher, Phys. Rev. Lett. **90** (2), 026101/1 (2003).

Publications since 2002 acknowledging DOE support:

"Sintering, Oxidation, and Chemical Properties of Size-Selected Nickel Clusters on TiO_2 (110)", by Masato Aizawa, Sungsik Lee, and Scott L. Anderson., J. Chem. Phys. **117** (2002) 5001-11

"Deposition dynamics and chemical properties of size-selected Ir clusters on TiO_2", Masato Aizawa, Sungsik Lee, and Scott L. Anderson, Surf. Sci. 542 (2003) 253-75.

"CO oxidation on Au_n/TiO_2 catalysts produced by size-selected cluster deposition" Sungsik Lee, Chaoyang Fan, Tianpin Wu, and Scott L. Anderson, JACS 126 (2004) 5682-3.

THERMOCHEMISTRY AND REACTIVITY OF TRANSITION METAL CLUSTERS AND THEIR OXIDES

P. B. Armentrout
315 S. 1400 E. Rm 2020, Department of Chemistry, University of Utah,
Salt Lake City, UT 84112; armentrout@chem.utah.edu

Program Scope

The objectives of this project are to obtain quantitative information regarding the thermodynamic properties of transition metal clusters, their binding energies to various ligands, and their reactivities. Using a guided ion beam tandem mass spectrometer, we examine the reactions of size-specific transition metal cluster ions with simple molecules and measure the absolute cross sections as a function of kinetic energy for each reaction.

Over the past three years, our DOE sponsored work has included studies of the kinetic energy dependences of the size-specific chemistry of V_n^+ (n = 2 - 13) and Ni_n^+ (n = 2 - 16) cluster ions reacting with D_2,[1,2] and of Ni_n^+ (n = 2 - 18) reacting with O_2.[3] Further, we have extended our studies to reactions with more complex molecules, specifically, the size-specific reactions of Fe_n^+ (n = 2 - 15) with ammonia (ND_3),[4] Ni_n^+ (n = 2 - 16) with methane (CD_4),[5] and studies of iron sulfide clusters: Fe_n^+ (n = 2 - 6) with COS and CS_2 and Fe_nS^+ (n = 2 – 4) with Xe and CS_2.[6] An invited review of our recent work that emphasizes the relationship to bulk phase properties was also published.[7] The latter point is illustrated in Figure 1 for the example of nickel clusters bound to hydrogen and oxygen where it is clear that bulk phase bond dissociation energies (BDEs) are approached for modest-sized clusters. Comparable behavior has been observed for V, Cr, and Fe clusters bound to D and O atoms.

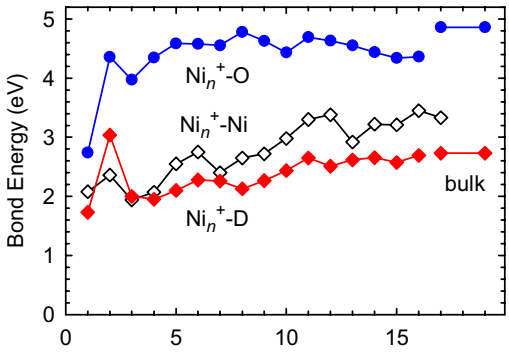

Figure 1. BDEs of D, Ni, and O to Ni_n^+ as a function of cluster size. Lines labeled bulk indicate the BDEs of H and O atoms to Ni films.

Recent Progress

Reactions of Clusters with D_2. We have now studied V_n^+ (n = 2 - 13),[1] Cr_n^+ (n = 2 - 14),[8] Fe_n^+ (n = 2 - 15),[9] and Ni_n^+ (n = 2 - 16)[2] cluster ions reacting with D_2. For all four metal systems, the only products observed are M_nD^+ and $M_nD_2^+$. The failure to observe M_mD^+ and $M_mD_2^+$ products where $m < n$ indicates that the M_nD^+ and $M_nD_2^+$ products dissociate exclusively by D and D_2 loss, consistent with the thermochemistry derived in this work.

In the Ni system, all clusters that form $Ni_nD_2^+$, $n \geq 5$, do so in barrierless exothermic processes. Comparison of the thermal rates of reaction for nickel clusters finds that they approach the collision limit for large clusters ($n \geq 12$) and are comparable to the rates observed for neutral nickel clusters,[10] showing that the charge on such large clusters is not influential in the reactivity observed. For smaller clusters, deviations in the reaction rates of neutral and cationic nickel clusters are found, indicating that the detailed electronic and geometric structures do influence the reactivity.

Using methods developed over the past decade,[11] we analyze the kinetic energy

dependence of the endothermic cross sections in order to determine threshold energies for these processes, which can then be directly related to $D_0(M_n^+\text{-D})$. The BDEs obtained are shown in Figure 1. For smaller clusters, variations in the BDEs must be related to the geometric and electronic structures of the metal cluster ions. Values for larger clusters can be compared to values for H atom binding to bulk nickel surfaces, between 2.70 and 2.74 eV for Ni(111), Ni(100), and Ni(110).[12,13] Figure 1 shows that the largest Ni_n^+-D BDEs ($n \geq 11$) equal the bulk phase value. Similar correspondences were observed in the Cr, V, and Fe systems even though the limiting values vary with the metal, which shows that the cluster bonds accurately track the variations in the bulk phase thermochemistry of different metals. Such correspondences with such small cluster sizes are somewhat surprising, but can be understood by the local nature of the chemical bond.

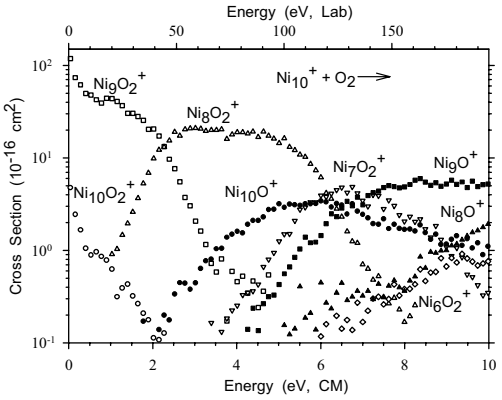

Figure 2. Reaction of Ni_{10}^+ with O_2.

Reactions of Clusters with O_2. Studies of the kinetic energy dependences of the V_n^+ (n = 2 - 17),[14] Cr_n^+ (n = 2 - 18),[15] Fe_n^+ (n = 2 - 18),[16] and Ni_n^+ (n = 2 - 18)[3] cluster ions reacting with O_2 have been completed. The reactions of metal cluster cations with O_2 are complicated as a large number of products are observed, e.g., the results of Figure 2 are representative of clusters larger than Ni_5^+. The magnitudes of the total reaction cross sections at thermal energies are all comparable to the collision cross section, indicating that the reactions are efficient and exothermic. Cluster dioxide ions are the dominant products at low energies. This work shows that metal-oxygen bonds are stronger than metal-metal bonds for all four metals, hence, primary products dissociate by sequential metal atom loss to form smaller cluster dioxide ions. Oxygen atom loss to form cluster monoxide ions, M_mO^+, is much less efficient. Analysis of the kinetic energy dependence is used to provide both $D_0(M_n^+\text{-O})$ and $D_0(M_n^+\text{-2O})$. As shown in Figure 1, the metal cluster oxygen BDEs measured in our work compare favorably to those for bulk phase surfaces.

Reactions of Clusters with CD_4. We have studied the kinetic energy dependences of reactions of Fe_n^+ (n = 2 - 16)[17] and Ni_n^+ (n = 2 - 16)[5] with CD_4. Figure 3 shows results for Ni_6^+, which are typical of most clusters. All observed reactions are endothermic. The lowest energy process for iron is dehydrogenation, whereas for nickel, double dehydrogenation is efficient enough that the $Ni_nCD_2^+$ species is not observed except for the smallest and largest clusters. These results are qualitatively consistent with reactivity observed for hydrocarbons on Fe and Ni surfaces, namely, carbide formation occurs in an activated process.

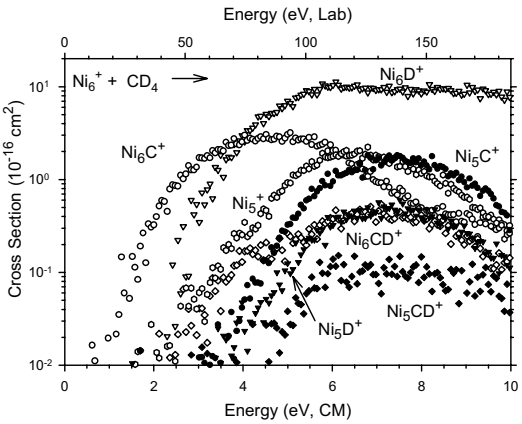

Figure 3. Reaction of Ni_6^+ with CD_4 with primary (open symbols) and secondary (closed symbols) products.

Thresholds for the various primary and secondary reactions are analyzed and BDEs for cluster bonds to C, CD, and CD_2 are determined. Importantly, the accuracy of these BDEs can be assessed because there are usually two independent routes to measure BDEs for each cluster to D, C, CD, and CD_2, e.g.,

$D_0(Ni_6^+\text{-D})$ can be measured in the primary reaction of Ni_6^+ or the secondary reaction of Ni_7^+. We find that the values obtained from the primary and secondary processes are in good agreement with one another for D (which also agrees with the results from reactions with D_2), C, and CD. For the CD_2 ligand, however, we find that the BDEs obtained from the primary reaction are generally low compared with those from the secondary reaction, which is evidence that there are barriers in excess of the endothermicity of the initial dehydrogenation reaction. For larger clusters, evidence suggests that the barrier lies in the initial dissociative chemisorption step.

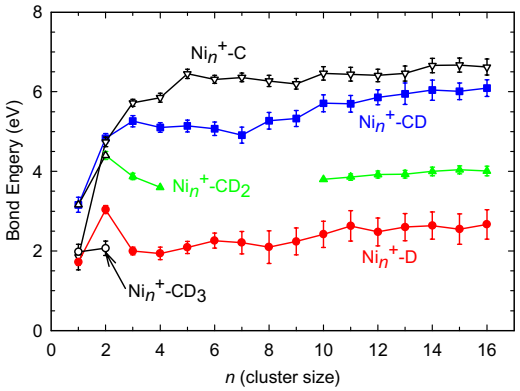

Figure 4. BDEs of D, C, CD, CD_2, and CD_3 to Ni_n^+ vs. cluster size.

Figure 4 shows the final BDEs determined in the nickel study.[5] We find that the values vary somewhat for small clusters but rapidly reach a relatively constant value with increasing cluster size. The magnitudes of these bonds are consistent with simple bond order considerations, namely, D (and CD_3) form one covalent bond, CD_2 forms two, and CD and C form three. Given the results of Figure 1, it seems reasonable that our experimental BDEs for larger clusters should provide reasonable estimates for heats of adsorption to surfaces. As little experimental information is available for *molecular* species binding to surfaces, the thermochemistry derived here for clusters bound to C, CD, and CD_2 provides some of the first experimental thermodynamic information on such molecular species.

Reactions of Clusters with ND_3. Irion and Schnabel (IS)[18] found that Fe_4^+ dehydrogenates ammonia at room temperature to form Fe_4NH^+, whereas no other iron cluster cations undergo the analogous reaction. Larger clusters add intact ammonia molecules (as do neutral iron clusters) and smaller clusters are essentially inert. Our work finds that the thermal reactivity of Fe_4^+ is indeed special, although both Fe_3^+ and Fe_5^+ dehydrogenate ammonia inefficiently at room temperature and all iron clusters (n = 2 – 10, 14) undergo this reaction if provided with sufficient energy, i.e., in activated processes. Figure 5 shows our results for Fe_4^+. The Fe_4ND^+ and $Fe_3ND_3^+$ products exhibit cross sections that decline with energy indicating a barrierless exothermic process, and then an endothermic feature above about 0.5 eV. For larger clusters, the dominant reactions at low energies are adduct formation of $Fe_nND_3^+$, consistent with the work of IS.[18]

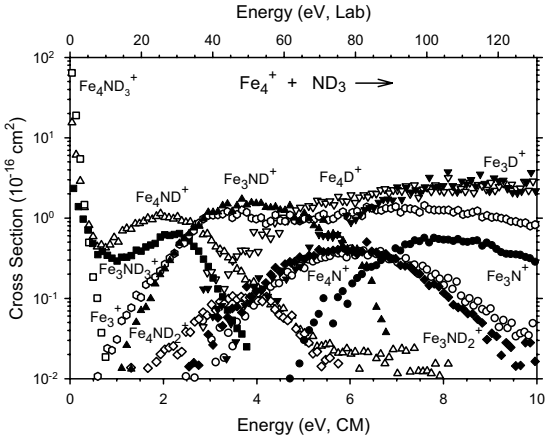

Figure 5. Reaction of Fe_4^+ with ND_3.

The two features in the dehydrogenation cross sections, observed for n = 3 – 5, are plausibly explained by a crossing between the potential energy surfaces corresponding to physisorption and chemisorption of ammonia to Fe_n^+. For most clusters, the surface crossing occurs above the reactant asymptotic energy, but for n = 3 – 5, the barrier is lower, which opens an alternate pathway that bypasses the barrier (reaction probability of ~5% for n = 4 and ~0.1% for n = 3 and 5). The alternate pathways could conceivably involve spin-conserving vs. spin-forbidden processes, or concerted vs. more direct mechanisms.

Iron-sulfur Clusters. Reactions of Fe_n^+ (n = 2 – 6) with COS and CS_2 and Fe_nS^+ (n = 2 - 4) with Xe and CS_2 were examined to elucidate the thermochemistry of iron-sulfur clusters,[6] of key importance in biology. Analyses of cross sections for endothermic reactions in these systems yield $D_0(Fe_n^+\text{-S})$, n = 2 - 5, $D_0(SFe_{n-1}^+\text{-Fe})$, n = 2 - 5, $D_0(SFe_n^+\text{-S})$, n = 1 - 3, and $D_0(S_2Fe_{n-1}^+\text{-Fe})$, n = 2, 3, as well as the ionization energy $IE(Fe_2S_2)$. Our results show that binding between sulfur and these small clusters strengthens as the cluster size increases up to n = 4, which suggests that sulfur occupies multifold coordination sites in the clusters Fe_nS^+ (n = 2 - 5) and $Fe_nS_2^+$ (n = 2 and 3). Such structures resemble those of bulk-phase iron-sulfur clusters, suggesting that Fe_nS^+ and $Fe_nS_2^+$ are useful gas-phase models for the bulk. We find that $Fe_2S_2^+$ is relatively stable, which may be of particular interest because this species mimics the core of the smallest ferredoxin.

Future Plans

Experimental work has begun on the reactions of Fe_n^+ with N_2, along with the reactions of Co_n^+ with D_2 and CD_4. The first study is designed to provide insight into the rate-limiting step in the Haber process, which uses a promoted iron catalyst to manufacture ammonia from N_2 and H_2 at high pressures and temperatures. The latter systems are designed to allow us to examine the periodic trends in the thermochemistry and reaction mechanisms for activation of methane. We also plan to initiate studies of the reactions of oxygenated iron clusters, $Fe_nO_m^+$, which might mimic the chemistry of metal oxide surfaces. The possibility that specific oxidation states of the iron clusters might induce efficient oxidation of species like methane will be explored.

Publications resulting from DOE sponsored research (1 – 7) and References

1. R. Liyanage, J. Conceição, and P. B. Armentrout, P. B. J. Chem. Phys. **116**, 936 (2002).
2. F. Liu, R. Liyanage, and P. B. Armentrout, J. Chem. Phys. **117**, 132 (2002).
3. D. Vardhan, R. Liyanage, and P. B. Armentrout, J. Chem. Phys. **119**, 4166 (2003).
4. R. Liyanage, J. B. Griffin, and P. B. Armentrout, J. Chem. Phys. **119**, 8979 (2003).
5. F. Liu, X.-G. Zhang, R. Liyanage, and P. B. Armentrout, J. Chem. Phys. accepted.
6. K. Koszinowski, D. Schröder, H. Schwarz, R. Liyanage, and P. B. Armentrout, J. Chem. Phys. **117**, 10039 (2002).
7. P. B. Armentrout, Eur. J. Mass Spectrom. **9**, 531 (2003).
8. J. Conceição, R. Liyanage, and P. B. Armentrout, Chem. Phys. **262**, 115 (2000).
9. J. Conceição, S. K. Loh, L. Lian, and P. B. Armentrout, J. Chem. Phys. **104**, 3976 (1996).
10. M. D. Morse, M. E. Geusic, J. R. Heath, and R. E. Smalley, J. Chem. Phys. **83**, 2293 (1985).
11. P. B. Armentrout, *Advances in Gas Phase Ion Chemistry*, Vol. 1; N. G. Adams and L. M. Babcock, Eds.; JAI: Greenwich, 1992; pp. 83-119.
12. K. Christmann, R. J. Behm, G. Ertl, M. A. Van Hove, and W. H. Weinberg, J. Chem. Phys. **70**, 4168 (1979).
13. J. Lapujoulade and K. S. Neil, J. Chem. Phys. **57**, 34 (1972).
14. J. Xu, M. T. Rodgers, J. B. Griffin, and P. B. Armentrout, J. Chem. Phys. **108**, 9339 (1998).
15. J. B. Griffin and P. B. Armentrout, J. Chem. Phys. **108**, 8062 (1998).
16. J. B. Griffin and P. B. Armentrout, J. Chem. Phys. **106**, 4448 (1997).
17. R. Liyanage, X.-G. Zhang, and P. B. Armentrout, J. Chem. Phys. **115**, 9747 (2001).
18. M. P. Irion and P. Schnabel, J. Phys. Chem. **95**, 105966 (1991).

"Electronic Structure of Transition Metal Clusters, and Actinide Complexes, and Their Reactivities"

K. Balasubramanian

Institute of Data Analysis and Visualization, University of California, Davis, Livermore, California 94550; Chemistry and Material Science Directorate, Lawrence Livermore National Laboratory, University of California, Livermore, California 94550; Glenn T. Seaborg Center, Lawrence Berkeley National Laboratory, Berkeley, California 94720

kbala@ucdavis.edu

Program Scope

This project concerns with computational chemistry of transition metal clusters and actinide complexes. We seek to understand many fundamental and intriguing questions related to the electronic structure of transition metal clusters and actinide complexes of relevance to environment. Transition metal clusters constitute a bridge between the molecular and solid states and consequently, interaction of adsorbing molecules with small metal clusters provides tractable models to enhance our understanding of chemisorption and catalysis. Gas-phase spectroscopic studies on these clusters are benefited by our computations. Computations of actinide complexes are important to understanding of the complexes found in geochemical and biochemical environment and are thus critical to management of high-level nuclear wastes. We are carrying out computational studies that aid in prediction and interpretation of gas-phase spectroscopic experiments of clusters and their reactivity. The geometrical and electronic properties such as ionization potentials, electron affinities, and binding energies of transition metal clusters vary dramatically with cluster sizes. We are investigating clusters of the third row transition metal clusters especially, Ta,W, Re, Os and Ir, and second-row clusters of Mo and Ru. Transition metal carbides and silicides of experimental interest are be considered. Uranyl and plutonyl complexes of environmental importance are being studied. These studies are made with relativistic complete active space multi-configuration self-consistent-field (CASSCF) followed by large-scale CI computations and relativistic CI (RCI) computations that include up to **60 million configurations** and thus electron correlation and spin-orbit effects simultaneously.

Recent Progress

We have made substantial progress in computing the electronic and spectral properties of transition metal clusters and actinide complexes of environmental importance as evidenced from our published work[1-23]. Our most recent works can be divided into 4 categories, namely, methods developments[17,18,20], electronic and spectral properties of transition metal clusters[4-7,14,19,], transition metal or actinide carbides and hydrides[1,3,8,11,12,13,15,16], actinide complexes of environmental importance.[2,9,10,21-23] Our computations on transition metal clusters have been focused on experimentally interesting niobium clusters, and our most recent paper[19] on the tetramer and pentamer and their ions computed several electronic states, equilibrium geometries, vibrational frequencies and dissociation energetics. Our work also facilitated assignment of observed spectra and shed light on some puzzling questions concerning these species. Substantial details of these works are in the respective references. We have developed a new relativistic double group spinor approach for non-rigid molecules. We expect these spinor representations to become valuable in dealing with the electronic and spectroscopic properties of very heavy non-rigid molecules containing transition metals or actinides.

We have carried out our computational work in collaboration with experiment. For example, our work on the excited states of the gold trimer, Au_3 was carried out in synergy with Prof. Andrews IR vibronic absorption spectrum. For the first time the upper spin-orbit state of AU_3 was observed and explained by our computational study. The most interesting feature of gold trimer is that spin-orbit effect inverts its potential energy surface by stabilizing the D_{3h} structure thereby quenching Jahn-Teller distortion. We have characterized this as relativistic inversion of sombrero. A recent study was carried out on $AuH_2$and its IR spectrum in solid hydrogen. Another fascinating and challenging study is that of AgSiO which exhibits a treacherous potential energy surface that has defied theorists and experimentalists for decades. We carried out high-level computations that included up to 50 million configurations to resolve these discrepancies. Ruthenium trimer (Ru_3) was found to be computationally challenging species due to the existence of numerous electronic states and also how different levels of theory led to different predictions. Ru_3 is an excellent case to demonstrate the challenges of computing transition metal clusters. Our predictions on Ru_3 agreed with experiments of Lombardi and coworkers who have obtained resonance Raman spectra of the Ru_3 trimer. Our works on transition metal carbides such as VC, RuC, VC_n, etc., were focused on computing a number of excited electronic states so that we could not only suggest assignments to the observed spectra but also make predictions of new yet to be observed spectral systems. We have also computed the dipole moments of these species, which are in very good agreement with experiment.

We have computed the geometrical and electronic properties as well as vibrational spectra of actinide complexes of environmental importance. These complexes are notoriously difficult and challenging for theoretical studies due to the difficult nature of both 5f and 6d shells and large relativistic and electron correlation effects. Particular complexes of considerable experimental interest have been uranyl and plutonyl complexes of carbonates and silicates, which occur in geochemical environment, and understanding sorption complexes formed in these environments are vital to our understanding of actinide transport in the environment. Our computed vibrational spectra and geometries have been compared with EXAFS spectra and Raman spectra of these species, and agreement is excellent when there are experimental data. We have predicted other vibrational modes and properties, which are yet to be observed. We are also computing the ionization energies of small actinide oxides with considerable accuracy.

Future Plan

We propose to continue our work on second, third row transition metal clusters, carbides and other complexes of transition metals and actinides. There are many challenges as we attempt to study these species. Both relativistic effects including spin-orbit effects and electron correlation effects must be considered accurately. There are spectroscopic studies on NbC, MoC, RhC etc., and we propose to obtain highly accurate potential energy curves of a number of excited states of these systems. Some of the larger carbides and hydrogenated carbide complexes have also been studied experimentally for V, Hf and Nb. These will of particular interest to us.

Transition metal clusters and hydrides are computationally quite challenging due to their multi-reference characters and large relativistic and electron correlation effects. The 5d and 4d shells continue to defy quantum chemists and as demonstrated by our work on Mo_2 large multi-reference CI expansions are needed for their spectroscopic properties. We propose to study trimers and tetramers of these species in collaboration with ongoing experimental efforts in various labs.

The actinide complexes of environmental interest continue to pose considerable challenges. For example, accurate treatment of these complexes in aqueous solution is very challenging. We propose to study these complexes in solution using a combination of relativistic quantum chemical models for the first hydration sphere and continuum types of models and other models. Such developments are in progress. Among the actinide complexes most of the past efforts have been on monocarbonates. We believe that the observed species are often tricarbonato complexes as these are limiting complexes of uranyl and plutonyl species. Thus geometries, vibrational spectra, and energetics dicarbonates and tricarbonates will be studied.

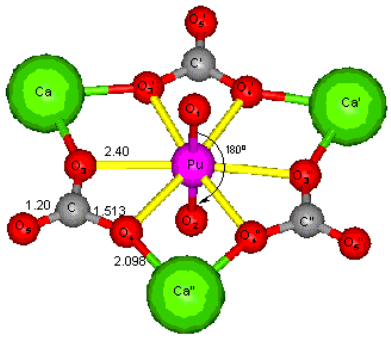

Optimized Geometry of the Plutonyl Tricarbonato Complex: $[PuO_2(CO_3)_3]Ca_3$

References to Publications of DOE-sponsored work in 2002-2004

1. K. Balasubramanian, "Potential Energy Surfaces for the insertion of Lawrencium and Nobelium into H_2", *J. Chem. Phys.* **116**, 3568-3575 (2002)

2. D. Majumdar, K. Balasubramanian, and H. Nitsche, "Theoretical Study of bonding in UO_2, UO_2^+,UO_2^-, UO_2^{+2} the $UO_2(CO_3)$", *Chem.Phys. Lett.* 262, 143-151 (2002).

3. Majumdar, S. Roszak and K. Balasubramanian, "Electronic structure and spectroscopic properties of electronic states of ScC_3 and ScC_3^-", *J. Chem. Phys.* **116**, 10238-10246 (2002)

4. Rui Guo ,K. Balasubramanian, Xuefeng Wang and Lester Andrews "Infrared Vibronic Absorption Spectrum and Spin-Orbit Calculations of the Upper Spin-Orbit Component of the Au_3 Ground State", *J. Chem. Phys.* **117**, 1614-1620 (2002)

5. K. Balasubramanian and X. Zhu "Spectroscopic constants and Potential Energy Curves for Mo_2 and Mo_2^+", *J. Chem. Phys.* 117, 4861-4870(2002)

6. K. Balasubramanian, "Spectroscopic Properties of Mo_2^- and Mo_2^+", *Chemical Physics Letters* **365**, 413-420 (2002)

7. R. Guo and K. Balasubramanian, "Theoretical study of the low-lying electronic states of ruthenium trimer (Ru_3)", *J. Chem. Phys.* **118**, 142-148 (2003)

8. S. Roszak and K. Balasubramanian, **"**Electronic structure and spectroscopic properties of electronic states of VC_2, VC_2^-, and VC_2^+", *J. Chem. Phys.* **118** 130-141 (2003).

9. D. Majumdar, S. Roszak K. Balasubramanian, and H. Nitsche," Theoretical study of aqueous uranyl carbonate (UO_2CO_3) and its hydrated complexes: $UO_2CO_3.nH_2O$ (n = 1 - 3)", *Chemical Physics Letters* **372**, 231-238 (2003).

10. V. Wheaton, D. Majumdar, K. Balasubramanian, L. Chauffe, and P. G. Allen, "A Comparative Theoretical Study of Uranyl Silicate Complexes", *Chemical Physics Letters* **371**, 349-356 (2003).

11. D. Majumdar and K. Balasubramanian, "A theoretical Study of Potential Energy Curves and Specroscopic Constants of VC", *Molecular Physics* **101**, 1369-1376 (2003).

12. R. Guo, K. Balasubramanian and H. F. Schaefer III, "The Treacherous Potential Energy hypersurface of AgSiO", *J. Chem. Phys.* **118**, 10623-10630(2003).

13. K. Balasubramanian, W. Siekhaus and W. McLean II, "Potential Energy Surfaces for the Uranium Hydridng and UH_3 Catalysis", *J. Chem. Phys.* **119**, 5879-5900(2003).

14. D. Majumdar and K. Balasubramanian, "Theoretical study of the electronic states of Niobium Trimer (Nb_3) and its anion (Nb_3^-)", *J. Chem. Phys.* **119**, 12866-12877 (2003).

15. R. Guo and K. Balasubramanian, "Spectroscopic Constants and Potential Energy Curves of Ruthenium Carbide: RuC", *J. Chem. Phys.* **120**, 7418-7425(2004).

16. Lester Andrews, Xuefeng Wang, and K. Balasubramanian, "The Gold Dihydride Molecule, AuH_2: Calculations of Structure, Stability and Frequencies, and the Infrared Spectrum in Solid Hydrogen", *J. Phys. Chem A.* **108**, 2936-2940 (2004).

17. K. Balasubramanian, "Relativity and the Periodic Table", (D. Rouvary & R. B. King, editors), Periodic Table into the 21st Century, 2004

18. K. Balasubramanian, "Relativistic Double Group Spinor Representations of Non-rigid Molecules", *J. Chem. Phys.* **120**, 5524-5535(2004).

19. D. Majumdar and K. Balasubramanian, "Theoretical Study of the Electronic States of Nb_4, Nb_5 clusters and their anions (Nb_4^-, Nb_5^-), *J. Chem. Phys.* **121,** 4014-4032 (2004).

20. K. Balasubramanian, "Mathematical Basis of Periodicity in Atomic and Molecular Spectrsocopy", Mathematics of the Periodic Table, Editors: R. B. King and D. H. Rouvray, Nova Press, NJ 2004

21. D. Chaudhuri and K. Balasubramanian, "Electronic Structure and Spectra of Plutonyl Complexes and their hydrated forms: PuO_2CO_3 and $PuO_2CO_3.nH2O$ (n=1,2)", *Chemical Physics Letters*, in press

22. D. Majumdar and K. Balasubramanian, "Theoretical studies on the electronic structures of $UO_2(CO_3)_2^{2-}$ and its metal salts: $M_2UO_2(CO_3)_2$ (M = Li^+, and Na^+)", *Molecular Physics,* submitted

23. D. Majumdar and K. Balasubramanian, "Theoretical studies on the nature of uranyl–silicate, uranyl–phosphate and uranyl–arsenate interactions in the model $H_2UO_2SiO4 \cdot 3H_2O$, $HUO_2PO_4 \cdot 3H_2O$, and $HUO_2AsO_4 \cdot 3H_2O$ molecules", *Chemical Physics Letters,* **397**, 26-33 (2004).

Role of Solvent: Reactions in Supercritical Fluids

David M. Bartels and Daniel M. Chipman
Notre Dame Radiation Laboratory
Notre Dame, IN 46556
e-mail: bartels.5@nd.edu; chipman.1@nd.edu

Background and significance

For a number of years this project has pursued the use of radiolysis as a tool in the investigation of solvent effects in chemical reactions. The project has now evolved toward the particular study of solvent effects on reaction rates in supercritical (sc-)fluids. Even more specifically, radical reactions in supercritical water are targeted because of interest to use sc-water as a coolant in future (GEN-IV) nuclear power plants. This has proven very fruitful from the basic science standpoint, as virtually any reaction we investigate exhibits behavior best characterized as "weird".

An anthropomorphic way to think about near-critical phenomena, is that the fluid is trying to decide whether it is a liquid or a gas. The cohesive forces between molecules that tend to form a liquid are just being balanced by the thermal entropic forces that cause vaporization. The result, on a microscopic scale, is the highly dynamic formation and dissipation of clusters and larger aggregates. The fluid is extremely heterogeneous on the microscopic scale. A solute in a supercritical fluid can be classified as either attractive or repulsive, depending on the average pair potential between the solute and solvent. If the solute-solvent pair potential is more attractive than the solvent-solvent potential, the solute will tend to form the nucleus of a cluster. A local density enhancement will prevail around the solute, which might have implications for various spectroscopies or for reaction rates. When the solute-solvent forces are repulsive, one might expect the solute to remain in a void in the fluid as the solvent molecules cluster together. Extremely large partial molal volumes are known for hydrophobic molecules in near-critical water. This effective phase separation should have significant implications for the chemical reactions in sc-fluids.

Our purpose in this work is to determine free radical reaction rates in supercritical fluids to develop an understanding of the important solvent effects. Among these will be the effect of local density enhancements (or depletions) on the solvation of reactants and transition states, potential of mean force in the relative diffusion (caging effects), and possible nonequilibrium energy and momentum transfer issues. Relatively few studies of free radical reactions have been carried out under supercritical conditions. We do not propose to extensively review the literature on this subject: an issue of Chemical Reviews [Chemical Reviews, 99, (1999)] contains several useful reviews of work up to 1999.

The ultimate goal of our study is the development of a predictive capability for free radical reaction rates, even in the complex microheterogeneous critical regime. No such capability now exists. The calculation of transition state geometries for free radical reactions by ab initio methods in the gas phase is still not completely reliable, though very good progress has been made. The calculation of condensed phase transition states is a much more difficult task because of the large number of configurations that must be considered, and the perturbation of the reaction energetics by the solvent.

The immediate goal of this work is to determine representative free radical reaction rates in sc-fluid and develop an understanding of the important variables to guide development and use of predictive tools. Electron beam radiolysis of water (and other fluids) is an excellent experimental tool with which to address these questions. The primary free radicals generated by radiolysis of water, $(e^-)_{aq}$, OH, and H, are respectively ionic, dipolar, and hydrophobic in nature. Their recombination and scavenging reactions can be expected to highlight the effects of clustering (i.e. local density enhancements) and solvent microheterogeneity both in terms of relative diffusion and in terms of static or dynamic solvent effects on the reaction rates. We already have transient absorption data for several of these species that highlights interesting and unexpected reaction rate behavior. A major thrust of the next several years will be to push time-resolved EPR detection of H atoms in sc-water. The Chemically Induced Dynamic Electron Polarization (CIDEP) generated in H atom recombination reactions is amenable to theoretical simulations, and provides another unique probe of the cage dynamics and potential of mean force. How different will be the potential of mean force between H atoms and between $(e\text{-})_{aq}$ and H? How easily will H atoms penetrate into water clusters?

Recent Progress

Nearly every reaction we have investigated in high temperature water has given unexpected results. Several reactions of the hydrated electron in supercritical water at 380°C have shown a minimum in reaction rate as a function of the density—at around 0.45 g/cc. This behavior remains to be explained. A most surprising result was obtained for the textbook reaction $H_2 + OH \rightarrow H + H_2O$. Arrhenius behavior was found up to 225°C, but then the reaction rate went *down*. We were unable to measure the lower reaction rate above 350°C. The reaction $H + OH^- \rightarrow H_2O + (e\text{-})_{aq}$ was carefully measured up to 350°C. This reaction is very unusual in that the entropy of activation seems to suddenly change sign at about 100°C. All of these reaction rate results have been reported in the papers listed at the end of this report.

The spectrum of the hydrated electron was carefully measured in high temperature and supercritical water. A moment analysis of the spectrum was carried out to determine the hydrated electron radius of gyration and kinetic energy as a function of the temperature and of density in supercritical water. The absolute free energy of hydration was also worked out as a function of temperature based on available data, in order to compare the gyration radius with the effective Born radius. Comparison of our results with recent simulation studies suggests that the "one quantum electron in classical MD water" models do not contain the relevant physics to fully explain the temperature dependence of the spectrum.

A large amount of transient absorption data is in process of analysis. Several thousand kinetics traces for the hydrated electron in H_2-saturated alkaline water up to 350°C are being analyzed to extract rate constants for (a) $(e\text{-})_{aq} + (e\text{-})_{aq} \rightarrow H_2 + 2OH^-$; (b) $(e\text{-})_{aq} + H \rightarrow H_2 + OH^-$; (c) $(e\text{-})_{aq} + H_2O_2 \rightarrow OH + OH^-$; and (d) the equilibrium $(e\text{-})_{aq} + H_2O \leftrightarrow H + OH^-$. The unusual reaction (a) of two hydrated electrons is diffusion limited up to 150°C, but by 250°C the reaction has essentially "turned off". Above this temperature the recombination is dominated by reaction (b). A large amount of kinetic data for the OH radical absorption at 250nm is also in process of analysis. The target is the second order recombination $OH + OH \rightarrow H_2O_2$. Unavoidably we obtain information on the $OH + H_2O_2$ reaction as well. The UV absorption of these species changes significantly with temperature, making this system a very difficult challenge. The preliminary result seems to be that OH + OH recombination rate hardly changes at all at 250bar pressure above 250°C, until the low density supercritical regime is reached at

about 375°C. Then the recombination rate drops dramatically and becomes too slow to measure easily. It is very unclear why recombination reactions of the OH radical should become so much less than diffusion limited at high temperature.

Planned Work

Immediate plans are to continue the optical transient absorption measurements of OH radical and hydrated electron reaction rates. Calculations will be initiated to characterize the nature of the OH absorption at 250nm in water, with a view toward understanding why this absorption seems to disappear in supercritical water. In the case of OH reactions, the transient absorption experiments will be complemented by measurements of product yields to infer reaction rates by competition. A most important target is the reaction H_2 + OH in supercritical water. Mechanisms of prototypical radiolytic reactions in aqueous solution such as H + OH → H_2O, H_2 + OH → H + H_2O, H_2 + O- → H + OH-, OH + OH → H_2O_2 and OH + OH- → O- + H_2O , as well as the OH/O- equilibrium, will be characterized by theoretical methods as initial steps toward the ultimate goal of understanding their unusual temperature dependences.

A major new effort will involve direct EPR measurements of free radicals in supercritical water. The primary target of this experiment is the hydrogen atom. The hydrogen atom is the prototypical free radical, and its reactions in condensed phase are naturally a subject of great theoretical interest. Moreover, extensive isotope effect information can be generated by comparison of D atom and muonium atom reactions. H (and D) atoms are readily generated in acidic water by electron beam radiolysis. Time-resolved EPR is found to be a convenient and specific technique for H atom detection. The large hyperfine coupling of H or D atoms make their signals unambiguous. Virtually always, time-resolved H atom signals are found to be polarized by Chemically Induced Dynamic Electron Polarization (CIDEP) in the radical recombination reactions.

Our goal in this work is once again to investigate reactions of the H (and D) atom in high temperature and sc-water, to provide data as a guide to development of predictive methods. Reaction rate measurements with H/D/Mu isotope effects will provide strong tests for theory. In the case of the H atom, we will be able to apply EPR techniques to investigate the solvent environment as well. It is known, from the EPR results, that H atoms are hydrophobic. We can expect them to occupy the voids between dynamic water clusters in the sc-fluid. In water at one atmosphere, the hyperfine coupling constants of the H and D atoms were shown to be sensitive to the frequency of collisions in their solvent cages, which depends on temperature and the H/D isotope mass. In the sc-fluid we can expect a strong dependence on the water density (pressure) as well. Both the hyperfine coupling and T_1, T_2 relaxation times will immediately provide information about the average solvation environment. If the solvent cages become very large, as suggested by partial molal volume measurements on hydrophobic gases, the H atom hyperfine coupling will approach the gas phase value.

The most exciting aspect of EPR detection of H and D atoms in sc-water is the potential to measure CIDEP in the H+H and D+D recombination reactions. One can calculate an average polarization enhancement per diffusional encounter, from a stochastic Liouville equation description of the combined spin and spatial diffusion. The enhancements depend upon the time-integrated spin exchange between the radicals of a pair during a diffusive encounter, and the degree of singlet triplet mixing (proportional to the difference in Larmor frequencies of the two radicals). Because spin exchange is typically very short-ranged and singlet-triplet mixing is slow, the phenomenon is sensitive to re-encounters and the full diffusional dynamics.

Polarization enhancements have been calculated for the simple case of spherical radicals freely diffusing in a continuum. H atoms in liquid water may come close to this idealization, but quantitative measurements on this system have never been successfully carried out even at room temperature. Diffusion is never fully free, and forces between the radicals will affect the size of the polarization enhancements. The size of polarization generated in these encounters can readily be estimated via the stochastic Liouville equation, assuming some relative diffusion governed by a potential of mean force. Will the mean force of the solvent in sc-water effectively keep H atoms apart or hold them together? How sensitive will the CIDEP be to the solvent density? Will the H + H recombination remain in the diffusion limit or become "third-body" limited?

Preprints available

REACTION OF H ATOMS WITH HYDROXIDE IONS IN HIGH-TEMPERATURE AND PRESSURE WATER, T.W. Marin, C.D. Jonah, and D.M. Bartels, J. Phys. Chem. A, submitted.

PULSE RADIOLYSIS OF SUPERCRITICAL WATER III. SPECTRUM AND THERMODYNAMICS OF THE HYDRATED ELECTRON, D. M. Bartels, K.Takahashi, J. Cline, T. Marin, and C. D. Jonah, J. Phys. Chem. A. , submitted.

Publications, 2002-2004

TRANSIENT NEGATIVE SPECIES IN SUPERCRITICAL CARBON DIOXIDE: ELECTRONIC SPECTRA AND REACTIONS OF CO_2^- ANION CLUSTERS, K. Takahashi, S. Sawamura, N. M. Dimitrijevic, D. M. Bartels, and C. D. Jonah, J. Phys. Chem. A ,106, 108-114, (2002).

REACTION RATES OF THE HYDRATED ELECTRON WITH NO_2-, NO_3-, AND HYDRONIUM IONS AS A FUNCTION OF TEMPERATURE FROM 125 TO 380^{o}C, K. Takahashi, D.M. Bartels, J.A. Cline, and C.D. Jonah, Chemical Physics Letters, 357, 358-364, (2002).

THE SECONDARY RESPONSE DISTORTION IN TRANSIENT ABSORPTION SPECTROSCOPY, J. Cline, C.D. Jonah, D.M. Bartels, Review of Scientific Instruments, 73, 3908-3915, (2002).

PULSE RADIOLYSIS OF SUPERCRITICAL WATER I. REACTIONS BETWEEN HYDROPHOBIC AND ANIONIC SPECIES, J. Cline, C. D. Jonah, T.Marin, D. M. Bartels, and K. Takahashi, J. Phys. Chem. A, 106, 12260, (2002).

PULSE RADIOLYSIS OF SUPERCRITICAL WATER II. REACTION OF NITROBENZENE WITH HYDRATED ELECTRONS AND HYDROXYL RADICALS, T. W. Marin, J A. Cline, D. M. Bartels, C. D. Jonah, and K.Takahashi, J. Phys. Chem. A , 106, 12280, (2002).

REACTION OF OH RADICALS WITH H_2 IN SUB-CRITICAL WATER, T. W. Marin, C. D. Jonah, and D.M. Bartels, Chem. Phys. Lett., 371, 144, (2003).

REACTION RATES OF HYDRATED ELECTRON WITH N_2O IN HIGH TEMPERATURE WATER AND POTENTIAL SURFACE OF THE N_2O^- ANION, Kenji Takahashi, Shintaro Ohgami, Yasushi Koyama, Sadashi Sawamura, Timothy W. Marin, David M. Bartels, and Charles D. Jonah, Chemical Physics Letters, 383, 445 (2004).

TOWARD AN ATOMIC LEVEL UNDERSTANDING OF HETEROGENEOUS CATALYSIS EMPLOYING GAS PHASE METAL OXIDE NANOPARTICLES

Elliot R. Bernstein
Colorado State University, Department of Chemistry, Fort Collins, CO 80523
erb@lamar.colostate.edu

This study deals with modeling of heterogeneous condensed phase and surface chemistry based on the behavior of small neutral clusters or nanoparticles. At present, our research is focused on small ($\leq$ 20 atoms) gas phase, neutral metal oxide clusters and small molecules as accessed by photoionization, time-of-flight mass spectroscopy, optical spectroscopy, and density functional theory calculations. The metal oxide nanoparticles serve as model systems for the local site surface structure at which heterogeneous catalysis can occur. Specifically, we are studying the following cluster/reaction systems: 1. Conversion of CO and NO to CO_2 and N_2 by gas phase, neutral iron oxide and copper oxide clusters; 2. Conversion of SO_2 to SO_3 by gas phase, neutral vanadium oxide clusters; 3. Decomposition of water into H_2 and O_2 by gas phase, neutral titanium oxide clusters and (possibly) UV radiation; and 4. Conversion of CO/H_2 (water gas) to CH_3OH by gas phase, neutral copper oxide and zinc oxide clusters and mixed metal oxide clusters.

The primary over-arching goal of our work is to obtain an atomic level (quantum mechanical) understanding of heterogeneous reaction rate enhancement. We will apply this understanding to generate a rational and analytical approach to the design and improvement of macroscopic catalytic systems. Specifically, we focus on elucidating the reaction mechanisms, energetics, electronic state, and structural dependencies of the metal oxide enhancement of the above reactions. We wish to answer the following questions concerning these reactions: 1) How do the reactions occur?; 2) What are the active site (geometric and electronic) structures at which these reactions occur?; and 3) What are the detailed mechanisms for the conversions of interest?

Our work over the past three years has focused on all phases of the present proposed effort: 1. establishment of the neutral metal oxide cluster distribution; 2. determination of the neutral cluster and product distribution following passage of the metal oxide clusters through the reaction cell with particular gas pressure of reactant molecules; 3. determination of the active cluster structures and properties by DFT calculations; and 4. DFT calculation of the reaction pathways and intermediates for the observed cluster generated reactions.

A. Neutral Cluster Distribution - Fe_mO_n, Cu_mO_n, Zr_mO_n, Ti_mO_n, V_mO_n.

Metal oxide neutral clusters are generated in the gas phase through laser ablation of the metal and reaction with various concentrations of O_2 in He. The mixture of expansion gas and neutral Fe_mO_n cluster species is expanded through a supersonic nozzle into a vacuum system. Ions are removed from this mixture by an electric field. The remaining neutral clusters are ionized by an ArF excimer laser at 193 nm, a ninth harmonic Nd/YAG laser at 118 nm, or a third harmonic Nd/YAG laser at 355 nm, and the ions are detected and identified in a TOFMS. The stable neutral clusters for saturated O_2 growth conditions are, in general, different for the different metal oxides.

Fe_mO_n: The stable neutral cluster for iron oxide are of the forms Fe_mO_m, Fe_mO_{m+1}, and Fe_mO_{m+2}; which one of these series of neutral clusters is most stable depends on the size of the cluster. For $m < 10$, Fe_mO_m is the most stable neutral cluster series, for $10 \leq m \leq 20$, Fe_mO_{m+1} is the most stable neutral cluster series, and for $21 \leq m \leq 30$, Fe_mO_{m+2} is the most stable neutral cluster series. With 118 nm radiation, the neutral clusters do not fragment because single photon absorption is sufficient to ionize all the clusters, and the energy/pulse is ca. 1 μJ. Comparison of the mass spectra obtained at 118 nm ionization (single photon) with those obtained at 193 nm and 355 nm ionization (through multiphoton processes), with regard to intensities and linewidths, leads to an understanding of the multiphoton neutral cluster fragmentation pathways. When fragmentation of clusters occurs, the multiphoton fragmentation mechanism for neutral iron oxide clusters during the ionization process that seems most consistent with all the data is the loss of one or two oxygen atoms.

V_mO_n: The stable neutral cluster mass spectral distribution for saturated oxygen growth conditions (O_2 concentration $\geq$ 3%) can be characterized by the cluster series $(V_2O_5)_x(VO_2)_y$. At lower oxygen concentrations, the growth of neutral clusters is kinetically controlled and oxygen deficient clusters dominate the distribution of neutral species.

Cu_mO_n: Based on the observed cluster patterns as a function of experimental conditions (e.g., copper oxide or metal sample, ablation laser power, expansion gas, …) and on the width of the TOFMS features, one can uncover the true neutral cluster distribution of Cu_mO_n species following laser ablation of the sample. Ablation of a metal

sample into 5% O_2/95% He generates only small neutral Cu_mO_n clusters with $m \lesssim 4$ and $n \sim 1, 2$. Ablation of copper oxide samples into the same expansion/reaction gas or pure He generates neutral clusters of the form Cu_mO_m ($m \leq 4$) and Cu_mO_{m-1} ($m > 4$). These clusters are directly detected without fragmentation (based on TOFMS linewidth studies using single photon, photoionization with 118 nm laser radiation. Using 355 and 193 nm multiphoton ionization, the observed cluster ions are mostly of the form $Cu_{2m}O_m^+$ for (193 nm ionization) and Cu_mO_1 and Cu_mO_2 (355 nm ionization) $4 \leq m \leq 10$. Neutral cluster growth takes place in the laser ablation generated plasma if both Cu and O are present. Apparently, copper metal is not very reactive with molecular oxygen, at least not at the temperatures achieved in the ablation/expansion gas mixture.

Zr_mO_n: Fragment ion features are observed in the mass spectra of $Zr_mO_n^+$ for only the 193 nm and 355 nm ionization schemes. The true neutral Zr_mO_n cluster distribution is obtained only through 118 nm single photon ionization, as verified by mass spectral peak linewidths and calculations of the cluster binding energies, ionization energies, and RRKM fragmentation rates. The neutral cluster distribution consists mainly of the series Zr_mO_{2m} and Zr_mO_{2m+1} for $m = 1, \ldots, \sim 30$.

Ti_mO_n: Again, only 118 nm (10.5 eV) radiation can ionize Ti_mO_n neutral clusters without fragmentation. The Ti_mO_{2m} and Ti_mO_{2m+1} series are found to be the most stable neutral cluster species for high oxygen content in the expansion gas. Fragmentation during the multiphoton ionization process for 193 nm light yields the stable cluster ions $Ti_mO_{2m-1,2}^+$. These ions are formed by loss of one or two oxygen atoms from $Ti_mO_{2m,2m+1}$ neutrals. For low oxygen content (<2%) in the expansion gas, oxygen deficient clusters of the form $Ti_mO_{2m-1,-2}$ are also produced. These latter series are not fragmented by the 193 nm ionization process. Based on structures calculated for the V_mO_n, Zr_mO_n, and Ti_mO_n cluster series, such stability can be associated with cluster structures in which singly bonded oxygen atoms are not present. Calculated ionization energies for small Ti_mO_n clusters are all between 9 and 10 eV and are thus consistent with the fragmentation results we have found experimentally.

B. Identification of Reactive Clusters, Product Species, and Complexes

This phase of our program has begun with the study of the following three reactions: 1) CO/NO → CO_2/N_2 employing Fe_mO_n neutral clusters as the reaction enhancement (catalyst) species; 2) SO_2 → SO_3 employing V_mO_n neutral clusters as the reaction enhancement (catalyst) species; and 3) H_2O → $H_2 + O_2$ employing Ti_mO_n neutral clusters as the reaction enhancement (catalyst) species. Additionally, we have explored a possible reaction for CO to CO_2 using very oxygen-deficient V_mO_n clusters.

The clusters are passed into a reaction cell with varying amounts of reaction gas (e.g., CO, NO, CO/NO, SO_2, H_2O). The cell is 6 cm long and the reaction gas pressure is varied between 0.1 to 50 x 10^{-4} torr.

TOFMS data for the Fe_mO_n/CO/NO system show that neutral clusters Fe_2O, Fe_2O_2, and Fe_3O_3 are preferentially removed from the beam as the pressures of CO and/or NO are increased in the reaction cell. Concomitant with this the mass signals for N_2, CO_2, C, N, and O increase with increasing reaction cell pressure. Product species signals are broad as expected for fragmentation of the clusters to generate product. A model theory has been generated to explain this behavior based on DFT reaction path calculations and is described below.

We have carried out similar studies for the SO_2/SO_3 V_mO_n system. Again, only a very few (small) clusters, VO_2, V_4O_n, $4 \leq n \leq 8$, appear to be active in the reaction. These clusters travel through the reaction cell in about 50-100 μs and undergo 0.1 to 5 collisions during this time, depending on the cell pressure (2 x 10^{-4} to 5 x 10^{-3} Torr). In this instance, both 118 nm and 193 nm ionization have been completed, and due to the more extensive fragmentation for these neutral clusters compared to the iron oxide neutral clusters, the 118 nm ionization results are more revealing and informative. We are presently engaged in an effort to detect the mass spectra of fragmented SO_2 and SO_3 reactant and product species under these conditions, employing a laser generating higher energy (26.5 eV) single photons. One can identify the growth of V_2O_3 in the TOFMS as the pressure of SO_2 is increased in the reaction cell. This observation will be discussed in the rection path calculation section (E) below.

We have also begun studies of the interaction of CO with very oxygen deficient, neutral vanadium oxide clusters. In this case, we have observed cluster complexes of the form V_8O_2CO, V_8O_3CO, V_8O_4CO as CO is added to the reaction cell. Most likely the interactions between V_8O_2, V_8O_3, and V_8O_4 and CO are too strong for a product molecule to be released from the cluster complex, but these results indicate that the V_8O_n, $2 \leq n \leq 4$, series of neutral clusters has an enhanced interaction/reaction with carbon monoxide. Smaller clusters do no react with CO, but V_9O_n and $V_{10}O_n$ clusters also appear to form CO/V_mO_n complexes.

Studies of the decomposition of H_2O to generate H_2 and O_2 are underway employing neutral Ti_mO_n species. The major observation thus far is that Ti_2O_4 is very reactive toward water and is effectively removed from the

mass spectrum of Ti_mO_n clusters. Ti_4O_8 can be seen as well to lose relative intensity as the H_2O pressure in the reaction cell is increased. These results are still under study and we are still characterizing other changes in the mass spectrum of the Ti_mO_n/ H_2O system and looking for other products.

These results demonstrate and reinforce two essential and important trends in all the metal oxide studies we have undertaken thus far: 1) the reactive species tend to be oxygen deficient with respect to the stable solid phase systems and often with respect to the most stable neutral clusters; and 2) the active clusters are small. This latter point is, of course, important for subsequent theoretical analysis and spectroscopic study.

C. Calculation of Neutral Cluster Structure for Reactive Species – DFT

We are calculating structures of reactive neutral clusters. We have made three choices for these calculations thus far: 1. of the two systems to calculate initially, Fe_mO_n and V_mO_n, we have chosen V_mO_n as the much simpler, more productive, and best suited to DFT calculations because Fe_mO_n have too many unpaired electrons and too many degenerate states to be ideally calculated; 2. the functional to yield the best and most reliable structures and energy levels is BPW91; and 3. the basis sets to employ are TZVP (triple zeta valence plus polarization) and LANL2DZ/D95. We believe that the choices are appropriate for the results needed to go beyond electronic and geometric cluster structure and to eventually calculate reactivity, transition states, and reaction/potential energy surfaces.

Two sets of structures are obtained: those calculated at the BPW91/TZVP level that are most likely accurate to ±5 kcal/mol, and those calculated at the BPW91/LANL2DZ/D95 level, most likely accurate to ± 10 k cal/mol for larger clusters. VO through V_2O_6 and V_4O_9 are completed at the highest level used, BPW91/TZVP. This level of theory has been bench marked for VO and VO_2 by us and seems to be near the state of the art for most DFT calculations reported. We are planning further bench mark spectroscopic studies for VO_2 (see below); other species will also be investigated if calculations suggest accessible excited states and low enough density of states to ensure analyzable, well resolved spectra. A few important points are worth noting about these calculated structures. First, a number of cluster stoichiometries (e.g., V_2O_4, V_2O_5, …) have isomers, and some isomers are within 10 kcal/mol of the calculated lowest energy structure (V_2O_4). In these instances, either isomer could be the lower energy structure and certainly both would be populated in the neutral cluster beam. Second, these clusters look like "surfaces" in the sense that all atoms are available for interactions/reactions with other species. Third, excited triplet states are calculated for V_2O_5 structures and could be spectroscopically accessed if the density of states and coupling between states are small, and relaxation processes are not too fast. Fourth, the V_4O_9 cluster begins to look "three-dimensional." Fifth, one can understand the fragmentation pattern (loss of nO and not M_xO_y, in general) we have observed for these clusters. For a parent neutral to lose an M_xO_y fragment, many (strong) M–O bonds must be broken; for a parent to lose an O atom, only one M–O bond is broken. The weaker M–M bonds are not present in these small clusters for the low energy isomers. Note too that terminal, bridging, oxo, and ozonide oxygen species are calculated for various cluster structures. One also finds that fragmentation of a cluster upon ionization could stop after only a few (terminal) oxygen atoms have been lost. These qualitative structural features are thus consistent with the neutral cluster fragmentation patterns discussed above for fragmenting ionization. Ionization energies, single photon energies, and RRKM calculations of fragmentation times, are all consistent with the qualitative behavior observed for these clusters.

Additionally, we have published BPW91/LANL2DZ/D95 (effective core potential basis set for V and D95 basis set for O) structures for Zr_mO_n clusters. These calculations are checked against three others for accuracy and are found to be quite consistent with structures and energies obtained with other algorithms and basis sets, as well as our experimental results for fragmentation and neutral cluster stability.

D. Spectroscopy of VO_2

We have just obtained spectra for the VO_2 $B(^2B_2) \leftarrow X\ (^2A_1)$ transition with an origin at 16,421 cm^{-1} and hot bands at 16,416 and 16,410 cm^{-1}. We have also assigned the 1_0^1, 2_0^1, 1_1^0, and 2_1^0 transitions. These spectra are detected in two ways: 1. scanning a dye laser about 610 nm and watching the fragment signal VO^+ appear in the TOFMS; and 2. watching the 118 nm VO_2 signal decrease as the resonances are scanned for the $^2B_2 \leftarrow {}^2A_1$ VO_2 transition. The 0_0^0 transition has a FWHM of less than 5 cm^{-1} under our present conditions. Hot band assignments give a T_{vib} ~ 700 K and the rotational structure for the 0_0^0 and 1_0^1 implies a T_{rot} ~50 K. These results confirm calculations at the BPW91/TZVP, BWP91/LANL2DZ/D95, and MP2 levels for VO_2.

E. Reaction Path Calculations – (Fe_2O/CO, Fe_2O/NO and V_mO_n/SO_2).

As a first attempt at using DFT calculations to explain the observed reactions, we have chosen Fe_2O with NO and CO. This work has been done in collaboration with S. Khanna and B. V. Reddy. The reaction CO to CO_2 occurs on this neutral cluster for three CO molecules added as the C-O bond elongates about 20-25%. CO_2 is

fragmented from the cluster in the ionization process as an ion and the $Fe_2O(CO)_2$ species or its fragments are neutral and thus not observed. This mechanism is consistent with all the experimental data generated for this system at Fe_2O. Further calculations are in progress now for other clusters and other pathways. Transition structures are generated for $Fe_2O(CO)$, $Fe_2O(CO)_2$, $Fe_2O(CO)_3$, and $Fe_2O(C)(CO) + CO_2$.

Calculations are being pursued for the V_mO_n/SO_2 system, as well. The chemistry here is quite rich and many stable species are present for $V_mO_n(SO_2)$ that are energetically accessible for $V_mO_n(SO_2)$ + 10.5 eV (ionization photon energy). Stable species are found for $VO_2(SO_2)$, $VO_3(SO)$, and $VO^+ + SO_3$. Additionally, V_2O_2 (SO_2) is found by one path to generate $V_2O_3^+ + SO$. Thus a number of our observations are found to be consistent with DFT/LANL2DZ/D95 calculated transition states and pathways.

These theoretical studies are being pursued actively at present in order to interpret the observed mass spectral data.

F. Summary and Future Effort.

The main goal of this research is to relate the findings and mechanisms obtained for these gas phase systems to condensed phase heterogeneous catalysis (gas/solid) or reaction rate enhancement. An obvious path to this goal would be to state that the neutral metal oxide species M_xO_y is most active in the gas phase for a given reaction and thus, such a structure (geometric and electronic), if it could be generated in the condensed, would increase catalytic activity for the condensed phase system. Note that this enhancement can be modest, ca. 1-10% or a 20% reduction in temperature, as cost savings can be large and this would still represent a step forward in the understanding of catalytical reaction behavior. Some of the pathways thus far calculated do regenerate the M_xO_y cluster, while other do not and we continue to search for more product species. These studies have thus far not focused on the regeneration step which is the final one in the catalytic process: regeneration of the original cluster from the reacted one would necessitate another species (O_2) in the reaction cell, as must occur for the condensed phase regeneration, as well, if the product is composed of an atom of the cluster. Otherwise, the desired product (CO_2, SO_3, …) must arise from reactant gas (O_2, CO, NO, SO_2, H_2O) and the reaction must be only "facilitated" by the cluster or active surface site.

Further work will involve more calculations, expanded reaction experiments, and the use of a table top x-ray laser (26.5 eV) for the detection/ionization of all clusters, reactants and products.

Publications:

1. M. Foltin, G. Stueber, and E. R. Bernstein, "On the Growth Dynamics of Neutral Vanadium Oxide and Titanium Oxide Clusters," *J. Chem. Phys.* **111**, 9577 (1999).

2. M. Foltin, G. J. Stueber, and E. R. Bernstein, "Investigation of the Structure, Stability, and Ionization Dynamics of Zirconium Oxide Clusters," *J. Chem. Phys.* **114**, 8971 (2001).

3. D. N. Shin, Y. Matsuda, and E. R. Bernstein, "On the Iron Oxide Neutral Cluster Distribution in the Gas Phase: I. Detection Through 193 nm Multiphoton Ionization," *J. Chem. Phys.* **120**, 4150 (2004).

4. D. N. Shin, Y. Matsuda, and E. R. Bernstein, "On the Iron Oxide Neutral Cluster Distribution in the Gas Phase: II. Detection Through 118 nm Single Photon Ionization," *J. Chem. Phys.* **120**, 4157 (2004).

5. Y. Matsuda, D. N. Shin, and E. R. Bernstein, "On the Neutral Copper Oxide Cluster Distribution in the Gas Phase: Detection Through 355 nm and 193 nm Multiphoton, and 118 nm Single Photon Ionization," *J. Chem. Phys.* **120**, 4165 (2004).

6. Y. Matsuda, D. N. Shin, and E. R. Bernstein, "On the Zirconium Oxide Neutral Cluster Distribution in the Gas Phase: Detection Through 118 nm Single Photon, and 193 and 355 nm Multiphoton, Ionization," *J. Chem. Phys.* **120**, 4142 (2004).

7. Y. Matsuda and E. R. Bernstein, "On the Titanium Oxide Neutral Cluster Distribution in the Gas Phase: Detection Through 118 nm Single Photon, and 193 and 355 nm Multiphoton, Ionization," *J. Phys. Chem.,* submitted.

8. Y. Matsuda, D. N. Shin, and E. R. Bernstein, "Identification, Structures, and Spectroscopy of Neutral Vanadium Oxide Clusters," *J. Chem. Phys.*, in preparation.

9. Y. Matsuda, E.R. Bernstein, B.V. Reddy, F. Rasouli, S.N. Khanna, "Dual Reactivity of Iron Oxide Clusters: Self-Stimulated CO Oxidation as Well as NO Reduction, *Nature*, to be submitted.

Precursor and Transient Species in Condensed Phase Radiolysis

Daniel M. Chipman, Jay A. LaVerne, and Simon M. Pimblott
chipman.1@nd.edu, laverne.1@nd.edu, pimblott.1@nd.edu
Radiation Laboratory, University of Notre Dame, Notre Dame, IN 46556

Program Scope

The final products of condensed phase radiolysis are largely governed by very early events (≤ picosecond) that occur immediately following the absorption of ionizing radiation. This program uses a multi-pronged approach employing heavy ion-, electron-, and gamma-radiolysis experiments in conjunction with stochastic kinetic modeling and electronic structure calculations to elucidate and interpret fundamental radiation chemical processes from their earliest stages. The specific goals are to characterize the precursor and transient species that are initially formed following absorption of high energy radiation in condensed systems, to determine the interactions of these species with their immediate environments, and to evaluate their effects on the mechanisms and kinetics of the various chemical reactions that dictate final product yields of radiolysis. Current focus is on aqueous solutions with some studies on other condensed phase systems, including hydrocarbons and related common heteroatomic solvents. The fundamental physical and chemical issues being addressed have direct applications to the underlying problems in design and operation of nuclear power plants, cleanup and management of radioactive wastes, nanotechnology, health physics, and other technological challenges of importance in the real world scenarios of significance to the mission of the Department of Energy.

Recent Progress

Scavenger studies clearly show that the precursors to the hydrated electron can lead to significant chemistry not normally associated with the hydrated electron. [1,2] Molecular hydrogen previously designated as unscavengable is now known to be due to the precursor to the hydrated electron. [3] These results gave a new appreciation to the role of extremely short lived transients on final product formation in the radiolysis of water. Techniques for the direct examination of these transients is not yet commonly available so the present experimental work depends on the indirect examination of stable products with varying concentrations of added scavengers for the transients.

Hydrogen peroxide is the main oxidizing molecular product ultimately produced in the gamma-radiolysis of water. The mechanism of hydrogen peroxide production has been examined [4] by varying the concentrations of scavengers for OH radical and of scavengers for the precursor to the hydrated electron. Hydrogen peroxide yields were found to decrease toward zero with increasing concentration of OH radical scavenger in all solutions, indicating that essentially all hydrogen peroxide is formed by combination reactions of OH radicals that are produced in the initial radiolytic decomposition of water. In nitrate and selenate solutions the yields of hydrogen peroxide were found to be closely associated with the scavenging capacity of the precursor to the hydrated electron, suggesting that its reactions have a significant role in hydrogen peroxide formation.

Observed hydrogen peroxide yields at high nitrate concentrations coupled with stochastic diffusion-kinetic modeling calculations showed that the molecular cation of water, H_2O^+, is the dominant precursor of the oxidizing species leading to hydrogen peroxide. Proton-transfer reactions of water molecular cations with neutral water molecules give 79% of the oxidizing species, whereas other reactions such as dissociative recombination reactions account for the rest. In radiolysis of selenate solutions a significant additional production of OH radicals was found due to the formation of $O^{\bullet -}$ and the scavenging of low-level excited water molecules.

A combined experiment with model approach is being used to examine the production of hydrated electrons and OH radicals in the heavy ion radiolysis of water. Scavenger capacity dependence studies give both the yields and temporal dependence of these main radical species in the radiolysis of water with protons, helium ions and carbon ions. Radical yields decrease with increasing particle linear energy transfer, LET, and the track reactions responsible for this decrease occur on very fast timescales ($\leq$ nanosecond). Monte Carlo calculations are found to agree well with experiments in most cases. The track model clearly shows that the variation in radical yield more closely follows the density of reactive species in the track and not the LET. A major limitation of the model seems to be due to defining the correct spatial distribution of the hydrated electron and its precursor in heavy ion tracks.

Electronic excitation of small water clusters has been examined [5] using high-level quantum chemical calculations. The lowest excited state energy of a central water molecule was found to be insensitive to stretching one of its OH bonds when the OH bond is hydrogen-bonded in an ice-like configuration to a neighboring water molecule. This result is in marked contrast to the behavior of the gas phase water monomer, where the lowest excited state is well known to be strictly dissociative along an OH stretching coordinate. The conclusions of this study may provide the basis for an explanation of the apparently long lifetime that has recently been experimentally inferred for excited water in irradiated thin ice films. [6] Analogous calculations are now being initiated to address electronic excitation in model systems more directly relevant to liquid water.

Future Plans

Experimental studies are focusing on the production and reaction of hydrated electrons and OH radicals in the heavy ion radiolysis of water. The specific scavengers for each of these radical species are glycylglycine and formic acid, respectively. Agreement between experiment and model calculations at low scavenger concentrations is satisfactory, especially since effects due to track ends are very uncertain. Experimental energy dependences of product yields will be used to determine track segment yields, a quantity more accurately calculated. Neither of the scavenger systems is ideal for studies at high scavenging capacity and new solutes are being evaluated.

A particularly promising approach for examining the effects of track structure on transient species is to examine the variation in formation of the main stable product, H_2 in the case of hydrated electrons and H_2O_2 in the case of OH radicals. The production of these products with increasing scavenging capacity for precursors to the hydrated electron and OH radical gives considerable information on the yields and spatial distributions of these very short lived transients. Eventually, the role of the excited water

molecule will be examined for its role in the formation of oxidizing species such as the O atom.

The poorly understood energetics and fragmentation patterns of the molecular cation, H_2O^+, in water will be studied with electronic structure methods. To model the situation in the liquid phase, small water clusters will be explicitly treated together with implicit solvation models that describe bulk effects by surrounding the clusters with dielectric continuum. All the available dissociation channels in low-lying states of the cation will be investigated, particularly focusing on the ultrafast deprotonation that produces OH and H_3O^+. It has recently been shown [2] that about 70% of the total molecular hydrogen ultimately produced in the gamma radiolysis of water comes from some previously unrecognized ultrafast process. Possible explanations involving dissociative electron combination with H_2O^+ will be studied along with alternatives such as dissociative electron combination with H_3O^+. The information obtained in these *ab initio* theoretical studies will guide stochastic simulations employing simulated fast electron and heavy ion track structures to study the ultra-fast reaction of the molecular cation of water with an adjacent water molecule to give H_3O^+ and OH radical, which is the dominant source of OH in liquid water radiolysis. There is no definitive observation of H_2O^+ in liquid water; however, there is evidence in photo-ionization studies suggesting a lifetime of < 100 fs. [7,8] The rate coefficient of the proton transfer reaction in the gas phase suggests a lifetime of ~18 fs at the density of liquid water. [9] Furthermore, theoretical calculations for the water dimer give a lifetime of 30-80 fs. [10] Simulations will be made employing a range of lifetimes from 10–100 fs, and the results analyzed by comparison with the well-established scavenger kinetics of OH radical decay and H_2O_2 formation. Further calculations will consider scavenging of the molecular cation, looking at the ultra-fast formation of Br_2^- in concentrated Br^- solution and at the effect of concentrated nitrate solutions on the yield of H_2O_2.

Not all the radiation induced reactive oxygen species are produced directly from H_2O^+. A number of additional sources have been postulated, including formation of O^- (OH) by a dissociative electron attachment reaction, direct formation of excited singlet states of H_2O by the primary radiation particle, and singlet and triplet states of H_2O produced by low-energy electron interactions, as well as the dissociative electron recombination reaction of H_2O^+ with e^- in producing singlet and triplet excited states of water. Transition states and potential energy surfaces governing dissociative channels of low-lying excited states of neutral water, H_2O^*, will be calculated with electronic structure methods that model the situation in liquid to evaluate their possible importance in direct production of transient radiolytic species. Production of these reactive oxygen species will also be the objective of a series of stochastic diffusion-kinetic calculations investigating the roles of direct excitation and the dissociative electron recombination reaction in producing singlet and triplet excited states of water, and the nonhomogeneous chemistry of $O(^1D)$ and $O(^3P)$ that have been postulated as the "extra" unobserved oxidizing species that is needed for material balance in kinetic and mechanistic models in high-LET water radiolysis. A final series of kinetic calculations will model the formation of HO_2 and O_2 in the high-LET radiolysis of aqueous Cu(II) – Fe(II) solutions, comparing predictions with available experimental data.

References

(1) B. Pastina and J. A. LaVerne *J. Phys. Chem. A*, **1999**, *103*, 209-212.
(2) B. Pastina, J. A. LaVerne and S. M. Pimblott *J. Phys. Chem. A*, **1999** *103*, 5841-5846.
(3) J. A. LaVerne and S. M. Pimblott *J. Phys. Chem. A*, **2000***104*, 9820-9822.
(4) A. Hiroki, S. M. Pimblott & J. A. LaVerne, *J. Phys. Chem. A*, **2002**, *106*, 9352-8.
(5) D. M. Chipman, submitted for publication.
(6) N. G. Petrik and G. A. Kimmel, *Phys. Rev. Lett.* **2003**, *90*, 166102-1-4.
(7) Y. Gauduel, S. Pommeret, A. Migus & A. Antonetti, *Chem. Phys.* **1990**, *149*, 1-10.
(8) F. H. Long, H. Lu & K. B. Eisenthal, *Phys. Rev. Lett.* **1990**, *64*, 1469-72.
(9) B. R. Rowe, F. Vallee, J. L. Queffelec, J. C. Gomet & M. Morlais, *J. Chem. Phys.* **1988**, *88*, 845-50.
(10) H. Tachikawa, *J. Phys. Chem. A*. **2002***, 106*, 6915-21.

DOE Sponsored Publications in 2002-2004

Hydrogen Peroxide Production in the Radiolysis of Water with High Scavenger Concentrations, A. Hiroki, S. M. Pimblott, and J. A. LaVerne, *J. Phys. Chem. A* **2002**, *106*, 9352-8.

Temperature Dependence of the Hydrogen Peroxide Production in the Gamma-Radiolysis of Water, I. Stefanic and J. A. LaVerne, J. Phys. Chem. A **2002**, *106*, 447-452.

Modeling of the Physicochemical and Chemical Processes in the Interaction of Fast Charged Particles with Matter, S. M. Pimblott and A. Mozumder, in "Charged Particle and Photon Interactions with Matter: Chemical, Physicochemical, and Biological Consequences with Applications", edited by A. Mozumder and Y. Hitano, Marcell-Dekker Inc. **2004**, chapter 4.

Radiation Chemical Effects of Heavy Ions, J. A. LaVerne in "Charged Particle and Photon Interactions with Matter: Chemical, Physicochemical, and Biological Consequences with Applications", edited by A. Mozumder and Y. Hitano, Marcell-Dekker Inc. **2004**, chapter 14.

Molecular Theory & Modeling

Transport and reactivity in amorphous solids

L. René Corrales
Chemical Sciences Division
Pacific Northwest National Laboratory
902 Battelle Blvd.
Mail Stop K1-83
Richland, WA 99352
rene.corrales@pnl.gov

The objectives of this work are to understand the factors that control the modifications to nuclear waste glasses, optical and micro-electronic devices, and biomolecular materials caused by chemical reaction, ion transport and irradiation processes that can compromise their fabrication and performance lifetime. Underlying the extent to which a material will undergo physical and chemical transformations are the molecular level structural characteristics, and the collective response to the operational environment. The former has a strong dependence on processing history and the latter depends on the particular composition, such as the concentration of radionuclides embedded into a glass, and physical state of the material that can include phase separated states or introduction of heterogeneous environments such as aqueous solid interfaces. **There is a great interest to DOE in networked oxide glasses, such as silicates and phosphates, because they are well suited for use in entombing nuclear waste and they form the basis of optical fibers, photonic devices, scintillators for radiation detection, and bio-inorganic composites for modern nanotechnology.** Fundamental issues relevant to these materials have to do with the distribution of ions that modify the network either by becoming part of the network, such as boron and aluminum in silica, or by breaking up the network, such as alkali, lanthanide and actinide ions. The former are network formers that become part of the network backbone and the latter are network modifiers that effectively breakup the backbone structure. The distributions of any type of ion in a glass can strongly affect the physical and chemical characteristics and, thereby, the response of the local structure to chemical reactions and electronic excitations. The correlation between the local molecular structure with chemical reactions and electronic excitations has been observed even in the homogeneous network structure of pure fused silica. Electronic excitations in fused silica are known to lead to the production of damage states that include the formation of color centers, but the molecular level mechanisms that lead to their formation remain unresolved. The reactions of water with silica are fairly well characterized by experiment, however, only recently has progress been made to understand the molecular level reaction mechanisms of reactions in the bulk and at surfaces. The reaction of water with silica is relevant to dissolution of silica at a glass/liquid interface, the leaching of ions from a glass, and in enhancing ion transport in the bulk that can induce or inhibit nucleation of new crystalline or non-crystalline phases. Further work is needed to characterize the significant changes in optical properties that are known to take place when chemical reactions take place at color centers and strained sites.

We have recently investigated the role of network relaxation in reactions, and the factors that control the range and source of the differences in the stability of reactants and products using density functional theory (DFT). The calculations were carried out using one water molecule inserted into two distinct bulk structures of fused silica, as well as into alpha-quartz and beta

cristobalite. All structures were computed using periodic images of a supercell. The quartz structure consisted of eight unit cells with a total of 72 atoms and that of cristobalite consisted of 8 unit cells with a total of 96 atoms. The fused silica structures consisted of 72 atoms in a cubic cell that were initially generated using classical molecular dynamics methods and optimized using DFT. Minimum energy pathways for reaction paths were determined using the nudged-elastic band method within the DFT calculations. In one glass, a diffusion-reaction path that takes a water molecule from one cavity to another cavity by a reaction path revealed that the SiOH groups undergo conformational rearrangement from which the water molecule can reform in a different cavity. In the same glass, a different conformational rearrangement of the SiOH groups leads to reforming a water molecule in the same cavity it came from, but with an exchange of an O atom from the network. A range of reaction barriers from 0.2 eV up to 1.7 eV (greater than that found for quartz) was determined for fused silica.

Electronic excitations in fused silica were studied by introducing the lowest lying triplet excited state into ten independent amorphous samples generated for specific use in density functional theory calculations. Key findings are that the experimentally observed red shift of the luminescence in going from crystalline quartz to fused silica is likely due to a different type of self-trapped exciton, one that has different characteristics presently distinguished theoretically by its structural properties. Further work is needed to resolve differences in optical properties that would be measurable by experiment. Another important finding is that defect pairs are able to form from non-activated processes in which the excited state energy decays via a non-radiative path. This is significant because it shows that inherent structural features can exist in fused silica in which an exciton could migrate towards and form a defect pair. The defect pair formed is not one which is detected experimentally, but it is thought to be a precursor defect pair that upon combining with a second similar defect pair could lead to the lower energy defect pair of an oxygen vacancy and peroxide radical. Two factors consistent with this hypothesis are that the meta-stabile defect pair can easily recombine back to the original ground state and that the defect pair can easily migrate. The former is consistent with experiments in which annealing leads to removal of high-energy configurations. The combination of meta-stable defect pairs is consistent with the observation that a threshold exists for observing low energy defect pairs and there is a delay before the stable defect pairs start to appear above this threshold. The threshold is related to the flux needed to create a substantial number of precursor defects that can then combine to form the stable defects.

The primary goal of this research is to develop a systematic understanding of physical and chemical transformations that can occur in amorphous covalently bonded materials during preparation and application. The complexity introduced by the amorphous phase necessitates development of creative approaches to study chemical reactions, electronic excitations, and structure evolution. The network response plays a major role in each of these processes such that electronic structure studies need to incorporate extended systems, and classical studies require potential interactions and simulation methodologies that correctly capture the physics. Albeit such approaches are approximate, our efforts combine classical simulations to create reasonably accurate descriptions of extended systems that can be used in electronic structure studies and, thus, what is learned from more accurate calculations can be iterated into the classical methods to systematically improve potentials and simulation methodologies for large-scale studies. Several important chemical reactions for nuclear waste and photonic glasses include those of the glass matrix with water, hydrogen, oxygen and other small reactive molecules that can come into contact with the glass or be created within the glass from radioactive decay and chemical

processes. Reactions with these particular molecules can occur at the surface or in the bulk. The network response differs because the reaction of a small molecule with different network formers leads to an interesting variety of responses when the network formers are mixed. One important reaction that has not been investigated theoretically to any significant extent is the reaction of hydrogen with network oxide materials. This reaction is important because electronic excitations in a glass containing or in contact with water can produce hydrogen gas that can then react with the glass itself. Ongoing experiments of the reaction of hydrogen with silica, and germanium doped silica show that there is limited reaction of silica with hydrogen, yet in the doped material, the reaction is greatly enhanced. Also, the experimental evidence shows an anomaly in that SiH bonds are not formed, something not well understood. Typically, when hydrogen reacts across a Si-O bond, a silanol group and a SiH group form. When a Ge atom is substituted for a Si and the same reaction is carried out, GeOH groups form, but no SiH or GeH groups are seen to form. This is an interesting and important mechanism that needs to be better characterized by theory, because the reaction mechanism is thought to be similar to that of water reacting with the same networks. The basic differences could be that for water the reaction path may be along a heterogeneous dissociation path, whereas the hydrogen pathway may be along a homogeneous dissociation path. These studies will be carried out using DFT plane wave calculations in simulated bulk systems, similar to our previous calculations of water reactions in silica. The calculations will first look at the energy differences between reactant and product states to determine what are stable product states. Substitution of silicon atoms with germanium atoms will then be done to create doped samples, and calculations carried out to determine possible product states. Comparison with more accurate cluster calculations using more accurate levels of *ab initio* theory will be made. Minimum energy pathways will then be determined using the nudged-elastic band method coupled with DFT calculations to obtain activation barriers. Results will be compared with available experimental data.

References to publications of DOE sponsored research (2002-present)

1. B. Park, L. R. Corrales, "Molecular dynamics simulation of La_2O_3-Na_2O-SiO_2 glasses: II. Clustering of the La^{3+} cations", J. Non-Cryst. Solids **311**, 107 (2002).
2. B. Park, L. R. Corrales, "Molecular dynamics simulation of La_2O_3-Na_2O-SiO_2 glasses: III. The driving forces of clustering", J. Non-Cryst. Solids **311**, 118 (2002).
3. R. Devanathan, WJ Weber, and LR Corrales. 2002. "Atomistic Simulation of Displacement Cascades in Zircon." In *Scientific Basis for Nuclear Waste Management XXV*, vol. 713, no. JJ11.36, ed. BP McGrail and GA Cragnolino, pp. 1-8. Materials Research Society, Warrendale, PA.
4. A. Chartier, C. Meis, W. J. Weber, L. R. Corrales, "Defect structure and migration in $La_2Zr_2O_7$ pyrochlores," Phys. Rev. B **65**, 134116 (2002).
5. B. Park, E. Bylaska, and L. R. Corrales, 'Energy dependence of vitreous B_2O_3 on boroxol ring concentration", *Phys. Chem. Glasses* **44**, 174 (2003).
6. F. Gao, G. Henkelman, W.J. Weber, L.R. Corrales, and H. Jónsson, "Finding Possible Transition States of Defects in SiC and Alpha Fe Using the Dimer Method," *Nuclear Instruments and Methods in Physics Res. B* **202**, 1 (2003).
7. R. C. Ewing, A. Meldrum, L. M. Wang, W. J. Weber, and L. R. Corrales, **Chapter 14: Radiation Effects in Zircon**, in *Zircon, Reviews in Mineralogy and Geochemistry*, Vol. **53**, edited by J. M. Hanchar and P. W. O. Hoskins (Mineralogical Society of America, Washington, DC, 2003), pp. 387-425.

8. A. Chartier, C. Meis, J-P. Crocombette, L. R. Corrales, W. J. Weber, "Atomistic modeling of displacement cascades in $La_2Zr_2O_7$ pyrochlore," *Phys. Rev. B* **67**, 174102 (2003).
9. R.M. Van Ginhoven, K.A. Peterson, M. Dupuis, L.R. Corrales and H. Jónsson, "An Ab Initio Study of Self-Trapped Excitons in Alpha-Quartz," *J. Chem. Phys.* **118**, 6582 (2003).
10. LR Corrales and W.J. Weber, "State of theory and computer simulations of radiation effects in ceramics", *Current Opinions in Solid State and Materials Science* **7**, 35 (2003).
11. LR Corrales, WJ Weber, A. Chartier, C Meis and J.-P. Crocombette, "Comment on 'Radiation Swelling and percolation in irradiated zircon'", *J. Phys. Conden. Matter* **15**, 6447 (2003).
12. LR Corrales, "Computational methods to study radiation effects in oxide materials" *Nuclear Instruments and Methods in Physics Res. B* **218**, 95 (2004).
13. R Devanathan, LR Corrales,WJ Weber, A Chartier and C Meis, "Molecular dynamics simulation of diordered zircon", *Physical Review B* **69**, 064115 (2004).
14. L. R. Corrales, "Free energy profiles of Al and La cation clustering in silica and soda silicate glasses", *J. Non-Cryst. Solids* 2004 (accepted).
15. L. R. Corrales, A. Chartier, R. Devanathan, "Excess kinetic energy dissipation in materials", *Nucl. Inst. Meth. B* 2004 (accepted).
16. R. Devanathan, L. R. Corrales, W. J. Weber, A. Chartier, and C. Meis, "Molecular dynamic simulation of defect production in collision cascades in zircon", *Nucl. Inst. Meth. B* 2004 (accepted).

Chemical Kinetics and Dynamics at Interfaces

Solvation/Fluidity on the Nanoscale, and in the Environment

James P. Cowin
Chemical Sciences Division
Pacific Northwest National Laboratory
P.O. Box 999, Mail Stop K8-88
Richland, Washington 99352
jp.cowin@pnl.gov

Program Scope

Interfaces have a unique chemistry, unlike that of any bulk phase. This is true even for liquid interfaces, where one might have (incorrectly) pre-supposed that a liquid's lack of rigidity might strongly suppress perturbations due to the interface. These interfacial effects include changes in fluidity and transport, solvation of ions, and stability of excited states. The applicability of the knowledge gained extends reactions and transport across two-phase systems (like microemulsions), electrochemical systems, and in many situations where a fluid is present in molecular-scale amounts… such as in cell membranes, enzymes and ion channels, or at environmental interfaces at normal humidities, such as the surfaces of atmospheric or soil particles. We explore these systems with several unusual methods. These include re-creating liquid-liquid interfaces using molecular beam epitaxy, and use of a molecular soft landing ion source. We also explore fundamental properties of bulk ice, that relate to such issues as proton transport, amorphous ice properties, and even the effect of ice in formation of planets.

Recent Progress

Probing Nano-Fluids: We use a unique approach to study interfacially perturbed materials: a soft-landing ion source and molecular beam epitaxy together allow us to re-create liquid-liquid interfaces with high precision. This has allowed us to probe fluidity with molecular precision near solvent interfaces, and solvation potentials for ions at or near these interfaces. As shown in Figure 1, left, we grow thin films of solvent, at cryogenic temperatures. While it is still too cold for any diffusion to occur, we add to the film, very gently, a fraction of a monolayer of molecular ions (Cs^+ in this case). These ions can be inserted at will at any precise, initial location in the solvent (3-methylpentane) film. We then warm the film, and follow the ion's motion with great precision, using an electrostatic Kelvin probe.

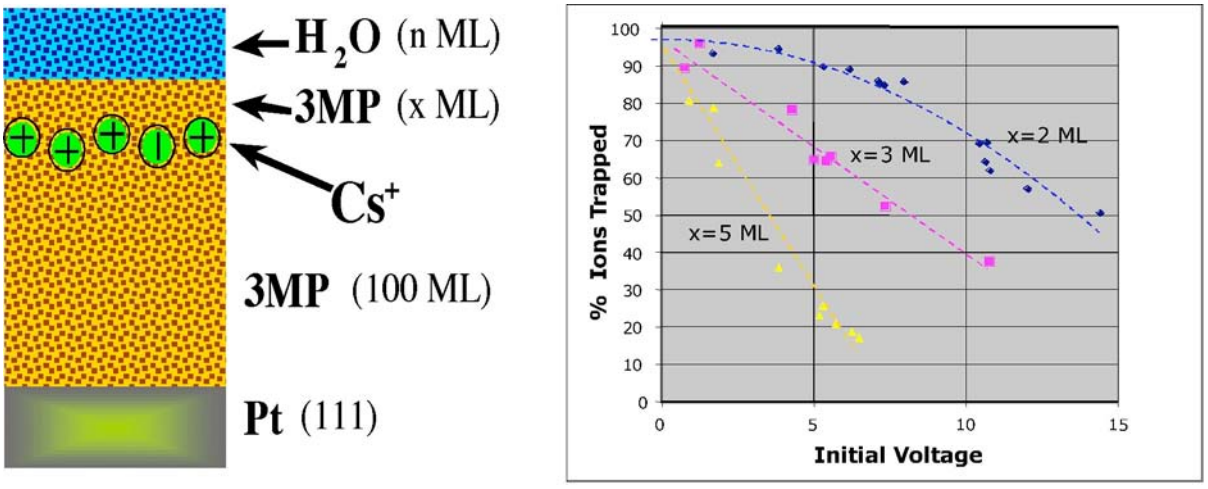

Figure 1. Probe ions placed at a distance x-monolayers (ML) away from an embedded water layer can either escape or get trapped when system is warmed (left). At right shows percent of ions that are trapped vs starting voltage

We used this approach to measure the nanometer dependence of the fluidity of 3 methyl pentane (3MP) at the 3MP-Pt, 3MP-vacuum, and 3MP-water interfaces. We were able to show that the film is orders of magnitude less viscous at the top of the film compared to the bulk material, and orders of magnitude more viscous at the bottom. (Bell et Al. 2003).

We then applied this precision ion-doping methods to map the solvation potential near the oil-water interface. Only a portion of the data is published from the first of many studies showing how we could determine the solvation potential minimum, and its maximum slope. (Wu et Al. 1999, 2001). Our most recent results include work where we gave ions a choice… by placing them x monolayers (ML) away from water interface, with a water thickness of n ML (Figure 1, right). The ions can either follow the collective ion-Pt induce potential gradient (V_f = 1 to 15 V across the 100 ML of 3MP), or fall backwards toward the water interface. We find that for n to many monolayers, the outcome is independent of n. But the fraction being trapped (Figure 1, right) varies strongly with V_f, and the distance away from the water interface. This provides information on the detailed shape of the solvation potential.

Atmospheric Dust Aging (with Alex Laskin): Dust in our atmosphere degrades our view, can make us sick, and influences climate and chemistry of the atmosphere. The dust's chemical properties that determine these effects constantly evolve, from the particle's birth until its removal from the atmosphere, typically days later. We explore atmospheric aging mechanisms of particles and their implications. These often involve solid particles with only monolayers of adsorbed water present, thus limited solvation (see "Nano-fluids" section). Analysis in the lab of samples of dust are done for each individual particles using computer controlled scanning electron microscopy with elemental analysis via emitted x-rays, and time of flight secondary ion mass spectrometry. The "Environmental" electron microscope permits imaging the particles at up to 100 % relative humidity, or several Torr of reactive gases present.

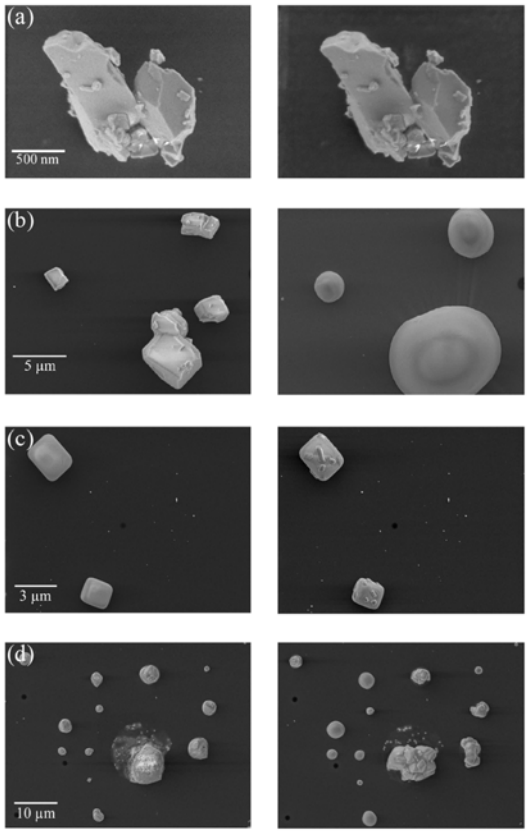

Figure 2. Single particle reaction with HNO_3 and water vapor: (a) SiO_2 before/after exposure to 1 Torr HNO_3 and ~25% RH for 20 minutes, (b) $CaCO_3$ before/exposure to 20 µTorr HNO_3 and 41% RH for 4 hours, (c) NaCl before/after exposure to 20 µTorr HNO_3 and 17% RH for 5 hours and (d) sea salt before/after exposure to 20 µTorr HNO_3 and 17% RH for 5 hours.

Collaborating with Prof. V.H. Grassian's group (U. of Iowa), we studied particles reacting with nitric acid, a pervasive trace pollution gas. Figure 1 shows changes observed for SiO_2, $CaCO_3$, NaCl and sea salt particles. Figure 2(a) shows a SiO_2 particle before and after exposure to nitric acid: no reaction is seen. Image (b) shows $CaCO_3$ dust reacting rapidly: its x-ray emission (not shown) confirms transformation to calcium nitrate (Krueger et al, 2003b). Images (c) and (d) show NaCl and sea salt particles. The NaCl particles showed only small amounts of $NaNO_3$ crystallites on the particle surfaces while sea salt particles reacted nearly completely. These transformations, accelerated by the hydroscopic nature of the products (especially Ca- and Mg- nitrate), may greatly alter common dust's lifetime and ability to seed clouds (Krueger, *et al.* 2003a; 2003b).

In a collaborative study with the group of Prof. B.J. Finlayson-Pitts (U. of California, Irvine) we probed the composition of NaCl particles reacted with hydroxyl radicals (Laskin, *et al.* 2003b). We showed that hydroxyl radicals transformed sea salt dust into both hypochlorites/perchlorates and hydroxides, via reactions with interfacial chloride ions. In the marine boundary layer, this increases particle alkalinity, increasing the uptake and oxidation of SO_2 to sulfate in sea salt particles. This may have an important impact on global warming. Other ongoing collaborative projects include; aging of diesel exhaust particles (Prof. M.J. Molina and L.T. Molina, Massachusetts Inst. of Technology) and biomass burning particles (with W.C. Malm and J.L. Hand, Nat. Park Service and Colorado State U.).

Bulk Water Ice: Two projects involving bulk water ice (amorphous and crystalline) were done recently, one on "nano-planets", another on the pryo- and piezo-electric properties.

Probing Nano-Planets: What is a nano-planet? A nano-planet is just a fanciful way to describe the micron-sized dust in a nebula around a newborn star, that may some day agglomerate to form planets. May form planets is emphasized, as the new star's stellar wind also begins to slowly strip the nebula of this dust. A planet must form within 1 million years, or the dust supply will be gone. The problem is, scientists have a hard time understanding how the dust can stick together fast enough, to reach gravitationally bound "planetesimals" (10's of meters of size). Our studies of the properties of low temperature water ices gave us insight into that process.

Most dust grains in the outer parts of the nebulae will be heavily coated or largely composed of water ice. Most of this ice forms amorphously via condensation from the vapor at from 10 to 100 K. At these temperatures, the water dipoles tend to slightly align, creating strong electrostatic fields within or around the ice grains (see Figure 3). Even in the presence of neutralizing charges, collisions and temperature changes re-expose these electric fields, which then greatly enhances the sticking rate of the ice grains. We also measured the elastic properties of the low temperature ice. As shown in Figure 3, it is very inelastic, which also makes it much easier for two colliding icy grains to stick together. (Wang et al. 2004)

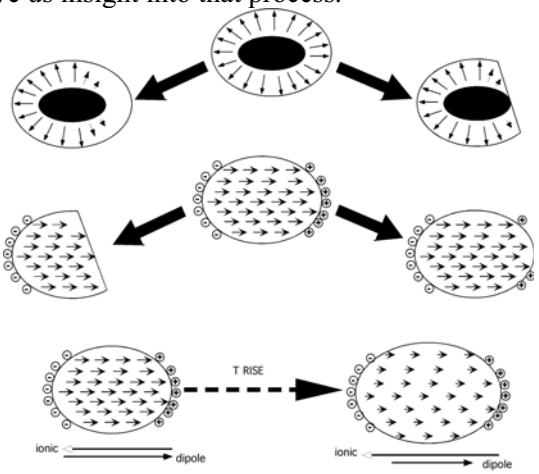

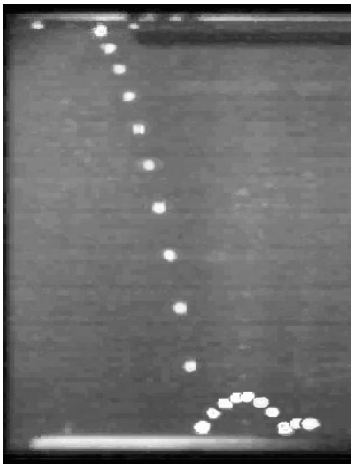

Figure 3. Left: Icy grains in pre-planetary nebula acquire electrostatic dipoles due to low temperature ice's spontaneous polarization (top). They spew charged fragments after collisions (middle), or polarize via subtle T-induced charge imbalances (bottom). Right: Time-lapse photo of a ball bouncing from an amorphous ice slab, shows how inelastic this low temperature ice is.

Pyro-and Piezo-electric Water Ice: We measured, for the first time, the pyro- and piezo-electric properties of water ice. These describe, respectively, how temperature and strain cause water ice to polarize. These properties are only non-zero for substances which possess no inversion symmetry, and most had supposed for water ice I, that it should be uniquely zero. However water ice that is slightly proton-aligned lacks inversion symmetry. So this does possess non-zero coefficients. Our soft-landed ions allow us to make water ice that is around 10% percent proton-aligned. It has strongly non-zero piezo- and pyroelectric coefficients. This has implications for the "nano-plane" work, and also can be very important in any study that attempts to probe low temperature water ice (<150 K) with electrical measurements. This work is written up, and will be submitted soon for publication.

Future Plans

A major ongoing effort is now finishing the publication of several papers related to solvation at the oil water interface, and a paper on ion motion in bulk 3 methyl pentane. The data backlogged mostly due to the need to resolve changes in fluidity at the various interfaces, as the activation barrier for diffusion basically adds to the effective solvation potential under some conditions.

New experiments are now just commencing. Our soft landing ion source has been re-laid out with new ion optics, which among other things makes our ion beam 20 to 50 times more intense. This will permit us to pursue a full accounting of the motion in water ice of hydronium ions, and hydrogen bond defects ("L" and "D" type), which form a basic for understanding many solvation processes and proton transport processes in liquid water, as well as water inside cells.

New experiments are in planning to re-create solutions with embedded ions, to look at solvation via photoemission, and with FTIR, and time-resolved optical probes. This involves a special small mobile ultrahigh vacuum system that can deliver our custom tailored films to optical probes located in other PNNL labs, and at synchrotrons. One important new goal of this work will be to understand the transport of excited state and electron-driven chemistry, under the influence of intense gradient s in electric field and solvation asymmetry.

References

Bell, R. (2003a), H-F Wang, K. Wu, M. J. Iedema, and J. P. Cowin, "Nanometer-Resolved Interfacial Fluidity." *J. Amer. Chem. Soc.* 125: 5176-5185

Bell, R.C. (2003 b) H.-F. Wang, M.J. Iedema, J.P. Cowin , Sculpting Nanoscale Liquid Interfaces, in "ACS Symposium Series 861: Mesoscale Phenomena in Fluid Systems" ed. F. Case and P. Alexandridis, Amer. Chem. Soc. , Chapter 12, pp. 191-203

Gallagher, M. C. (2003), M. S. Fyfield , L. A. Bumm, J. P. Cowin and S. A. JoyceStructure of Ultrathin MgO films on Mo(001), Thin Solid Films 445, 96

Krueger, B. J.(2003a), V. H. Grassian, M. J. Iedema, J. P. Cowin and A. Laskin "Probing Heterogeneous Chemistry of Individual Atmospheric Particles Using Scanning Electron Microscopy and Energy Dispersive X-ray Analysis. " *Anal. Chem.,* 75: 5170-5179 .

Krueger, B.J. (2003b), V.H. Grassian, A. Laskin and J.P. Cowin "Laboratory Insights Into the Processing of Calcium Containing Mineral Dust Aerosol in the Troposphere." *Geophysical Research Letters* 30: 1148-1151 .

Laskin, A., (2003a), M. J. Iedema and J.P. Cowin "Time-Resolved Aerosol Collector for CCSEM/EDX Single-Particle Analysis." *Aerosol Sci. Technol,* 37: 246-260 .

Laskin, A.(2003b), D. J. Gaspar, W.-H. Wang, S.W. Hunt, J. P. Cowin, S. D. Colson, and B. J. Finlayson-Pitts "Reactions at Interfaces As a Source of Sulfate Formation in Sea-Salt Particles." *Science,* 301: 340-344 .

Laskin, A. (2004), D. J. Gaspar, W.-H. Wang, S.W. Hunt, J. P. Cowin, S. D. Colson, and B. J. Finlayson-Pitts, "Response to Comments on "Reactions at Interfaces As a Source of Sulfate Formation in Sea Salt Particles", Science 303, 628

Wang, H.-F. (2004), RC Bell, MJ. Iedema, AA. Tsekouras, JP Cowin, "Sticky Ice Grains Aid Planet Formation". (submitted to J. Astrophysics)

Wu , K. (1999), M.J. Iedema, J.P. Cowin, Ion Penetration of the Oil-Water Interface, Science 286, 2482

Wu, K (2001), M.J. Iedema, G.K. Schenter, J.P. Cowin Invited Feature Article: Sculpting the Oil-Water Interface to Probe Ion Solvation, J. Phys Chem. B 105, 2483

New Ultrafast Techniques for Electron Radiolysis Studies

Robert A. Crowell, David Gosztola, and Ilya A. Shkrob
Chemistry Division
Argonne National Laboratory
9700 S. Cass Ave.
Argonne, IL 60439
rob_crowell@anl.gov

Program:

Reaction Intermediates in Condensed Phase: Radiation and Photochemistry

Scope:

It is the goal of this project to develop ultrafast techniques for electron pulse radiolysis. Ultrafast ($<10^{-11}$ps) physical processes play a pivotal role in all chemical reactions. Detailed knowledge of primary events such as energy (charge) transfer, thermalization, solvation and the chemistry of pre-thermalized electrons is essential in order to produce a complete picture of reactivity. Due to the lack of a suitable femtosecond source of ionizing radiation, experimental studies on the primary events in radiation induced chemical reactions are virtually nonexistent. Understanding of these ultrafast processes will be beneficial to areas as diverse as photochemistry, materials processing, device fabrication, catalysis, astro and environmental chemistry and radiation processing. It is the ultimate goal of this project to provide such information so that we can gain a full understanding of the radiation chemistry. Achievement of this goal requires the implementation of ultrafast laser, radiolytic and x-ray spectroscopic techniques, techniques that currently do not collectively exist for this purpose. Recent advances in super-intense ultrashort laser technology have led to the ability to generate subpicosecond electron, proton and x-ray pulses *without* the use of a traditional electron accelerator. The objective of our current efforts is to develop a state-of-the-art table-top 5-20 TW terawatt laser system that will produce these types of pulses for chemical physics studies. Utilized in conjunction with our ultrafast laser system the electron pulses will provide unprecedented insight into many of the contemporary issues concerning the primary processes of radiation induced chemical reactions.

Recent Progress:

TUHFF Laser System. The Terawatt Ultrafast High Field Facility (TUHFF) has been constructed in the Chemistry Division. TUHFF contains a homebuilt 20TW laser system whose output is currently being used to relativistically accelerate subpicosecond electron pulses to the MeV level. TUHFF represents the only effort in this country to use a terawatt laser to generate subpicosecond electron pulses for chemical studies. The TUHFF laser system is based on the chirped pulse amplification scheme and utilizes three Ti:Sapphire amplification stages. The laser currently operates in the 2-10TW region reliably over extended periods of time. Future upgrades in the laser stretcher and

Table 1. TUHFF Laser Specifications

	Wavelength	Rep.	Pulsewidth	Energy
Oscillator	780 nm	100 MHz	15 fs	2 nJ
Amp 1	800 nm	10 Hz	~350 ps	2 mJ
Amp 2	805 nm	10 Hz	~350 ps **30 fs**	0.35 J **0.15 J (5 TW)**
Amp 3	805 nm	10 Hz	~350 ps **30 fs**	1.3 J **0.6 J (20 TW)** **after pulse compression**

compressor components will permit reliable operation at the full power of 20TW. The TUHFF laser specifications are shown in Table 1.

Generation of Subpicosecond Electron Pulses. By focusing the output of the TUHFF laser into a specially designed supersonic helium gas jet we have succeeded in the generation of intense electron pulses. Using metal filters we are able to determine that ~30% of the electrons that are produced have been accelerated to energies in excess of 5 MeV. The maximum in the electron energy spectrum is approximately 2.5 MeV. A Faraday cup has been designed and constructed to measure the electron pulse charge. Presently, the pulse charges are in the range of 80-100 pC. In addition to the pulse charge and energy spectrum it is important to characterize the electron beam's transverse (spatial) profile. Figure 1 shows the transverse profile of the electron beam at two different laser powers. At 7 TW of laser power the electron beam divergence is actually less than that of the laser beam that is used to generate them. The combination of the current electron pulse charge, energy dispersion and spatial profile will enable us to begin time-resolved measurements with ~5 ps time resolution.

Development of Single-Shot Ultrafast Transient Absorption Spectroscopy. Due to large shot-to-shot variations in the yield of high-energy electrons and low repetition rate of the setup (10 Hz), the standard pump-probe detection of transient absorption kinetics is not an efficient approach for ultrafast measurements at TUHFF. For these reasons, high priority was put on the development of a robust single-shot detection methodology that provides an alternative way to sample ultrafast kinetics. Our current solution is ultrafast Frequency Domain Single-Shot (FDSS) transient absorption. This spectroscopy is based upon frequency encoding with chirped femtosecond. This method takes advantage of the bandwidth of subpicosecond optical pulses. In this technique a femtosecond probe pulse is stretched out to several picoseconds. The stretching process assigns each frequency component of the probe pulse a specific time delay. The stretched probe pulse is passed

through the sample at the same time as a femtosecond pump pulse and the measured kinetic trace is imprinted in the spectrum of the transmitted probe pulse. The modulated probe pulse spectrum is then converted into a time scan using a monochromator and a photodiode array (PDA).

Future Plans:

The main focus of our current effort is directed towards using TUHFF to perform our first time-resolved measurements. It is expected that our first measurements will have a time resolution of ~5ps, limited by the electron pulse charge and energy dispersion. As the pulse charges increases the experimental time resolution will also improve. Our target is 1 nC of charge which should reduce the time resolution to 1-2 ps. Recently our group has carried out several femtosecond photoionization studies of liquid water (see abstract of Shkrob et. al and references therein). This work has provided a significant amount of insight into the dynamics of solvation and thermalization for above-the-gap ionization of liquids. We will use this knowledge as the starting point for our first radiolysis experiments. The first studies will focus on thermalization and solvation dynamics of electrons that are generated in water radiolysis. This work will be followed by studies of the reactivity of electron precursors (i.e., chemistry that occurs before thermalization). An upgraded version of the TUHFF laser system has been designed and will be implemented in the future. The improvements will allow for reliable operation at 20 TW and an increase in the charge of the electron pulses. Other future projects include development of ultrasensitive methods to characterize the longitudinal (temporal) characteristics of the electron pulses and the generation of hard x-rays via Thompson scattering.

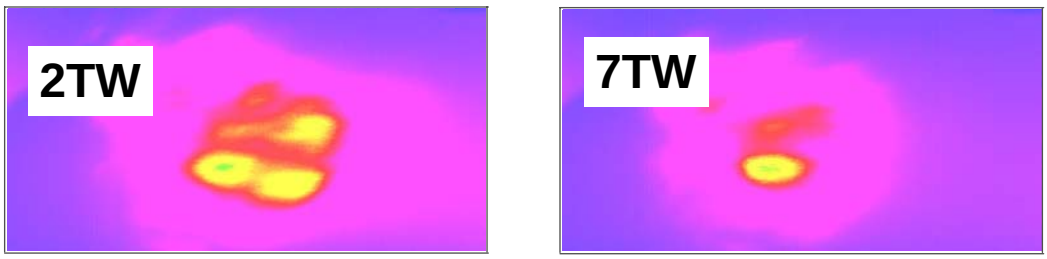

Figure 1. The spatial profile of the electron beam. The full angle beam divergence goes from ~15º at low power (2TW) to ~3º at higher power (7TW). At the highest laser power (23TW) the divergence is expected to be on the order of 1º. This effect is a result of relativistic self focusing of the electron beam.

Recent Publications

1. M. C. Sauer Jr., I. A Shkrob**,** R. Lian, R. A. Crowell, D. M. Bartels, X. Chen, D. Suffren, and S. E. Bradforth, "Electron photo-detachment from aqueous anions. II. Ionic strength effect on geminate recombination dynamics and quantum yield for hydrated electron," J. Phys. Chem. A., accepted.

2. R. Lian, R. A. Crowell, I. A. Shkrob, D. M. Bartels, D. A. Oulianov, and D. J. Gosztola, "Recombination of Geminate ($OH:e^-$) Pairs in Concentrated Alkaline Solutions: Lack of Evidence for Hydroxyl Radical Deprotonation," Chem. Phys. Lett. 389, 379 (2004).

3. M. C. Sauer Jr., I. A. Shkrob* and R. A. Crowell "Electron Photodetatchment from Aqueous Anions. I. Quantum Yields for Generation of Hydrated Electron by 193 and 248nm Laser Photoexcitation of Sundry Inorganic Anions," J. Phys. Chem A, 108, 5490 (2004).

4. R. A. Crowell, R. Lian, I. A. Shkrob, J. Qian, D. A. Oulianov, and S. Pommeret, "Light-induced temperature jump causes power-dependent ultrafast kinetics of electrons generated in multiphoton ionization of liquid water," J. Phys. Chem. A, accepted.

5. R. Lian, D. A. Oulianov, I. A. Shkrob and R. A. Crowell, "Geminate recombination of electrons generated by above the gap (12.4eV) photoionization of liquid water," Chem. Phys. Lett., accepted.

6. R. Lian, R. A. Crowell, I. A. Shkrob, D. M. Bartels, X. Chen, and S. E. Bradforth, "Ultrafast Dynamics for the Electron Photodetachment of Aqueous Hydroxide," J. Chem. Phys. 120, 11712 (2004).

7. I. A. Shkrob, D. A. Oulianov, R. A. Crowell, and S. Pommeret "Frequency Domain single-shot (FDSS) ultrafast transient absorption spectroscopy" J. Appl. Phys. 96, 25 (2004).

8. R. A. Crowell, R. Lian, D. A. Oulianov, and I. A. Shkro* "Geminate recombination of the hydroxyl radicals generated from the 200nm photodissociation of hydrogen peroxide," *Chem. Phys. Lett.* 383, 481 (2004).

9. R. A. Crowell, D. J. Gosztola, I. A. Shkrob, D. Oulianov, C. D. Jonah, and T. Rajh "Ultrafast Processes in Radiation Chemistry," Radiat. Phys. Chem. 70, 501 (2004)

10. L. Zhao, R. Lian, I. A. Shkrob, R. A. Crowell, S. Pommeret, E. L. Chronister, A. D. Liu, and A. D. Trifunac,, "Ultrafast studies on the photophysics of matrix-isolated radical cations of polycyclic aromatic hydrocarbons," submitted to J. Phys. Chem. A 108, 25 (2004).

Molecular Theory & Modeling

Ions at interfaces of hydrogen bonded liquids

Liem X. Dang
Chemical Sciences Division
Pacific Northwest National Laboratory
902 Battelle Blvd., Mail Stop K1-83
Richland, WA 99352
liem.dang@pnl.gov

Summary. The adsorption and distribution of ions at aqueous liquid interfaces are fundamental processes encountered in a wide range of chemical and biological systems. In particular, the manner in which solvent molecules solvate ions is relevant to problems in chemical and physical processes. For example, solvation of ions affects chemical reactions at interfaces and the distribution of ions and/or counter-ions influences the structure and stability of large molecules and membranes. The focus of research on this project is the characterization of solvation processes at aqueous liquid interfaces using molecular dynamics (MD) computer simulation techniques. We develop fundamental, molecular-scale information about the interactions of ions and molecules in solvent phases and across aqueous liquid interfaces. We focus special effort on understanding the precise mechanism and dynamics of the transfer process, and on learning the role of many-body effects on the transfer mechanism of solutes across the aqueous liquid interface. We use MD simulations to compute potentials of mean force for dilute solutions and density profiles in concentrated solutions. In addition, research on chemical separation science involves the development of methods and potential models for use in the simulation of crown ether molecules mediating ion transport across water-organic liquid interfaces. Results of this research further our understanding of ion transport across liquid-liquid interfaces, which in turn, provides basic knowledge needed to address DOE's environmental restoration issues.

HI at the water liquid/vapor interface. We carried out simulations to characterize solvation properties of hydronium-iodide (HI) salt at the water liquid/vapor interface. In Figure 1, we present the density profiles for water center-of-mass, oxygen atoms in H_3O^+ ions, and I^- ions obtained from a MD simulation. Upon examining these density profiles as well as the MD simulation snapshots, we can make the following observations. 1) A significant number of iodide anions are present near the Gibbs dividing surface (GDS) and form well-defined maximum, and

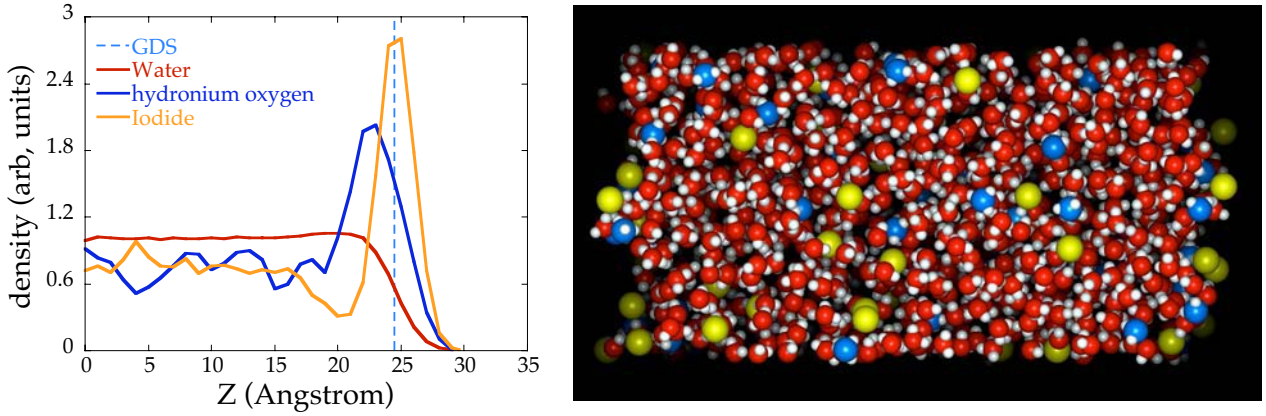

Figure 1. Computed density profiles of HI and a molecular dynamics snapshot of HI at the liquid/vapor interface of water. The Gibbs dividing surface (GDS) is the location where the solvent density is half its bulk value. At the right, O atoms in H_3O^+ and I^- ions are indicated by blue and yellow spheres, respectively. Interfaces are at the left and right of the right image.

the H_3O^+ molecules are found to have enhanced concentration near the interface with significant population at the interface. 2) These results differ from the results of NaI salt at the water liquid/vapor interface, in which the width of the electric double layer is smaller. The new results are supported by our earlier studies on the potential of mean force for the transport mechanism of an ion (Na^+ and H_3O^+) across the water liquid/vapor interface. In the previous studies, the computed H_3O^+ potential of mean force indicates that H_3O^+ is found closer to the dividing surface than the Na^+, and the computed free energy for H_3O^+ is lower (about 6 kcal/mol) at the dividing surface. 3) It is interesting to point out that the hydration energies of H_3O^+ and Na^+ are nearly identical; therefore, the different behavior of these ions at the aqueous interface can be attributed to the differences in the shape, charges distribution, as well as the polarizability of the ion used in our classical simulations.

The mechanism of proton transport in liquid water is quantum mechanical in nature; therefore, our classical polarizable model for H_3O^+ (*i.e.*, fixed charge) may not accurately capture the H_3O^+ - H_2O interaction. It is well known that the proton diffusion mechanism in water will strongly influence the results and this mechanism is also known to have non-negligible quantum effects. An accurate study of the proton transport mechanism requires quantum statistical treatment of the hydrogen motion in liquid water. Thus, extension of our study to include quantum effects and comparison of the results to the results presented in this paper will be a worthwhile next step. It remains to be seen whether the mechanism of proton transport will have a significant effect on the distribution of H_3O^+ at the interface. Finally, the present study may also contribute to the understanding of ion-induced nucleation of water vapor, which is thought to be an importance in many atmospheric processes

NaI at liquid/vapor interfaces of water and methanol. The liquid/vapor interface of methanol has been studied experimentally, and it has been established that the methanol surface molecules oriented so that their methyl groups point away from the bulk liquid. This result is quite different from the liquid/vapor interface of water where significant amounts of dangling OH bonds (~25%) are present at its interface. As part of our ongoing research on ions at liquid/vapor interfaces, we performed a detailed study of the solvation properties of sodium iodide salt at the liquid/vapor interfaces of methanol and water and a description of the transport mechanism of an iodide anion across the liquid/vapor interface. There have been some studies of ion solvation in liquid methanol, and it has been established that, while the hydration structure of an ion in methanol is very similar to that of an ion in water, the dynamical property (i.e., residence time as characterized by velocity correlation functions) is quite slow compared to ion solvation in the liquid water. In addition, the density of liquid methanol (0.8 gram/cm3) is about 20 % lower than the density of liquid water (1.0 gram/cm3) at room temperature and there is a difference in the ion solubility, which could play a significant role in the solvation of ions at their liquid/vapor interfaces. We performed MD simulations of a 2.2 M NaI methanol liquid/vapor interface. In Figure 2, we present preliminary density profiles of the methanol center-of-mass,

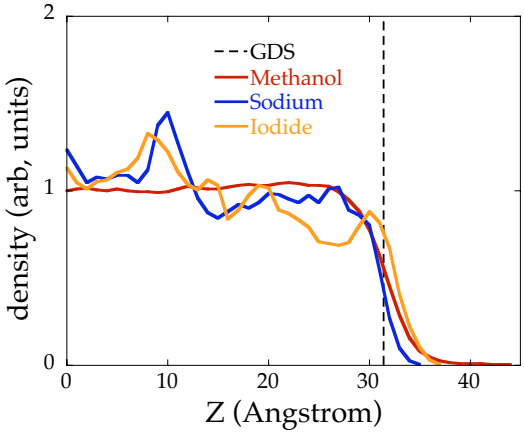

Figure 2. Computed density profiles across the interface of NaI methanol solution.

iodide, and sodium ions obtained from averages over 3 ns of MD simulations. Several observations are in order. 1) The characteristic of the methanol center-of-mass density profile of the salt methanol interface is very similar to the corresponding pure methanol interface, except that the density is now around 0.7 g/cm^3 instead of 0.8 g/cm^3 for pure methanol. The decrease in liquid density is likely caused by the reorganization of methanol molecules around the NaI salt. 2) The density profiles of the iodide and sodium ions are asymmetrical around Z = 0 Å, which is indicative of slow dynamics/equilibration processes of ions in liquid methanol. However, we can conclude from these computed density profiles that the iodide anions were found nearer to the interface than the sodium cations. Figure 3 presents a snapshot of the NaI methanol system, which was taken during the MD simulations of 2.2 M salt concentration. The snapshot clearly indicates that the ions distribute randomly along the axis perpendicular to the interface and some iodide anions were found at or near the interface. In addition to the above calculations, we also carried out the simulations of 2.2 M NaI salt water liquid/vapor interface using our own set of polarizable potential models for water and ion-water. In Figure 4, we present the density profiles for water center-of- mass, sodium and iodide ions obtained from a 500-ps MD simulation. Upon examining these density profiles as well as the MD simulations snapshots, we conclude that iodide anions have enhanced concentration at the interface, as shown by a well-defined maximum at the Gibbs dividing surface of the iodide's density profile. This result indicates that the probability of finding an iodide anion at the interface of water is far greater than finding an iodide anion at the methanol liquid/vapor interface (see Figure 2). We can attribute this effect to the difference between the liquid water and liquid methanol interfaces as well as the difference in the liquid densities and solubility's of the ions in these solvents. We also note here that the computed density profiles in the simulation of the water liquid/vapor interface converged quickly when compared to the corresponding methanol simulations. Future work will include simulations of hydronium ions at the methanol interface and comparing to the corresponding water interfaces.

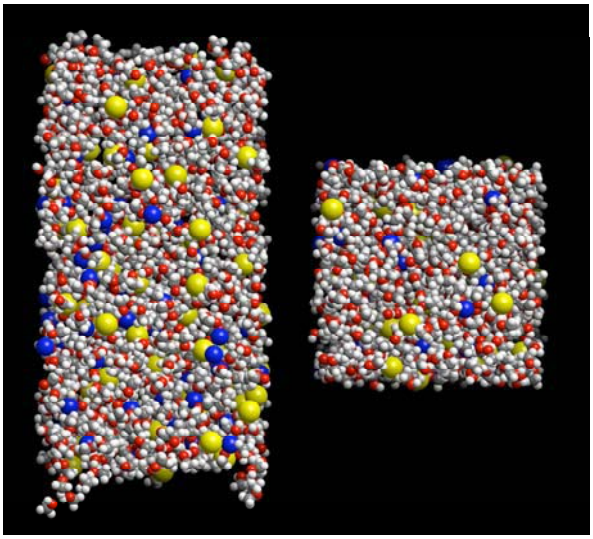

Figure 3. A molecular dynamics snapshot of NaI methanol interface. Na^+ and I^- ions are indicated by blue and yellow spheres, respectively. Interfaces are at the top and bottom of the left image. The right image is looking down onto one of the interfaces.

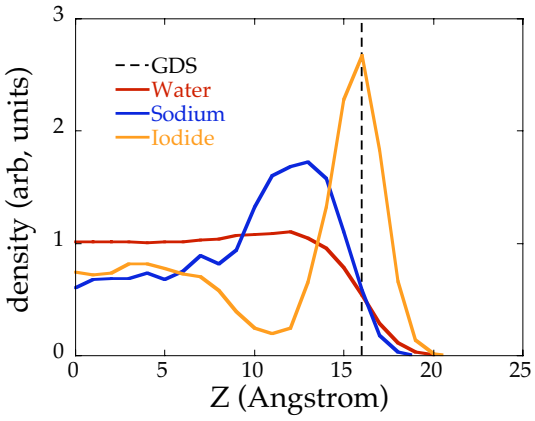

Figure 4. Computed density profiles across the NaI aqueous interface.

Collaborators on this project include Tsun-Mei Chang, Collin Wick , Matina Roeselova and Douglas J. Tobias (UC, Irvine).

References to publications of DOE sponsored research (2002-present)

1. L. X. Dang and T. M. Chang, "Computational Studies of Liquid Water Interfaces," in Water in Confined Geometries, edited by V. Buch and J. P. Devlin (Spring-Verlag, New York, 2003), pp. 227-247.
2. L. X. Dang and T. M. Chang, "Molecular Mechanism of Ion Binding to the Liquid/Vapor Interface of Water," *Journal of Physical Chemistry B* **106**, 235 (2002). **Featured on Journal Cover.**
3. L. X. Dang, T. M. Chang, and AZ Panagiotopoulos, "Gibbs Ensemble Monte Carlo Simulations of Thermodynamic Properties of a Polarizable Potential Model of Water," *Journal of Chemical Physics* **11**7, 3522-3523 (2002).
4. L. X. Dang, "Computational Studies of Ions Binding to the Liquid Interfaces of Water," *Journal of Physical Chemistry* **B 106**, 10388-10394 (2002).
5. L. X. Dang, "Solvation of the Hydronium Ion at the Water Liquid/Vapor Interface," *Journal of Chemical Physics* **11**9, 6351 (2003).
6. T. M. Chang and L. X Dang, "On Rotational Dynamics of an NH_4^+ Ion in Water," *Journal of Chemical Physics* **11**8, 8813 (2003).
7. L. X Dang and T. M. Chang, "Many-Body Interactions in Liquid Methanol and its Liquid/Vapor Interface: A Molecular Dynamics Study," *Journal of Chemical Physics* **11**9, 9851 (2003).
8. L. X. Dang, Gregory K. Schenter and John L. Fulton "EXAFS Spectra of Dilute Solutions of Ca^{2+} and Sr^{2+} in Water and Methanol," *Journal Phys. Chem*. **B 107**, 14119 (2003).
9. L. X. Dang and Bruce C. Garrett. "Molecular Mechanism of Water and Ammonia Uptake by the Liquid/Vapor Interface of Water" *Chemical Physics Letters 385, 309 (2004).*
10. L. X. Dang*, "*Ions at the Liquid/Vapor Interface of Methanol*" Journal of Physical Chemistry* **A 108**, 0000 (2004). **Featured on Journal Cover.**

Molecular Theory & Modeling

Electronic Structure and Reactivity Studies in Aqueous Phase Chemistry

Michel Dupuis
Chemical Sciences Division
Pacific Northwest National Laboratory
902 Battelle Blvd.
Mail Stop K1-83
Richland, WA 99352
michel.dupuis@pnl.gov

Summary. Our current work involves developing and applying computational electronic structure models of solvation. We use *continuum models* for theoretical characterization of organic radicals in solution (reduction potentials, acidities, bond dissociation energies, activation energies) to obtain a mechanistic understanding of these radicals and to contribute to thermochemical kinetic models. These studies support experimental projects aimed at characterizing reactions and at measuring properties of organic radicals in solution relevant to DOE programs in environmental management sciences. Collaborators include D.M. Camaioni and J.A. Franz (PNNL), and D.M. Chipman (U. Notre Dame). Important limitations in the accuracy of *continuum models* of solvation for describing organic radical ions have been traced to the definition of molecular cavities. This finding has lead to proposing novel semi-empirical and *ab initio* definitions of molecular cavities for accurate predictions of molecular properties.

We use *discrete solvent models*, including mixed Hamiltonian representations (QM/MM-vib, QM/MM-pol-vib, and QM/MM-vib/CONT) of solute-solvent systems, combined with Direct ab initio Dynamics (DD) and free energy perturbation methods to study chemical reactions in the aqueous phase. These models are applied to processes relevant to DOE programs in contaminant fate and transport, such as the reduction of chlorocarbons and H_2 formation induced by ionizing radiation in aqueous systems. The DD methodology is yielding new qualitative insights into reactivity. Finally, we systematically apply the method of *Direct ab initio Dynamics* to the characterization of vibrational spectra of small ion-water clusters while accounting for anaharmonicities and mode couplings. This work is in collaboration with Prof. M. Aida (Hiroshima U.).

***Ab Initio*-based Characterization of Aqueous Solvation of Organics (*Dupuis and Camaioni*)**

Motivation: After extensive experimental characterization of tank wastes during the 1990s (Mecham et al. 1998; Camaioni et al. 1998; Meisel et al. 1993, Meisel et al. 1991), theoretical input, based on *ab initio* theories, is now needed to obtain an improved understanding of chemical reactions in aqueous phase and to provide fundamental data (thermochemical, spectroscopic, and reactivity data of organic radical ions) that cannot be easily measured and yet is needed for the development of reliable thermochemical kinetic models.

Approach: We apply existing solvation models (e.g., COSMO, and Chipman's SS(V)P) with MO and DFT theories using large basis sets with the solute residing in a molecular shaped cavity embedded in a dielectric continuum.

Results: Continuum solvation models provide a practical way to characterize solvation effects on the energetics of many chemical reactions; however, they are unable to yield **consistently** chemical accuracy for many systems outside the type of molecules used to calibrate the models.

The errors are most acute on pK scales because of the logarithmic dependence. Systematic investigations of electrostatic properties of solutes are showing that current cavity approximations do not reproduce well the detailed solute-solvent interactions. We are developing more accurate and consistent chemical functionality-based schemes of defining cavities involving atomic radii dependent on atomic charges. Our calculations showed that the electrostatic potential around nitrate NO_3^- is consistent with small cavity radii around O and a large cavity radius around N, in contrast to models based on scaled Van der Waals radii. The protocol was initially defined for oxoanions and is being extended to other organic functional groups. Another protocol involves rolling a solvent molecule around the solute, as depicted for OH radical (picture at right).

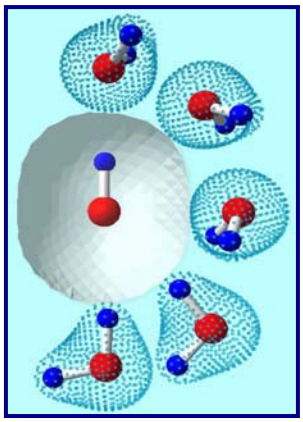

T. Autrey, A.K. Brown, D.M. Camaioni, M. Dupuis, N.S. Foster, and A. Getty, "Thermochemistry of Aqueous Hydroxyl Radical From Advances in Photoacoustic Calorimetry and ab initio Continuum Solvation theory",J. Am. Chem. Soc. Communication,

<u>Quasi-Classical Direct ab Initio Dynamics for Vibrational Spectroscopy</u> *(Dupuis and Aida)*

Motivation: Fundamental insights about the forces involved in hydrogen bonds, proton transfer, and ionic solvation can be obtained from measured cluster properties. Recent high resolution spectroscopic studies of water clusters and ion-water clusters are proviting data in need of "fresh theoretical treatments, both to refine assignments and elucidate structures."[W.H. Robertson *et al.*, Science 299, 1367 (2003); K.R. Amis *et al.*, Science 299, 1375 (2003); C. Chaudhuri *et al.*, Molec. Phys. 99, 1161 (2001)].

Approach: We apply the method of direct dynamics to generate quasi-classical trajectories with forces calculated 'on the fly' at the quantum chemical MP2/aug-cc-pVDZ level of theory to account for anharmonicities and mode couplings. We calculate the density of vibrational states from the velocity autocorrelation function (ACF), the IR intensities from the dipole ACF, and the Raman intensities from the molecular polarizability ACF. Initial atomic velocities are defined consistent with the harmonic vibrations. The analysis can be performed on a subset of internal coordinates to assign DOS peaks to selected internal coordinates, akin to traditional FG analyses.

Results: Spectra for $(H_2O)X^-$ for X=F, Cl, OH have been computed and are shown on the right, along those for $(H2O)_nH^+$ with n=2,3 (not shown). The simulation data are in accord

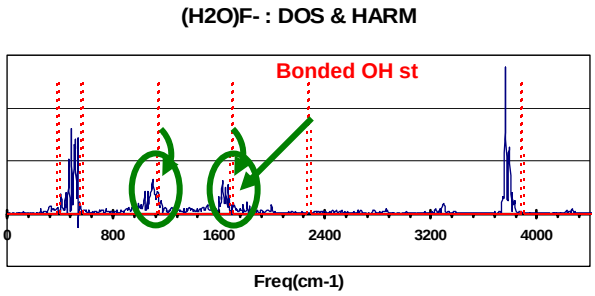

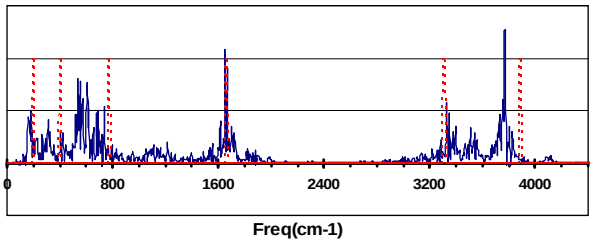

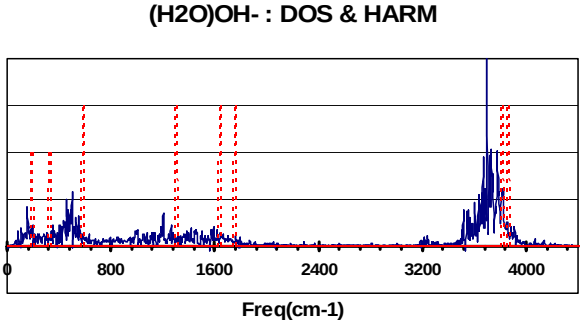

with the VSCF results of Chaban *et al.* [J. Phys. Chem. A 107, 4952 (2003)] for $(H_2O)F^-$, in particular showing the large shift of the H-bonded stretch (harmonic ~ 2400 cm^{-1} and anharmonic ~ 1500 cm^{-1}) and with quantum dynamics results of Schenter *et al.* [J. Chem. Phys. 113, 5171 (2001)] for $(H_2O)Cl^-$. Thus the methodology is found to account well for anharmonicities and mode couplings, as well as to capture the most significant quantum effects of zero point vibrations.

Direct Dynamics Study of Chemical Reactions (*M. Dupuis with M. Aida and H. Yamataka)*

Motivation: A critical role is traditionally assigned to transition states (TSs) and minimum energy pathways (IRCs) in interpreting organic reactivity. Such an interpretation, however, ignores vibrational and kinetic energy effects of finite temperature. Recently W. L. Hase et al. (Science 296, 875 (2002)) showed that reactions do not necessarily follow the intermediates along the IRC and Hase's work broadly suggests that kinetic and temperature effects must be accounted for in the interpretation of chemical reactivity. Our studies highlighted below supports that dynamics effects may lead to qualitatively different interpretations of reaction mechanisms.

Approach: We apply the method of *direct dynamics* to generate classical trajectories by integrating Newton's equations of motion with forces calculated 'on the fly' from quantum chemical wavefunctions at the HF, MP, or DFT levels of theory.

Results: We studied the heterolysis rearrangement of protonated pinacolyl alcohol Me_3C-CHMe-OH_2^+ for which the IRC pathway suggests a *concerted* mechanism. The finite temperature MD pathway suggests a *stepwise* route with C-O bond cleavage followed by Me migration [S. Ammal *et al.*, Science 299, 1555 (2003)]. A stepwise mechanism might lead to racemized products.

We also studied borderline reactions, i.e. reactions that appear to follow different mechanisms in different circumstances. We studied a prototype of Substitution/Electron-Transfer borderline reactions:

$H_2CO^- + CH_3Cl \rightarrow H_2CO\text{-}CH_3 + Cl^-$ [S_N2]

$H_2CO^- + CH_3Cl \rightarrow H_2CO + CH_3 + Cl^-$ [*ET*]

using the direct dynamics approach (see panels below) [Y. Yamataka *et al.*, Chem. Phys. Lett. 353, 310 (2002)]. The S_N2 and ET products originate from a single transition state branching to a S_N2 valley and an ET valley. The finite temperature direct MD simulations suggest that at low temperature most trajectories appear to lead to the S_N2 product. At higher temperature more ET products are obtained, as more trajectories cross over from the S_N2 valley to the ET valley if

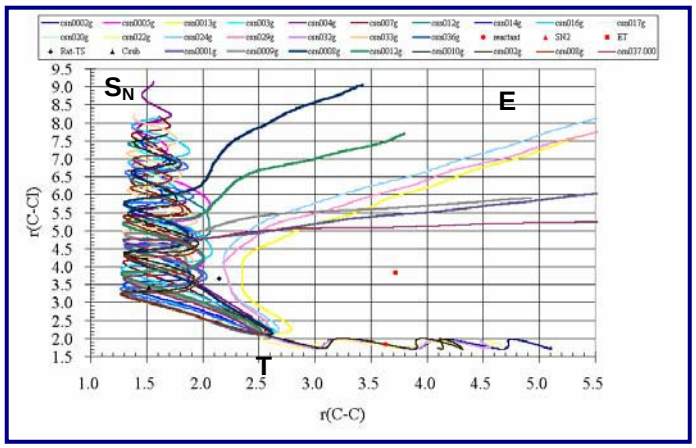

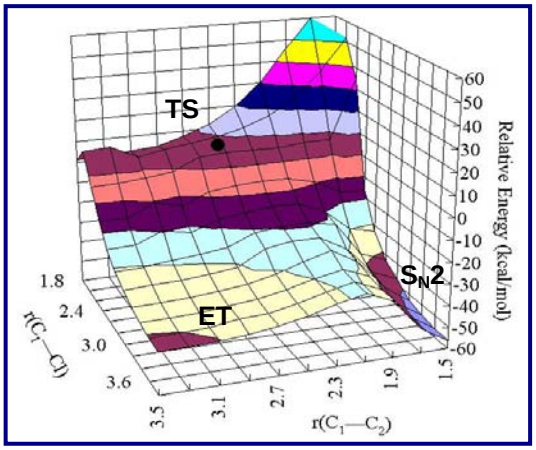

energy flows into the C-C bond of the S_N2 product, thus dissociating to the ET products. A traditional interpretation would call on two TS's with different barrier heights, the higher barrier being more accessible at higher temperature. In the present case internal energy redistribution appears responsible for the higher ET product yield at higher temperature.

References to publications of DOE sponsored research (2002-present)

1. D.M. Chipman and **M. Dupuis**, "Implementation of Solvent Reaction Fields for Electronic Structure," *Theoretical Chemistry Accounts* **107**, 90 (2002).
2. H. Yamataka, M. Aida, and **M. Dupuis**, "Analysis of Borderline Substitution/Electron Transfer Pathways From Direct ab initio MD Simulations," *Chemical Physics Letters* **353**, 310 (2002).
3. **M. Dupuis**, M. Aida, Y. Kawashima, and K. Hirao, "A Polarizable Mixed Hamiltonian Model of Electronic Structure for Micro-solvated Excited States: I. Energy and Gradients Formulation and Application to Formaldehyde ($^1A_2$)," *Journal of Chemical Physics* **117**, 1242 (2002).
4. Y. Kawashima, K. Hirao, and **M. Dupuis**, "Monte Carlo Micro-Solvation Simulations for Excited States using a Mixed-Hamiltonian Model with Polarizable and Vibrating Waters: Application to the Blue Shift of the H_2CO $^1(\pi^*\leftarrow n)$ Excitation," *Journal of Chemical Physics* **117**, 248 (2002).
5. **M. Dupuis**, Y. Kawashima, and K. Hirao, "A Polarizable Mixed Hamiltonian Model of Electronic Structure for Solvated Excited States: II. Application to the Blue Shift of the H_2CO $^1(\pi^*\leftarrow n)$ Excitation in Water," *Journal of Chemical Physics* **117**, 1256 (2002).
6. S. Ammal, H. Yamataka, M. Aida, and **M. Dupuis**, "Dynamics-Driven Reaction Pathway in An Intramolecular Rearrangement," *Science* **299**, 1555 (2003).
7. R. M. Van Ginhoven, H. Jonsson, K. A. Peterson, **M. Dupuis**, and L. R. Corrales, "An ab initio tudy of Self-Trapped Excitons in α–quartz," *Journal of Chemical Physics* **118**, 6582 (2003).
8. M. Aida and **M. Dupuis**, "IR and Raman Intensities in Vibrational Spectra from Direct Ab Initio Molecular Dynamics: D_2O as an Illustration," *Journal of Molecular Structure (Theochem)* **633**, 247 (2003).
9. D. Camaioni, **M. Dupuis**, and J. Bentley, "Theoretical Characterization of Oxoanions XO_m^{n-} Solvation," *Journal of Physical Chemistry A* **107**, 5778 (2003).
10. **M. Dupuis**, G. K Schenter, B. G. Garrett, and E. E. Arcia, "Potentials of Mean Force with Ab Initio Mixed Hamiltonian Models of Solvation," *Journal of Molecular Structure (Theochem)* **632**, 173 (2003).
11. T. Autrey, A. K. Brown, D. M. Camaioni, **M. Dupuis**, N. S. Foster, and A. Getty, "Thermochemistry of Aqueous Hydroxyl Radical from Advances in Photoacoustic Calorimetry and ab initio Continuum Solvation Theory", J. Am. Chem. Soc. (Communication), **126**, 3680 (2004).
12. **M. Dupuis** and M. Aida, "Vibrational Spectra from Quasiclassical Direct ab Initio Dynamics", Electronic Encyclopedia of Computational Chemistry, Wiley & Sons, (2004).

Photochemistry at Interfaces

Kenneth B. Eisenthal
Department of Chemistry
Columbia University
New York, NY 10027
eisenth@chem.columbia.edu

The scope of the program is the development of a molecular level description of the equilibrium and time dependent chemical and physical properties of interfaces using as the primary methods the interface selective second harmonic and sum frequency spectroscopies.

Recent Progress

Ultrafast Dynamics of Liquid Interfaces

The dynamics of chemical reactions, structural changes, and the motions of chemical species, in what is the intrinsically asymmetric interface, are dependent on solvation response times, e.g. charge transfer reactions. In addition these dynamical processes are dependent on the frictional forces which control molecular motions such as rotations. Because of the pervading influence of interface dynamical processes we are investigating excited state solvation and rotational dynamics at liquid interfaces.

(A) Effect of a Charged Interface on Solvation Dynamics

The investigations of solvation dynamics studies in our lab have extended from organic probe molecules at air/water, silica/water, to our current studies on neutral and charged surfactant interfaces. We find that the solvation of coumarin 314 (C314) is four times faster at the neutral stearic acid/water interface than at the charged stearate/water interface. This large difference, which we attribute to a change in the interfacial water structure, possibly reversing the interfacial water orientations, is a consequence of the electrostatic interactions between the water dipole and the negatively charged surfactant plane. It should be noted that the solvation dynamics of C314 at the negatively charged dodecylsulfate/water interface indicates that it is the charge and not the chemical identity of the surfactant head group that determines the solvation dynamics.

(B) Rotational Dynamics at Water Interfaces

Measurement of Out of Plane Rotational Motions

We have found that coumarin 314 at water interfaces can be treated as a uniaxial molecule with regard to the generation of second harmonic light. Thus its interfacial orientation can be described by the polar angle θ, which gives the orientation with respect to the interface normal, and the in plane angle φ. To separate out of plane and in plane rotational motions we excited C314 molecules with a circularly polarized pump that is incident normal to the interface plane. Because the circular pump has equal intensities for all in plane directions, it does not disturb the in plane orientational isotropy intrinsic

to an equilibrium interface. However the pump, being polarized in the interface plane, preferentially excites molecules whose transition moments have large values of θ, i.e. closer to an in plane orientation. The pump thereby perturbs the out of plane equilibrium ground state orientational distribution and creates a nonequilibrium excited state orientational distribution. The rotational relaxation of the ground and excited molecules to their equilibrium orientational distribution is monitored by a time delayed probe pulse incident at 70˚ to the interface normal. An important result was finding that the out of plane rotation time for C314 at the air/water interface was independent of the pump and probe wavelength. This supports the idea that the C314 can be approximated as a two state system. Furthermore the single exponential dynamics for the out of plane rotations indicate that the ground and excited state molecules have equal out of plane rotational relaxation times, within our experimental error. The fact that they are equal, despite the much larger dipole moment (12D vs 8D) of the excited molecule indicates that dielectric friction effects on out of plane rotations are not significant.

(C) Effect of a Negatively Charged Surfactant Interface on Rotational Motions

We find that the out of plane rotation is 386±9ps at a sodium dodecyl sulfate (SDS) monolayer coverage of 100$Å^2$/surfactant molecule. This is a very small increase relative to the rotational time constant of 352±9ps at the air/water interface. In bulk water the rotation time is 100ps. It is of direct interest that molecular dynamics simulations predict that the rotational relaxation should be faster at the air/H_2O interface because of the lower water density in the interfacial region. In their simulations however, a different probe molecule was used. I have informed them of our findings and they will repeat their simulations with the molecule that we used in our experiments. The small effect of surface charge is surprising because we know that C314 and dodecylsulfate are strongly interacting. Measurements of the equilibrium orientation of C314 changes considerably from a dipole orientation of 67±3˚ at the air/H_2O interface to the more upright 33±4˚ at an 80 $Å^2$ monolayer SDS/water interface. The surface tension phase diagram also shows a marked coumarin-SDS interaction. The small effect of surface charge on rotations is puzzling and has important implications for interfacial rotations at other negatively charged interfaces, among which are mineral oxide/water interfaces and the cell membrane/water interface, which is negatively charged due to anionic phospholipids in the cell membrane. Studies of other negatively charged and positively charged surfactant interfaces are necessary to get a more complete picture. We are talking also with colleagues about carrying out a molecular dynamics simulation, which though clearly not trivial, could be helpful.

(D) Molecular Ion Transport Across a Membrane in Real Time

A few years ago we demonstrated that SHG and SFG are dipole allowed for centrosymmetric structures, contrary to general thinking including my own. The key factor is the centrosymmetry length scale. If it is of the order, or some fraction (not too small) of the incident wavelength, then second harmonic and sum frequency light generated at the particule interface is allowed. Using centrosymmetric structures extending from 1μm polymer beads to ~100nm size emulsions, liposomes, semiconductor particles to 40nm gold particles, we showed that SHG was a surface sensitive method. These results open up the entire field of colloidal particles as well as other nano-

microparticles to the application of SHG and SFG to the study of their equilibrium and dynamic surface properties.

We have succeeded in using SHG to observe an organic cation, malachite green (MG), crossing a membrane bilayer in real time. Because of symmetry the orientation of MG on the outer surface of a liposome bilayer will be opposite to MG that have crossed the bilayer and are on the inner bilayer surface. The second order polarizations of the oppositely aligned molecules will cancel each other. Thus as MG crosses the bilayer the SHG signal should decay, and indeed does. However we find that the SHG signal does not decay to a value close to zero. This indicates that there are unequal populations of MG at the inner and outer surfaces. A possible explanation is based on the idea that the positively charged MG that has crossed the bilayer creates a positively charged inner surface that opposes further MG molecules from crossing the bilayer. To test this idea we sought to eliminate this electrostatic barrier by using the antibiotic valinomycin, which is a well known alkali ion transporter across membranes. With valinomycin present the transport of MG to the inner surface will favor the valinomycin transporting Na^+ ions to the outer region of the liposome solution for which the potential is negative, and thereby prevent the buildup of a positive inner potential. We see from Figure 1 that valinomycin at a concentration of $1x10^{-8}$M brings the SHG to a value close to zero in 36± 1s, which is to be compared with the partial decay of the SHG signal in 90±2s in the absence of valinomycin.

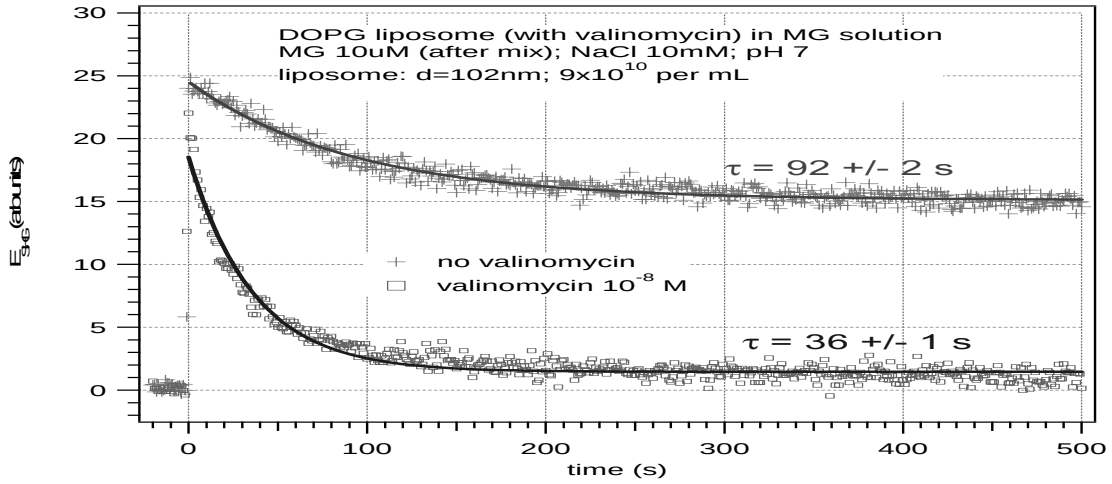

(E) Detection of SH Labeled Molecules

In many systems it can prove difficult to detect large molecules of interest at an interface, e.g. proteins and peptides, because their hyperpolarizabilities are small or the interface concentration is small, or other SHG active molecules are present. We have shown that by labeling the protein cyctochrome C, with a resonantly enhanced strongly SHG active label, such as oxazole, we can detect very small interface populations. Furthermore because we know the position and orientation of the label within the protein, we can obtain from the SHG polarization measurements the orientation of the protein at the interface of interest.

Future Plans

We are setting up a laser system to carry out interfacial vibrational sum frequency generation measurements. This new system, which should be up and running

in a few months, assuming that we will receive all the components needed in the near term, will have a major impact on our program in extending our interfacial spectroscopic capabilities. With SFG we can obtain the vibrational spectra of interfacial molecules and thereby probe their interactions, e.g. hydrogen bonding, with neighboring chemical species. By selecting the incident infrared to a frequency corresponding to that of a vibrational chromophore in a given molecule, e.g. C≡N, we can use SFG to measure the rotational motions with respect to the C≡N axis. By then selecting a different vibrational chromophore in the same molecule, perhaps C=O or C-D, we can determine the rotations about their axes. This will provide a powerful new way to investigate interfacial rotations and interfacial friction. The complementary SHG measurements of rotations will further improve the molecular level description of interfacial rotations, in that the SHG measures rotation about a symmetry axis defined by the nonlinear polarizability, which for the uniaxial molecules that we have been studying is along the molecule's electric dipole axis. Another research direction is the dynamics of interfacial chemical reactions at liquid interfaces. To begin with we will use SHG and SFG to study unimolecular reactions, such as isomerization and intramolecular proton transfer because of their relative simplicity. These unimolecular reactions can serve as "simple" models of the effects of solvent on chemical reactions. Among the solvent properties of interest are size, shape, rigidity, and hydrophobicity of the solvent molecules, interfacial roughness, (especially at liquid/liquid interfaces such as water/non polar hydrocarbon), and the orientational structure of the solvent molecules at the interface. We will seek to determine whether the measurements of rotational motions at various interfaces can provide a molecular level scale of friction, with possible use in interpreting the dynamics of isomerization reactions. The barrierless isomerization reactions of some triphenylmethane dyes should be particularly amenable to a connection between rotations and isomerizations because for the triphenylmethane dyes it is the solvent friction that determines the isomerization dynamics.

DOE Supported Publications

Liu, J., Shang, X., Pompano, R., Eisenthal, K.B., "Antiobiotic assisted molecular ion transport across a membrane in real time", Faraday Soc. Dis., 2004, accepted.

Benderskii, A.V., Henzie, J., Basu, S., Shang, X., Eisenthal, K.B., "Femtosecond aqueous solvation at a positively charged surfactant/water interface", J. Phys. Chem. B., 2004, 108, 14017-14024.

Benderskii, A.V., Eisenthal, K.B., "Dynamical timescales of aqueous solvation at negatively charged lipid/water interfaces", J. Phys. Chem. A., 2002, 106, 7483-7490.

Eisenthal, K.B., Salafsky, J., "Attachment of second harmonic-active moiety to molecules for detection of molecules at interfaces", USPTO patent #WO0246764, 2002.

Program Title: Time Resolved Laser Studies of the Proton Mechanism of Bacteriorhodopsin

Principal Investigator: **M. A. El-Sayed**
Georgia Institute of Technology
Laser Dynamics Lab
School of Chemistry and Biochemistry
Atlanta, Georgia, 30332-0400
e-mail: mostafa.el-sayed@chemistry.gatech.edu

Program Scope: The understanding of the molecular mechanisms involved in the proton pump process responsible for the conversion of solar to electric energy in the other photosynthetic system in nature: bacteriorhodopsin.

Recent Progress: The recent work was focused on **the involvement of water molecule networks in the proton transport process in the bacteriorhodopsin pump by following the changes in the infrared continua during its photocycles**. (Florian Garczarek, Jianping Wang, Mostafa A. El-Sayed and Klaus Gerwert; Biophysical Journal, in Press. This paper was selected by the editorial office to be the subject of New and Notable).

The question of whether or not protons are transferred via protonated hydrogen-bonded networks in proteins is of general interest at present. The membrane protein bacteriorhodopsin (bR), a light-driven proton pump, is the most suitable protein in which to study proton transfer processes (for recent reviews see [1] and [2]).

Protonated hydrogen-bonded networks are monitored by the so-called continuum absorbance over a broad spectral range covering several hundred wavenumbers in the infrared region. This is shown in experimental and theoretical studies of numerous model systems[3,4,5,6]. In order to monitor proton transfer via the protonated hydrogen-bonded networks in proteins, broad IR absorbance changes in the region> 1800 cm^{-1} are investigated during the photocycle of bR.

The bleach continuum in the 1900-1800-cm^{-1} region was reported during the photocycle of bacteriorhodopsin (bR) and was assigned to the dissociation of a polarizable proton chain during the proton release step[7]. More recently, a broad band pass filter was used and additional IR continua have been reported by Wang and El-Sayed[8]: a bleach at > 2700 cm^{-1}, a bleach in the 2500-2150-cm^{-1} region and an absorptive behavior in the 2100-1800-cm^{-1} region. In order to fully understand the importance of the hydrogen bonded chains in the mechanism of the proton transport in bR, a detailed study is carried out. Comparisons are made between the time-resolved FTIR experiments on wild type bR and its E204Q mutant (which has no early proton release), and between the changes in the continua observed in thermally or photothermally heated water (using visible light-absorbing dye) and those observed during the photocycle. The results strongly suggest that except for the weak bleach in the 1900-1800-cm^{-1} region and > 2500 cm^{-1}, all the other IR continua observed during the bR photocycle are inseparable from the changes in the absorption of the solvent water molecules that are photothermally excited via the nonradiative relaxation of the

photoexcited retinal chromophore. A possible structure of the hydrogen-bonded system, giving rise to the observed bleach in the 1900-1800-cm^{-1} region and the role of the polarizable proton in the proton transport is shown in figure (1) and discussed below.

The proposal that a polarizable proton chain is involved in the proton release, was supported at the structural level. The $H_5O_2^+$ complex is believed to be stabilized between Glu204 and Glu194 in the proton release pathway (See fig. 1). This is based on an integrated approach combining high resolution x-ray data, FTIR measurements, pK_a calculations and MD simulations[7,9,10]. There are two internal water densities within the proton release pathway that might contain protonated hydrogen-bonded water networks at the proton release site. One is close to the Schiff base, Asp85, Tyr185 and Asp212, and the other between Arg82, Glu204 and Glu194. Mutations of residues in the cavity close to the Schiff base do not affect the continuum absorbance between 1900 and 1800 cm^{-1}, but mutations in the lower pocket do. Therefore, the protonated network of internal water molecules giving rise to the observed absorbance changes between 1900 and 1800 cm^{-1} is located in the lower pocket as shown in Fig. (1).

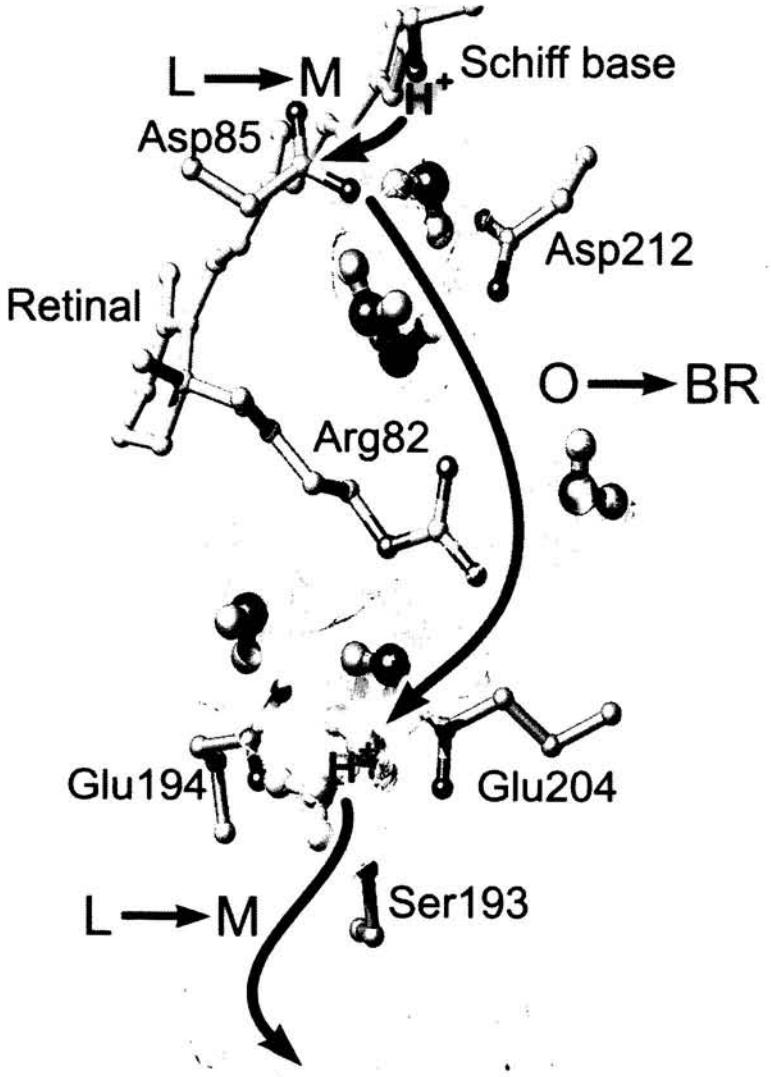

Fig 1

Figure 1 Proton release pathway of bR. There are two internal water cavities on the proton release pathway which could contain protonated hydrogen-bonded networks. One is close to the Schiff base, Asp85, Tyr185 and Asp212, and the other between Arg82, Glu204 and Glu194. The protonated network of internal water molecules, which gives the observed changes in the continuum absorbance between 1900-1800 cm^{-1}, is located in the lower cavity since only mutation in this region changes the observed continuum absorption.

References:

1. Haupts U., Tittor J., Oesterhelt D. 1999. Closing in on bacteriorhodopsin: Progress in understanding the molecule. *Annu. Rev. Biophys. Biomolec. Struct.* 28:367-399.
2. Lanyi J. K. 2000. Molecular mechanism of ion transport in bacteriorhodopsin: Insights from crystallographic, spectroscopic, kinetic, and mutational studies. *J. Phys. Chem. B* 104:11441-11448.
3. Kim J., Schmitt U. W., Gruetzmacher J. A., Voth G. A., Scherer N. E. 2002. The vibrational spectrum of the hydrated proton: Comparison of experiment, simulation, and normal mode analysis. *J. Chem. Phys.* 116:737-746.
4. Lobaugh J., Voth G. A. 1996. The quantum dynamics of an excess proton in water. *J. Chem. Phys.* 104:2056-2069.
5. Vuilleumier R., Borgis D. 1999. Transport and spectroscopy of the hydrated proton: A molecular dynamics study. *J. Chem. Phys.* 111:4251-4266.
6. Zundel G. 2000. Hydrogen Bonds with Large Proton Polarizability and Proton Transfer Processes in Electrochemistry and Biology. *Advances in Chemical Physics* 111:1-218.
7. Rammelsberg R., Huhn G., Lubben M., Gerwert K. 1998. Bacteriorhodopsins intramolecular proton-release pathway consists of a hydrogen-bonded network. *Biochemistry* 37:5001-5009.
8. Wang J., El-Sayed M. A. 2001. Time-resolved Fourier transform infrared spectroscopy of the polarizable proton continua and the proton pump mechanism of bacteriorhodopsin. *Biophys. J.* 80:961-71.
9. Luecke H., Schobert B., Richter H. T., Cartailler J. P., Lanyi J. K. 1999. Structure of bacteriorhodopsin at 1.55 angstrom resolution. *J. Mol. Biol.* 291:899-911.

Future Plans: Studies of the spectroscopy and photocycle of the newly synthesized crystals of bacteriorhodopsin in which the lipids have been replaced by suitable detergents and the relative orientation and separation of the protein molecules are different from those present in the native. This will enable us to answer questions regarding the photocycle and the proton pump in the native bacteria itself.

DOE Supported Publications (2002-2004):

1. Jianping Wang, Colin D. Heyes, and Mostafa A. El-Sayed, "Refolding of Thermally Denatured Bacteriorhodopsin in Purple Membrane", J. Phys. Chem. B, **106** (3), 723-729 (2002).

2. Colin D. Heyes, Mostafa A. El-Sayed, "The role of the native lipids and lattice structure in bacteriorhodopsin protein conformation and stability as studied by temperature-dependent Fourier transform-infrared spectroscopy", Journal of Biological Chemistry, **277** (33), 29437-29443 (2002).

3. Jianping Wang, Stephan Link, Colin D. Heyes, Mostafa A. El-Sayed, "Comparison of the dynamics of the primary events of bacteriorhodopsin in its trimeric and monomeric states", Biophysical Journal, **83** (3), 1557-1566 (2002).

4. Jianping Wang, Mostafa A. El-Sayed, "Time-resolved long-lived infrared emission from bacteriorhodopsin during its photocycle", Biophysical Journal, **83** (3) 1589-1594 (2002).

5. Colin D. Heyes, Jianping Wang, Laurie S. Sanii, Mostafa A. El-Sayed, "Fourier transform infrared study of the effect of different cations on bacteriorhodopsin protein thermal stability", Biophysical Journal, **82** (3), 1598-1606 (2002).

6. Colin D. Heyes, Mostafa A. El-Sayed, "Thermal Properties of Bacteriorhodopsin", Journal of Physical Chemistry B, Vol. **107**, Number 44, 12045-12053, (2003). (Feature Article)

7. Colin D. Heyes and Mostafa A. El-Sayed, "Proton Transfer Reactions in Native and Deionized Bacteriorhodopsin Upon Delipidation and Monomerization," Biophysical Journal, **85**, 426-434, (2003).

8. Colin D. Heyes, Keith B. Reynolds, Mostafa A. El-Sayed, "Eu^{3+} Binding to Europium-Regenerated Bacteriorhodopsin upon Delipidation and Monomerization", FEBS Letters, **562** (2004) 207-210.

Molecular Theory & Modeling

Accurate Descriptions of Chemical Reactions in Aqueous Systems

Bruce C. Garrett
Chemical Sciences Division
Pacific Northwest National Laboratory
902 Battelle Blvd.
Mail Stop K1-83
Richland, WA 99352
bruce.garrett@pnl.gov

The long-term objective of this project is to understand the factors that control the chemical reactivity of atomic and molecular species in aqueous environments. Chemical reactions in condensed phase environments play crucial roles in a wide variety of problems important to the Department of Energy (DOE), for example:

- Corrosion in nuclear reactors promoted by reactive radical species, such as OH.
- Release of hydrogen from chemically-bound hydrogen for use as a fuel.
- Chemical production using catalysis to provide efficient energy use.
- Contaminant degradation in the environment by natural and remedial processes.
- Degradation of materials used for nuclear waste entombment.
- Destruction of hazardous waste by supercritical oxidation.

The need in all of these areas is to control chemical reactions to produce desired products without generating harmful or wasteful byproducts. The control of transport and reactivity in these complex systems demands knowledge of the factors that drive the chemical reactions and requires understanding how the driving factors of the systems can be manipulated to affect the reaction rates. The goals of this research are the development of theoretical methods for describing reactions in condensed phases (primary aqueous liquids) and the application of these methods to prototypical problems of interest to DOE.

The calculation of accurate rate constants for reactions in condensed phases remains a major challenge. Electronic structure calculations of molecular interaction energies for extended systems are necessarily approximate. Accurate dynamical calculations require a quantum mechanical treat and for extended systems they are also necessarily approximate - variety of approximations but few benchmark studies. A wide variety of approximate methods for both energetics and dynamics exist with little or no accurate benchmarks to validate their performance for extended systems. Our approach builds upon the success of variational transition state theory (VTST) for predicting rate constants of gas-phase reactions. VTST provides a systematically improvable framework for computing rate constants of liquid-phase reactions, including both nonequilibrium solvation and quantum mechanical effects. The reaction energetics are treated by a hierarchical approach (from accurate first principles calculations on model systems to approximate treatment of solvation energies by QM/MM and continuum solvation models), in which in which higher accuracy calculations on model systems provide benchmarks for more approximate methods that can be applied to more realistic models of the reactive system. In the VTST approach to condensed-phase reactions the solvent influence on reaction energetics is computed from equilibrium averages over solvent configurations to give a potential of mean force (PMF). A cluster model of the reactive system is treated explicitly, so the PMF is

multidimensional. The coupling of solvent dynamics to the reactive system is included by a generalized Langevin model of solvent friction.

We have carried out benchmark calculations for microsolvated versions of the nucleophilic substitution (S_N2) and proton transfer (PT) reactions of OH^- with $CH_{4-n}Cl_n$:

$$OH^-(H_2O)_m + CH_{4-n}Cl_n \rightarrow CH_{4-n}Cl_{n-1}OH(H_2O)_{m-m'} + Cl^-(H_2O)_{m'} \quad (S_N2)$$

$$OH^-(H_2O)_m + CH_{4-n}Cl_n \rightarrow (H_2O)_{m-m'+1} + CH_{3-n}Cl_n^-(H_2O)_{m'} \quad (PT)$$

Critical geometries were optimized at the MP2/aug-cc-pVDZ level of theory and single point calculations were performed at these geometries using MP2, MP3, CCSD, and CCSD(T) with complete basis set (CBS) estimates obtained using the augmented correlation consistent basis sets through quadruple zeta and extrapolated to the complete basis set (CBS) limit. The results of these studies are shown in Figure 1. Both reactions (S_N2 and PT) proceed through a reactant complex in which OH^- forms a complex with the chlorinated methane molecule. The barrier for the S_N2 reaction, relative to the energy of the reactant complex, increases with increasing solvation. Note also that the reaction energy (the energy of the product) increases (or becomes less negative) as the solvation increases. Barriers for the PT reaction are small and can change significantly with changes in the chlorination and hydration. Minimum energy paths (MEPs) were calculated for the S_N2 reactions at the MP2/aug-cc-pVDZ level of theory and the accurate cluster energies were used in a layered QM/MM approach to estimate the barrier for the reaction in bulk water (see Figure 2). To account for the effects of bulk solvation, we use a computationally tractable and efficient procedure for the calculation of potentials of mean force using mixed Hamiltonian models of electronic structure where quantum subsystems are described with computationally intensive ab initio wavefunctions. The mixed Hamiltonian is mapped into an all-classical Hamiltonian that is amenable to a thermodynamic perturbation treatment for the calculation of free energies. A small number of statistically uncorrelated (solute-solvent) configurations are selected from the Monte Carlo random walk generated with the all-classical Hamiltonian approximation. Those are used in the averaging of the free energy using the mixed quantum/classical Hamiltonian. The effects of solvation on this reaction are shown to increase the barrier height by over 18 kcal/mol.

Our VTST approach to reactions in solution is accurate when classical dynamics are valid and solvent dynamics can be treated by linear response. Benchmark calculations are needed to test this approach, based upon the on the potential of mean force, when quantum mechanical effects are important. We have conducted a careful analysis of a model proton transfer reaction in polar solvent. The system models the reaction of a weak acid (AH) with a base (B), in which A and B are treated as atoms, and the polar solvent is a model of methylchloride, in which the

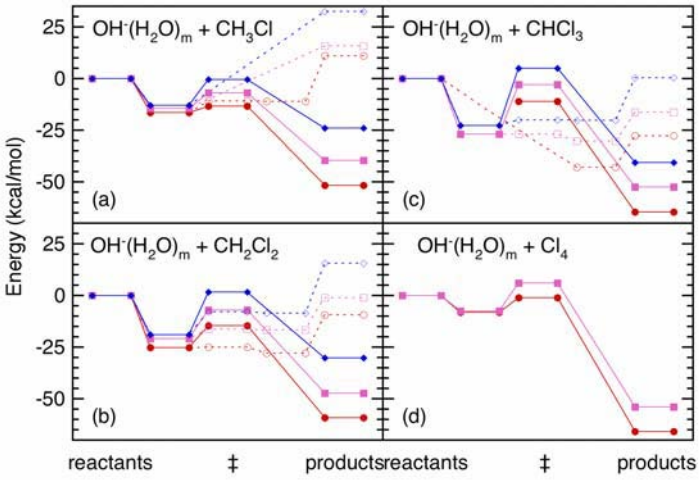

Figure 1. Energetics of the microsolvated S_N2 (solid lines) and PT (dashed lines) reactions $OH^-(H_2O)_m + CH_{4-n}Cl_n$ for n = 1 – 4 (a-d, respectively) and with m = 0 (circles), 1 (squares), and 2 (diamonds). The zero of energy in all cases is defined for $OH^-(H_2O)_m$ infinitely separated from $CH_{4-n}Cl_n$

methyl group is treated as a united atom. The PMF for this reaction is shown in Figure 3. Rate constants have been calculated for this system by other researchers using a variety of different methods (e.g., surface hopping, curve-crossing, and centroid TST) resulting in computed rate constants that range over 2 orders of magnitude. By examining a systematic sequence of 18 different sets of approximations, we clarify some of the factors (such as classical vibrations, harmonic approximations, quantum character of reaction-coordinate motion, and nonequilibrium solvation) that contribute to the different predictions of various approximation schemes in the literature. The large variability in computed rate constants indicates a need for accurate benchmark calculations of the dynamical methods. In more recent work we have uncovered a weak temperature dependence and nearly constant H/D kinetic isotope effect for this model system, indicating that contributions to the rate constants are dominated by tunneling energies near threshold. Therefore, this system provides an extreme test of methods for including quantum mechanical effects in condensed phase reactions.

Since accurate quantum dynamical benchmarks are not possible for condensed phase systems, careful calculations using a variety of approximate methods are needed to understand the regions of validity and limitations of each of these methods. Our future work will provide a systematic study of different approaches to treating the model proton transfer problem described above. Different theoretical methods will be used including VTST and centroid-path-integral based methods. In addition, the treatment of the condensed phase system will compare treating the solvent as frozen (sudden approximation for the solvent) with the PMF approach (adiabatic approximation for the solvent). In addition, we will use embedded cluster techniques to examine the effects of the solvent dynamics on tunneling.

Studies of the reactions of OH^- with chlorinated hydrocarbons will continue with the goal of understanding the of degradation mechanism of these compounds. We have recently initiated studies of the interaction of OH radical with aqueous systems, with the long-term goal of understanding how the open-shell nature of this species affects its reactivity in aqueous solution.

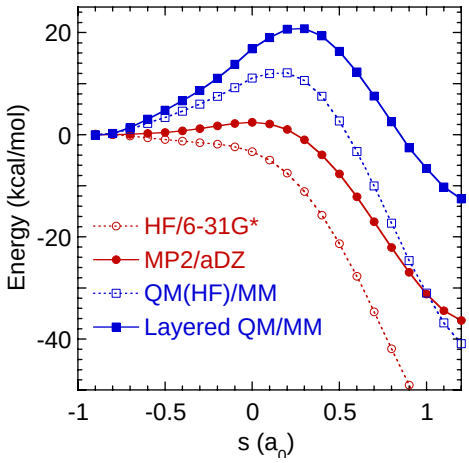

Figure 2. Energetics along the MEP for the reaction OH^- + CH_3Cl, computed at the MP2/aug-cc-pVDZ (MP2/aDZ) level of theory. Energies for geometries along the MEP are computed at the HF/6-31G* level, which is used in the QM/MM calculation and these results are used with the MP2/aDZ results to give the layered QM/MM results.

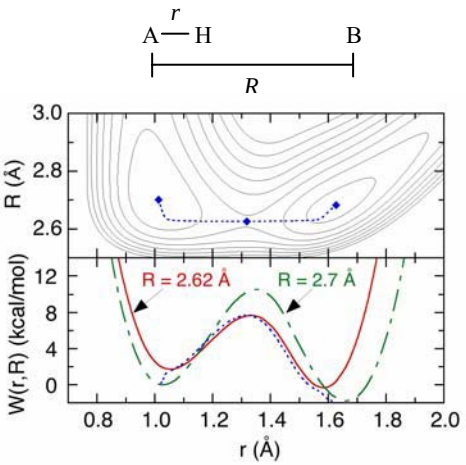

Figure 3. (a) Equipotential contours of the potential of mean force *W(r,R)*. Contours (solid curves) are plotted for energies of 0, 4, 8, 12, 16, 20, 24, and 28 kcal/mol. The zero of energy is taken as the minimum of the reactant well at r = 1.01 A, R = 2.70 A. The solid diamonds indicate the locations of the reactant and product minimum and the saddle point. The dashed curve depicts the minimum energy path. (b) Potential *W(r,R)* as a function of r for R fixed at 2.6265 A (solid curve), for R fixed at 2.7 A (chain curve), and along the minimum energy path (dotted curve).

Collaborators on this project include G. K. Schenter, R. P. McRae, D. G. Truhlar, E. E. Arcia, D. T. Chang, Y. A. Borisov, S. L. Mielke, T. H. Dunning, M. Dupuis, S. S. Xantheas, J. Li, S. Du, J. Francisco

References to publications of DOE sponsored research (2002-present)

1. S. M. Kathmann, G. K. Schenter, and B. C. Garrett, "Understanding the Sensitivity of Nucleation Kinetics: A Case Study on Water," *Journal of Chemical Physics* **116**, 5046-5057 (2002).
2. S. L. Mielke, B. C. Garrett, and K. A. Peterson, "A Hierarchical Family of Global Analytic Born–Oppenheimer Potential Energy Surfaces for the H + H_2 Reaction Ranging in Quality from Double-Zeta to the Complete Basis Set Limit," *Journal of Chemical Physics* **116**, 4142-4161 (2002).
3. G. K. Schenter, S. M. Kathmann, and B. C. Garrett, "Equilibrium Constant for Water Dimerization: Analysis of the Partition Function for a Weakly Bound System," *Journal of Physical Chemistry A* **106**, 1557-1566 (2002).
4. G. K. Schenter, S. M. Kathmann, and B. C. Garrett, "Dynamical Benchmarks of the Nucleation Kinetics of Water," *Journal of Chemical Physics* **116**, 4275-4280 (2002).
5. R. J. Duchovic, Y. L. Volobuev, G. C. Lynch, D. G. Truhlar, T. C. Allison, A. F. Wagner, B. C. Garrett, J. C. Corchado, "POTLIB 2001: A Potential Energy Surface Library for Chemical Systems," *Computer Physics Communications* **144**, 169–187 (2002).
6. B. C. Garrett, S. M. Kathmann, and G. K. Schenter, "Thermochemistry and Kinetics of Evaporation and Condensation for Small Water Clusters," in Water in Confining Geometries, edited by V. Buch and J. P. Devlin (Springer, Berlin, 2003), p. 25-51.
7. D. G. Truhlar and B. C. Garrett, "Reduced Mass in the One-Dimensional Treatment of Tunneling," *Journal of Physical Chemistry A* **107,** 4006-4007 (2003).
8. G. K. Schenter, B. C. Garrett, and D. G. Truhlar, "Generalized Transition State Theory in Terms of the Potential of Mean Force," *Journal of Chemical Physics* **119,** 5828-5833 (2003).
9. S. L. Mielke, K. A. Peterson, D. W. Schwenke, B. C. Garrett, D. G. Truhlar, J. V. Michael, M.-C. Su, and J. W. Sutherland, "H + H_2 Thermal Reaction: A Convergence of Theory and Experiment," *Physical Review Letters* **91,** 063201 (2003).
10. M. Dupuis, G. K. Schenter, B. G. Garrett, and E. E. Arcia, "Potentials of Mean Force with Ab Initio Mixed Hamiltonian Models of Solvation," *Journal of Molecular Structure-Theochem* **632,** 173-183 (2003).
11. Y. A. Borisov, B. C. Garrett, Y. A. Kolbanovskii, I. V. Bilera, and N. N. Buravtsev, "On the Relationship between the Enthalpy of Formation of Carbenes Upon Cleavage of the Double Bond in Fluoroolefins and the Electron Density on the Pi Bond: An Ab Initio Study," *Doklady Physical Chemistry* **392,** 212-216 (2003).
12. L. X. Dang and B. C. Garrett, "Molecular Mechanism of Water and Ammonia Uptake by the Liquid/Vapor Interface of Water," *Chemical Physics Letters* **385,** 309-313 (2004).
13. B. C. Garrett, "Ions at the Air/Water Interface," *Science* **303,** 1146-1147 (2004).
14. S. M. Kathmann, G. K. Schenter, and B. C. Garrett, "Multicomponent Dynamical Nucleation Theory and Sensitivity Analysis," *Journal of Chemical Physics* **120,** 9133-9141 (2004).
15. S. M. Kathmann, G. K. Schenter, and B. C. Garrett, "Dynamical Nucleation Theory: Understanding the Role of Aqueous Contaminants," in Proceedings of the 16th International Conference on Nucleation and Atmospheric Aerosols, edited by M. Kulmala and M. Kasahara (Kyoto University Press, 2004), p. 243-246.

Abstract

Program Title: **Chemical Reaction Dynamics in Nanoscale Environments**
DOE Grant No. DE-FG02-01ER15212

Principle Investigator:

Evelyn M. Goldfield,
Department of Chemistry
Wayne State University
Detroit, MI 48202
evi@sun.science.wayne.edu

Program Scope:

The major focus of the research in this program is the study of the behavior of molecular systems confined in nanoscale environments. The goal is to develop a theoretical framework for predicting how chemical reactions occur in nanoscale environments. To achieve this goal we have employed ab initio quantum chemistry, classical dynamics and quantum dynamics methods. Most of our work has focused on systems confined within single walled carbon nanotubes (SWCNT). This abstract will focus on the work of our group done in collaboration with Stephen K. Gray of Argonne National Laboraory and that of H. Bernhard Schlegel, a co-PI on this project and his research group.

Recent Progress:

Our research has focused on the behavior of hydrogen atoms and molecules confined within SWCNT's of various shapes and sizes. We completed a study of the discrete energy levels of H_2 and its isotopes confined within single-walled carbon nanotubes (SWCNTs) of various shapes and sizes. These four-degree-of-freedom quantum calculations explicitly treat both translation of the H_2 center-of-mass orthogonal to the nanotube axes and rotation about the center of mass. These are the first calculations on this type of system to treat hindered rotation and translation together. For H_2, D_2 and T_2, we computed all of the bound energy levels for five SWCNTs: (3,6), (8,0), (2,8), (6,6) and (10,10). Employing an empirical potential that was included in the Brenner MD package, we solved for the energy levels and the wavefunctions iteratively, using the ARPACK (Arnoldi package) software library, a collection of subroutines designed to solve large-scale eigenvalue problems. We used these energy levels and wavefunctions to explore several issues, including the potential use of nanotubes as quantum sieves for isotope separation, the effects of confinement on the ortho/para energy separation and equilibrium constants as a function of temperature for a single H_2, binding to a SWCNT. This research has been published in Ref. [1] and [2]

Quantum sieving is a purely quantum effect that relies on the differences in zero point energy in binding of molecules to the nanotube to achieve separations. Our calculations predicted far more modest selectivities than those predicted by other previous calculations of Karl Johnson and coworkers (see S.R. Challa, D. S. Sholl, and J. K.

Johnson, Physical Review B, **63** 245419), who employed a 1-D model in their calculations. The differences in our results, however, are due more to a difference in the interaction potentials than in the model. The interactions of H_2 and the nanotube are long range forces and quite difficult to compute using ab initio methods. Several different potentials have been suggested in the literature and we have recomputed our results using three of these, including one set that we believe is closest to the one used by Johnson and coworkers. (It is not possible to compare directly due to the differences in the models.) Our recent results are very interesting, showing a large and systematic variation of several quantities with the potential parameters and the form of the potential including quantum sieving selectivities, number of bound energy levels and energy spacings, and ortho-para energy separations. The results of this research are currently being analyzed and will be written up soon.

Most of our current energy has focused on the calculation of the interaction of $H + H_2$ within SWCNT's. Because the transition state of this reaction is collinear, it is possible that the restriction of impact parameters that may occur will enhance the probability of reaction. However, this may depend quite strongly on the diameter of the nanotube. It is also the case that hydrogen atoms that are close to the walls of the nanotube will react strongly with carbons. Therefore, we ran wavepacket calculations to see whether H atoms at one end of a nanotube with momentum directed along the central tube axis were capable of traveling through to the other end of the tube. Portions of the wavepacket that were attracted to the walls were absorbed. We computed the distance traveled as a function of tube diameter and initial wavepacket momentum. Not surprisingly, the larger the tube, the more wavepacket density reached the other end. But, except for the smallest tubes studied, a large portion of the hydrogen did emerge on the other end of the tube.

There are a number of theoretical, computational and technical challenges involved in this project. Even with if we do not consider motion of the carbons in the nanotube, we are left with nine degrees of freedom which is very large for a quantum dynamics calculation. Thus, we are developing reduced dimensionality models that include the relevant degrees of freedom. The smallest such model, we believe contains five degrees of freedom. The code to describe that model is currently being written and debugged. Because we want to exploit the cylindrical symmetry of the tube, we are developing and testing a version of our Dispersion Fitted Finite Difference (DFFD) method for computing the action of the kinetic energy operator that is consistent with these coordinates. This has turned out to be a bit trickier than one might anticipate.

Another challenge is finding an appropriate description of the hydrogen-nanotube interactions that describes properly the change in character of the H – nanotube interactions as the system goes from $H + H_2$ to the transition state and then on to products (or back to reactants). We are currently considering the "AIREBO" potential from the Steve Stuart group at Clemson. (J. Stuart, A. B. Tutein and J. A. Harrison, J. Chem. Phys. **112** 6472 (2000).

An important parameter in this research will be the size of the tube. In large tubes, the H_2

will bind near the wall of the tube, preferring to be parallel to the central nanotube axis. In smaller tubes, the H_2 will be aligned in the center of the nanotube along the central axis. While this may seem to be the optimal situation to achieve enhanced reactivity, in these smaller tubes, such as the (3,6) with a radius of ~3 Å, more of the H atoms will react with the walls. Small nanotubes are more difficult to synthesize although much progress is being made in this direction. We anticipate that if our model does show enhanced reactivity, it will be for somewhat larger nanotubes.

A new related research project that is just getting started is using quantum chemistry to compute interaction potentials for small molecules such as NO_2, CO_2, and O_2 binding to the outer and to the inner walls of semi-conducting SWCNT' s. The current project studies binding of NO_2 to a (10,0) SWCNT which is 20 Å in length. At this state, we are exploring the most optimal level of theory to use which balances accuracy and computational cost. This work is in conjunction with a member of our computer and electrical engineering department who is developing a nanotube based chemical sensor.

Recent projects in the Schlegel group include a study of the effects of constrained environments on the molecular dissociation dynamics. They have initiated a study of the dissociation of formaldehyde, $H_2CO \rightarrow H_2 + CO$, with a (7,7) SWCNT. Molecular dynamics calculations were carried out with ONIOM type quantum mechanics molecular mechanics (QM/MM) methods. The nanotube was treated with the UFF molecular mechanics force field and the H_2CO was treated quantum mechanically. Compared to the dissociation in the gas phase, a smaller fraction of the available energy goes into product translation and more into H_2 vibration. A possible explanation for this could be that when H_2 hits the wall of the tube, some of its translational energy gets converted to vibrational energy.

A current focus of the Schlegel group is the study of ionization of molecules within SWNT's. When molecules are confined inside single walled carbon nanotubes, they experience a unique physical and electronic environment. This environment has a pronounced effect on the ionization potential of molecules within them. The ionization of neutrals to cations becomes easier than in the gas phase, whereas the ionization of anions to neutrals becomes more difficult. To gain insight into this process, ionization potentials were calculated for a set of anions and neutral molecules inside carbon nanotubes of different lengths and diameters. They have optimized series a (7,7) armchair nanotubes ranging in length from 13-30 Å as well as (8,8) and (9,0) nanotubes of ca 15 Å length, in both the neutral and mono-cation states at the B3PW91/3-21G level of theory. Hückel theory can be used to explain the periodic changes in the orbital energies, ionization potentials and electron affinities as the tube is lengthened. A series of molecules were placed in the nanotubes and calculated at the B3PW91/6-311++G(d,p) level to see the overall environmental effects on the ionization of them. Five categories with distinct characteristics can be identified: (i) the molecule always ionizes but the nanotube does not, (ii) the nanotube always ionizes but the molecule does not, (iii) the molecule ionizes spontaneously as soon as it is placed inside the nanotube, (iv) the nanotube ionizes spontaneously as soon as the molecule is placed inside, and (v) either

the molecule or the nanotube ionizes, depending on the length of the tube. HF and Na are simple examples for cases (ii) and (iii), respectively. Halogens can serve as examples for case (iv). The CN radical is an example of case (v). Because the IP oscillates by more than 0.5 eV as the length is incremented, the electron is removed from CN for some lengths and from the nanotube for other lengths. The results of this research are currently being written up.

References:

1. T. Lu, E. M. Goldfield and S. K. Gray, " The equilibrium constants for molecular hydrogen in carbon nanotubes based on iteratively determined nano-confined bound states", Journal of Theoretical and Computational Chemistry, special issue on Iterative Methods in Quantum Mechanics and Applications to Chemical Problems" **2**, 621 (2003).

2. T. Lu, E. M. Goldfield and S. K. Gray, "Quantum states of molecular hydrogen and its isotopes in single-walled carbon nanotubes ",J Phys Chem B **107,**12989),2003

3. M. D. Halls and H. B. Schlegel, "Chemistry Inside carbon nanotubes: Enhancement of the Menshutkin S_N2 reaction. J. Phys. Chem. B, **106**, 1921(2002).

X-ray Absorption Study of TiO_2 Nanocrystalline Films Under Electrochemical Control

David Gosztola, Zoran Saponjic, Lin Chen, Tijana Rajh
Argonne National Laboratory, Chemistry Division
9700 S. Cass Avenue
Argonne, IL 60439
gosztola@anl.gov

Program:

Reactive Intermediates in Condensed Phase: Radiation and Photochemistry

Scope:

The Radiation and Photochemistry program at Argonne National Laboratory primarily studies the initial events and ensuing chemistries that follow energetic excitation. The fundamental mechanisms of internal energy conversion following excitation are studied by probing the dynamics and structural changes that unravel electronic structure and mechanisms of relaxation of transient species in the condensed phase.

Recent progress:

The mechanism of semiconductor assisted radio- and photo-catalysis is based on the principle that particulate semiconductors behave as miniature electrochemical cells driven by radiolytic or photoinduced charge separation. The efficiency of such systems is often determined by energy loss pathways such as charge recombination and charge trapping. The complex interplay between structure and electronic properties in nanoparticulate metal oxide semiconductors has been shown to affect both the lifetime and electrochemical potential of radiolytically and photochemically produced charge carriers.

Excitation of nanocrystalline TiO_2 with photon energies larger than its band gap results in the formation of conduction band electrons and valence band holes. Localization of conduction band electrons into lower energy electronic sites occurs in less than 30 ps. Due to the large number of electron surface trapping states in nanocrystalline particles, electrons localize preferentially at the TiO_2 surface. Surface-trapped electrons exhibit broad absorption in the visible region of the spectrum with a maximum around 620 nm in acidic solution. The position of the absorption maximum varies some 50 nm depending on the size of the nanoparticles and the number of excess electrons. On the other hand, the absorption of electrons in larger particles increases steadily from 400 nm towards longer wavelengths, having a plateau near 900 nm. This absorption feature has been attributed to delocalized electrons. Although much less studied, excitation of nanocrystalline TiO_2 with ionizing radiation (e.g. 3-20 MeV electron beam) also produces conduction band electrons and valence band holes often with multiple electron/hole pairs formed for each initial ionizing event. One benefit of radiolytically producing charge separation is that very wide bandgap semiconductors can be studied in which suitable laser sources may not be available for direct optical excitation.

We have coupled spectroelectrochemical approaches with X-ray absorption spectroscopy in order to begin to reveal the electronic nature of injected charge carriers and the structural changes due to their localization. In particular, localization of charge carriers may be manifested by changes in both local oxidation state and local structure and symmetry as well as in new optical absorption transitions. Concurrently we have been developing the means and methods to investigate and understand the response of the structure of wide bandgap nanocrystalline metal oxide semiconductor films to the controlled injection and localization of charge carriers using electrochemical methods.

Using an electrochemical cell specifically designed to be used simultaneously for optical (UV-vis-NIR) as well as x-ray studies, we have shown that slow (10's-100's seconds) electrochemical trap filling is a quasi-reversible process and is accompanied with changes in the X-ray absorption spectrum of the film. The X-ray absorption changes were found to be consistent with a lowering of the oxidation state of the metal-oxide film along with a change in symmetry of its crystal structure.

Figure 1 (below) shows the spectroelectrochemical response of a 650 nm thick nanocrystalline TiO_2 film at various potentials. The nanocrystalline film was deposited on an optically transparent conductive (ITO) glass substrate immersed in acetonitrile with 0.2 M $LiClO_4$ supporting electrolyte. As the potential of the TiO_2 film was made more negative, an increase in absorption throughout the visible-NIR region was observed. This increase has been attributed to the accumulation of electrons in the film. At potentials negative of -1.3 V, a weak broad band centered at 1030 nm began to appear which has been attributed to conduction band electrons. At potentials negative of -1.8 V, a much stronger pair of absorption bands appeared at 740 nm and 385 nm. These intense bands have been attributed to shallow (740 nm) and deep (385 nm) surface trap sites.

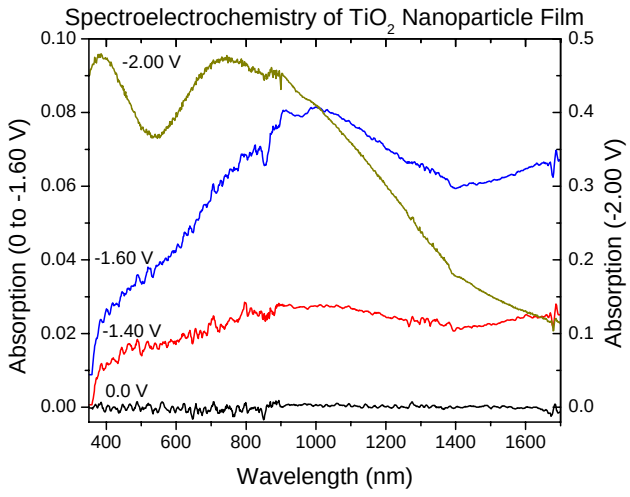

Figure 1: Absorption spectra of TiO_2 nanocrystalline film in acetonitrile at various potentials. Substrate: ITO coated glass. Potentials are versus $Ag/AgNO_2$.

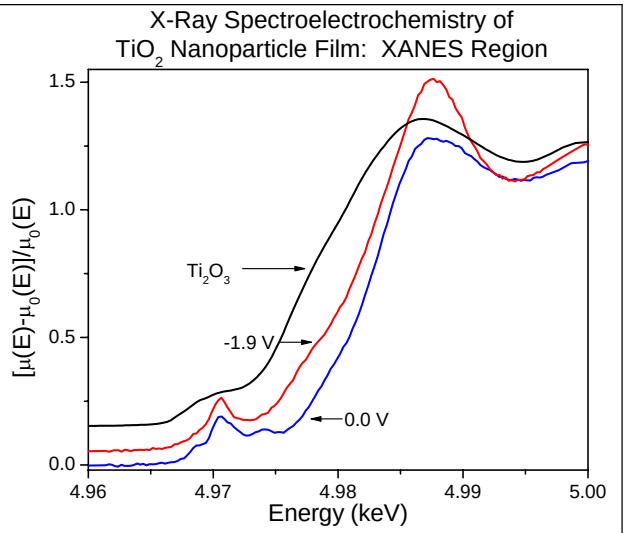

Figure 2: X-Ray absorption spectra of TiO_2 nanocrystalline film in acetonitrile at various potentials and powered Ti_2O_3. Electrochemical substrate: ITO coated Mylar.

Figure 2 (above) shows the X-ray absorption spectra in the near edge region (XANES) of a nanocrystalline TiO_2 film at 0 V and -1.9V deposited on a transparent ITO-Mylar substrate in acetonitrile/$LiClO_4$ as well as the XANES of a bulk sample of Ti_2O_3. Upon reduction, the X-ray absorption edge shifted to lower energies consistent with the reduction in oxidation state of Ti^{4+} and a decrease in the fine structure was observed consistent with the decrease in symmetry upon formation of Ti^{3+} ions (Ti_2O_3 has a D3d symmetry , significantly different from the D2d symmetry of anatase TiO_2).

Future plans:

Since the electronic structure and energy levels of charge carriers ultimately determine their capability to perform redox reactions, it is imperative that we develop the necessary tools to better reveal the issues associated with structure and energetics in nanoparticles. While we continue to investigate the structural and electronic changes that accompany charge localization, we will begin

dynamic studies of the time-evolution of the trapping process itself. We will also begin time-resolved measurements using films in which electron trap sites are electrochemically pre-filled in order to better understand the detrapping process and charge mobility in the absence of available trap sites and thus gain unique insights into the relationship between excited state dynamics and structure. Ultrafast time-resolved radiolytic measurements will also be carried out using our new picosecond laser plasma based electron accelerator.

Acknowledgment: This work was supported by the U.S. DOE, Office of BES, Division of Chemical Sciences, under contract W-31-109-Eng-38.

Publications 2002 – 2004:

Toward Electronically Coupled Bio-Inorganic Conjugates.
D. Gosztola, Z. Saponjic, L. Chen, L. De La Garza, N. Dimitrijevic, and T. Rajh,
Proceedings of the Electrochemical Society 205th Meeting, (2004).

Efficient, Rapid One-Electron Photooxidation of Chemisorbed Polyhydroxyl Alcohols and Carbohydrates by TiO_2 Nanoparticles in an Aqueous Solution.
I. A. Shkrob, M. C. Sauer, Jr., and D. Gosztola, *Chem. Phys.*, In Press, (2004).

Recombination of Geminate (OH,E_{aq}^-) Pairs in Concentrated Alkaline Solutions: Lack of Evidence for Hydroxyl Radical Deprotonation.
R. Lian, R. A. Crowell, I. A. Shkrob, D. M. Bartels, D. A. Oulianov, and D. Gosztola,
Chem. Phys. Lett., 389(4-6), 379-384, (2004).

Ultrafast Processes in Radiation Chemistry.
R. A. Crowell, D. J. Gosztola, I. A. Shkrob, D. A. Oulianov, C. D. Jonah, and T. Rajh,
Radiation Physics and Chemistry, 70(4-5), 501-509, (2004).

Photoinitiated Charge Separation: From Photosynthesis to Nanoparticles.
M. C. Thurnauer, N. M. Dimitrijevic, O. G. Poluektov, and T. Rajh, *The Spectrum*, 17(1), 18-24 (2004).

Charge Transfer Across the Nanocrystalline-DNA Interface: Probing DNA Recognition
T. Rajh, Z. Saponjic, J. Liu, N. M. Dimitrijevic, N. F. Scherer, M. Vega-Arroyo, P. Zapol, L. A. Curtiss, and M. C. Thurnauer, *Nano Letters* 4(6), 1017-1023 (2004).

Assembly of Topo-Capped Silver Nanoparticles into Multilayered Film.
Z. V. Saponjic, T. Rajh and N. M. Dimitrijevic, "Material Syntheses", U. Schubert, R. M. Laine, and N. Huesing, Eds., John Wiley & Sons, submitted (2004).

Light-Induced Charge Separation and Redox Chemistry at the Surface of TiO_2/Host-Guest Hybrid Nanoparticles.
N. M. Dimitrijevic, T. Rajh, Z. Saponjic, L. de la Garza, and D. M. Tiede,
J. Phys. Chem. B. 108(26), 9105-9110 (2004).

Charge Separation in Titanium Oxide Nanocrystalline Semiconductors Revealed by Magnetic Resonance.
T. Rajh, O. G. Poluektov and M. C. Thurnauer, "Chemical Physics of Nanostructured Semiconductors", Chapter 1, A. I. Kokorin and D. W. Bahnemann, Eds., NOVA Science Publ., Inc., The Netherlands, pp. 1-34, (2003).

Surface Modification of TiO_2: A Route for Efficient Semiconductor Assisted Photocatalysis.
T. Rajh, O. V. Makarova, D. Cropek, and M. C. Thurnauer,
"Synthesis, Functionalization and Surface Treatment of Nanoparticles", Chapter 9, M.-I. Baraton, Ed., American Scientific Publishers, California, pp. 147-171, (2003).

Explaining the Enhanced Photocatalytic Activity of Degussa P25 Mixed Phase TiO_2 Using EPR.
D. C. Hurum, A. G. Agrios, K. A. Gray, T. Rajh, and M. C. Thurnauer,
J. Phys. Chem. B, 107, 4545-4549 (2003).

Biology of TiO_2 – Oligonucleotide Nanocomposites.
T. Paunesku, T. Rajh, G. Wiederrecht, J. Maser, S. Vogt, N. Stojicevic, M. Protic, B. Lai, J. Oryhon, M. Thurnauer, and G. Woloschak,
Nature Materials, 2, 343-346 (2003).

Revealing the Nature of Trapping Sites in Nanocrystalline Titanium Dioxide by Selective Surface Modification.
N. M. Dimitrijevic, Z. V. Saponjic, D. M. Bartels, M. C. Thurnauer, D. M. Tiede, and T. Rajh,
J. Phys. Chem. B, 107(30), 7368-7375 (2003).

Computational Studies of Catechol and Water Interactions with Titanium Oxide Nanoparticles.
P. C. Redfern, P. Zapol, L. A. Curtiss, T. Rajh, and M. Thurnauer, *J. Phys. Chem. B*, 107, 11419-11427 (2003).

Theoretical Study of The Ionization Potential of Thymine: Effect of Adding Conjugated Functional Groups.
M. Vega-Arroyo, P. R. LeBreton, T. Rajh, P. Zapol, and L. A. Curtiss, *Chem. Phys. Lett.*, 380, 54-62 (2003).

Self-Assembly of Topo-Derivatized Silver Nanoparticles into Multilayered Film.
Z. V. Saponjic, R. Csencsits, T. Rajh, and N. M. Dimitrijevic, *Chem. Mater.*, 15(23), 4521-4526 (2003).

Rapid Excited-State Structural Reorganization Captured by Pulsed X-Rays.
L. X. Chen, G. Jennings, T. Liu, D. J. Gosztola, J. P. Hessler, D. V. Scaltrito, G. J. Meyer,
J. Am. Chem. Soc., 124(36), 10861-10867, (2002).

Functional Asymmetry of Photosystem II D1 and D2 Peripheral Chlorophyll Mutants of *Chlamydomonas Reinhardtii.*
J. Wang, D. Gosztola, S. V. Ruffle, C. Hemann, M. Seibert, M. R. Wasielewski, R. Hille, T. L. Gustafson, and R. T. Sayre, *Proceedings of the National Academy of Sciences of the United States of America,* 99(2), 4091-4096, (2002).

Analytical Treatment of EPR Spectra of Weakly Coupled Spin Correlated Radical Pairs in Disordered Solids: Applications to the Charge Separated State in TiO_2 Nanoparticles.
A. A. Dubinski, G. D. Perekhotsev, O. G. Poluektov, T. Rajh, and M. C. Thurnauer,
J. Phys. Chem. B, 106 (5), 938-944 (2002).

Electron and Hole Adducts Formed in Illuminated InP Colloidal Quantum Dots Studied by Electron Paramagnetic Resonance.
O. I. Micic, A. J. Nozik, E. Lifshitz, T. Rajh, O. G. Poluektov, and M. C. Thurnauer,
J. Phys. Chem. B, 106 (17), 4390-4395 (2002).

Fe_2O_3 Nanoparticle Structures Investigated by X-Ray Absorption Near-Edge Structure, Surface Modifications, and Model Calculations.
L. X. Chen, T. Liu, M. C. Thurnauer, R. Csencsits, and T. Rajh, *J. Phys. Chem. B*, 106 (34), 8539-8546 (2002).

Surface Restructuring of Nanoparticles: An Efficient Route for Ligand - Metal Oxide Crosstalk.
T. Rajh. L. X. Chen, K. Lukas, T. Liu, M. C. Thurnauer, and D. M. Tiede,
J. Phys. Chem. B, 106(41), 10543-10552 (2002).

Photon and Electron Stimulated Chemistry of Adsorbates

Ian Harrison
Department of Chemistry, University of Virginia
Charlottesville, VA 22904-4319
harrison@virginia.edu

This research program aims to employ non-thermal electron transfer chemistry to investigate the nature of the transition states for activated dissociative chemisorption of small molecules on metal surfaces. Two important scientific hypotheses are under investigation. The first hypothesis is that catalytic dissociative adsorption reactions on metal surfaces are primarily surface mediated electron transfer reactions for many hard-to-activate small molecules. Accordingly, the lowest lying affinity levels of these adsorbates, which are accessible by surface photochemistry and scanning tunneling microscopy (STM), will play a key electronic structure role in determining barrier heights for dissociative chemisorption. The second hypothesis is that electron transfer excitation into these adsorbate affinity levels followed by image potential acceleration towards the surface and rapid quenching may leave the adsorbate in the "transition state region" of the ground state potential relevant to thermal catalysis from where desorption and/or dissociation will ultimately occur.[1] It follows that a design principle for selecting potentially active photocatalysts (that initiate "hot" ground state dynamics) is to choose surfaces that already exhibit relatively low barriers in thermal catalysis. The research will explore the effect of alkali metal promotion of transition metal surfaces, which in some instances leads to improved thermal dissociative chemisorption catalysts (e.g., N_2 dissociation on Cs/Ru), and will work to quantify electronic structure features relating to the reactive potentials for dissociative chemisorption. The possibility that work function reductions introduced by coadsorption of alkali metals can lower the adsorbate affinity levels sufficiently that dissociative photochemistry can be red-shifted into the visible or infrared will be examined. The local bonding, electron transfer reactivity, and the energetic position of the affinity level of the adsorbates will be probed as a function of distance away from the alkali metal promoters using low temperature STM.

Initial experiments with our homebuilt, low and variable temperature STM (T_s > 15 K) examined the non-activated dissociative chemisorption of Br_2 on Pt(111)[2] and the photochemical deposition of Br on Pt(111) [3] by photoinduced dissociative electron attachment (DEA) to physisorbed CH_3Br. Although our long term goal has been to investigate DEA of particularly hard-to-activate physisorbed molecules such as N_2, CH_4, and CO_2, using electrons from the STM tip, our experience to date has been that we can only image islanded aggregates of these physisorbed molecules that desorb by 90 K on Pt(111). Consequently, we've concentrated our attention on the CH_3Br/Pt(111) system which is an important model system in surface photochemistry[4] and which should undergo activated dissociative chemisorption with a threshold energy intermediate between CH_4 (E_0 = 59 kJ/mol)[5] and CH_3I (E_0 < 48 kJ/mol).[6] Both CH_4 and CH_3Br desorb rather than dissociate on Pt(111) when they are dosed on a low temperature surface and heated in thermal programmed desorption experiments. In contrast, heating adsorbed CH_3I leads to C-I bond scission at T_s > 190 K. The CH_3Br photochemistry proceeds through photoinduced DEA into an affinity band that begins at roughly 2 eV above the Fermi level.

Dosing CH_3Br on to a K promoted Ag(111) surface leads to DEA through a non-thermal electron harpooning mechanism.[7] Here, we are interested in first characterizing the CH_3Br/Pt(111) system by STM and then pre- and post-dosing alkali metal to examine local effects in the thermal and electron transfer chemistry of CH_3Br.

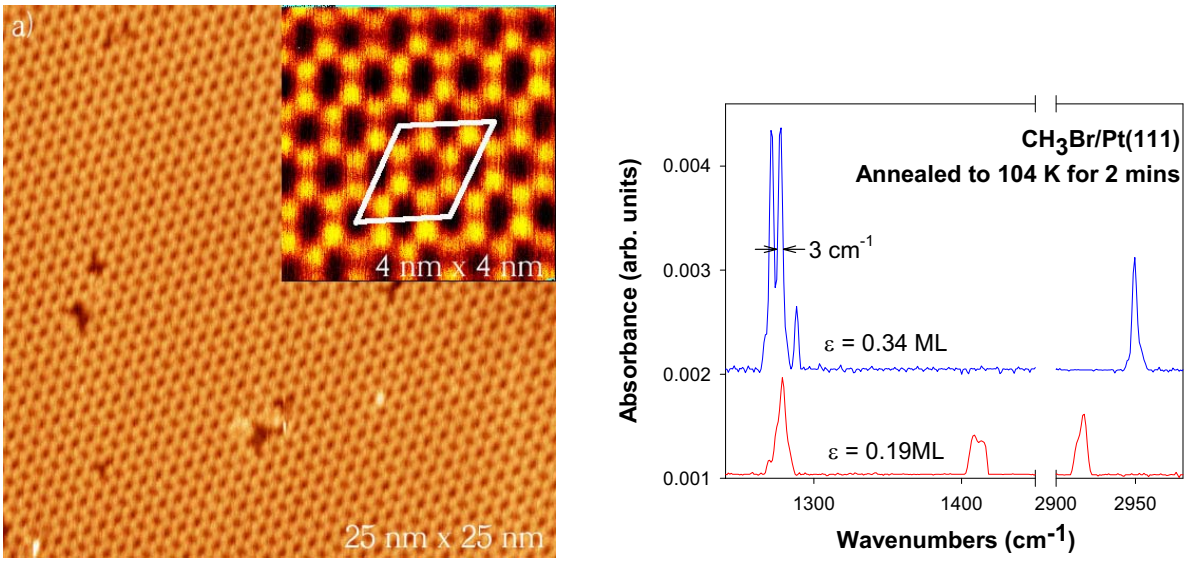

Fig. 1 (a) STM image of saturation coverage (θ = 0.255 ML) of CH_3Br on Pt(111) at 20 K formed by dosing multilayers and annealing off overlayers slowly to 104 K. The inset shows the CH_3Br unit cell holds molecules, imaged as bright spots, in two kinds of local environment – it may be easier to see that the molecules surround two kinds of "central black holes", round and slightly oblong. (b) RAIRS spectra of adsorbed CH_3Br after several gas exposures, ε, at 20 K surface temperature followed by annealing at 104 K for 2 minutes. The disappearance of the ν_5 perpendicular CH_3 deformational mode at 1412 cm^{-1} at higher exposures indicates the CH_3Br molecules are all standing up. The sharp splitting of the ν_2 parallel CH_3 deformational mode at 1283 cm^{-1} at the highest exposure (leaving saturation coverage behind) is consistent with the ordered CH_3Br pattern observed by STM whose unit cell contains two kinds of inequivalent CH_3Br molecules.[8]

Methyl bromide is a sausage shaped molecule with a 1.8 Debye dipole moment whose highly structured TPD spectrum on Pt(111) extends from 250 K to 100 K.[9] Figure 1 illustrates the ordered CH_3Br monolayer on Pt(111) as imaged by STM and the evolution of CH_3Br RAIRS spectra as a function of increasing exposure after sustained annealing to a surface temperature that will desorb overlayer molecules. To observe the ordered CH_3Br monolayer it was essential to use the STM with picoamp currents and bias voltages near the Fermi energy. Such ordered CH_3Br structures have not been observed in the past using conventional surface science techniques because CH_3Br undergoes efficient DEA by electrons with energies greater than ~2 eV above the Fermi energy so that the adsorbate ordering is easily disrupted, and also because CH_3Br undergoes significant restructuring within its monolayer and overlayer due to intermolecular electrostatic interactions with kinetics that are relatively slow. Earlier surface science and photochemical studies of CH_3Br on Pt(111)[9] that did not employ such an aggressive annealing procedure failed to find such an ordered and oriented monolayer, but clearly provided evidence that the molecular orientation was metastable when dosed at 20 K and evolved with annealing at least through 85 K. We are able to induce DEA in CH_3Br using electrons from the STM tip and can also image individual CH_3Br molecules at low temperatures. We are currently

improving our STM tip preparation procedures to allow for more robust field emission that should improve our imaging/spectroscopic capabilities and long term tip stability. We plan to examine photoinduced and STM tip induced DEA of the ordered CH_3Br monolayer and look particularly for site specific preferences in DEA. We will look also for DEA differences at low coverages and for single molecules. A Cs doser will be used to vary the local work function at the CH_3Br/Pt(111) surface and to allow the local DEA chemistry to be examined by STM. The next step will be to examine the DEA of physisorbed CH_4 and CO_2 on Pt(111) by imaging the chemisorbed dissociation products by low temperature STM.

DOE Publications in 2002-2004: none

References:

[1] R. Zehr, A. Solodukhin, B. C. Haynie et al., "Low-temperature and photon-induced chemistry of nitrogen on Pt(111)," Journal of Physical Chemistry B **104**, 3094-3106 (2000).

[2] H. Xu and I. Harrison, "Dissociative adsorption of Br_2 on Pt(111): Hot atom dynamics," Journal of Physical Chemistry B **103**, 11233-11236 (1999).

[3] H. Xu, R. Yuro, and I. Harrison, "The structure and corrosion chemistry of bromine on Pt(111)," Surface Science **411**, 303-315 (1998).

[4] V. A. Ukraintsev, T. J. Long, T. Gowl et al., "Photoinduced Dissociative Electron-Attachment of CH_3Br on Pt(111) - the Role of the Local Work Function," Journal of Chemical Physics **96**, 9114-9121 (1992).

[5] A. Bukoski, D. Blumling, and I. Harrison, "Microcanonical unimolecular rate theory at surfaces. I. Dissociative chemisorption of methane on Pt(111)," Journal of Chemical Physics **118**, 843-871 (2003).

[6] C. French and I. Harrison, "Orientation and Decomposition Kinetics of Methyl-Iodide on Pt(111)," Surface Science **342**, 85-100 (1995).

[7] X. L. Zhou, S. R. Coon, and J. M. White, "Potassium Promoted Decomposition Of Methyl-Bromide On Ag(111)," Journal Of Chemical Physics **94**, 1613-1625 (1991).

[8] T. Schwendemann and I. Harrison, unpublished observations, (2004).

[9] C. French and I. Harrison, "Site preferences, energetics and orientation of CH_3Br on Pt(111): investigation by RAIRS, TPD and photofragment angular distributions," Surface Science **387**, 11-27 (1997).

Chemical Kinetics and Dynamics at Interfaces

*Control of laser desorption and reaction in wide gap materials**

Wayne P. Hess (PI), Kenneth M. Beck, and Alan G. Joly
Chemical Sciences Division, Pacific Northwest National Laboratory
P.O. Box 999, Mail Stop K8-88, Richland, WA 99352, USA

Program Scope

The elucidation of physical and dynamic processes of electronically excited solids is essential to understanding radiation chemistry of condensed matter. Radioactive decay (from waste or other sources) releases huge quanta of energy that can induce reactions in the surrounding material. The initial high energy quantum is absorbed by the host material and ionization tracks are formed along the decay vector. The high energy species thus produced, such as core holes and free electrons, relax very quickly to form electron-hole pairs, excitons, and other species. These much less energetic secondary products then induce the transformations commonly regarded as radiation damage. It is therefore possible to study most radiation chemistry using initial excitation energies in the chemically relevant range between roughly 2 and 20 eV. The lower end of this range is easily generated by table top laser sources. Photo-stimulated desorption, of atoms or molecules, provides a direct window into many important processes and is particularly indicative of electronic excited state dynamics. Excited state chemistry in solids is inherently complex and greater understanding is gained using a combined experiment/theory approach. We collaborate with leading solid-state theorists using *ab initio* calculation and analysis to model laser desorption and photoemission experiments. The experiments are designed specifically to test hypothetical models and theoretical predictions resulting from the calculations. We have developed laser techniques to study solid-state chemistry using tunable femtosecond and nanosecond lasers to excite wide-gap materials under highly controlled conditions. We monitor particle emission using quantum-state specific laser ionization and probe surface chemical transformations using surface sensitive techniques such as x-ray photoelectron spectroscopy.

Laser control of chemical reactions has been actively pursued since the development of tunable lasers. Control schemes typically involve gas-phase reactant molecules prepared under isolated or single-collision conditions. Small molecules are used to reduce the number of reactive pathways and decrease energy redistribution rates from laser-prepared states. Laser control is currently pursued through active control schemes described as coherent control, quantum control, and two-pulse control. Coherent control utilizes interference between multiple excitation pathways to a final state to influence the overall reaction. Quantum control uses tailored femtosecond pulses to create initial excited state wavepackets specifically designed to optimize a particular reactive outcome. Two-pulse, or pump dump control, has been proposed to redirect wavepacket motion to enhance a particular reaction channel. The goals of laser control research are the same for active and passive schemes. To date we have explored mainly incoherent or passive control strategies although both approaches mean to drive the reaction towards a particular optimal outcome. We have demonstrated that laser control of desorbed products and quantum states is possible by judicious choice of laser wavelength, pulse duration, and delay between femtosecond pulse pairs.

Recent Progress and Future Direction

My team's laboratory studies are based on UHV surface science and laser excitation and ionization techniques. We probe desorbed atoms or molecules from ionic crystals using resonance enhanced multiphoton ionization and time-of-flight mass spectrometry. In single-pulse experiments, photon energies are chosen to excite specific surface structural features that lead to

particular desorption reactions. In pulse pair experiments, the initial laser pulse induces formation of transient species in the near surface region. A subsequent pulse then further excites either the sample or the nascent transient species to induce specific particle emission. Our laser systems are a combination of excimer, Nd:YAG, ultrafast, and tunable solid state or dye lasers. Pump laser output may be frequency converted using nonlinear techniques to produce photon energies ranging from 1 to 8 eV. The radiation sources are tuned to excite either bulk or surface states leading to controlled laser desorption of atoms or molecules.

The photon energy selective approach takes advantage of energetic differences between surface and bulk exciton states and probes the surface exciton directly. Application of this approach to controlling the yield and state distributions of desorbed species requires detailed knowledge of the atomic structure, optical properties, and electronic structure within a developing surface exciton desorption model. Our model indicates that it is possible to excite the surface over the bulk of ionic crystals using tunable excitation and thus induce controllable surface specific reactions. We recently demonstrated nearly exclusive surface excitation of KBr, KI, NaCl and other alkali halides. Previously, all other excitation sources (e.g. lasers, synchrotron, and electron) produced a mixture of surface and bulk excitation leading to multiple reactions. By generating the hyperthermal (surface) channel without significant thermal emission (bulk channel), we proved that a particular channel could be selected.

Direct surface excitation, in principle, allows incoherent control over product quantum state and velocity distributions. Control of such state distributions is, in effect, a confirmation of our exciton desorption model. Figure 1 displays the Br atom velocity and kinetic energy profiles for excitation photon energies between 5.5 and 6.5 eV. The photon energy range overlaps the threshold region of the KBr bulk absorption band. The kinetic energies decrease markedly with photon energy. The peak kinetic energies of desorbed Br atoms are 0.37, 0.24, 0.18 and 0.12 eV using pump photon energies of 6.46, 6.07, 5.94, and 5.56 eV, respectively. These selected kinetic energy distributions none-the-less exceed the thermal distribution (0.03 eV) expected from bulk excitation. Demonstration of controlled velocity distributions effectively confirms the theoretical model.

A method for extending laser control to the particle *electronic state* (spin-orbit) distribution is also predicted from our model. Such control has been demonstrated for subset of crystals that meet specific conditions. The factors required for electronic state control are the relative size of energetic shift between the surface and bulk exciton bands and the spin-orbit energy of the desorbed halogen atom. A large shift between the surface and bulk exciton band in combination with a small relative spin orbit splitting is required for effective control. If the relative level separations are reversed laser control is not possible due to interference between the bulk and surface channels. These factors predict that electronic state control is possible for all alkali- chlorides and fluorides and no alkali- bromides and iodides.

Figures 2 displays relative spin-orbit yields measured for room temperature KCl and KI as a function of photon energy. For KCl, Φ_{Cl^*}, varies from near zero to 80% for excitation energies from 6.4 to 7.5 eV. For KBr, Φ_{Br^*}, varies from near zero to just above 10% for excitation energies over a similar range. The suggested positions of the *surface* and bulk exciton maxima, for each alkali halide, are indicated to provide a common reference. One can clearly see a strong difference in behavior between chloride and iodide. The relative Cl* yield, Φ_{Cl^*}, increases markedly with photo-excitation energy. In contrast, Φ_{Br^*}, is always small when excited at energies similar in relative position to the surface exciton. Although Φ_{Br^*} indeed increase with photo-excitation energy, the value of Φ_{Br^*} remains small due to the large I-atom ground state yield derived from bulk absorption.

Figure 3 displays a schematic of bulk and surface energy levels. Significantly, the spin-orbit splittings are considerably smaller than the surface and bulk exciton shifts for alkali chlorides but larger for the alkali iodides. The spin-orbit splitting in alkali chlorides is small (ΔE

~ 0.1 eV) such that both the $\Gamma_{3/2}$ and $\Gamma_{1/2}$ exciton states are located within the lowest absorption feature at room temperature. Furthermore, the shift between the surface and bulk exciton is large (> 0.5 eV) in comparison. These two factors constitute the requirements for laser control over the halogen atom electronic state distribution and predict that a high degree of control for al chlorides and fluorides but the opposite for bromides and iodides.

Technological applications of alkali halides are limited compared to oxide materials. Oxides serve as dielectrics in microelectronics and form the basis for exotic semi- and super-conducting materials. Although the electronic structure of oxides differs considerably from alkali halides, it now appears possible to generalize the exciton model for laser surface reactions to these interesting new materials. We ask the question "Can an oxide surface excitons or a combination of excitons lead to controllable desorption and hence specific surface modification?" If exciton based desorption can be generalized to oxides then selective excitation of surface excitons could lead to controllable surface sculpting, on an atomic scale, for many important materials. Figure 4 displays the O-atom velocity and kinetic energy profiles for 4.7 eV photo-excitation. The O-atom KE distribution is clearly hyperthermal indicating that a surface exciton mechanism could likely be responsible. While exciton-based desorption is plausible for MgO, we note that the higher valence may require a bi- or tri-exciton mechanism. The details of this mechanism need to be delineated and, when confirmed, laser control schemes then developed. Future plans include development of coherent control schemes using tailored femtosecond pulses or pulse-pairs and photo-emission electron microscopy to probe dynamics of oxide nanostructures on surfaces.

Fig. 1

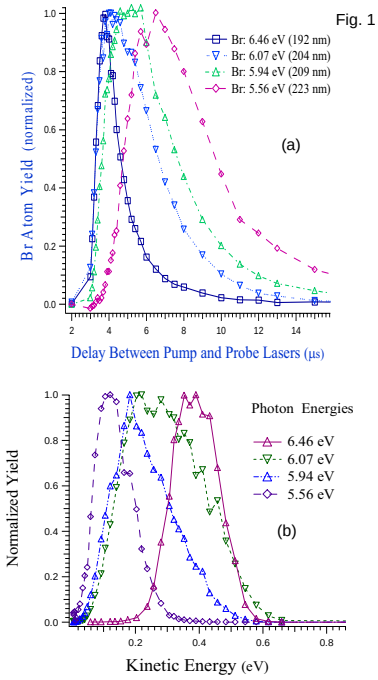

Velocity profiles (a), and kinetic energy distributions (b), of Br emission following tunable band edge excitation. The velocity profiles are obtained by plotting the Br atom yield as a function delay between pump and probe lasers. The kinetic energy distributions result from transformation of the velocity profiles and show the predicted photon energy dependence.

Fig. 2

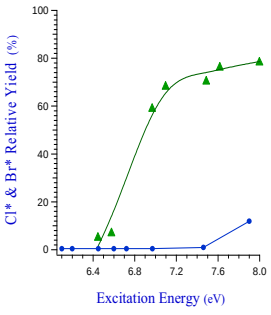

Relative spin-orbit yields measured for room temperature KCl and KBr as a function of photon energy.

Fig. 3

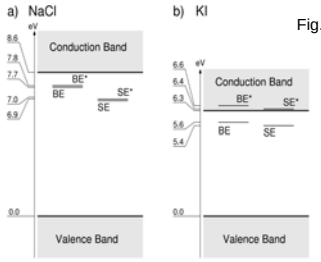

Generalized schematic diagram of bulk electronic bands and bulk and surface exciton states for (a) NaCl; and (b) KI. SE and SE* are surface exciton states with J = 3/2 and 1/2 corresponding to $\Gamma^{S}_{3/2}$ and $\Gamma^{S}_{1/2}$ states respectively. BE and BE* are bulk exciton states with J = 3/2 and 1/2, corresponding to $\Gamma^{B}_{3/2}$ and $\Gamma^{B}_{1/2}$ states respectively.

Fig. 4

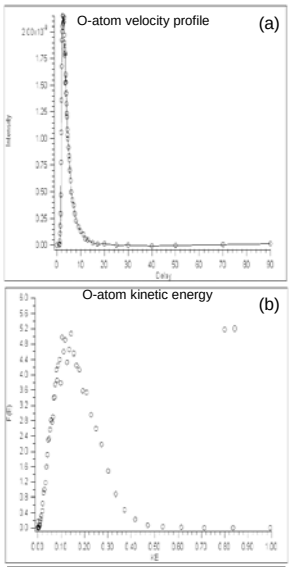

Velocity profile (a); and hyperthermal kinetic energy distribution (b); of O-atom desorption from ballistic deposition grown MgO film. The hyperthermal kinetic energy distribution and theoretical calculations indicate that the exciton model may be extendable to oxides in general. Units as in Fig. 1.

References to publications of DOE BES sponsored research (FY2002 to present)

1. WP Hess, AG Joly, DP Gerrity, KM Beck, PV Sushko, and AL Shluger, "Selective laser desorption of ionic surfaces: resonant surface excitation." J. Chem. Phys. **115**, 9463 (2001).

2. "Analysis of Hanford-related organics using matrix assisted laser desorption/ionization time-of-flight mass spectrometry." JA Campbell, WP Hess, JR Lohman, and SC Goheen, J. Radioanal. and Nuc. Chem. **250**, 247 (2001).

3. "Nitric acid-water complexes: Theoretical calculations and comparison to experiment." PR McCurdy, WP Hess, and SS Xantheas, J. Phys. Chem. **106**, 7628 (2002).

4. "Femtosecond Time-Resolved Photo-Stimulated Desorption from Ionic Crystals." AG Joly, WP Hess, KM Beck and JT Dickinson, Appl. Surf. Sci. **186**, 339 (2002).

5. "Control of laser desorption using tunable single pulses and pulse pairs." WP Hess, AG Joly, DP Gerrity, KM Beck, PV Sushko, and AL Shluger, J. Chem. Phys. **116**, 8144 (2002).

6. "Solid-state halogen atom source for chemical dynamics and etching." WP Hess, AG Joly, KM Beck, DP Gerrity, PV Sushko, and AL Shluger, Appl. Phys. Lett. **81**, 1140 (2002).

7. "Wavelength dependence of UV-laser induced emission of neutral and ionic species from single crystal $NaNO_3$." LP Cramer, SC Langford, WP Hess, and JT Dickinson, Appl. Surf. Sci. **197-198**, 35 (2002).

8. "What do MALDI mass spectra reveal about ionization mechanisms?" MR Papantonakis, J Kim, WP Hess, and RF Haglund, Jr., J. Mass Spectrom. **37**, 639 (2002).

9. "Transient Center Photodecomposition in Potassium Bromide." K.M. Beck, A.G. Joly, W.P. Hess, DP Gerrity, NF Dupuis, PV Sushko, and AL Shluger, Appl. Surf. Sci. **197-198**, 581 (2002).

10. "Photon stimulated desorption from KI: Laser control of I-atom velocity distributions" M Henyk, AG Joly, KM Beck, and WP Hess, Surf. Sci. **528**, 219 (2003).

11. "Synergistic effects of exposure of surfaces of ionic crystals to radiation and water." JT Dickinson, KH Nwe, WP Hess, and SC Langford, Appl. Surf. Sci. **208**, 2 (2003).

12. "Surface excitons detected by atomic desorption." AG Joly, KM Beck, M Henyk, WP Hess, PV Sushko, and AL Shluger, Surf. Sci. **544**, L683 (2003).

13. "The origin of temperature-dependent yield of Frenkel-pairs generated by valence excitation in NaCl", K Tanimura and WP Hess, Phys. Rev. B, **69**, 155102 (2004).

14. "Laser control of product electronic state: desorption from alkali halides." KM Beck, AG Joly, N Dupuis, P Perozzo, W Hess, P Sushko, and A Shluger, J. Chem. Phys. **120**, 2456 (2004).

15. "Determination of surface exciton energies by velocity resolved atomic desorption." WP Hess, AG Joly, KM Beck, PV Sushko, and AL Shluger, Surf. Sci. **564**, 62 (2004).

*Collaborators include AL Shluger, PV Sushko, DP Gerrity, and M Henyk

The Cluster Studies Program at Argonne National Laboratory

Julius Jellinek, Mark B. Knickelbein, and Stefan Vajda

Chemistry Division, Argonne National Laboratory, Argonne, Illinois, 60439
jellinek@anl.gov

Program Scope

This integrated experimental/theoretical program aims at acquiring fundamental knowledge and understanding of a broad variety of physicochemical properties of gas phase and deposited metal and organometallic clusters, cluster-ligand systems, and nanoparticles assembled from them. The immense interest in clusters is fueled by the unparalleled novelty and variety of their features and by the revolutionary impact they are expected to have on many technologies. An added role of clusters and cluster studies is to provide a fundamental, microscopic foundation for the broader areas of nanoscience and nanotechnology. Size- and composition-selected clusters expand the periodic table of elements as new, "superatomic" building blocks for assembly of novel (nano)materials and (nano)systems. We focus on metal and metal-containing clusters because of their particular relevance in many applications, e.g., catalysis, electronics, coatings, thin films, magnetic recording and storage, and others. Our studies cover structural, thermal, electronic, magnetic, dielectric, and chemical properties of both homogeneous and heterogeneous (including alloy) clusters as a function of their size and composition. We investigate cluster-substrate interactions and assembly of deposited clusters into larger nanoparticles. We take full advantage of the unique capabilities available at Argonne, such as the Advanced Photon Source (APS), and carry out activities in close contact with the recently established Center for Nanoscale Materials (CNM). The presence of both experimental and theoretical components in our program provides for a highly stimulating environment and strong synergism. Below we give a brief account of recent progress in select areas of our activities and outline our plans.

Recent Progress

Experimental Studies of Cluster Magnetism. Bare clusters[1-4] and polynuclear organometallic complexes[5] of transition or rare-earth metal atoms are two broad classes of molecular magnets with potentially useful properties as building blocks in novel magnetic materials. Studies of isolated metal clusters and their complexes offer the opportunity to probe the emergence of novel magnetic properties on the atom-by-atom basis[1-2]. Such experiments allow intrinsic cluster magnetic properties to be probed in the absence of a perturbing solvent or matrix. Conversely, the effects of solvents and matrices on magnetic properties can be mimicked for isolated species via the study of clusters that are partially or fully covered with adsorbates.[3,4] For smaller clusters and complexes, high-level theoretical methods can be applied (see below), which provide valuable interpretation of (and feedback to) the experiments. Specific topics of interest include: 1) Magnetic ordering in clusters composed of normally nonmagnetic elements;[1,2] 2) Orbital contributions to magnetism in clusters of iron, cobalt and nickel;[3,4] 3) Adsorbate-induced modification of magnetism in ferromagnetic clusters;[3,4] 4) Multidecker sandwich complexes: One-dimensional molecular magnets;[5] and 5) Synthesis and characterization of cluster-based magnetic materials (see below). Here, we focus on the first of these topics to exemplify some of the conceptual issues motivating our studies.

Band structure calculations demonstrate that *Stoner enhancements* in paramagnetic susceptibilities of bulk transition metals, e.g., in chromium, manganese, and palladium, are largely due to their unusually high densities of states $N(E_f)$ at the Fermi level. One of the strategies that has been successfully used to "induce" ferromagnetic ordering in these metals is to further increase their $N(E_f)$ values by spatial confinement in one or more directions. Clusters are spatially confined in three dimensions and thus may be expected to display novel confinement-induced magnetic phenomena. Our method of probing the magnetic properties of isolated metal clusters employs a *molecular beam magnetic deflection* approach.[2]

In this technique, a beam of neutral clusters (or cluster-ligand complexes, or sandwich complexes) is passed through an inhomogeneous magnetic field. The susceptibility of the cluster "sample" is determined by measuring the field-induced spatial deflection.[2] The intrinsic magnetic moments are determined from the measured susceptibilities via the Curie Law. The per-atom moments for Mn_n in the size range n=5-99 vary from ~0.3 μ_b to ~1.7 μ_b. Manganese thus joins chromium and rhodium in the class of normally nonmagnetic transition elements that become magnetically ordered when produced as clusters. Our preliminary studies indicate that small clusters of the group IIIB transition metals - scandium, yttrium, and lanthanum - also display magnetic ordering even though their bulk phases are simple paramagnets at all temperatures.

Experimental Studies of Deposited Clusters. This is a new activity in our program that aims at understanding and characterizing the interactions of deposited clusters with different supports and with each other as a function of the cluster size and material; the material, morphology, and temperature of the support; and the deposition parameters, such as energy, angle, and coverage. The understanding of these interactions and how they affect the thermal stability of the deposited clusters, as well as the kinetics/mechanisms of their aggregation into larger particles, is a prerequisite for rational use of clusters as building blocks in nanoassembly. It is also central to the field of nanocatalysis, where the ability to utilize the unique size-specific catalytic properties of particles depends on the ability to preserve their size.

Our first experiments were performed on Pt_n clusters. The clusters were generated in a laser vaporization source at room temperature and the entire distribution of sizes was deposited on a naturally oxidized surface of a silicon wafer (SiO_2/Si(111) placed at 90° to the cluster beam. The samples then were taken to the APS and studied using the grazing incidence X-ray scattering (GISAXS) technique. To analyze the thermal stability of the initially formed deposited particles, the samples were gradually heated from room temperature to above 400 °C and GISAXS images were taken at time intervals sufficient for thermal equilibration. The analysis of the data revealed that the originally formed particles preserved their averaged size over a broad temperature range (up to about 330 °C in the case of a coverage equivalent to 6.8×10^{14} atoms/cm^2), but further heating caused a sudden onset of rapid aggregation. Interestingly, the particles grew laterally, whereas their average height remained unchanged. We have also determined that the shape of the aggregated particles was preferentially cylindrical. Higher levels of coverage (up to an equivalent of 1.7×10^{16} Pt atoms/cm^2) led to larger initial average size of the deposited particles and larger final aggregated particles. The shape of these larger particles was preferentially (semi)spherical. The kinetics of aggregation at 400 °C was studied by recording GISAXS images as a function of time. The results indicate a two-step growth process, with the initial fast step completed within about 30 minutes.

In a set of recent, more refined experiments we used a high-flux cluster source and a quadrupole mass spectrometer to select and deposit a narrow size distribution of cationic Au_n^+ clusters with n=1, 2, .., 10. By varying the cluster generation conditions and the settings on the ion optics, the position and the number of the dominant peaks in the distribution could be varied. As supports we used SiO_2/Si(111) and thin alumina films [one monolayer of Al_2O_3 on SiO_2/Si(111) and 1 nm thick Al_2O_3 film on Si(111)] prepared by the atomic layer deposition (ALD) technique. We studied the effect of the coverage with different initial cluster size distributions on the onset of particle aggregation and the average final size of the particles. Whereas the analysis of the accumulated data is still in progress, the results indicate a number of interesting findings. For example, when one uses n=7-10 as the dominant sizes in the distribution and deposits an amount of Au equivalent to surface coverage of 2.5% ML, the GISAXS data indicate formation of cluster dimers and trimers, which are quite resistant to further aggregation – they retain their size up to about 390 °C.

Other experimental studies. Other areas of our recent experimental studies include electric deflection measurements of dipole moments and dielectric susceptibilities of metal clusters,[6,7] and reactions of CO, O_2, and NO with Ag_n clusters.[8] The latter are of relevance to catalysis, in general, and selective oxidation of CO, in particular.

Theoretical/Computational Studies. Our theoretical/computational studies cover structural, dynamical, electronic, magnetic, and chemical properties of one- and two-component (alloy) metal clusters and organometallic complexes. They involve both development of new concepts and methodologies especially appropriate for finite systems and large-scale numerical simulations. One of the recent developments is *computational electron spectroscopy of metal clusters.* We have formulated a new rigorous and highly accurate scheme[9] for computation of spectra of electron binding energies (EBE) within density functional theory (DFT) and applied it to study the effects of size, structure, charge state, and composition on the electronic properties of Mg_n, Al_n, and mixed Ni/Al clusters.[10-13] Our computed EBE spectra are not only in excellent agreement with the available experimental data,[14,15] but they provide for the understanding of the true meaning of these data. We have shown that the charge state may have a major effect on other (e.g., structural and electronic) properties of finite systems and this has to be taken into account in the interpretation of the results of photodetachment experiments traditionally performed on anionic species. We have analyzed the intriguing and important phenomenon of size-induced transition to metallicity and identified the separate roles of structure/symmetry and elemental composition in defining the electronic properties of bimetallic clusters. We have shown that high-accuracy computations of EBE used in conjunction with measured photoelectron spectra (PES) allow for identification of the isomeric forms of clusters generated under specific experimental conditions. (For more details on our computational electron spectroscopy scheme and its applications see a separate abstract in this book).

Another new initiative in our theoretical/computational studies is DFT explorations of structural, electronic, and magnetic properties of linear sandwich V_nBz_{n+1} ($Bz=C_6H_6$) complexes. These are motivated by the experimental studies in our group,[5] which have shown that these complexes are magnetic. So far we have covered the size range n=1-6. We obtained the equilibrium configurations for different spin-multiplicity states, and for the most stable configuration of each size characterized the binding energy, HOMO-LUMO gap, ionization potential (IP), electron affinity, and the energy of breaking away a terminal VBz unit. The computed IPs are in excellent agreement with the measured values. Our study shows that the complexes are magnetic and that the total magnetic moment, as judged by the most stable configurations, changes linearly with the size n ($1\mu_b$ per V atom). We also computed the infrared spectra of the most stable structures of the complexes and analyzed the changes in them as a function of size. Except for VBz_2, our results on the infrared spectra are predictions, which have yet to be verified experimentally.

Yet another area of our recent studies is structural, electronic, and magnetic properties of Be_n[16] and Mn_n clusters. For beryllium we have covered the size-range n=2-9, and for each size obtained up to six isomeric forms considering different packing of the atoms and different multiplicities of the total spin. For the most stable structures we have also characterized the vertical and adiabatic IPs. A particularly interesting finding is that for n=6-9 the energetically most preferred configurations correspond to higher multiplicity states. The work on manganese clusters is motivated by the measurements of magnetic moments of these systems in our group[1] and the availability of PES data for them.

Among our other recent studies are an integrated theoretical/experimental work in our group on the structures of mixed Ni/Al clusters[17], explorations of thermal fragmentation[18] and chemical reactivity of nickel clusters,[19] and an investigation of the effect of the bosonic *vs* fermionic nature of He on the Raman spectra of Br_2 solvated in He_n clusters.[20,21] The latter three studies were performed within the framework of international collaborations.

Future Plans

Our future work on cluster magnetism will be extended to bimetallic cluster systems. Clusters composed of a transition metal (e.g., Fe) and a lanthanide metal (e.g., Tb), are expected to exhibit both high magnetic moments and large magnetic anisotropy (both are necessary for ultrahigh density magnetic storage applications). Another major component of our future program will be studies of the magnetic behavior of size-selected metal clusters deposited onto surfaces or into matrices. These studies will provide models of how substrates, matrices, overlayers and dipolar and/or exchange coupling(s) affect the

overall magnetic properties of a macroscopic sample composed of nanometer (or subnanometer) scale building blocks.

Our near-future work on cluster deposition and cluster-based nanoassembly will focus on single-sized clusters, including those of relevance in nanomagnetism (see above) and nanophotonics; controlled deposition conditions; and use of various, including patterned, supports (oxide surfaces, nanopores, SAMs, PCN membranes, rare gas matrices). We will add fields and chemical reactions to our tools of post-deposition processing. Our more distant plans include studies of chemical reactivity of deposited clusters and cluster-assembled nanoparticles of relevance to nanocatalysis. These will be complemented by gas phase reactivity studies, which will supply data necessary for evaluation of the support effects. All aspects of the studies will be extended from one- to multi-component clusters and nanoparticles.

Our planned theoretical/computational studies will expand our explorations of structural, electronic, and magnetic properties of metal clusters to systems of larger sizes and various compositions. In particular, we will investigate systematically the coupling between the changes in structural, electronic, and magnetic properties of bimetallic clusters as a function of size and composition (both elemental and percentile). We will continue to study the phenomenon of size-induced transition to metallicity. The central task here is to develop the concept of the finite-size metallicity and its physical characteristics. The studies of sandwich complexes will be extended to V_nBz_n and $V_{n+1}Bz_n$ systems, as well as other organometallic complexes. We will perform dynamical simulation studies of cluster deposition on substrates, cluster-based nanoassembly, and cluster reactivity of relevance to our planned experimental studies. An important part of our future work will be conceptual and methodological developments directed at formulation of novel dynamical and statistical analysis tools that explicitly incorporate and account for finite size effects.

References

1. M. B. Knickelbein, Phys. Rev. B 70, 014424 (2004).
2. S. N. Khanna, B. K. Rao, P. Jena, and M. B. Knickelbein, Chem. Phys. Lett. 378, 374 (2003).
3. M. B. Knickelbein, J. Chem. Phys. 116, 9703 (2002).
4. M. B. Knickelbein, Chem. Phys. Lett. 353, 221 (2002).
5. K. Miyajima, A. Nakajima, S. Yabushita, M. B. Knickelbein, and K. Kaya, JACS, in press.
6. M. B. Knickelbein, J. Chem. Phys. 118, 6230 (2003).
7. M. B. Knickelbein, J. Chem. Phys. 120, 10450 (2004).
8. L. D. Socaciu, J. Hagen, J. Le Roux, D. Popolan, D. M. Bernhardt, L. Woste, and S. Vajda, J. Chem. Phys. 120, 2078 (2004).
9. J. Jellinek and P. H. Acioli, J. Chem. Phys. 118, 7783 (2003).
10. P. H. Acioli and J. Jellinek, Phys. Rev. Lett. 89, 213402 (2002).
11. J. Jellinek and P. H. Acioli, J. Phys. Chem. A 106, 10919 (2002); 107,1670 (2003).
12. P. H. Acioli and J. Jellinek, Eur. Phys. J. D 24, 27 (2003).
13. J. Jellinek and P. H. Acioli, in *Metal-Ligand Interactions in Molecular-, Nano-, Micro-, and Macro-Systems in Complex Environments*, N. Russo, D. R. Salahub, and M. Witko, Eds., Kluwer Academic Publishers, Dordrecht, 2003, p. 121.
14. O. C. Thomas, W. Zheng, S. Xu, and K. H. Bowen, Phys. Rev. Lett. 89, 213403 (2002).
15. X. Li, H. Wu, X. Wang, and L.-S. Wang, Phys. Rev. Lett. 81, 1909 (1998).
16. S. Srinivas and J. Jellinek, J. Chem. Phys. (in press).
17. E. F. Rexer, J. Jellinek, E. B. Krissinel, E. K. Parks, and S. J. Riley, J. Chem. Phys. 117, 82 (2002).
18. H. Avci, M. Civi, Z. B. Guvenc, and J. Jellinek, J. Phys. B 36, 3487 (2003).
19. S. Ozcelik, Z.B. Guvenc, P. Durmus, and J. Jellinek, Surf. Sci. 566, 377 (2004).
20. D. Lopez-Duran, M. P. de Lara-Castells, G. Delgado-Barrio, P. Villarreal, C. D. Paola, F. A. Gianturco, and J. Jellinek, Phys. Rev. Lett. 93, 053401 (2004).
21. D. Lopez-Duran, M. P. de Lara-Castells, G. Delgado-Barrio, P. Villarreal, C. D. Paola, F. A. Gianturco, and J. Jellinek, J. Chem. Phys. 121, 2975 (2004).

Molecular Theory & Modeling

Understanding the Chemical Physics of Nucleation in Solution

Shawn M. Kathmann
Chemical Sciences Division
Pacific Northwest National Laboratory
902 Battelle Blvd.
Mail Stop K1-83
Richland, WA 99352
shawn.kathmann@pnl.gov

The long-term objective of this project is to develop a fundamental understanding of the chemical physics governing nucleation of nano-sized solid phases in solution. A recent DOE report underscored the importance of nucleation by stating "Since most phase transitions involving nanostructured materials occur under conditions far from equilibrium, *the kinetic pathways available to these systems are numerous and not well understood. ... It will be important for making progress in the areas of synthesis and processing, therefore, to develop our understanding of nanochemistry and the broader general issues of nucleation and growth.*" Nanostructured materials are currently of great technological interest because their properties depend strongly on size, shape, and composition that differ significantly from either bulk or isolated molecules. This complex dependence of properties is precisely the reason there is so much interest, demand, and potential for exploiting nano-sized systems. The physical, electronic, and optical properties, in principle, can be "tuned" to create new materials with desired characteristics. However, the promise of "materials by design" has been replaced by a "cook and look" approach simply because there are too many degrees of freedom in relevant systems and appropriate chemical physics insight and is needed to bridge the gap.

Our development of Dynamical Nucleation Theory (DNT) at PNNL has provided a more detailed understanding of nucleation processes, and in the work proposed here, we wish to capitalize on this understanding to develop new, physically justified, models of nucleation in solution. DNT was formulated as a molecular-level approach to study gas-to-particle nucleation. DNT utilizes a step-by-step reaction kinetics perspective and thus provides a formalism in which the kinetic parameters, necessary for the construction of a consistent nucleation theory, can be obtained. DNT does not require bulk thermodynamic properties such as the density or surface tension. Significant progress has been made in developing DNT over the last few years and these advances provide the basis for a true molecular-level understanding of nucleation involving multiple components. Using DNT, an extreme sensitivity of the kinetic parameters, and thereby the nucleation rates, to the underlying interaction potentials has been discovered. These results indicate the major source of this sensitivity depends upon the Helmholtz free energies of the clusters. For example, a change of -0.5 kcal/mole in each of the chemical potentials of water clusters leading up to the critical size can alter the nucleation rate by 10 orders of magnitude. To make the magnitude of this variation in free energy more concrete, -0.5 kcal/mole is equivalent to the difference in zero-point-energies between $(H_2O)_2$ and $(D_2O)_2$. Prior to the development of DNT, the molecular nature of the intrinsic instability regarding the kinetics of the nucleation process has eluded theoretical efforts. The Helmholtz free energy is related to the interaction potential through the partition function and thus changes in the interaction energies between the atoms or molecules, in turn, alters the reaction free energies and rate constants underlying each

mechanistic step of nucleation. Since DNT is a molecular-level approach the effect of various impurities can be explicitly included to determine their affect on nucleation.

A brief summary of the advances made using DNT is provided here:

- An expression for the evaporation rate constant was *directly* obtained by using variational transition state theory with a spherical dividing surface centered on the center of mass of the cluster. The surprising result is that the evaporation rate constant is proportional to the derivative of the Helmholtz free energy for cluster formation with respect to the radius of the spherical dividing surface, although many previous molecular theories have assumed the Helmholtz free energy is independent of the constraining radius.
- The optimum value of the constraining radius is uniquely determined by the variational criteria of VTST, which minimizes the rate constant. The variational criteria can be understood simply – it is the location of the reaction bottleneck. Therefore, DNT provides the first physically justified procedure for selecting a unique volume for an *i*-cluster, which has been a source of controversy in the literature for over 70 years. This volume is physically justified because it defines the clusters that are most stable (i.e., with the slowest rate) to evaporation.
- A consistent theoretical approach was provided for calculating condensation rate constants using detailed balance and equilibrium constants that are consistent with the evaporation rate constants. It is important to note that in this approach, the condensation rate constants are determined without assuming the condensation rate is given by the gas-kinetic collision rate.
- The formalism has been extended to nucleation involving multiple components.
- Computational methods were developed to calculate (i) the dependence of the Helmholtz free energy of cluster formation on the radius of the constraining volume, which is needed to determine the evaporation rate constants, and (ii) the relative differences in Helmholtz free energies for clusters of different sizes, which are needed for the equilibrium constants and condensation rate constants.
- Explicit molecular dynamics simulations of the reaction kinetics confirmed the validity of VTST for the evaporation and condensation rate constants.
- Sensitivity studies of the nucleation kinetics were implemented for multi-component systems (for the first time). These studies determined novel and computationally efficient procedures for calculating the parameters needed to obtain nucleation rates.
- An extreme sensitivity of the kinetic parameters, and thereby the nucleation rates, to the underlying interaction potentials used in the molecular simulations has been discovered. These results indicate the extreme sensitivity of nucleation experiments to contaminants, since trace species in a small molecular cluster can significantly alter the molecular interactions and consequently affect the thermodynamics and kinetics of the nucleation processes.

The physical reason why nucleation is so sensitive can be understood intuitively. Since the nucleation process involves many mechanistic steps (typically 10's to 100's), small changes in each step can be amplified over the total number required to reach the critical cluster – defined as the cluster at the top of the nucleation barrier. The sensitivity of nucleation to interaction potentials motivates to look for relative effects on nucleation rates due to seeds (ions, impurities, contaminants, etc.). We investigated the variations in the water cluster Helmholtz free energies (chemical potentials) resulting from a single ion (of different sign and size). Figure 1 shows a comparison of the molecular calculations with those from Classical Ion-Induced Nucleation

Theory. It is obvious that the molecular-level chemical potentials are quite different from the continuum description and hence predict very different nucleation rates.

Using the statistical mechanical framework of Dynamical Nucleation Theory (DNT), a molecular-level model of cluster formation will be developed for nucleation in solution. The extension of DNT to solution phase crystallization requires a cluster definition. This is equivalent to choosing a dividing surface separating reactants (clusters) from products (not clusters) in the solution configuration space (see Figure 2). A statistical mechanical formalism will be constructed utilizing VTST to relate the variation in the cluster Helmholtz free energy with respect to the relevant dividing surface for cluster dissolution rate constant. The cluster dissolution rate constants (α_i) and equilibrium constants K^{EQ} allow determination of association rate constants (β_{i-1}). Given these dynamical parameters the nucleation rates for crystallization can be calculated and compared with experiment for consistency/validation and/or refinement of the interaction potentials and/or formalism. The essence of DNT is that it is a true theoretical description of nucleation as compared to the more simulative approaches mentioned above. The relevant timescale for the nucleation event is dictated by the potentials of mean force via the thermodynamic and kinetic properties of the clusters. This is particularly useful since nucleation is inherently a rare occurrence and trying to observe these events directly during a simulation at realistic conditions is computationally very demanding – the majority of time is spent searching irrelevant regions of the solution configuration space. We propose to calculate the rates of cluster dissolution directly by characterizing the dynamical bottlenecks for each cluster leading up to

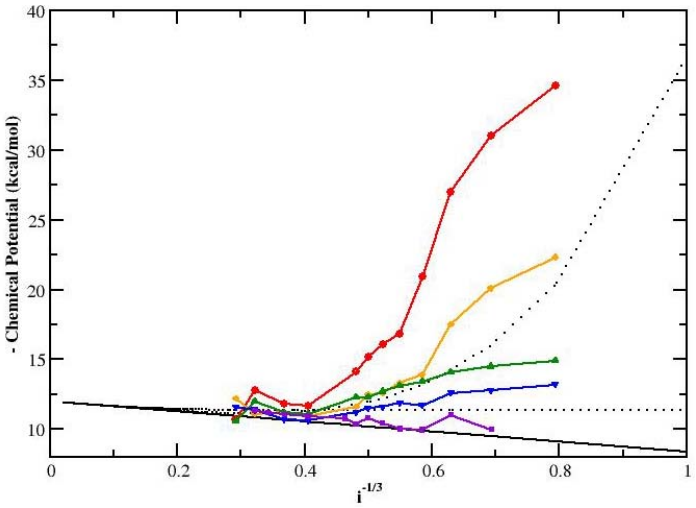

FIGURE 1. Size dependence of the chemical potentials of aqueous ionic clusters using ions of different size (2.35Å and 4.40Å) and sign (+/-): red (- and 2.35Å), yellow (+ and 2.35Å), green (- and 4.40Å), blue (+ and 4.40Å), purple (pure TIP4P water), upper dotted (CNT w/ion radius = 0.1Å), lower dotted (CNT w/ion radius = 10 Å), solid black (CNT pure water).

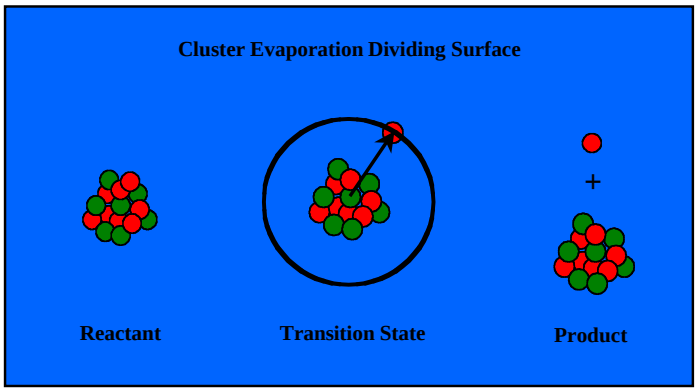

FIGURE 2. VTST scheme within DNT: The reactant is defined as the *ij*-cluster containing *i* atoms (red) of species A and *j* atoms of species B within a spherical constraining volume with origin coincident with the cluster center-of-mass. The dissolution channel transition state for species A is defined as having one monomer of a particular species (red) lying on the dividing surface (black circle) at a particular distance from the cluster center-of-mass (black arrow) – this distance defines the reaction coordinate. A product is defined as the (*i*-1)*j*-cluster plus one monomer at infinity. The cluster reactive flux is minimized with respect to the dividing surface to obtain the variational bottleneck for dissolution.

critical size. This will be done using interaction potentials benchmarked against accurate electronic structure calculations and potential of mean force Molecular Dynamics (MD) simulations performed within our group. The proposed extension of DNT will provide a framework in which increasingly more accurate calculations on crystallization in solution can be readily incorporated. In particular, we will determine the thermodynamic and kinetic properties for the clusters relevant to solution phase crystallization of various alkali halide and metal salts (LiCl, NaCl, KCl, AgCl, and AuCl). The choice of these salts is threefold: (1) atomistic simulations have been performed on several of these systems, and (2) they represent simple chemical series of alkali halides and metal halides, and (3) both series display different solubilities (e.g., aqueous LiCl has a solubility of 19.9M whereas aqueous AgCl is 1.3×10^{-6} M). The solvents for the alkali halide and metal halide salts will be chosen such that the solute concentrations to achieve crystallization are consistent with the VTST dividing surface defining the monomer reaction channels - solvents in which the salts have low solubilities meet this criteria. As mentioned previously, the solute (salt) will be treated explicitly, whereas the solvent (aqueous, organic, inorganic) will be treated implicitly via the potential of mean force used in the Monte Carlo (MC), Brownian Dynamics (BD) or Generalized Langevin Dynamics (GLD) simulations. Monte Carlo simulations will be used to determine the Helmholtz free energies and evaporation rate constants for the nucleating clusters. We will begin by testing existing potentials against accurate ab initio calculations on the various salts mentioned above. Exploratory MD simulations with explicit treatment of solvent molecules will be performed to determine the potentials of mean force employed in the MC and BD/GLD simulations.

In summary, once the proposed work is successfully completed, we will have a more fundamental understanding of the chemical physics of nucleation. The proposed research will provide the theoretical formalism, computational methodologies, and analysis for further application on more technologically relevant materials and explore the effect of interactions, and conditions (temperature, solubility, electromagnetic fields, etc.) on nucleation. We anticipate that this research will lead to meaningful results that can be compared with experimental data as an independent validation of theoretical and computational developments.

Publications of DOE Sponsored Research (2002-present)

1. Understanding the Sensitivity of Nucleation Kinetics: A Case Study on Water, S.M. Kathmann, G.K. Schenter, and B.C. Garrett, *J. Chem. Phys.*, **116**, 5046 (2002).
2. Dynamical Benchmarks of the Nucleation Kinetics of Water, G.K. Schenter, S.M. Kathmann, and B. C. Garrett, *J. Chem. Phys.*, **116**, 4275 (2002).
3. Equilibirum Constant for Water Dimerization: Analysis of the Partition Function for a Weakly Bound System, G.K. Schenter, S.M. Kathmann, and B.C. Garrett, *J. Phys. Chem. A*, **106**, 1557 (2002).
4. "Thermochemistry and Kinetics of Evaporation and Condensation for Small Water Clusters" B.C. Garrett, S.M. Kathmann, and G.K. Schenter in *Water in Confining Geometries*, Eds. V. Buch and J.P. Devlin (2003 Springer-Verlag Berlin Heidelberg NewYork).
5. Multi-Component Dynamical Nucleation Theory And Sensitivity Analysis, S.M. Kathmann, G.K. Schenter, and B.C. Garrett, *J. Chem. Phys.*, 120, 9133 (2004).
6. Dynamical Nucleation Theory: Understanding the Role of Aqueous Contaminants, Shawn M. Kathmann, Gregory K. Schenter, and Bruce C. Garrett, Proceedings of the 16th International Conference on Nucleation and Atmospheric Aerosols, Eds. M. Kasahara and M. Kulmala, (2004 Kyoto University Press).

Radiolysis of Water at Solid Interfaces

Jay A. LaVerne, Dan Meisel, Simon M. Pimblott, and I. Carmichael
laverne.1@nd.edu; meisel.1@nd.edu, pimblott.1@nd.edu, carmichael.1@nd.edu
Radiation Laboratory, University of Notre Dame, Notre Dame, IN 46556

Program Scope

Solid – liquid interfaces have long been known to enhance the radiolytic decomposition of the liquid, but comprehensive radiation chemical studies of heterogeneous systems are relatively new. Experimental radiation chemical studies of aqueous dispersions of nanoparticles are of considerable importance as these systems provide the opportunity to investigate energy and charge exchange across interfaces, which open pathways for wholesale exchange of reactive intermediates between the two phases. Understanding the transport of charge and energy across an interface is relevant to many practical technological problems of importance to the Department of Energy as heterogeneous systems are frequently encountered in the management of nuclear materials and nuclear waste, and in nuclear power plant infrastructure. Examples include sludge and slurries in storage facilities, and porous oxide deposits on metal surfaces of the primary circuit in nuclear reactors. A potential medical application is the use of bio-molecular targets tagged with metallic nanoparticles in radio-therapeutic treatment of patients.

This program is devoted to an experimental examination and theoretical prediction of the kinetics and yields of transient species produced in the radiolysis of aqueous nanoparticle dispersions and stable products from the radiolysis of water adsorbed on particle surfaces. Pulse radiolysis experiments are used to probe the escape of carriers into the bulk water and adsorbed scavengers are employed to trap these carriers at the particle surface. This technique gives information on the role of transient species passing to or through the solid oxide – water interface. Another major experimental thrust is the examination of the influence of oxide interfaces on the stable products in the radiolysis of water. Aqueous suspensions or slurries are used to determine the effect of different oxide interfaces on the radiolytic production or destruction of H_2 and H_2O_2. Effects due to modifications in surface morphology and the formation of adsorbed species are also being examined. Stochastic modeling of energy deposition across interfaces enhances the experimental program and gives insight into the fundamental processes at the interface. Computational quantum chemistry provides an atomistic-level description of the effect of surface morphology on the spectroscopic properties of the adsorbed transients and quantifies the thermochemistry of product formation. Elucidation of initial energy deposition and the subsequent migration of energy, charge or other carriers are vitally important to understanding the ultimate radiolytic outcome in heterogeneous systems.

Recent Progress

Pulse radiolysis experiments using scavengers of OH radicals have shown that when an aqueous suspension of silica particles is irradiated essentially no holes cross the particle – water interface to generate OH radicals. (1,2) All of the holes that are originally generated by the ionizing radiation in the silica remain in the particle, even at the smallest

size used (7 nm diameter). In contrast, picosecond pulse radiolysis experiments directly observing the yield of e_{aq}^- by absorption suggest that electrons escape from the SiO_2 particles into the water, even with particles of 22 nm diameter. (3) This limited data suggests that a fundamental understanding of the radiation-induced chemistry will require not only the elucidation of the effects of radiation on the constituent media, but also a description of the physical and chemical processes of both low-energy electrons and holes occurring at or passing through the interface.

Recent experiments on aqueous suspensions of silica nanoparticles containing adsorbed electron acceptors (e.g., methyl viologen, MV^{2+}) and irradiated using pulse radiolysis, show that the yield of the reduced radical cation, MV^+, increases with increasing weight percent of SiO_2 in the sample. (4) Furthermore, the MV^+ is formed within the electron pulse indicating the fast migration of electrons to the surface of the SiO_2 nanoparticle following their formation in the bulk of the oxide. Yields of MV^+ as high as 6.5 radicals per 100 eV are found, which is significantly higher than the 4.5 hydrated electrons per 100 eV initially formed in neat water. The high yields suggest that an additional source of reducing equivalents is generated in the SiO_2 nanoparticle that is capable of reducing MV^{2+}. The source and nature of these species are not known, but kinetic analysis suggests that they come from the oxide and are not due to species diffusing to the interface from the bulk water. Monte Carlo simulations concur with the hypothesis that these additional reduction equivalents are due to excitons captured by the electron acceptor at the interface. Equilibrium studies of different adsorbates on SiO_2 nanoparticles have been used to characterize the binding site density of the surface probes used in these studies. (5) These studies allow an estimate of the size of the particle beyond which no escape of charge carriers will occur. For the silica particles studied here this size is 30 nm in diameter.

Molecular hydrogen production from water adsorbed on various ceramic oxide particles has been shown to be significantly greater than can be accounted from energy directly absorbed by the adsorbed water layers. (6-8) The effect appears to be especially prominent with oxides of band gap of about 5 eV, but the relationship between hydrogen formation and band gap energy is tenuous. The results suggest that energy initially deposited in the bulk oxide is transferred to the surface to initiate water decomposition, presumably by excitons. Particle type, size, and other parameters will have significant influence on the nature of the carriers and the probability of reaching the surface.

In suspensions of SiO_2 nanoparticles of 7 and 22 nm diameter, the yield of H_2 increases as the weight fraction of silica increases. (9) On the other hand, the production of H_2 in the radiolysis of slurries of large SiO_2 particles (~343 nm diameter) is virtually identical to that obtained in water alone, suggesting little escape of electrons from the bulk oxide to the water. However, aqueous slurries of smaller SiO_2 particles (~8 nm diameter) can double the H_2 production from water. Scavenger studies varying the concentration of selenate, suggest that electron reactions occurring on the μs time domain are responsible for the additional H_2 produced in aqueous SiO_2 dispersions. The radiolysis of aqueous ZrO_2 slurries shows even greater H_2 production than with comparable weight percent of SiO_2. Particle size has some effect, but surface morphology seems to have a greater influence on H_2 formation in these systems.

Monte Carlo track structure calculations have been performed using inelastic cross sections derived from the differential dipole oscillator strength distributions of

water and SiO_2. A collision-by-collision approach shows that the density of energy transfer events in SiO_2 is shifted to higher energy (27 eV) than in the case of liquid water (24 eV). The mean energy losses are estimated to be 87 and 64 eV in SiO_2 and water, respectively, showing a substantial difference between the oxide and water. Furthermore, the ionization and excitation yields in SiO_2 are found to be 4.1 and 2.2 per 100 eV. Combined with the experimental studies, these results suggest that the excited states are capable of reducing MV^{2+}.

Future Plans

Radiolysis studies of aqueous suspensions of SiO_2 and ZrO_2 suggest that energy deposited directly in the oxide can lead to formation of hydrated electrons in the liquid phase and excess production of H_2. (6-9) Other oxides of technical importance, such as Al_2O_3, and TiO_2, will be examined as a function of the weight percent of oxide power in water. Particle sizes will range from a few nm to about 1 μm, so the nature of the systems will vary from suspensions to slurries. Variation in particle size is especially important in determining the transport of energy or material through the interface. Mixtures of similar weight percent but different particle sizes will give information on the efficiency of electron or mass transport, since the relative surface areas determine transport through the interface. Another method to determine the identity of transients is to induce defects in the solid; trapping at these defects then competes with transient migration to the surface. Defect sites will be radiolytically produced in the solid oxide followed by the adsorption of water and further irradiation and the measurement of the radiolytic formation of H_2. The storage of energy in defect sites and the eventual manifestation of this energy in hazardous gas formation may have important implications in the long term storage of sealed containers of radioactive materials.

The radiolysis of adsorbed water can produce copious quantities of H_2, but no corresponding oxidizing species are observed to evolve from the surface. (7,8) Peroxides or other oxygen species must be adsorbed on the surface or absorbed into the oxide. (10-13) Water adsorbed on SiO_2, Al_2O_3, and ZrO_2 will be irradiated and the surface examined with FT-IR and EPR techniques. Techniques of computational quantum chemistry will be employed to determine energetically favored surface structures and terminations and the relevant spectroscopic properties of candidate species on such surfaces will be evaluated from theory. The presence of peroxides and several other oxygen species should be readily observable if they are radiolytically produced. Hydrogen peroxide thermal decomposition is known to be affected by the presence of surfaces. (14) The thermal and radiolytic decomposition of aqueous solutions of H_2O_2 in the presences of several solid oxides will be examined with selected scavengers to determine the mechanism involved.

References

(1) T. Schatz, A. R. Cook, and D. Meisel *J. Phys. Chem. B* **1999**, *103*, 10209-10213.
(2) N. M. Dimitrijevic, A. Henglein, and D. Meisel *J. Phys. Chem. B* **1999**, *103*, 7073-7076.
(3) T. Schatz, A. R. Cook, and D. Meisel *J. Phys. Chem. B* **1998**, *102*, 7225-7230.
(4) B. H. Milosavljevic, S. M. Pimblott and D. Meisel *J. Phys. Chem. B*, **2004**, *108*, 6996-7001.

(5) B. H. Milosavljevic and D. Meisel *J. Phys. Chem. B*, **2004**, *108*, 1827-1830.
(6) N. G. Pretrik, A. B. Alexandrov, and A. I. Vall *J. Phys. Chem. B* **2001**, *105*, 5935-5944.
(7) J. A. LaVerne and L. Tandon *J. Phys. Chem. B* **2002**, *106*, 380-386.
(8) J. A. La Verne and L. Tandon *J. Phys. Chem. B* **2003**, *107*, 13623-13628.
(9) J. A. LaVerne and S. E. Tonnies *J. Phys. Chem. B* 2003, *107*, 7277-7280.
(10) C. Corbel, G. Sattonnay, J. F. Lucchini, C. Ardois, M. F. Barthe, F. Huet, P. Dehaudt, B. Hickel, and C. Jegou *Nucl. Instrument. Methods Phys. Res. Sect. B-Beam Interact. Mater. Atoms* **2001**, *179*, 225-229.
(11) H. P. Boehm *Disc. Faraday Soc*. **1971**, *52*, 264-289.
(12) V. B. Kazansky, G. B. Pariisky and V. V. Voevodsky *Disc. Faraday Soc*. **1962**, *31*, 203-208.
(13) R. Gao, A. Safrany, and J. Rabani *Radiat. Phys. Chem.* **2002**, *65*, 599-609.
(14) Croiset, E.; Rice, S. F.; Hanush, R. G. *AIChE* **1997**, *43*, 2343.

DOE Sponsored Publications in 2002-2004

J. A. LaVerne and L. Tandon, "H_2 Production in the Radiolysis of Water on CeO_2 and ZrO_2," *J. Phys. Chem. B* **2002**, *106*, 380-386.

D. Meisel, "Radiation Effects In Nanoparticle Suspensions," in "Nanoscale Materials", Ed. L. Liz-Marzan and P. Kamat, Kluwer Publishers, 119-34 (**2003**).

P. V. Kamat and D. Meisel, "Nanoparticles in Advanced Oxidation Processes," Current Opinion in Colloid & Interfacial Sci. **2003**, 7, 282-7.

J. A. La Verne and L. Tandon, "H_2 Production in the Radiolysis of Water on UO_2 and Other Oxides," *J. Phys. Chem. B* **2003**, *107*, 13623-13628.

J. A. La Verne and S. E. Tonnies, "H_2 Production in the Radiolysis of Aqueous SiO_2 Suspensions and Slurries," *J. Phys. Chem. B* **2003**, *107*, 7277-7280.

B. H. Milosavljevic, S. M. Pimblott and D. Meisel, "Yields and Migration Distances of Reducing Equivalents in the Radiolysis of Silica Nanoparticles," *J. Phys. Chem. B*, **2004**, *108*, 6996-7001.

B. H. Milosavljevic and D. Meisel, "Kinetic and Thermodynamic Aspects of Adsorption on Silica Nanoparticles. A Pulse Radiolysis Study," *J. Phys. Chem. B*, **2004**, *108*, 1827-30.

D. Meisel, "Radiation Effects on Nanoparticles", Proceedings of the International Atomic Energy Agency Workshop on Emerging Applications of Radiation in Nanotechnology, IAEA Press, Vienna, ISSN 1011-4289, pp. 130-141 (**2004**).

EXPERIMENTAL AND COMPUTATIONAL STUDIES OF CHARGE AND ENERGY TRANSFERS IN MULTICHROMOPHORIC AROMATIC SYSTEMS

Edward C. Lim, P.I.
Department of Chemistry
The University of Akron
Akron, OH 44325-3601
Email: elim@uakron.edu

Abstract

A concerted experimental (laser spectroscopy) and theoretical (quantum chemistry) study of photoinduced charge and energy transfer in multichromophoric aromatic systems is carried out to deduce the role intermoiety interactions (CT, van der Waals, and H-bonding) play in the charge/energy transfer processes. The project is composed of three parts. In part I, we study the geometries and binding energies of jet-cooled aromatic clusters to probe the geometry dependence of photoionization and photoisomerization (i.e., excimer formation), and to deduce the time evolution of the formation of dimer core structures in electronically excited neutral clusters and ground-state ionic clusters. Part II is devoted to the study of the role the intramolecular singlet excimers play as electron donors in photoinduced CT processes of aromatic clusters and diarylalkanes. This study, also carried out in supersonic jet, is concerned with real-time probe of the excimer formation and photoionization, which will provide a rigorous test for the occurrence of excimer-mediated photoionization and photoinduced CT. In part III, we investigate the mechanism of intramolecular charge transfer in *para*-disubstituted aromatic molecules containing electron-donating and electron-accepting groups. Since this last project has been the subject matter of our very recent focus, we describe the major findings of part III in detail.

Intramolecular charge transfer (ICT) in photoexcited donor-acceptor (EDA) molecules, in which an electron is transferred from one group to another of the same molecule, has been the subject of very considerable interest during the past four decades. The best known, and certainly the best studied, prototype of such systems is 4-dimethylaminobenzonitrile (DMABN), which exhibits fluorescence from both the locally excited (LE) state and the ICT state in polar solvents.[1] The picosecond transient absorption spectrum of DMABN in polar solvents is characteristic of the benzonitrile anion,[2] indicating that the ICT state is composed of dimethylamino radical cation and benzonitrile anion. Despite the very many experimental and theoretical studies that have been carried out for DMABN,[3] neither the mechanism of the ICT state formation nor the structure of the ICT state is presently known with any certainty. Four different models have been proposed for the structure of the ICT state. Three of these differ mostly in the orientation of the dimethylamino group relative to the plane of the phenyl ring in DMABN: the twisted ICT (TICT),[4] the planar ICT (PICT)[5] and the wagged ICT (WICT).[6] Of these, WICT model can be dismissed on the basis of the calculations that show that a low-lying highly polar $\pi\pi^*$ excited state cannot be generated for DMABN by increasing the angle of inversion. The fourth model, referred to as RICT (for rehybridized ICT),[7] identifies the ICT state with a bent $\pi\sigma^*_{C\equiv N}$ state that is formed by the rehybridization of the cyano carbon atom from sp to sp^2. This model has also been rejected in favor of the TICT model on energetic grounds.

While the identification of the ICT state with the πσ* (RICT) state is almost certainly wrong, the role of the πσ* state in electron-transfer dynamics cannot be ruled out by calculations that do not take into account the effects of solvation.

Recently, we have presented the results of TDDFT (time-dependent DFT), CIS, and CASSCF calculations of the low-lying excited singlet states of diphenylacetylene (DPA),[8,9] DMABN,[10] and related molecules. The results demonstrate the occurrence of low-energy crossing between the initially excited ππ* state and a highly polar $\pi\sigma^*$ state of bent geometry. The barrier for the ππ* → πσ* state switch was found to be strongly dependent on the nature of the substituent. The πσ* state formed from the state switch is expected to be dark due to the small πσ* → S_0 radiative decay rate and very efficient πσ* → S_0 internal conversion that arises from the small energy gap, and large geometry difference, between the πσ* and ground states. The formation of the πσ* state can, however, be probed via the very strong πσ* ← πσ* absorption[8-10] that occurs in the near infrared region of the spectrum. As the $\pi \rightarrow \sigma^*_{C\equiv N}$ (or $\pi \rightarrow \sigma^*_{C\equiv C}$) is an intramolecular charge transfer transition in which an electron localized on the phenyl π orbital is promoted to the σ* orbital localized on the C≡N (or C≡C) group, it is natural to wonder if the πσ* state (with computed dipole moment larger than that of low-lying ππ* states) could play an important role in the photoinduced ICT reaction of p-substituted DPA, DMABN and related molecules.[9,10]

The above supposition has very recently been put to a definitive test through the measurements of time-resolved absorption spectra of the LE (ππ*) state, $\pi\sigma^*_{C\equiv N}$ state, and benzonitrile anion for DMABN in polar solvents.[11] The results of this study, carried out with sub-picosecond time resolution, clearly demonstrate that the πσ* state is a precursor of the intramolecular charge-transfer (ICT) reaction, which leads to the formation of benzonitrile ion.[11] More specifically, the formation rate of the anion corresponds to the decay rate of the πσ* state, indicating that the fully charge-separated ICT state is formed from the initially excited ππ* state vy charge shift (CS), viz.,

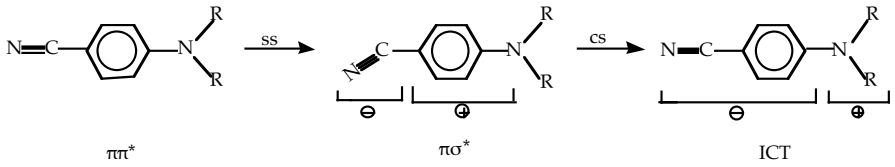

A similar mechanism can also account for the formation of benzonitrile anion and dimethylaminophenylacetylene cation in p-dimethylamino-p′-cyano-diphenyacetylene.[9]

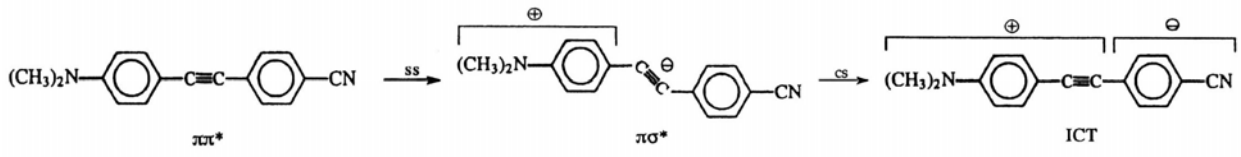

Extension of the computational and experimental studies to other *para*-disubstituted electron donor-acceptor molecules, including those that lack low-lying πσ* states, is presently in progress.

References

1. E. Lippert, W. Lüder and H. Boos, in: *Advances in Molecular Spectroscopy*, edited by A. Mangini, ed. (Pergamon Press, Oxford, 1962), pp. 443-457.
2. T. Okada, N. Mataga and W. Baumann, *J. Phys. Chem*. **91**, 760 (1987),
3. See, for a recent review, W.M. Kwok, C. Ma, P. Matousek, A.W. Parker, D. Phillips, W.T. Toner, M. Towrie, P. Zuo, and D. L. Phillips, *Phys. Chem. Chem. Phys.* **5**, 3643 (2003).
4. K. Rotkiewicz, K.H. Grellmann, and Z.R. Grabowski, *Chem. Phys. Lett*. **19**, 315 (1973).
5. Th. von der Harar, A. Hebecker, Yu V. Il'ichev, Y.-B. Jiang, W. Kühnle, K.A. Zachariasse, *Recl. Trav. Chim. Pays-Bas***, 114**, 430 (1995).
6. W. Schuddeboom, S.A. Jonker, J.H. Warman, U. Leinhos, W. Kühnle, K.A. Zachariasse, J. Phys. Chem. **96**, 10809 (1992).
7. A.L. Sobolewski, W. Domcke, *Chem. Phys. Lett*. **250**, 428 (1996).
8. M.Z. Zgierski and E.C. Lim, *Chem. Phys. Lett*.,**387**, 352-355 (2004).
9. M.Z. Zgierski and E.C. Lim, *Chem. Phys. Lett*. **393**, 143-149 (2004).
10. M.Z. Zgierski and E.C. Lim, *J. Chem. Phys*. **121**, 2462-2465 (2004).
11. E.C. Lim et al., "Evidence for the Direct Involvement of the $\pi\sigma^*$ State in the Intramolecular Excited-State Charge Transfer of 4-Dimethylaminobenzonitrile", in preparation.

List of Publications (2002-2004)

1. D.C. Moule, T. Fujiwara and E.C. Lim, "Thiophosgene, A Tailor-Made Molecule for Photochemical and Photophysical Studies", *Advance in Photochemistry*, in press.
2. M.Z. Zgierski and E.C. Lim, The Role of $\pi\sigma^*$ State in Intramolecular Electron-Transfer Dynamics of 4-Dimethylaminobenzonitrile and Related Molecules, *J. Chem. Phys*., **121**, 2462-2465 (2004).
3. M.Z. Zgierski and E.C. Lim, On the Mechanism of Intramolecular Charge Transfer in para-Disubstituted Diphenylacetylenes Containing Electron-Donating and Electron-Accepting Groups: Role of $\pi\sigma^*$ State in Electron-Transfer Dynamics, *Chem. Phys. Lett*., **393**, 143-149 (2004).
4. M.Z. Zgierski and E.C. Lim, Nature of the "Dark" State in Diphenylacetylene and Related Molecules: State Switch from the Linear $\pi\pi^*$ State to the Bent $\pi\sigma^*$ State, *Chem. Phys. Lett*., **387**, 352-355. (2004).
5. T. Fujiwara, D.C. Moule, and E.C. Lim, Optical-Optical Double Resonance Probe of the Dark State of Thiophosgene in Supersonic Free Jet, *Chem. Phys. Lett*., **389**, 165-170 (2004).
6. T. Fujiwara, D.C. Moule, and E.C. Lim, Thiophosgene, A Molecule Tailor-Made for Testing Fundamental Theoretical Concepts of Radiationless Transitions: Intramolecular Dynamics of S_1 Cl_2CS, *J. Phys. Chem. A*, **107**, 10223-10227 (2003).
7. C. Gonzalez and E.C. Lim, Evaluation of the Hartree-Fock Dispersion (HFD) as Practical Tools for Probing Intramolecular Potentials of Small Aromatic Clusters: Comparison of the MP2 and HFD Intermolecular Potentials, *J. Phys. Chem. A*, **107**, 10105-10110 (2003).
8. T. Fujiwara, D.C. Moule, and E.C. Lim, A One-Photon Laser Induced Fluorescence and a Sequential Two-Photon Optical-Optical Double Resonance Excitation Study of the

Vibrational Structure of the $\tilde{B}\ ^1A_1$ ($\pi\pi^*$) State of Thiophosgene, Cl_2SC, *J. Chem. Phys.*, **119**, 7741-7748 (2003).
9. T. Fujiwara and E.C. Lim, Binding Energies of the Neutral and Ionic Clusters of Naphthalene in Their Ground Electronic States, *J. Phys. Chem.*, **107**, 4381-4386 (2003).
10. E.C. Lim, Aromatic Excimers as Electron Donors in Photoinduced Charge Transfer Processes, *Res. Chem. Intermed.*, **28**, 779-794 (2002).
11. L.M. Beaty-Travis, D.C. Moule, E.C. Lim, and R.H. Judge, A Conformational Study of the $S_1(\mathbf{n}\pi^*)$ Excited State of Formic Acid, *J. Chem. Phys.*, **117**, 4831-4838 (2002).
12. C. Gonzalez and E.C. Lim, On the Equilibrium Geometries of Anthracene Trimer and Naphthalene: Comparison of the Exp-6-1 and HFD Structure Predictions with Experiment, *Chem. Phys. Lett.*, **357** 161-167 (2002).
13. J.-K. Lee, R.H. Judge, B.H. Boo, and E.C. Lim, Conformation-Selective Photoionization of Covalently Linked Diaryl Compounds: Excimer-Mediated One-Color Two-Photon Ionization in Seeded Beams of 1,3-Diphenylpropane, *J. Chem. Phys.*, **116** 8809-8816 (2002).
14. D.C. Moule and E.C. Lim, Highly Varying Photophysical Properties of Thiocarbonyls: Validation of Fundamental Theoretical Concepts of Electronic Radiationless Transitions, *J. Phys Chem. A,* **106**, 3072-3078 (2002).

Solvation, Spectroscopy, and Electron Transfer

Mark Maroncelli

Department of Chemistry 104 Chemistry Building,
Penn State University, University Park, PA 16802
mpm@chem.psu.edu

Our DOE sponsored work focuses on understanding solvation, especially dynamical aspects of solvation, its influence on charge transfer processes. The main emphasis of the past few years (and the near future) is in two areas: i) exploring the distinctive features of solvation and charge transfer in ionic liquids and ii) using time-dependent emission spectroscopy learn about dynamical solvent control of charge transfer reactions. Some of our recent work and future directions are summarized below.

1) Unusual? Interactions in Perfluorinated Solvents[2,3,6,10]: As a result of interests developed during a sabbatical semester spent in Peter Rossky's lab, we devoted some time to examining energetic and frictional aspects of perfluoroalkane + alkane interactions. Electrical interactions are of negligible importance in alkane + perfluoroalkane systems, and this work represents a detour from the primary focus of our DOE-sponsored research on polar solvent dynamics and electron transfer. However, most charge transfer reactions (for example the TICT reactions described in Section 3) involve both electrical and nonpolar coupling to solvent. What we have learned about nonpolar interactions and "mechanical" friction in these completely nonpolar systems is of relevance for modeling the mixed interactions present in the more general case.

Paper #2 concerns an experimental study of the nature of friction in perfluoroalkanes. Here we examined whether the unusually weak coupling between perfluoroalkanes and aromatic solutes suggested by electronic spectroscopy is also manifest in unusually small friction on isomerization and rotation of a probe solute such as diphenylbutadiene (DPB). (We chose this particular solute because we had been studying it in other contexts.) Comparing the behavior of DPB in perfluoroalkane solvents to that in other solvents we came to mixed conclusions regarding unusual frictional effects. Whereas the rotational friction sensed by DPB in perfluoroalkane solvents was no different from what would be expected based on the behavior in other solvents, friction on the isomerization reaction was found to be anomalously small. At this point we can only conjecture that the difference may reflect the different spatial extents and/or frequencies of the motions involved in isomerization compared to rotation. Verification of this idea will have to await simulation or other modeling studies. During the course of this work we also learned several new things about the photophysics of DPB and proposed a model for the isomerization that was able to correlate a great deal of literature data that has accumulated on this reaction.

DPB

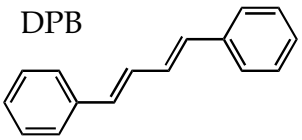

(*trans*,*trans*-1,4-diphenyl-1,2-butadiene)

Paper #3 is a computational study of perfluoroalkane + alkane mixing. It asks whether standard potential models, consisting of all-atom potentials, together with commonly used combining rules are capable of reproducing the anomalous mixing behavior observed in perfluoroalkane + alkane systems. The answer is no. Only with more exotic mixing rules were we able to achieve a good fit to experimental perfluoroalkane + alkane mixing data, however the same approach did not appear to be extendable to atoms other than C, F, and H. As one part of this study, we considered the use of electronic structure calculations in order to understand whether there is something peculiar about F + H interactions. At least to the level explored to date (MP2 with large and diffuse basis sets) we find that

such calculations are not accurate enough to reproduce the subtle differences in intermolecular potentials that give rise to the interesting mixing behavior.

The use of simple potentials of the sort studied in paper #3 is central to all of our simulation work (and that of most other people as well). For this reason we continued to explore the issues raised by #3 in more detail. We have been testing the ability of a variety of simple conformal potentials and mixing rules to reproduce experimental 2nd-pressure virial data on a wide range of nonpolar molecules. Virial data provides some of the most direct thermodynamic information on intermolecular interactions, and highly accurate data is available on many small molecules. We are currently in the process of writing up this work as paper #10. Perhaps the most important finding reported there is that the Lorentz-Berthelot (LB) combining rules, the default rules used in most simulation work, are a poor choice for most purposes. More sophisticated combining rules, especially when used in conjunction with slightly improved versions of the venerable Lennard-Jones potential, are much more accurate, and can reproduce most available virial data with an accuracy of ~10%. When viewed in the context of this larger body of experimental data, we find that perfluoroalkane + alkane interactions do not look particularly anomalous. Rather the anomaly is only a reflection of false trust in standard methods (especially use of LB combining rules).

2) Solvation Dynamics in Ionic Liquids[1,4,5,7]: Ionic liquids are an emerging class of solvents made up of large asymmetric organic cations and a variety of anions so chosen to be liquid at or near room temperature. They are receiving considerable attention as possible replacements for volatile organic solvents in a range of processes. We have been exploring solvation in ionic liquids with an eye toward understanding how they may differ from traditional polar solvents as media for electron transfer. To date, our published work has entailed the use of steady-state and ps time-resolved emission measurements of solvation and rotational dynamics of probe solutes in a variety of room temperature ionic liquids.

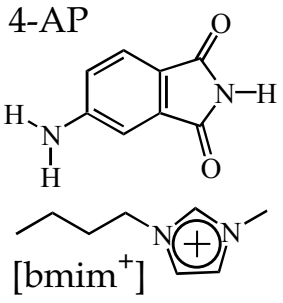

Paper #1, which was one of the first investigations of this type, focused on measuring the behavior of a single probe solute, 4-AP, in the prototypical ionic liquid [bmim$^+$][PF_6^-]. In that study, we found that there is nothing unusual about solute rotation in these highly viscous liquids. Rotation is slow and proportional to solvent viscosity in conformity to simple hydrodynamic models. We discovered that solvation dynamics *are* surprising in that they are dramatically bimodal. Roughly 50% of the solvation takes place in less than 5 picoseconds, whereas the remainder occurs in the nanosecond range at room temperature.

This initial work, and related results from other groups seemed to suggest that biphasic dynamics was characteristic of all ionic liquids. But, paper #4, which involved study of three distinct classes of ionic liquids, showed that the ultrafast component is absent in liquids based on ammonium or phosphonium cations. It now appears that the alkylimadazolium cation, the cation used thus far in most solvation studies, is the source of the ultrafast dynamics. We conjectured (with some support from simulations) that the ultrafast dynamics involves small amplitude motions of an imidazoium cation which lies adjacent to and coplanar with the solute. This aspect of the dynamics remains to be explored further (see Proposal).

Paper #4 and paper #5 served to characterize the general features of the slow (ns) component of the solvation response. We showed that the latter dynamics are highly non-exponential with an overall time scale that is approximately proportional to solvent viscosity. The relationship between solvation rate and viscosity appears to be primarily related to the size of the cation, which is the larger of the two components in all of the ionic liquids studied. It seems likely that the nanosecond solvation dynamics being observed in ionic liquids is analogous to the structural relaxation process observed in many glass-

forming liquids at low temperatures, presumably involving large-amplitude motions of solvent molecules and reorganization of the charge-structure of the liquid. In phosphonium ionic liquids we also observed highly non-exponential solute rotation, similar to what is found in highly viscous supercooled liquids.

Paper #7 presents a brief examination of how much the identity of the probe solute used to measure solvation dynamics affects this dynamics. This study was prompted by the fact that emerging literature reports suggested that solvation times might vary by as much as a factor of 5-6 as a function of solute. Our work showed that the majority of this variation reflects ambiguities in comparing results from different laboratories rather than a real solute effect. Measuring dynamics in a single ionic liquid using six varied probes, we found no more than a 2-fold variation of solvation times.

3) TICT Reactions in PnC Compounds[6,8]: The bulk of Kevin Dahl's Ph.D. thesis (#6) and paper #8 concern a comprehensive experimental study of twisted intramolecular charge transfer ("TICT") reactions in a series of substituted aminobenzonitriles, the "PnC" series. The parent compound ABN does not undergo reaction in the excited state and it is used as a control. In the alkylated solutes, small changes in hybidization with ring size make the driving force and rate of reaction increase systematically in the order P4C< P5C< P6C. Moreover, in the latter cases these rates are comparable to or larger than solvation rates at room temperature. The ultimate goal of our work with these compounds, the pursuit of which will extend into the next grant cycle, is to construct accurate solvent-dependent potentials with which we can model the reaction dynamics and thereby discover how dielectric and mechanical friction control reaction in these and similar systems.

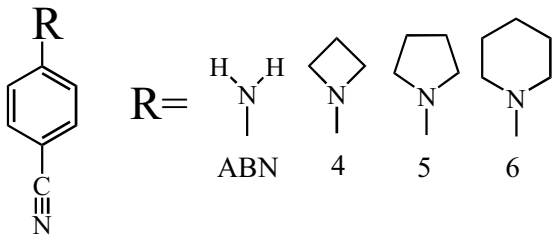

Publication #8 documents our progress to date by reporting characteristics of the steady-state spectra, quantum yields, and time-resolved emission kinetics of the four solutes shown above in 25 room-temperature solvents. Paper #6 also describes the model we employ, which is outlined in Sec. 5 below. In this initial work, we attempted to understand the solvent dependence of the steady-state spectra using a simplified model, one which ignores the distributions over torsional and solvation coordinates, focusing only on the minima in the reaction potentials. Whereas the frequencies of the steady-state absorption and emission spectra of all of the probes could be reasonably modeled in this way using only a dielectric continuum treatment of the solvent, the relative intensities of the LE and CT states could not. Evidently, either the representation of relative radiative rates or of the relative populations of the states requires explicit consideration of the distribution of molecules on the S_1 surface. This requirement is not surprising given the fast kinetics observed in these systems, where reaction times of 10-200 ps are typical. Such times together with semi-empirical calculations indicate small <5 k_BT barriers to reaction and broad minima in the reactive surface. Time-resolved emission experiments also displayed a range of kinetic behavior as a function of solute and solvent. The emission of P4C in most solvents conforms to the behavior expected for classical 2-state kinetics, whereas the emission of P5C and P6C is sometimes of this simple type but often much more complex, displaying multi-exponential LE decays and time-dependent spectral shifts in many solvents. These differences could be rationalized in terms of a combination of solute- and solvent-dependent changes to reaction barriers and solvent frictional effects. We were able to estimate both the free energy change $\Delta_r G$ and rate constant k_f in many solute + solvent combinations. Using correlations between these two observables to approximately determine transmission coefficients for reaction revealed that solvent friction partially controls the rates of the P5C and especially P6C reactions in many solvents, but plays little role in the reactions of P4C. The variable role of solvent friction can be rationalized in terms of systematic variations in the reaction surfaces as

functions of solute and solvent. Such variations were anticipated, and were the motivation for undertaking this extensive study. As hoped, our work thus far has shown the PnC series to be an excellent testing ground for understanding dynamical solvent effects on charge-transfer processes. Further experiments and modeling of these reactions will be an important part of future research.

4) Construction of a Kerr-Gated Emission Spectrometer[9]: Over the past several years Sergei Arzhantsev has devoted most of his time to construction of the general-purpose femtosecond emission spectrometer described in Paper #9. In our previous work, whenever time-resolved emission spectra were desired, we sequentially measured emission decays at a series of wavelengths and reconstructed instantaneous spectra from this series. This approach provides good results in many cases, but when one wishes to examine changes to the shapes of spectra, of importance for examining ultrafast electron transfer systems, the high temporal and spectral resolution provided by the new "Kerr-gated emission spectrometer" are advantageous. The spectrometer uses the dynamic Kerr effect in a medium such as liquid benzene to shutter the spontaneous emission recorded by a spectrograph+CCD combination. Whereas other workers have only demonstrated the technique with solutes having a few ps lifetime, we have sacrificed some time resolution in order construct a spectrometer of general applicability. The current system is capable of providing high-quality spectra of fluorophores such as coumarin 153 (C153; 5-6 ns lifetime) with an instrumental response function of 450 fs (FWHM).

DOE Sponsored Publications:

1. J. A. Ingram, R. S. Moog, N. Ito, R. Biswas, and M. Maroncelli, "Solute Rotation and Solvation Dynamics in a Room-Temperature Ionic Liquid," *J. Phys. Chem. B* **107,** 5926-5932 (2003).
2. K. Dahl, R. Biswas, and M. Maroncelli, "Photophysics and Dynamics of Diphenylbutadiene in Alkane and Perfluoroalkane Solvents," *J. Phys. Chem. B* **107,** 7838-7853 (2003).
3. W. Song, M. Maroncelli, and P. J. Rossky, "Simulations of Alkane - Perfluoroalkane Mixing Behavior using All-Atom Potentials, Failure of the Usual Combining Rules," *J. Chem. Phys.* (2003).
4. S. Arzhantsev, N. Ito, M. Heitz, and M. Maroncelli, "Solvation dynamics of coumarin 153 in several classes of ionic liquids: cation dependence of the ultrafast component," *Chem. Phys. Lett.* **381,** 278-286 (2003).
5. N. Ito, S. Arzhantsev, M. Heitz, and M. Maroncelli, "Solvation Dynamics and Rotation of Coumarin 153 in Alkylphosphonium Ionic Liquids," *J. Phys. Chem. B* **108,** 5771-5777 (2004).
6. K. Dahl, "Experimental Assessment of the Effects of Solvent on the Rate of Excited State Chemical Reactions," Ph.D. Thesis, The Pennsylvania State University, 2004.
7. N. Ito, S. Arzhantsev, and M. Maroncelli, "The probe dependence of solvation dynamics and rotation in the ionic liquid 1-butyl-3-methyl-Imidazolium hexafluorophosphate," *Chem. Phys. Lett.* **396,** 83-91 (2004).
8. K. Dahl, R. Biswas, N. Ito, and M. Maroncelli, "Solvent Dependence of the Spectra and Kinetics of Excited State Charge Transfer in Three Alkylaminobenzonitriles," *J. Phys. Chem. B* in press (2004).
9. S. Arzhantsev and M. Maroncelli, "Design and characterization of a femtosecond fluorescence spectrometer based on optical Kerr gating," submitted to *Appl. Spectrosc.* (2004).
10. W. Song and M. Maroncelli, "Transferable All-Atom Force Fields based on 2-Parameter Potential Functions: How Accurate can They Be?," manuscript in preparation (2004).

Spectroscopy of Organometallic Radicals

Michael D. Morse
Department of Chemistry
University of Utah
315 S. 1400 East, Room 2020
Salt Lake City, UT 84112-0850
morse@chem.utah.edu

I. Program Scope:

In this project, we seek to obtain fundamental physical information about unsaturated, highly reactive organometallic radicals containing open *d* subshell transition metal atoms. Gas phase electronic spectroscopy of jet-cooled transition metal molecules is used to obtain fundamental information about ground and excited electronic states of such species as the transition metal carbides and organometallic radicals such as CrC_2H, $CrCH_3$, and $NiCH_3$. High resolution infrared spectroscopy is applied to the unsaturated transition metal carbonyls, MCO, $M(CO)_2$, $M(CO)_3$, etc.

II. Recent Progress:

A. Optical spectroscopy of NiC, WC, RuC, CrC_2H, $CrCH_3$, and $NiCH_3$

During the past two years, we have carried out resonant two-photon ionization (R2PI) and dispersed fluorescence (DF) spectroscopic studies of the transition metal carbides NiC,[1] WC,[2] and RuC.[3] Our work has established that NiC has an $X\ ^1\Sigma^+$ ground state, with a bond length of $r_e'' = 1.6273(2)$ Å and vibrational constants of $\omega_e'' = 875.155$ cm^{-1} and $\omega_e''x_e'' = 5.38$ cm^{-1} for $^{58}Ni^{12}C$.[1] We have now demonstrated that all three isovalent molecules, NiC, PdC, and PtC, have $X\ ^1\Sigma^+$ ground states.

In another recently published study, we have reported on the R2PI and DF spectra of tungsten carbide, WC.[2] Unlike its congener, MoC, which has a δ^2, $^3\Sigma^-$ ground state, WC has a $\delta^1\ \sigma^1$, $^3\Delta_r$ ground state. This discrepancy results from the relativistic stabilization of the 6*s* orbital in the 5*d* series. From our work, ground state parameters of $r_0'' = 1.7135$ Å, $\omega_e'' = 983$ cm^{-1}, and $\omega_e''x_e'' = 11$ cm^{-1} have been determined.

Our paper on the spectroscopy of RuC in the 18,000 – 24,000 cm-1 region is now in press at J. Chem. Phys.[3] In this paper, our analysis of the $v'=0$-4 levels of the $[18.1]^1\Pi$ state has yielded an RKR potential for this state. Three additional new band systems are also reported in this manuscript, along with RKR analyses of all previously known states.

We are now in the process of making minor revisions to a paper on the vibrationally resolved R2PI and DF spectra of CrC_2H, $CrCH_3$, and $NiCH_3$, which will be published in J. Chem. Phys.[4] Well-characterized vibronic spectra have been recorded for CrC_2H and $NiCH_3$, and these have allowed metal-carbon vibrational frequencies to be measured for these species in both the ground and the excited states. Rotationally resolved scans over all three molecules have been accomplished, but these have not yet yielded to analysis.

Finally, during the collection of data on CrC_2H, we also recorded the spectrum of the minor isotopomer of chromium hydride, $^{50}Cr^1H$. We measured the excited state lifetime of this species, which is currently of considerable interest in astrophysics. Our paper is currently undergoing revision for publication in the Astrophysical Journal.[5]

B. Infrared Spectroscopy of unsaturated transition metal carbonyls

We have recently developed a slit-jet discharge source diode laser spectrometer for high-resolution investigations of unsaturated transition metal carbonyls. The device uses a slit orifice with a width of 200 μm and a length of 15 mm. A Teflon insulator separates the slit aperture from a pair of stainless steel discharge electrodes. During the operation of the pulsed valve, the discharge electrodes are biased to a negative potential, inducing a discharge in which electrons are accelerated into the slit channel, completing the circuit at the grounded slit nozzle body. Volatile organometallic molecules such as $Cr(CO)_6$ and $Fe(CO)_5$, seeded in the argon carrier gas, are exposed to the discharge, producing fragment species such as CrCO, $Cr(CO)_2$, $Cr(CO)_3$, *etc*.

Following supersonic expansion into vacuum, the beam of molecular fragments is crossed with the output of a lead-salt diode laser that is multipassed across the length of the slit jet expansion using a Perry cell. The transmitted laser intensity is detected using a HgCdTe detector. In order to increase the detection efficiency and discriminate against precursor molecule absorptions and noise, the discharge is pulsed at 15 kHz (33.3 μs on, 33.3 μs off) and the preamplified signal is detected using a lock-in detector.

In addition to the main IR laser beam, which is multipassed across the output of the pulsed slit jet discharge, partial reflections are used to record (1) fringes from a 0.048 cm^{-1} free spectral range Ge étalon, and (2) the spectrum of a reference gas, typically OCS, N_2O, or allene. These are used for absolute calibration of the instrument.

We have shown that the pulsed discharge, operating at 15 kHz, destroys the $Fe(CO)_5$ molecule, leading to the formation of fragment species. This is illustrated below, where the IR absorption is plotted as a function of time during the nozzle pulse, with the IR laser tuned to an $Fe(CO)_5$ parent molecule absorption. The profile of the nozzle pulse (approximately 2 ms in duration) is evident. It is also apparent that roughly 30% of the $Fe(CO)_5$ molecules are destroyed when the pulsed discharge is turned on.

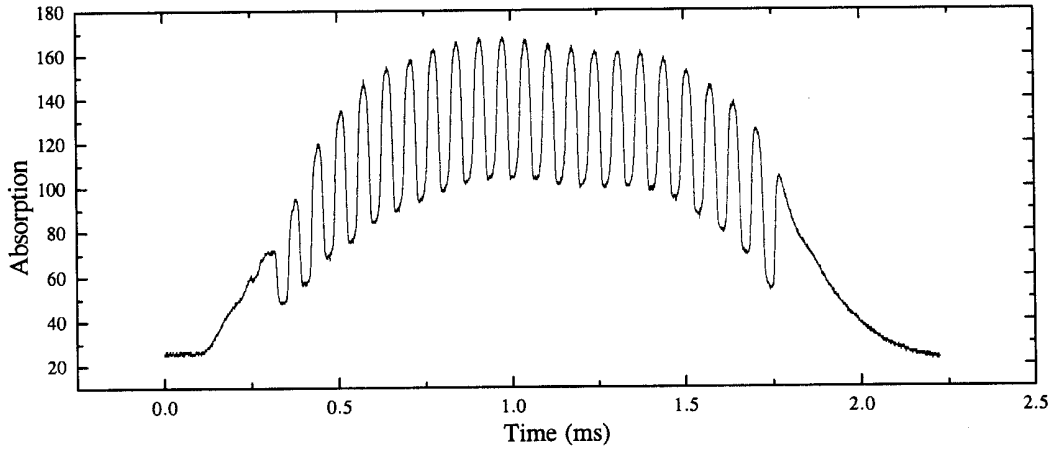

Figure 1. The diode laser is tuned to an absorption in the spectrum of $Fe(CO)_5$, allowing a profile of the nozzle pulse to be recorded. A discharge is pulsed on and off during this nozzle pulse, at a rate of 15 kHz, significantly depleting the $Fe(CO)_5$ molecules during each pulse of the discharge.

We have tested this system by recording the previously known spectra of the fragment molecules FeCO and $Fe(CO)_2$. Shown below are portions of the spectra:

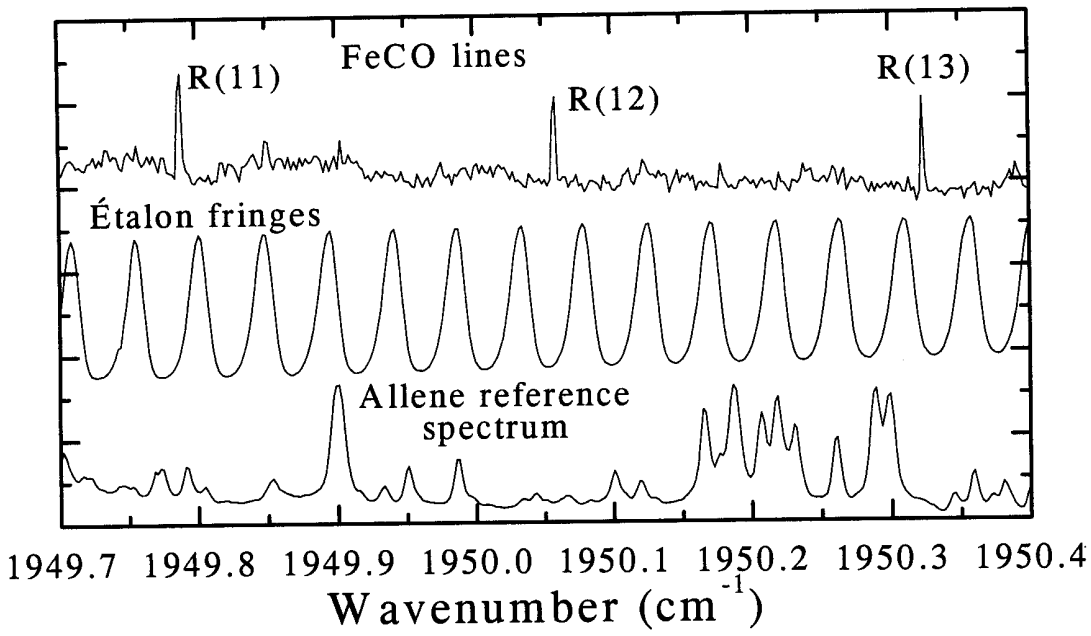

Figure 2. A scan of the diode laser over the 1949.7-1950.4 cm^{-1} range, showing absorption lines of the FeCO radical, fringes of the reference étalon, and the absorption spectrum of allene, which is used for absolute calibration.

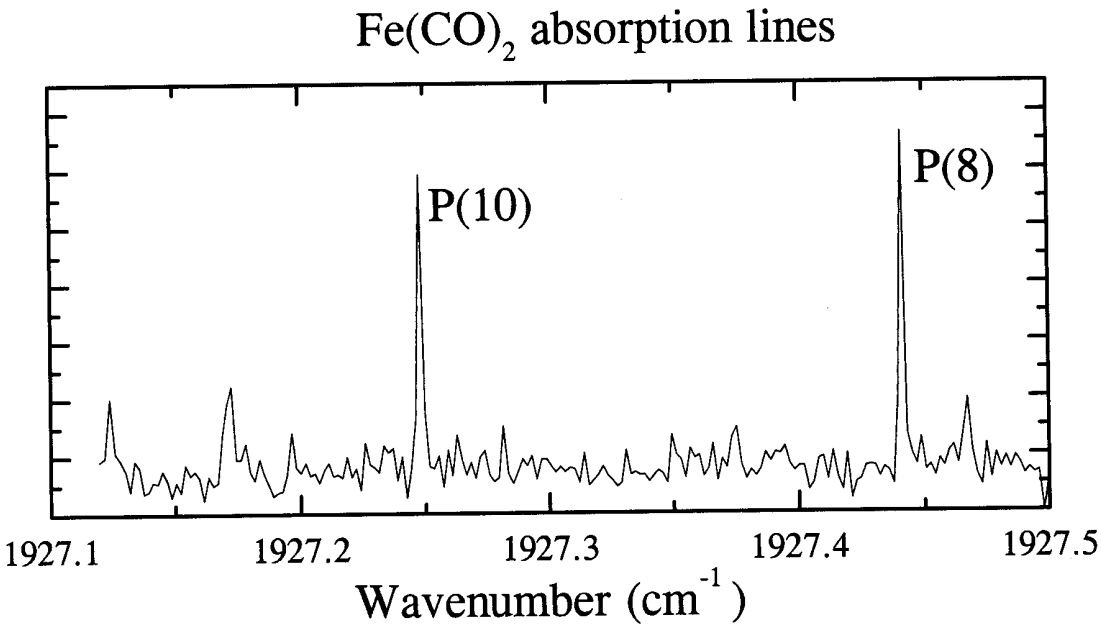

Figure 3. A scan of the diode laser over the 1927.1-1927.5 cm^{-1} range, showing the P(8) and P(10) absorption lines of the $Fe(CO)_2$ radical. The P(9) line is absent due to nuclear spin statistics in this linear molecule.

III. Future Plans

A. R2PI and DF spectroscopy of transition metal carbides and radicals

We have recorded spectra of TiC, at rather high rotational temperatures. During the upcoming period, we plan to analyze the rotational structure and thereby measure the ground and excited state symmetries and rotational constants. This molecule is important for understanding the growth processes leading to formation of metallocarbohedrenes (met-cars). In addition, TiC is likely present in the interstellar medium and knowledge of its spectrum will enable a search for this species. We also plan to study transition metal carbides that have high ionization energies, which have previously been inaccessible to our R2PI method. These include CuC, AgC, AuC, OsC, and IrC. We hope to obtain a satisfactory rotational analysis of the more complicated transition metal radicals CrC_2H and $NiCH_3$ as well. Finally, we plan to begin work on species that are related to catalyst support materials by investigating Mg_2O, Mg_3O, LiMgO, etc.

B. IR spectroscopy of unsaturated transition metal carbonyls

Having successfully generated FeCO and $Fe(CO)_2$, and detected their IR absorptions, we now plan to move to molecules that have not previously been investigated by high-resolution IR spectroscopy. Luckily, the locations of strong IR absorptions are known from matrix isolation and some low-resolution gas phase studies. Target molecules to be sought are listed below, along with the expected IR frequencies:

		$Fe(CO)_3$	1950 cm^{-1}		
NiCO	2015 cm^{-1}	$Ni(CO)_2$	1990 cm^{-1}	$Ni(CO)_3$	2030 cm^{-1}
CrCO	2010 cm^{-1}	$Cr(CO)_2$	1990 cm^{-1}	$Cr(CO)_3$	2000; 1880 cm^{-1}
MoCO	1890 cm^{-1}	$Mo(CO)_2$	1900 cm^{-1}	$Mo(CO)_3$	2000; 1888 cm^{-1}
WCO	1870 cm^{-1}	$W(CO)_2$	1890 cm^{-1}	$W(CO)_3$	1890 cm^{-1}

The aim of this work will be to establish the vibrational frequencies, rotational constants, geometries, bond lengths, and electronic symmetries of these molecules. After success on several of these molecules, we hope to move on to studies of the transition metal nitrosyls, such as CoNO, FeNO, etc.

IV. Publications from DOE Sponsored Research 2002-2004:

[1] D. J. Brugh and M. D. Morse, "Resonant two-photon ionization spectroscopy of NiC," J. Chem. Phys. **117**, 10703-10714 (2002).

[2] S. M. Sickafoose, A. W. Smith and M. D. Morse, "Optical spectroscopy of tungsten carbide (WC)," J. Chem. Phys. **116**, 993-1002 (2002).

[3] N. F. Lindholm, D. A. Hales, L. A. Ober and M. D. Morse, "Optical spectroscopy of RuC: 18 000 - 24 000 cm^{-1}," J. Chem. Phys. in press, (2004).

[4] D. J. Brugh, R. S. DaBell and M. D. Morse, "Vibronic spectroscopy of unsaturated transition metal complexes: CrC_2H, $CrCH_3$, and $NiCH_3$," J. Chem. Phys. submitted, (2004).

[5] S. Shin, D. J. Brugh, and M. D. Morse, "Radiative lifetime of the v=0,1 levels of the A^{6+} state of CrH," Astrophys. J., submitted, (2004).

Localized Photoemission from Gold Nanostructures and Electromagnetic Friction

Lukas Novotny (novotny@optics.rochester.edu)
University of Rochester, The Institute of Optics, Rochester, NY, 14627.

1 Program Scope

We study the local interaction between a laser-irradiated local probe, such as a metal tip, and a sample placed in close proximity. Under certain conditions, the local probe is able to confine and enhance the incoming radiation. For metal tips it has been theoretically predicted that the enhancement factor can be three to four orders of magnitude, i.e. the intensity at the metal tip is a factor $10^3 - 10^4$ stronger than the intensity of the incoming radiation. The enhanced field at the tip acts as a highly confined light source for a local, spectroscopic interaction with the sample surface. The field enhancement originates from a combination of electrostatic lightning-rod effect (quasi-singularity at the tip) and surface plasmon resonances which are strongly material and geometry dependent. The experimentally determined enhancement factors are not as strong as the theoretically predicted ones and it is the focus of our project to understand the critical parameters for maximizing the enhancement effect.

By moving the sample underneath the laser-irradiated metal tip and acquiring an optical response for different tip-sample positions we are able to record an optical raster-scan image with a resolution that solely depends on the tip sharpness. The principle of this *tip-enhanced spectroscopy* is shown in Fig. 1. So far, we were able to demonstrate resolutions better than 20nm using 1) two-photon excited fluorescence [1], 2) second-harmonic generation [2], and 3) Raman scattering [3]. Our work has enabled systematic studies of single molecule fluorescence in inhomogeneous environments and of defects and dopants in single-walled carbon nanotubes.

While studying the electromagnetic response of laser-irradiated gold tips we discovered that the tips emit radiation over a broad range of frequencies when excited with femtosecond laser pulses. We have further investigated the origin of this radiation and determined that it is due to second-harmonic generation [2] and broadband photoluminescence [4]. It was found that in both cases the emission originates from the tip end and hence it constitutes a highly confined light source. The yield of photoluminescence was found to be a good indicator for the strength of local field enhancement and we performed a study on metal nanoclusters to demonstrate this effect [5].

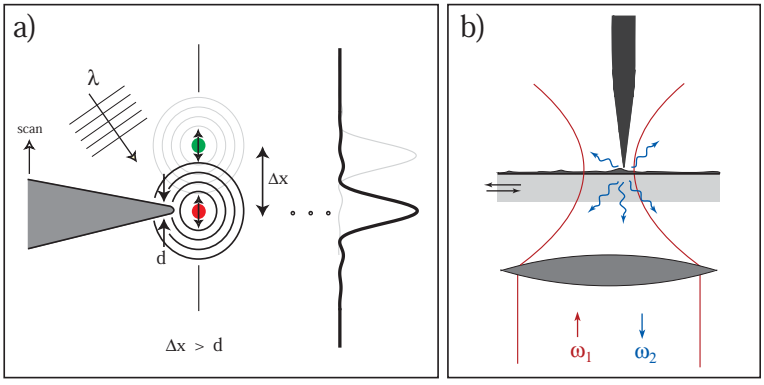

Figure 1: *Principle of the local field-enhancement technique. A laser-irradiated metal tip (polarization along tip axis) enhances the incident electric field near its apex thereby creating a localized photon source. a) Schematic of the method. b) Practical implementation: a higher-order laser beam is focused on a sample surface and a sharply pointed metal tip is positioned into the laser focus. The enhanced fields at the tip locally interact with the sample surface thereby exciting a spectroscopic response that is collected by the same objective and directed on a detector.*

2 Recent Progress

In the past year, we have investigated the photoluminescence from laser-irradiated metal tips. We have determined that the luminescence intensity is an indirect measure for the strength of field enhancement and we developed a technique for the characterization of so-called hot-spots associated with aggregates of metal particles [5]. In a parallel effort, we have investigated theoretically the nature of friction between tip and sample [6]. This study led to some remarkable predictions associated with so-called electromagnetic friction: 1) strong friction is associated with dielectric bodies in relative motion, and 2) electromagnetic friction is even present in for a single body if it interacts with thermal background radiation. This means that any object will ultimately come to rest. However, typical friction forces are in the range of atto-Newtons which makes it difficult to be observed at ambient conditions. Both projects, locally excited photoluminescence and electromagnetic friction, will be described in the following separate sections.

2.1 Localized photoluminescence

The optical properties of metal nanoparticles are strongly influenced by their size, their shape, and by their environment such as the proximity to other particles. When the dimensions of nanoparticles becomes smaller than the wavelength of the exciting light, energy can be confined in small spatial regions through the local excitation of surface plasmon resonances. The enhanced fields in these regions are used in a wide range of applications including surface enhanced Raman scattering (SERS), near-field microscopy, and nanoscale optical devices. Direct experimental measurements of electromagnetic fields localized between closely spaced nanostructures are needed to validate theoretical predictions and to develop systems with improved properties. In our study, we investigated the three-dimensional spatial variation of the electromagnetic field as a function of the separation between a gold nanoparticle and a sharp gold tip. We took advantage of the intrinsic photoluminescence properties of gold nanostructures. Two-photon excited luminescence was found to be sensitive to the local field enhancement on rough metal films [4]. In our experiments, we localize regions of strong field enhancement by measuring the spatial distribution of the photoluminescence yield.

Individual nanoparticles deposited on a transparent substrate were excited by the field of a tightly focused femtosecond laser, similar to the situation shown in Fig. 1b. The high peak intensity ($\approx 110\,\mathrm{GW}\ /\ \mathrm{cm}^2$) associated with ultrashort pulses $\approx 120\,\mathrm{fs}$ excites electrons in the metal particles from the d band to the sp conduction band by two-photon absorption [4]. Subsequent photoluminescence is collected with the same objective as used for excitation and is directed toward either a sensitive avalanche photodetector for imaging purposes or to a CCD spectrometer to acquire luminescence spectra.

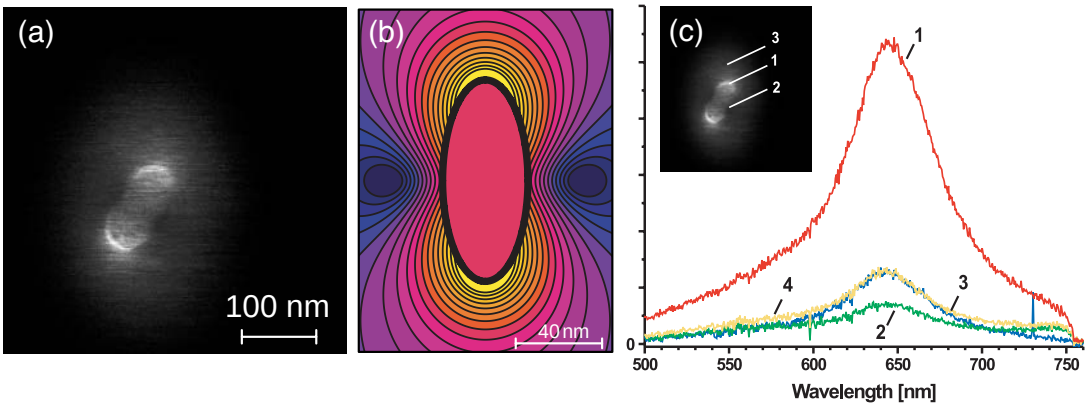

Figure 2: *(a) Two-photon excited photoluminescence image of an elliptical cluster of gold particles. The halo corresponds to the farfield luminescence. (b) Calculated intensity distribution of ellipsoid with the same dimensions excited near resonance* $\approx 650\,nm$. *(c) Photoluminescence spectrum (excitation at* $780\,nm$*) acquired for different tip positions.*

Fig. 2a shows the photoluminescence image originating from an elliptical gold particle as it is raster-scanned underneath the gold tip. The luminescence originates from the gold particle and not from the tip. The tip is used to locally scatter the near-field of the generated photoluminescence and hence to enable diffraction-unlimited imaging. As seen in Fig. 2a, the photoluminescence is strongly enhanced at the extremities of the ellipsoidal particle. On the other hand, the signal intensity is reduced at the two diametrically opposed points along the short axis. The photoluminescence image strongly resembles the calculated surface intensity distribution of an ellipsoid excited at resonance, as shown in Fig. 2b. The image demonstrates the dipolar character of the excited particle: charge accumulation at both ends along the long axis and charge depletion along the short axis. The calculation was based on the multiple multipole method (MMP) for an excitation wavelength of 650 nm and a dielectric constant of $\varepsilon_{Au} = -12.9 + 1.09i$.

We have determined that there is no resonant coupling between tip and particle. This is evidenced by the recorded spectra shown in Fig. 2c. The gray curve in represents the emission of the ellipsoidal particle without the tip present. The spectrum is peaked at 644 nm, in agreement with the calculated resonance. The particular shape of the spectrum originates from the convolution of the density of states available at these energies with the intrinsic surface plasmon resonance of the particle [4]. The spectrum was also recorded as a function of particle position (positions 1, 2, 3 and 4). No shift of the resonance peak is observed. Only the signal amplitude is affected by the tip and the overall shape of the spectrum is conserved. Therefore, the tip has a negligible influence on the intrinsic response of the particle. We thus have the analogous situation to two coupled oscillators, one of which is much weaker than the other. Because the tip can be regarded as a passive probe, we obtain a direct measurement of the field enhancement and thus of the local charge distribution on the surface of the dimer.

In conclusion, in this study we showed that local field enhancement at nanoscale metal structures leads to local photoluminescence excited by two-photon absorption. A direct map of the distribution of local fields (hot spots) can be recorded by locally scattering the photoluminescence intensity using a metal tip. The presented method is a promising approach for the characterization of field enhancing structures used in future plasmonic devices. It will also be useful in the study of hot spots responsible for the giant enhancement of Raman cross sections in SERS.

2.2 Electromagnetic Friction

To maintain a sharp metal tip at a distance of ≈ 1 nm from the sample surface a highly sensitive feedback mechanism is needed. A common approach is to oscillate the tip with an amplitude of less then $1\mathring{A}$ parallel to the sample surface and to measure the friction force as a function of tip-sample distance. Interestingly, this shear-force can even be measured in UHV conditions and at temperatures as low as 4 K [7]. There is no theory which would render an order-of-magnitude agreement with experimental measurements.

We performed a general study of electromagnetic friction arising from charge correlations between two bodies in relative motion [6]. It is well known that electromagnetic interactions between two charge-neutral objects give rise to an attractive force, known as the *dispersion force*. Our study shows that if the two objects are in relative motion to each other then there appears an additional non-conservative force which brings the motion ultimately to rest. We determined that the force is much stronger for dielectric objects than for metal objects. In addition, it was found that only fluctuations in the frequency range $0 \,..\, 100$ Hz contribute significantly to the force. This force has direct consequences for the development of future nanoscale systems and for various proposals in the field of quantum information. Dissipative interactions limit the performance of nano-electro-mechanical systems (NEMS) and will lead to increased decoherence in miniaturized particle traps such as ion-traps and atom chips.

A remarkable outcome of our theory is that friction is even present in empty space as long as the temperature is finite. Thus, an object moving in empty space comes ultimately to rest. This result is consistent with earlier existing theories. In another limit, for short distances between particle and surface, we can neglect retardation and find that friction becomes strongly material dependent, i.e. friction is many orders of magnitude stronger for dielectric materials than for conducting materials. Also important is the finding that only thermal fluctuations in the low-frequency range of $0 \,..\, 100$ Hz are significant.

3 Future Plans

In a continuation of our project we will investigate the possibility of performing absorption spectroscopy on single molecules using the localized emission near a metal tip as a photon source. We will explore metal tips of finite length to increase the field enhancement factor further by imitating concepts known from antenna theory.

References

[1] E. J. Sanchez, L. Novotny, and X. S. Xie, "Near-field fluorescence microscopy based on two-photon excitation with metal tips," *Phys. Rev. Lett.* **82**, 4014 (1999).

[2] A. Bouhelier, M. Beversluis, A. Hartschuh, and L. Novotny, "Near-field second-harmonic generation induced by local field enhancement," *Phys. Rev. Lett.* **90**, 13903 (2003).

[3] A. Hartschuh, E. J. Sanchez, X. S. Xie, and L. Novotny, "High-resolution near-field Raman microscopy of single-walled carbon nanotubes," *Phys. Rev. Lett.* **90**, 95503 (2003).

[4] M. R. Beversluis, A. Bouhelier, and L. Novotny, "Continuum generation from single gold nanostructures through near-field mediated intraband transitions," *Phys. Rev. B.* **68**, 115433 (2003).

[5] A. Bouhelier, M. R. Beversluis, and L. Novotny, "Characterization of nanoplasmonic structures by locally excited photoluminescence," *Appl. Phys. Lett.* **83**, 5041 (2003).

[6] J. R. Zurita-Sanchez, J.-J. Greffet, and L. Novotny, "Near-field friction due to fluctuating fields," *Phys. Rev. A* **69**, 022902 (2004).

[7] B. C. Stipe, H. J. Mamin, T. D. Stowe, T. W. Kenny, and D. Rugar, "Noncontact friction and force fluctuations between closely spaced bodies," Phys. Rev. Lett. **87**, 96801 (2001).

[8] J. R. Zurita-Sanchez and L. Novotny, "Multipolar interband absorption in a semiconductor quantum dot. II. Magnetic dipole enhancement," *J. Opt. Soc. Am. B* **19**, 2722 (2002).

[9] J. R. Zurita-Sanchez and L. Novotny, "Multipolar interband absorption in a semiconductor quantum dot. I. Electric quadrupole enhancement," *J. Opt. Soc. Am. B* **19**, 1355 (2002).

[10] A. Bouhelier, M. R. Beversluis, and L. Novotny, "Near-field scattering of longitudinal fields," *Appl. Phys. Lett.* **82**, 4596 (2003).

[11] A. Bouhelier, J. Renger, M. Beversluis, and L. Novotny, "Plasmon coupled tip-enhanced near-field microscopy," *J. Microsc.* **210**, 220 (2003).

[12] A. Hartschuh, H. N. Pedrosa, L. Novotny, and T. D. Krauss, "Simultaneous fluorescence and Raman scattering from single carbon nanotubes," *Science* **301**, 1354 (2003).

[13] A. Bouhelier, A. Hartschuh, M. R. Beversluis, and L. Novotny, "Near-field optical microscopy in the nanosciences," in *Microscopy for Nanotechnology*, N. Yao and Z. L. Wang (eds.), Springer Verlag, in print (2004).

[14] A. Hartschuh, M. R. Beversluis, A. Bouhelier, and L. Novotny, "Tip-enhanced optical spectroscopy," *Phil. Trans. R. Soc. Lond. A* **362**, 807 (2004).

DOE sponsored publications (2002-2004): Refs. [2], [4], [5], [6], [8], [9], [10], [11], [12], [13], [14].

LASER DYNAMIC STUDIES OF PHOTOREACTIONS ON SINGLE-CRYSTAL AND NANOSTRUCTURED SURFACES

R. M. Osgood, Columbia University, New York, NY 10027

ABSTRACT

This research program examines the photon-initiated reaction mechanisms, half-collision dynamics, and other optically induced dynamics effects, which occur for adsorbates on well-characterized, semiconductor or metal-oxide surfaces. The research is directed toward achieving the fundamental understanding necessary for several DOE-based photochemistry needs including surface photodecomposition of contaminants, photoelectrochemical energy conversion, and heterogeneous photocatalysis. Our current program has yielded several new research results on the basic chemical dynamics of surface photofragmentation. These include the following:

First, adsorbed thiolate layers have been used to investigate heterogeneous electron-transfer to surface-adsorbed electron-detector molecules. Our earlier work on photoinitiated substrate-electron bond-cleavage showed that tunneling of electrons across the surface barrier to target surface molecules is an important phenomenon in UV photoreactions. One approach to investigating this process is to use inert organic-overlayer tunneling barriers, with variable electron properties in conjunction with methyl-halide

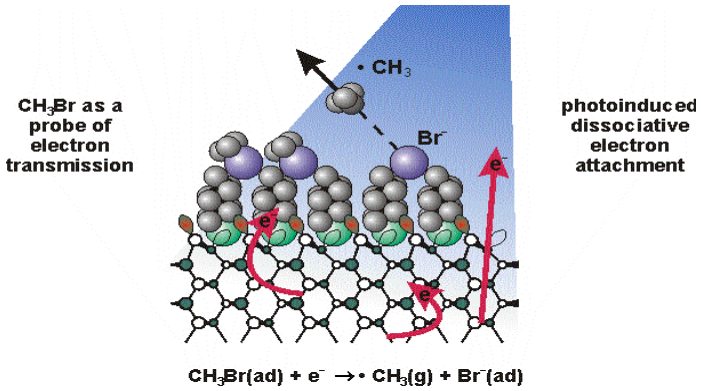

Fig. 1: Using the system: CH_3Br/Organic Spacer/GaAs(110) to probe how spacer chain length affects photoiniated electron transport through a thiolate surface layer

adsorbates as surface electron "detectors" or target molecules; see schematic sketch in Fig. 1. Variable property spacer layers had been used earlier, for example, in electron-transport studies for electrochemistry; in this case, barriers of thiols of varying thickness were employed. With regard to a specific system for our studies, our measurements of adsorbed alkyl sulfides show that these species exhibit negligible photoreactivity when adsorbed in monolayer quantities upon GaAs(110) and that methyl bromide is an excellent electron detector, since each attachment event yields one desorbed CH_3 moiety. Using this surface system, our photoreactions experiments have shown that surface UV photoreactions increase monotonically with the thickness of the spacer layer. The simplest interpretation of our results builds upon detachment physics discussed earlier by Sanche and coworkers using external electron-beam irradiation. In this model, the probability for transmission through the chain is essentially unity, however, the process of recapture, which is included in heuristic theories as the survival rate, is decreased through increased distance of the attaching molecule from the surface.

Second, a REMPI probe has been employed to correlate photofragment vibronic excitation with bond-scission mechanism, i.e., either electron-mediated, or via direct photodissociation. For example, we have used this technique to examine the internal-state distributions of methyl fragments that are produced by photoinduced dissociative electron attachment on surfaces. These experiments have given the first insight into the vibronic distributions for the process of dissociative electron attachment, showing that electron attachment yields more vibrational excitation than does direct photodissociation, a result, which can be explained by the geometry of the negative-ion transition state.

Third, our program has investigated photofragmentation on small-band-gap, metal-oxide surfaces and showed that unlike that on wide-band-gap surfaces, electron-mediated chemistry dominates the photochemistry. In this case, the model system used was CH_3I adsorbed on the (2×2) magnetite-selvedge surface of single-crystal hematite. Our experiments identified the electron-attachment process by use of quadrupole TOF mass spectroscopy to measure the velocity of the ejected CH_3 photofragments. The measurements also showed the coverage-dependent change in the relative ratio of the direct dissociation TOF peak and that of the dissociative electron-attachment peak.

We are now altering our research focus to photochemical dynamics on nanostructured surfaces and the surfaces of nanoobjects. Thus, we will explore photoreaction dynamics, i.e., fragment energetics and angular distributions from UV-irradiated adsorbates, on heavily reconstructed oxide surfaces and oxide nanocrystals. The research tools will be time-of-flight detection, SXPS, STM, standard UHV probes, and theoretical *E&M* and molecular computational tools. We have *already* begun collaboration with the Nanocatalysis Group (Hrbek) at Brookhaven National Laboratory

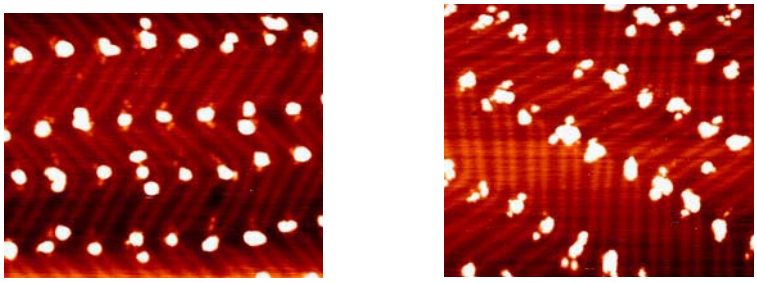

Fig. 2: STM images made in collaboration with Jan Hrbek(BNL) and Zhen Song(Columbia) at BNL showing Mo nanocrystals formed on an covered and bare Au(111) surface. Note that the clusters are present at the Au-elbow sites.

with the goal of examining the growth of narrow size distributions of nanoclusters on TiO_2 surfaces or of TiO_2 nanoclusters on metal surfaces. Our first approach to synthesizing these clusters is based on metal deposition on various ice films, such as water and ammonia; initially we have examined Mo – see Fig. 2. The experiments involve the STM probes and SXPS probes at BNL. After the nanocluster preparation method is clearly established and characterized, photochemical-dynamics experiments will be undertaken.

Publications, 2002-2004

1. N. Camillone, III, K. Adib, J.P. Fitts, K.T. Rim, G.W. Flynn, S.A. Joyce, and R.M. Osgood, Jr., "Surface-Termination-Dependence of the Reactivity of Single-Crystal Hermatite with CCl_4." Surf. Sci., 511, 267 (2002).
2. K. Adib, N. Camillone III, J.P. Fitts, K.T. Rim, G.W. Flynn, S.A. Joyce and R.M. Osgood, Jr., "CCl_4 Chemistry on the Magnetite Selvedge of Single-Crystal Hematite: Competitive Surface Reactions." Surf. Sci 497, 127 (2002).
3. K. Adib, D.R. Mullins, G. Totir, N. Camillone III, J.P. Fitts, K.T. Rim, G.W. Flynn and R.M. Osgood, Jr., "Dissociative Adsorption of CCl_4 on the Fe_3O_4 (111)-(2x2) Selvedge of α-Fe_2O_3 (0001)." Surf. Sci. 524, 113 (2002).
4. A. Srivastava, and R.M. Osgood, Jr., "Photoreaction Dynamics of CH_3I Multilayers on GaAs (110): REMPI Probing of the CH_3 Umbrella Mode." Chem. Phys. Lett. 355, 371 (2002).
5. N. Camillone III, K. Adib, A. Khan, D. Mocuta and R..M. Osgood, Jr., "Dimethyl Sulfide Formation from Adsorbed Methanethiol: Surface-trapping of UV-generated Reaction Intermediates." J. Phys. Chem B 106, 12491 (2002).
6. K. Adib, G.G. Totir, J.P. Fitts, T. Miller, G.W. Flynn, S.A. Joyce and R.M. Osgood, Jr., "Chemistry of CCl_4 on Fe_3O_4(111)-(2x2) Surfaces in the Presence of Adsorbed D_2O." Surf. Sci. 537, 191 (2003).
7. Z. Zhu, A. Srivastava, and R.M. Osgood, Jr., "Reactions of Organosulfur Compounds with Si(100)," J. of Phys. Chem. B 107, 13939 (2003).
8. A. Srivastava and R.M. Osgood, Jr., "State-Resolved Dynamics of 248 nm Methyl-Iodide Fragmentation on GaAs(110)." J. of Chem. Phys. 119, 10298 (2003).
9. K.T. Rim, J.P. Fitts, T. Muller, K. Adib, N. Camillone III, R.M. Osgood, Jr., S.A. Joyce and G.W. Flynn, "CCl_4 Chemistry on the Reduced Selvedge of a α-Fe_2O_3(0001) Surface: A Scanning Tunneling Microscopy Study." Surface Science 541, 59 (2003).
10. K.T. Rim, T. Muller, J.P. Fitts, K. Adib, N. Camillone III, R.M. Osgood, Jr., E.R. Batista, R.A. Friesner, B.J. Berne, S.A. Joyce, and G.W. Flynn, "An STM Study of Competitive Surface Reactions in the Dissociative Chemisorption of CCl_4 on Iron Oxide Surfaces." Accepted by Surf. Sci. (2003).
11. G. G. Totir, Y. Le and R. M. Osgood, Jr., "Photoinduced Reaction Dynamics of Halogenated Hydrocarbons on Iron Oxide Surfaces: CH_3I on Fe_3O_4 (111)-(2x2)", Subm. JCP.
12. Z. Zhu, T. Andelman, M. Ying, S. O'Brien, R. Osgood and S. Ehrlich, "Synchrotron X-ray Scattering by ZnO Nanorods: Self-Assembly and Growth," subm to Nanoletters.
13. Z. Zhu, A. Chen, A. Srinivastava and R. Osgood, "A Comparative Study of Metal-Catalyzed Growth of Nanowires," subm to J. Crystal Growth.

Optical manipulation of ultrafast electron and nuclear motion on metal surfaces

Hrvoje Petek (petek@pitt.edu)
Department of Physics and Astronomy
University of Pittsburgh
Pittsburgh, PA 15260

Program scope. Alkali atom covered metal surfaces are of interest as models for chemisorption, and for practical applications in catalysis and as cathode materials.[1] Despite being the object of numerous experimental and theoretical studies spanning more than 70 years, the nature of chemisorption of alkali atoms on metals is still poorly understood.[2, 3] Upon chemisorption at low coverage alkali atoms are thought to be nearly completely ionized with the outermost *ns* electron delocalized in the conduction band of the substrate. Since it is difficult to detect the additional DOS contributed by the *ns* electron by most elsctron spectroscopic techniques, the nature of the chemisorption bond is not well understood.[4] By contrast, the excited electronic states of alkali atom covered surfaces are characterized by a sharp anti-bonding resonance appearing at ~3 eV above the Fermi level E_F and designated by A in Fig. 1.[5, 6] The lifetime of this state strongly depends on the nature of the metal substrate, the crystal orientation, and the size of the alkali atom.[7] Excitation of this state on the Cs/Cu(111) leads to the nuclear motion along the desorption coordiante, which we study by time-resolved two-photon photoemission spectroscopy.[3, 8, 9] We are undertaking a systematic study the electronic structure and desorption dynamics of alkali atom covered noble metal surfaces. Here we present preliminary studies on the changes in the electronic structure as a function of coverage of alkali atoms (K, Rb, and Cs) on Cu(111) surface. We specifically focus on the change in the properties of the intrinsic Shoclkley surface state (SS) on Cu(111) in the presence of impurities.

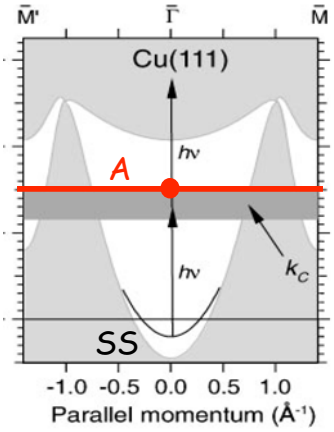

Figure 1. The L-projected band structure of Cu(111).

Recent progress. We investigate one and two-photon photoemission (1PP and 2PP) excited with the second (3.1 eV) and fourth (6.1 eV) harmonics of a <10 fs Ti:sapphire laser. The normal photoemission is detected by scanning a 7-channel hemispherical electron energy analyzer. The photoemission spectra are recorded by repetitively scanning the analyzer energy while depositing alkali atoms from SAES getter sources. The alkali atom source is equipped with getters for Cs, Rb, and K, and can be tilted to achieve uniform flux from each source onto the surface. The surface is either at room temperature or 90 K during the deposition.

Figure 2 shows a series of 2PP spectra obtained by exposing the clean Cu(111) surface to a constant flux of Cs and repetitively scanning the analyzer. The spectra show the well-known decrease in the work function as the surface concentration of Cs increases. We estimate the Cs concentration from the change of the work function with Cs coverage reported in literature.[10] The p(2x2) structure is defined as 1 monolayer ML. In addition to the work function change, the spectra show the appearance of the Cs

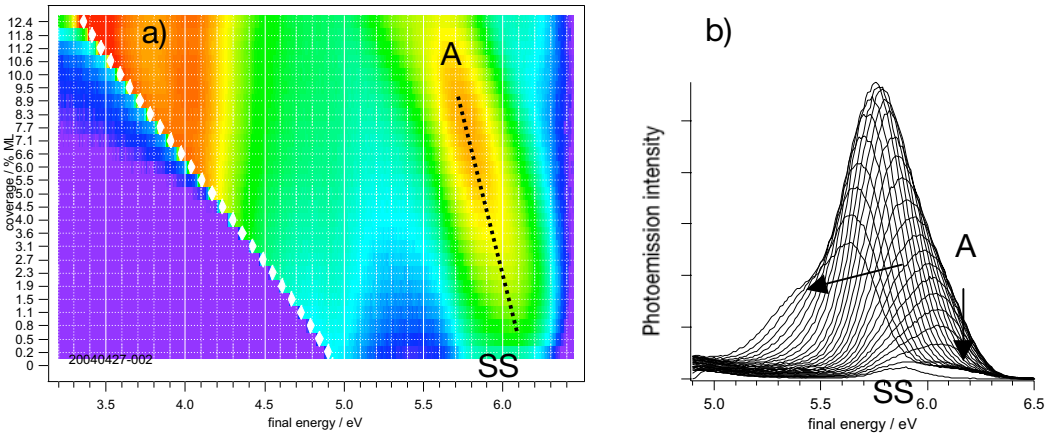

Figure 2. a) 3D plot of 2PP spectra of Cs/Cu(111) at 300 K as a function of Cs coverage. The doted line indicates approximate shift in the energy of the antibonding state A with coverage. b) detail of the photoemission spectra in a) showing the tuning of A through the resonance with SS.

antibonding state at ~3.1 eV above E_F, which shifts to ~2.7 eV at the highest coverages studied. We are limitied to studying this coverage range because one photon photoemission becomes prominant for >0.1 ML of Cs, and the resulting increase in the photoelectron yield leads to distortion of the spectra due to space charge effects.

Figure 2b shows a detail of the photoemission spectra near the resonant excitation from the Shockley surface state to the antibonding state; at low and high coverages we observe distinct SS and A peaks, while for intermediate coverage the two peaks blend and 2PP is resonance enhanced. The 2PP spectra of Rb and K covered Cu(111) surfaces are very similar with A appearing at 3.1 eV, except that the linewidths are broader due to faster resonant charge transfer from A to the conduction band of copper.[7]

In order to be able to interpret the changes in the 2PP spectra of Fig. 2, especially the resonant excitation process A ← SS, we have measured independently the changes in the occupied surface structure induced by the alkali atom adsorption. Figure 3 shows a series of photoemission spectra as a function of Cs coverage as in Fig. 2, but here the photoemission is induced by one-photon absorption of 6.1 eV light. The 1PP spectra show the change in the work function of copper and shift to lower energy of SS, which

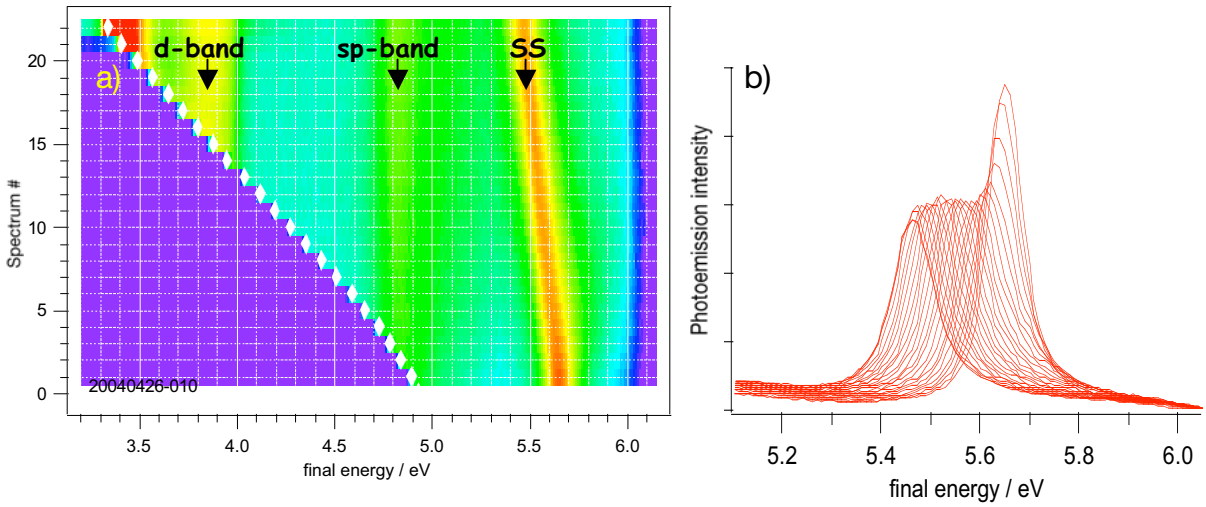

Figure 3. a) 3D plot of 1PP spectra of Cs/Cu(111) at 300 K as a function of Cs coverage. b) detail of the photoemission spectra in a) showing the tuning and broadening of SS.

are both consequence of the change in the surface potential by the alkali atom adsorption. Such independent measurement of the SS energy and width is necessary to extract quantitative information on the A ← SS resonant excitation in Fig. 2.

A close inspection of the SS spectra in Fig. 3b shows a remarkable and unexpected result. The intensity of SS decreases and the linewidth increases in the first few scans; however, above the coverage of 0.01 ML, the SS lineshape does not change. The linewidth changes as a function of coverage are plotted in Fig. 4a. Although the change in the line shape saturates for higher coverages, the change in the work function and the SS energy is essentially linear with time and hence, coverage. The linear shift is expected if the flux and sticking coefficient of alkali atoms is constant, and if the surface does not undergo a structural phase transition. Cs atoms are known to exist in a hexactic liquid structure for the entire coverage range, so we do not expect to encounter a structural phase transition.[1] This is supported by our measurements with Rb and K, which show essentially the same behavior as Cs, except that the linewidth at saturation increases by ~10% for the lighter alkali atoms.

In order to gain better understanding of the alkali atom results, we have studied the effect of other adsorbates on the SS linewidth and other properties. For exmple, Fig. 4b shows the results for the adsorption of water on Cu(111). Water is known to form bilayers on copper at exposures necessary for multilayer coverages.[11] Significantly, the SS linewidth increases linearly with exposure of the surface to water vapor at all coverages until the maximum coverage at which SS can be observed. Such behavior is expected for a classical scattering center, as has been assumed for the interaction of SS with impurity atoms.[12] Ironically, the primary citation for the effect on impurity scattering on photoemission linewidths (K/Cu(111)) is limited to the range of coverages of K up to the point of saturation (data reproduced in Fig. 4a).[12] The data in Fig. 4 rise two key questions: 1) What physical process is responsible for the saturation of the SS linewidth; and 2) Why do different adsorbates behave in a dramatically different manner?

To answer the first question, we examined various length scales that could impact the scattering processes. Saturation of cross sections in solid state materials is well documented in high-energy physics experiments where it is usually associated with the wavelength of the scattering particle exceeding the interscatterer distance. In surface experiments, the Fermi wavelength is one significant parameter that will influence the ineraction among adsorbate atoms and the screening of carges on surfaces. Remarkably,

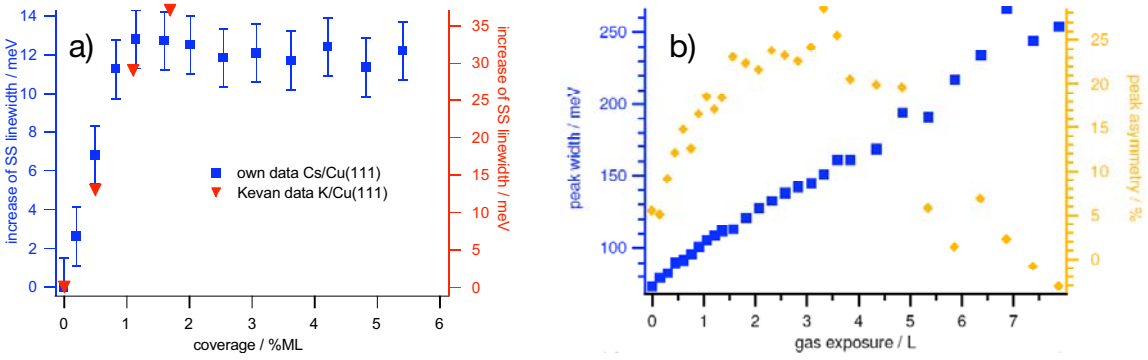

Figure 4. a) The SS linewidth as a function of Cs atom coverage. Red triangles show data from Ref. 12. b) The SS linewidth and asymmetry as a function of exposure to water at 90 K.

the interadsorbate spacing at the point of saturation corresponds exactly to the Fermi wavelentgh of 30 Å for the SS. However, we cannot explain why the propreties of electrons at the Fermi level with momentum k_F should should be expressed in holes generated at ~0.4 eV below the Fermi level with k = 0.

To address the second question, we consider the nature of alkali atom adsorption. Unlike other adsorbates, alkali atoms can be considered as point positive charges. The similar spectroscopic properties of Cs, Rb, and K (e.g. the same energy of A at low coverage) point to similar electronic properties of alkali atoms, which would be concisitent with the point charge model. Adsorbates such as water do not undergo complete electron transfer, and have structure related to both the intra and inter molecule bonding. The behavior of a point positive charge may be different from other scatering centers, because theory shows that the screened potential for a Z=1 charge in 2D free electron gas supports a bound state.[13] It may be that this unique property of alkali atoms also contributes to the unusual scattering processes.

To conclude, we have discovered highly unusual scattering properties of alkali atom impurities interacting with a 2D free electron gas. Considering the pominent role the interaction of SS electrons with impurity atoms and molecules plays in the emerging field of atomic scale device physics, such as embodied by quantum corrals,[14] it is imperative that we gain a deeper understanding of the factors that lead to the nonclassical scattering behavior of alkali atoms.

Future plans. We plan to further explore the line broadening induced by alkali atoms for Ag(111) surface. This should confirm whether the satureation of the linewidth really occurs when the interimpurity spacing is less than Fermi wavelength, which is 75 Å for Ag(111). We also plan to search for a theoretical explanation through a collaboration with Prof. Pedro Echenique and his group (see Ref. 13). In parallel, we are conducting experiments on the Suface Femtochemistry of alkali atoms.

Publications. We have had not publications yet from this project. We will publish the above results once we have a good theoretical model for the nonclassical broadening.

References

1 R. D. Diehl and R. McGrath, J. Phys. C **9**, 951 (1997).
2 I. Langmuir, J. Am. Chem. Soc. **54**, 2798 (1932).
3 H. Petek and S. Ogawa, Annu. Rev. Phys. Chem. **53**, 507 (2002).
4 B. Woratschek, et al., Phys. Rev. Lett. **55**, 1231 (1985).
5 M. Bauer, S. Pawlik, and M. Aeschlimann, Phys. Rev. B **55**, 10040 (1997).
6 H. Petek, et al., Surf. Sci. **451**, 22 (2000).
7 A. G. Borisov, et al., Phys. Rev. B **65**, 235434 (2002).
8 H. Petek, et al., J. Phys. Chem. B **105**, 6767 (2001).
9 H. Petek, et al., Science **288**, 1402 (2000).
10 S. Å. Lindgren and L. Walldén, Solid State Commun. **25**, 13 (1978).
11 C. Gahl, et al., Surf. Sci. **532-535**, 108 (2003).
12 S. D. Kevan, Phys. Rev. B **33**, 4364 (1986).
13 E. Zaremba, I. Nagy, and P. M. Echenique, Phys. Rev. Lett. **90**, 046801 (2003).
14 E. J. Heller, et al., Nature **369**, 464 (1994).

X-Ray Spectroscopy of Aqueous Solution Surfaces

R.J. Saykally Group(FWP#CH03SAY01)
College of Chemistry
University of California
Berkeley, CA 94720
saykally@cchem.berkeley.edu

Program Scope

The goal of this project is to explore and develop new methodologies for probing the nature of liquid-vapor interfaces of volatile liquids and solutions

Our recent work using liquid microjets [1-5] has demonstrated that the electronic and geometric structures of volatile liquid surfaces can be characterized via X-ray absorption spectroscopy. Utilizing the intense monochromatic soft X-Rays available at the LBNL Advanced Light Source (ALS), we have completed and published the first studies ever made of surface relaxation in a liquid (both water and methanol).[4] Additionally, we have made the first observation and characterization of a new type of hydrogen bonded species in the liquid/vapor interface of water-"acceptor only" molecules. These NEXAFS studies on water have now been extended to methanol.[8]

Ongoing and future studies will comparatively examine the effects of temperature, ion concentrations, and pH on both the surface and bulk structure of liquid water, small primary alcohols (methanol, ethanol, proponal), and binary water / alcohol systems. We shall investigate the chemical charge state and surface structure of amino acids and polypeptides, as well as the adsorption and solvation of ions at the liquid water surface. Longer-term goals include investigations of the comparative surface vs. bulk reactivities of active species such as OH, HO_2,ClO, and solvated electrons.

Recent Progress

A detailed description of the first generation experimental design and performance has been published.[5] A second generation experiment has been designed and constructed, and is still under development and refinement. We have recently investigated the temperature dependence of the bulk structure of deeply supercooled liquid water.[6] A strong temperature dependence of oxygen K-edge x-ray absorption fine structure features was observed for supercooled and normal liquid water droplets prepared from the breakup of a liquid microjet. Analysis of the data over the temperature range 251 to 288 K (-22° to +15°C), which is ca. 30% of the stability range of liquid water at 1 atmosphere pressure, yields the average energy required to effect an observable rearrangement between the fully coordinated ("ice-like") and distorted ("broken donor") local hydrogen bonding configurations responsible for the pre-edge and post-edge features, respectively, as 1.5 ± 0.5 kcal/mole. This energy equals the latent heat of melting of ice Ih and is consistent with the distribution of hydrogen bond strengths obtained for the "overstructured" ST2 model of water. A paper on this work has been accepted by Science.

In order to further our understanding of aqueous biological systems, the carbon, nitrogen, and oxygen K-edge spectra were measured for aqueous solutions of glycine by total electron yield near edge x-ray absorption fine structure (TEY NEXAFS).[7] The bulk solution pH was systematically varied while maintaining a constant amino acid concentration. Spectra were assigned through comparisons with both previous studies and ab initio computed spectra of isolated glycine molecules and hydrated glycine clusters. Nitrogen K-edge solution spectra recorded at low and moderate pH are nearly identical to that of solid glycine, while basic solution spectra strongly resemble that of the gas phase. The carbon 1s $\rightarrow \pi^*_{C=O}$ transition exhibits a 0.2 eV red shift at high pH due to the deprotonation of the amine terminus. This deprotonation also effects a 1.4 eV red shift in the nitrogen K-edge at high pH, as well as the appearance of two new sharp pre-edge features at 401.3 eV and 402.5 eV. These resonances, previously observed in the vapor phase ISEELS spectrum of glycine,[1] have been reassigned as transitions to σ^* bound states. The observation of these peaks indicates that the amine moiety is in an acceptor -only configuration at high pH. At low pH, the oxygen 1s $\rightarrow \pi^*_{C=O}$ transition exhibits a 0.25 eV red shift due to the protonation of the carboxylic acid terminus. These spectral differences indicate that the variations in electronic structure observed in the NEXAFS spectra are dominated by the internal charge state of the molecule, rather than by the condensed phase interactions.

Our investigations of aqueous ionic solutions have shown that the addition of alkalai halides engenders strong changes in the x-ray spectrum of bulk liquid water. We have observed a systematic increase in these changes as a function of both anion size and concentration. We intend to further our understanding of the aqueous environment by determining what cation effects exist in these systems, as well as utilizing theoretical calculations to understand the spectral changes observed in the bulk and at the surface.

Future Plans

In addition to the work described above, we have recently begun studying non-aqueous systems. Our preliminary work has resulted in the characterization of liquid methanol surface and bulk.[8] Additionally we have begun comparative studies into the bulk and surface properties of a variety of liquid hydrocarbons, including toluene, cyclohexane, nonane, and heptane. The high spectral resolution available at the ALS has allowed us to observe detailed electronic structure in the NEXAFS spectra of these hydrocarbon systems not previously available. We intend to continue this work, investigating the effect of conjugation and branching on the surface and bulk structure .

In a continuation of studies on aqueous systems, we intend to compare the electronic structure of a variety of solutes in solution and at the surface. One interesting system is the uranyl ion(UO_2^{+2}), which can form a variety of complex ions with both chloride and hydroxide, such that the surface interactions could be studies as a function of ion charge. From such experiments we hope to further our understanding of transport processes and surface reactivity for a wide range of atmospheric, industrial, and biological systems.

References and Recent Publications

1) K.R. Wilson, J.G. Tobin, A.L. Ankudinov, J.J. Rehr, and R.J. Saykally, *Phys. Rev. Lett.* **85**, 4289 (**2000**)
2) K.R. Wilson, B.S. Rude, T. Catalano, R.D. Schaller, J.G. Tobin, D.T. Co, and R.J. Saykally, *J. Phys. Chem. B* **105**, 3346-3349 (**2001**).
3) K.R. Wilson, M. Cavalleri, B.S. Rude, R.D. Schaller, A. Nilsson, L.G.M. Pettersson, N. Goldman, T. Catalano, J.D. Bozek, and R.J. Saykally, *J. Phys.: Condens. Matter* **14**, L221-L226 (**2002**).
4) K.R. Wilson, R.D. Schaller, B.S. Rude, T. Catalano, D.T. Co, J.D. Bozek, and R.J. Saykally, *J. Chem. Phys.* **117**, 7738-7744 (**2002**).
5) K.R. Wilson, B.S. Rude, J.D. Smith, C.D. Cappa, D.T. Co, R.D. Schaller, M. Larsson, T. Catalano, and R.J. Saykally, *Rev. Sci. Instrum.* **75**, 725-736 (**2004**).
6) J.D. Smith, C.D. Cappa, B.M. Messer, K.R. Wilson, and R.J. Saykally, Accepted by *Science*, August 2004.
7) B.M. Messer, C.D. Cappa, J.D. Smith, K.R. Wilson, and R.J. Saykally, Submitted to *J. Phys. Chem. B* ,September 2004.
8) K.R. Wilson, B.S. Rude, R.D. Schaller, T. Catalano, M. Cavalleri, A. Nilsson, L.G.M. Pettersson, and R.J. Saykally, Accepted by *J. Phys. Chem. B* , August 2004.

Reactive Intermediates in High Energy Chemistry.

Principal Investigators: Ilya A. Shkrob, * Robert A. Crowell, and David Gosztola

Radiation and Photochemistry Group, Chemistry Division, Argonne National Laboratory, Argonne, Illinois 60439; tel.: 630-2529516; FAX: 630-2524993; e-mail: shkrob@anl.gov

1. Scope.

Our program aims to study localization, thermalization, and chemical transformations of short-lived reaction intermediates (e.g., electrons and holes) generated by ionization, electron detachment, and energetic photoexcitation of molecules in condensed matter systems. We also study the dynamics of trapped charges (e.g., solvated electrons) in liquids (e.g., water), ionic and molecular solids (e.g., glasses), and nanomaterials (e.g., TiO_2 nanoparticles). Of special interest are chemical processes initiated by high-power lasers and radiation chemistry caused by accelerated particles. By nature of electron scattering process, the excitation and ionization events in radiolysis are clustered in "spurs", viz. nanosize domains separated by vast distances. We are trying to "dissect" these spurs and learn about rapid, concerted processes occurring in the initial phase of their evolution. Presently, the main approach is modeling such processes using short laser pulses. The reaction intermediates are studied using ultrafast pump-probe spectroscopy, pulse radiolysis, time-resolved conductivity and magnetic resonance. The use of fast and slow techniques, short-pulse lasers and particle accelerators, kinetic and structural methods are constitutents of our multifaceted approach. Our ability to pursue such studies will soon be aided by a 5-20 TW table-top laser system capable of generating subpicosecond electron pulses (T3 system). Once this system is operational, spurs on the picosecond time scale could be studied.

2. Progress report.

The focus of our recent work has been ultrafast studies of electron dynamics following UV excitation of water and aqueous anions, such as HO^-. Understanding of these dynamics is required for modeling the evolution of radiolytic spurs. E.g., knowing the dynamics of the $\left(HO, e^-_{aq}\right)$ pairs generated by electron detachment from HO^- is important since the same pairs occur in radiolysis of water. Below we summarize these recent studies.

2.1. Ionization of water and electron solvation and thermalization following above-the-gap photoexcitation.

The optical gap of liquid water is 8-9 eV, and the conduction band is directly accessible to photon with energies > 11 eV. At lower photon energy, the ionization occurs either via autoionization or a concerted proton and electron transfer. Only this low-energy regime has been studied previously using ultrafast laser spectroscopy. Ours is the first study in which the electron dynamics were studied following above-the-gap (12.4 eV total energy) ionization of water, using 200 nm, 300 fs laser pulses. The analysis of geminate recombination kinetics for electron generated by two photon ionization of H_2O and D_2O indicates that the average separation between the electron and its geminate partners in D_2O is 13% shorter than in H_2O (2.1 nm vs. 2.4

nm). Thus, quite unexpectedly, even at this high ionization energy, autoionization of water competes with direct ionization. Temporal evolution of transient absorption (TA) spectra (0.5 - 1.7 μm) for electron has been studied. Two distinctive regimes of the spectral evolution were observed. In both of these regimes, the spectral profile changes considerably with the delay time of the probe pulse. Currently popular "continuous blue shift" and the "temperature jump" models, in which the spectral profile does not change as it shifts to the blue are not supported by our data. Furthermore, no *p*-state electron, postulated by several authors was observed. For $t < 1$ ps, two new TA features (the 1.15 μm band and 1.4 μm shoulder) were observed for the electron in the spectral region where O-H overtones appear in the spectra of H_2O. These two features were not observed in D_2O. Vibronic coupling to the modes of water molecules lining the solvation cavity is a possible origin of these features. On the sub-picosecond time scale, the absorption band of solvated electron progressively shifts to the blue. At later delay times ($t > 1$ ps), the position of the band maximum is "locked", but the spectral profile continues to change by narrowing on the red side and broadening on the blue side; the oscillator strength is constant. The time constant of this narrowing is 0.56 ps for H_2O and 0.64 ps for D_2O, respectively. Vibrational relaxation and time-dependent decrease in the size and sphericity of the solvation cavity are suggested as possible causes for the observed spectral transformations in both of these regimes.

Geminate recombination kinetics for electrons generated by multiphoton ionization of liquid water become power dependent when the irradiance of the excitation light is greater than 0.3-0.5 TW/cm^2 (the terawatt regime). We found that in tri- 400 nm photon ionization of water, the observed kinetic transformations are caused by a rapid temperature jump in the sample. Such a jump is inherent to multiphoton ionization in the terawatt regime, when the absorption of the pump light along the optical path becomes very nonuniform. The heating of water is substantial (tens of K) because the quantum yield of the ionization is only 0.42, and a large fraction of the excitation energy is released into the solvent bulk as heat. Evidence of the temperature jump is the observation of a red shift in the absorption spectrum of (thermalized) electron and characteristic "flattening" of the thermalization dynamics in the near IR. The temperature jump in the terawatt regime must be common in multiphoton ionization of molecular liquids. The implication of these observations for femtosecond pulse radiolysis is that the "spur" is quite hot in the first few tens of picoseconds, as > 10 eV of heat is deposited in the nanodomain of the liquid. This study has been conducted in collaboration with S. Pommeret of CEA/Saclay, France.

2.2. Photodetachment from aqueous anions.

Mono- (1 x 6.2 eV) and bi- (2 x 3.1 eV) photonic excitation of aqueous hydroxide and iodide in their charge transfer to solvent (CTTS) bands were studied over the temperature interval of 10 to 100 ^oC and concentration range of 10^{-3} to 10 M. This work has been carried out in collaboration with S. E. Bradforth's group at the USC. For HO^-, both the electron and OH radical dynamics were studied. Pairing of the photodetached electron with the residual radical/atom in a solvent cage was observed for all halide and pseudohalide anions; these caged pairs remain in proximity (0.5-0.7 nm) for 4-15 ps and then decay by diffusion out of the cage. For hydroxide, there is a considerable barrier for recombination of the caged pairs, ca. 85 meV. For iodide, 1- and 2-photon processes of the same total energy result in nearly identical electron distributions. For hydroxide, the electron distribution in much broader in the biphotonic excitation. The latter is also much less efficient than that of I^-. We attribute this inefficiency of the 2- photon process to a changeover of the electron wavefunction from *s*- (1-photon excitation) to *p*- (2-photon

excitation) and spin-orbital mixing in the heavier anion. Understanding this effect and the role of spin-orbital coupling is the current emphasis of our CTTS studies. Currently we are studying other aqueous anion systems, including Br^-, HS^-, $Fe(CN)_6^{4-}$, SO_3^{2-}, SO_4^{2-}, and SCN^-. The objective is to obtain accurate data on the quantum yields of photoelectron in 1-photon excitation at 5-6.2 eV and 2-photon excitation at 3.1 eV of these anions and to study the electron dynamics. We already established that photoexcited polyvalent anions yield electrons via direct ionization. The latter process becomes more prevalent with the increasing photon energy, for all anions. An unexpected finding is that while all halides exhibit near unity quantum yield of electron photodetachment, pseudohalides show significantly lower yields (ca. 1/3) which, in some systems, are wavelength-dependent. These observations challenge current CTTS theories. Another one of unexpected findings is our discovery that for all aqueous anions, the yield of free photoelectrons decreases by 10% per M ionic strength of the solution. The rate of this decrease varies for different anions, from 100 ps for halides to > 1 ns for sulfite and hydroxide. Cation association with the solvated electron and its parent anion are thought to cause this ionic strength effect.

2.3. Photoprocesses in aqueous TiO_2 nanoparticles.

Understanding of the mechanisms for charge dynamics and electron/hole reactions in/on titania nanoparticles and nanocrystalline films, has important ramifications for photocatalysis and solar energy conversion. We study light absorption, photoexcitation, and chemical properties of free carriers and band tail charges in titania. Our results implicate ultrafast charge-transfer reaction of free holes with chemisorbed molecules at TiO_2 surface as the most important pathway for photocatlytic degradation of hydroxylated compounds. Complete separation of the spectral contributions from trapped electron and hole is demonstrated using polyols as selective hole scavengers. Some holes are scavenged by the polyols promptly within the duration of the excitation pulse, some are scavenged at a slower rate over 200 ns, and the rest are not scavenged, even at high concentration of the polyols (> 10 vol. %). A reaction with chemi- and physi-sorbed polyols is responsible for the prompt and the slow decay, respectively. Vis-IR photoexcitation of trapped electron causes its promotion into the conduction band of TiO_2 followed by rapid recombination of the free electron and a trapped hole. The quantum yield for this process is 0.28 for 532 nm and 0.024 for 1064 nm photoexcitation. The photobleaching spectra indicate rapid equilibration between free and bandtail electrons and midgap states. Contrary to the previous studies, we found that the holes in titania absorb over the entire visible. The characteristic 650 nm band of photoexcited TiO_2 nanoparticles is, in fact, composite. These vis-absorbing *O 2p* holes might originate from a common impurity in TiO_2, e.g. Al^{III} ions. The scavenging efficiency of polyols increases with the number of OH groups. A specific binding site is suggested that involves an octahedral Ti^{IV} atom chelated by the $–CH_2(OH)-CH_2(OH)-$. This mode of binding accounts for the depletion of 5-coordinated Ti atoms observed in the XANES spectra of coated TiO_2 nanoparticles. These binding sites trap a substantial fraction of holes before the latter descend to surface traps and/or recombine with electrons. The resulting hole center rapidly loses a proton to the environment, yielding a ketyl radical.

3. Future plans.

Our nearest goal is to improve the time resolution of pulse radiolysis using the T3 source. We will also use free-electron laser facility (ALFF) at the APS (Argonne) and high harmonic

generation using a Ti:sapphire laser system to pursue ultrafast studies of photoionization in liquids that is induced by the absorption of vacuum UV light. The higher is the excitation energy, the stronger is the similarity of the photoexcitation to the processes occurring in radiolytic spurs.

Recent publications (2004).

R. Lian, D. A. Oulianov, I. A. Shkrob, and R. A. Crowell, *Geminate recombination of electrons generated by above-the-gap (12.4 eV) photoionization of liquid water.* Chem. Phys. Lett. (2004) in press; preprint on http://arXiv.org/abs/physics/0407148

M. C. Sauer, Jr., I. A. Shkrob, R. Lian, R. A. Crowell, D. M. Bartels, X. Chen, S. Suffern, and S. E. Bradforth, *Electron Photodetachment from Aqueous Anions. II. Ionic Strength Effect on Geminate Recombination Dynamics and Quantum Yield for Hydrated Electron.* J. Phys. Chem. A. (2004), in press; preprint on http://www.arXiv.org/abs/physics/0404056

R. A. Crowell, R. Lian, I. A. Shkrob, Jun Qian, D. A. Oulianov, and S. Pommeret, *Light-induced temperature jump causes power-dependent ultrafast kinetics of electrons generated in multiphoton ionization of liquid water.* J. Phys. Chem. A (2004), in press; preprint on http://arXiv.org/abs/physics/0405013

I. A. Shkrob, *Geminate recombination dynamics studied via electron reexcitation: Kinetic analysis for anion CTTS photosystems*, Chem. Phys. Lett. **395** (2004) 264.

I. A. Shkrob and M. C. Sauer, Jr., *Hole Scavenging and Photo-Stimulated Recombination of Electron-Hole Pairs in Aqueous TiO_2 Nanoparticles*. J. Phys. Chem. B **108** (2004) 12497.

M. C. Sauer, Jr., I. A. Shkrob, D. Gosztola, *Efficient, rapid photooxidation of polyatomic alcohols and carbohydrates by aqueous TiO_2 nanoparticles.* J. Phys. Chem. B **108** (2004) 12512.

R. Lian, R. A. Crowell, I. A. Shkrob, D. M. Bartels, X. Chen, and S. E. Bradforth, *Ultrafast Dynamics for the Electron Photodetachment of Aqueous Hydroxide*, J. Chem. Phys. **120** (2004) 11712.

R. Lian, R. A. Crowell, I. A. Shkrob, D. M. Bartels, D. A. Oulianov, and D. Gosztola, *Recombination of Geminate (OH,e_{aq}^-) Pairs in Concentrated Alkaline Solutions: Lack of Evidence For Hydroxyl Radical Deprotonation.* Chem. Phys. Lett. **389** (2004) 379.

R. A. Crowell, R. Lian, M. C. Sauer, Jr., D. A. Oulianov, and I. A. Shkrob, *Geminate recombination of hydroxyl radicals generated in 200 nm photodissociation of aqueous hydrogen peroxide.* Chem. Phys. Lett. **383** (2004) 481.

I. A. Shkrob, D. A. Oulianov, R. A. Crowell, and S. Pommeret, *Frequency-domain "single-shot" (FDSS) ultrafast transient absorption spectroscopy using compressed laser pulses*. J. Appl. Phys. **96** (2004) 25.

M. C. Sauer, Jr., R. A. Crowell, and I. A. Shkrob, *Electron Photodetachment from Aqueous Anions. I. Quantum Yields for Generation of Hydrated Electron by 193 and 248 nm Laser Photoexcitation of Miscellaneous Inorganic Anions*. J. Phys. Chem. A **108** (2004) 5490.

I. A. Shkrob and M. C. Sauer, Jr., *Radical Ions in Liquids*, in *"Charged Particle and Photon Interactions with Matter.",* eds. Y. Hatano and A. Mozumder, Marcel Dekker, New York, 2004; Ch. 11, pp. 301-331.

R. A. Crowell, E. L. Chronister, R. Lian, A. D. Liu, S. Pommeret, I. A. Shkrob, A. D. Trifunac, and L. Zhao, *Ultrafast studies on the photophysics of matrix-isolated radical cations of polycyclic aromatic hydrocarbon*s. J. Phys. Chem. A **108** (2004) 25.

Understanding Nanoscale Confinement Effects in Solvent-Driven Chemical Reactions

Ward H. Thompson
Department of Chemistry, University of Kansas, Lawrence, KS 66045
Email: wthompson@ku.edu

Project Overview. It is now possible to synthesize nanometer-sized cavities in sol-gels, reverse micelles, vesicles, zeolites, organic and inorganic supramolecular assemblies, and even proteins. This gives strong impetus to improving our understanding of chemical reactions in nano-confined solvents. The benefits could include new ways of controlling chemistry, designing micro- and mesoporous catalysts, and developing chemical sensors. We are investigating the energetics and dynamics of chemical reactions in solvents confined within nanometer-sized cavities, or "nanocavities." The fundamental question we are addressing is *How does a chemical reaction occur differently in a nano-confined solvent than in a bulk solvent?*

Solvent-driven reactions, typically those involving charge transfer, should be most affected by confinement of the solvent and thus provide the greatest opportunity for manipulating the chemistry. The limited number of solvent molecules, geometric constraints of a nanocavity, and solvent-wall interactions should have dramatic effects on both the reaction energetics and dynamics. Our focus is on proton transfer – a key class of solvent-driven reactions of widespread importance in chemistry and biology – and related processes. Thus, a fundamental understanding of proton transfer reactions in nano-confined solvents will impact many areas of chemistry in addition to providing important insights into the larger class of solvent-driven reactions. The diversity among nanocavities (*e.g.*, in their size, shape, flexibility, and interactions with the solvent and/or reactants) makes it difficult to translate studies of one system into predictions for another. Thus, we are focusing on developing a unified understanding of reaction dynamics in the diverse set of confinement frameworks.

Recent Progress. *Charge Transfer Spectra and Time Dependent Fluorescence.* We have studied charge transfer spectra because they provide insight into solvation properties in confined solvents relevant to proton transfer and are frequently measured experimentally. We have found that a chromophore with a charge transfer transition in polar, aprotic solvents confined in hydrophobic spherical nanocavities displays different trends in the steady-state absorption and fluorescence spectra with cavity size.[1] Specifically, the fluorescence spectrum is red-shifted as the cavity radius is increased while the absorption spectrum is essentially unchanged. This behavior can be understood based on the solute position: In the ground state the solute has a relatively small dipole moment and is most likely found near the cavity wall, excluded by the solvent. In the excited state, the solute dipole moment is large and the solute is most likely to be found fully solvated near the center of the cavity.[2] The fluorescence spectrum is therefore more sensitive to changes in the cavity size than the absorption spectrum. In addition, these results led us to predict that the time dependent

fluorescence (TDF) of such a chromophore in a spherical nanometer-scale cavity will exhibit characteristics due to the change in the chromophore position in the cavity after excitation.

This prediction, combined with the numerous experimental measurements of TDF in a variety of confined solvent systems, motivated us to simulate the TDF for this model with nonequilibrium molecular dynamics (MD).[3] In addition, TDF provides information about solvation dynamics relevant to proton transfer reactions. We found that the time decay of the normalized Stokes shift function, $S(t)$, is tri-exponential. The three time scales can be roughly attributed to inertial motion (< 300 fs), solvent reorientational dynamics ($\sim 1.5-3$ ps), and solute motion toward the cavity interior ($\sim 15-40$ ps). Thus, the appearance of this longest time scale in these simulations confirmed our prediction. The solute motion that is observable in the long-time component of $S(t)$ is slower the larger the solution density. The time-dependent average solute position is single-exponential at the low density considered here but bi-exponential at the higher density.

While the Stokes shift increases with the cavity radius, the normalized Stokes shift function, $S(t)$, does not show a consistent trend with cavity size. Ultimately this is a result of the changes in the solute molecule position distribution with cavity size in the ground and excited electronic states. These affect the amplitudes of the different time-components of $S(t)$ while the solvent reorientation times are not found to depend strongly on solute position (for CH_3I and CH_3CN). These results indicate that TDF measurements may not be indicative of cavity size, even when the steady-state fluorescence spectra are.

We have investigated the effect of the shape of the confining framework by Monte Carlo simulations of the absorption and fluorescence spectra of the same model chromophore confined in nanoscale ellipsoidal cavities (with two identical semi-axes, a, and one unique one, c).[4] In addition, the solute and solvent (center-of-mass) probability distributions have been calculated and used to interpret the spectra. Both prolate and oblate ellipsoidal cavities of varying size have been considered along with several solvent densities. As for spherical cavities,[1] the absorption spectrum for the model solute is insensitive to the cavity dimensions. In contrast, in the fluorescence spectra for prolate ellipsoidal cavities (a=10 Å, c= 10, 15, 30, 50 Å), the maximum peak shifts to the red with increasing semi-axis c, but quickly becomes independent of c. For the oblate ellisoidal cavities (a=10, 15, 30 Å, c=10 Å), the fluorescence spectra shift to the red steadily as the semi-axis a increases as was found for spherical cavities.[1] These results can be understood by the same analysis used to explain the spectra in spherical cavities. A new feature, however, is that the effective solvent polarity in the cavity interior is limited by the minor semi-axes a.

It is important to note that in all cases the solute positions are affected by the solvent structure in the cavities. Specifically, the solvent packs in "layers" separated roughly by the diameter of the solvent molecule. The layering of a liquid at the interface with a solid surface is a well-known phenomenon but here is also modified by packing effects and we have found that the structure depends on the properties of the solvent (*e.g.*, CH_3I and CH_3CN line up parallel to the cavity wall while CH_3OH lies perpendicular, H_2O adapts an intermediate structure). As the major semi-axis c is increased in the prolate ellipsoid cavities, the solvent density quickly approaches cylindrical symmetry near the cavity center.

The solvent density naturally affects the solute position distributions leading to layered structures and a significant density in the solute ground state to be found near the ellipsoid "ends" where the solvent density is smaller.

Vibrational Dynamics. The vibrational dynamics investigated by Raman spectra and time-resolved vibrational pump-probe experiments in confined solvents have not been as well studied as electronic spectra. These measurements probe processes in which the solvent-solute short-range repulsive interactions play a large role. Thus, they provide a valuable complement to measurements that are sensitive to the longer-range electrostatic interactions. In addition, they provide insight into activated processes including reaction dynamics.

We have investigated the vibrational dynamics of a model diatomic anion solute dissolved in a methyl iodide solvent confined in a nanoscale spherical cavity by molecular dynamics simulations.[5] The effect of confining the solvent on the vibrational energy relaxation time T_1, solvent-induced frequency shift $\langle\delta\omega\rangle$, and pure dephasing time T_2^* were examined by comparing the results from confined systems of varying size (cavity radius 0.8-2 nm) to those from the bulk system. We found that T_1 increases monotonically toward the bulk solvent value with increasing cavity size. The changes in T_1 are attributed to the presence of high local density solvent layers induced by the confinement. In these solvent layers, the repulsive, Lennard-Jones forces play an important role and the enhancement of the local density leads to faster vibrational energy relaxation. In contrast to T_1, the solvent-induced frequency shift and the dephasing time do not change monotonically with cavity size. This is due to the overlap of the solute position distribution with the solvent layers and the differences in solvent properties to which $\langle\delta\omega\rangle$ and T_2^* are sensitive compared to that for T_1. We believe that the trends will be strongly system-dependent (and preliminary results for the same solute in other solvents seem to support that contention).

Proton Transfer. A model intramolecular phenol-amine proton transfer system in a CH_3Cl solvent confined in a smooth, hydrophobic spherical cavity has been investigated. We have developed a valence bond description for the reaction complex based loosely on a widely applied model. Monte Carlo simulations have been used to calculate the reaction complex position distribution and the free energy curves, as a function of a collective solvent coordinate, for several fixed reaction complex radial positions (based on the center-of-mass); cavity radii of 10 and 15 Å have been considered. Quantum effects associated with the transferring proton have been included by adding the proton zero point energy to the classical free energy. Mixed quantum-classical MD simulations are also being carried out to investigate the reaction mechanism and dynamics.

The key results of the Monte Carlo simulations are that 1) The reactant proton transfer complex is located near the cavity wall while the product complex is found primarily in the interior (analogous to the charge transfer chromophore). 2) The reaction free energy depends strongly on the reaction complex position, varying from endothermic (by ~ 1 kcal/mol) near the cavity wall to exothermic (by ~ 5 kcal/mol) deep in the cavity interior. Together these demonstrate that the reaction coordinate must involve motion of the reaction complex from near the cavity wall to the interior as a component. We do not observe strong cavity size effects on the position distributions or free energy curves. Our results also indicate that

this proton transfer system is in the (vibrationally) nonadiabatic regime and should display significant kinetic isotope effects due to tunneling.

These results strongly indicate that the reaction complex position is part of the reaction coordinate for proton transfer in these nanoconfined solvents. We are currently carrying out mixed quantum-classical MD to determine the details of the reaction mechanism. The proton motion is treated quantum mechanically while all the other coordinates are described classically. (The proton vibrational Schrödinger equation is solved at every time step using a sinc-function discrete variable representation basis and a Lanczos algorithm.[6]) Both vibrationally adiabatic and nonadiabatic (surface hopping) dynamics are being simulated. Our results indicate that multiple mechanisms exist, *i.e.*, the solvent coordinate changes first followed by solute motion, the solute moves first followed by a change in the solvent coordinate, or the two change in a concerted manner – we have observed all three mechanisms in the trajectories, though the first appears to be the most prevalent. We are currently investigating the kinetic isotope effect.

Future Plans. We are currently implementing several extensions of the work described above. Specifically, we are developing cavity models with atomically rough surfaces and different chemical functionalities. We are also developing cylindrical pore models to explicitly simulate dimensionality effects. We are implementing mixed quantum-classical MD simulations of surface proton transfer (where the acid is covalently bound to the cavity wall) and of intermolecular proton transfer reactions (in which the heavy atom coordinate is quantized). We are developing models for larger solutes, particularly inter- and intramolecular phenolamine proton transfer systems. We are simulating confined systems with a wider variety of solvents. Finally, we are investigating conformational energetics and dynamics in confined solvents, beginning with 1,2-dichloroethane.

References

[1] W.H. Thompson, *J. Chem. Phys.* **117**, 6618-6628 (2002).

[2] These simple energetic arguments, while ultimately decisive, are modulated by a geometric one: the space available for a solute molecule a distance r from the cavity center is proportional to r^2. This cooperation/competition between energetic and geometric effects provides a simple model for extrapolating to confining frameworks of different dimensionality (*e.g.*, spherical cavities vs. cylindrical pores vs. slit pores).

[3] †W.H. Thompson, *J. Chem. Phys.* **120**, 8125-8133 (2004). "Simulations of Time-Dependent Fluorescence in Nano-Confined Solvents"

[4] †J.A. Gomez and W.H. Thompson, *J. Phys. Chem. B* ASAP (2004). "Monte Carlo Simulations of Absorption and Fluorescence Spectra in Ellipsoidal Nanocavities"

[5] †S. Li, T.D. Shepherd, and W.H. Thompson, *J. Phys. Chem. A* **108**, 7347-7355 (2004). "Simulations of the Vibrational Relaxation of a Model Diatomic Molecule in a Nanoconfined Polar Solvent"

[6] W.H. Thompson, *J. Chem. Phys.* **118**, 1059-1067 (2003).

†DOE-sponsored publication.

STRUCTURAL STUDIES OF THE SOLVATION EFFECTS AND CHEMICAL INTERACTIONS IN OPEN-SHELL SYSTEMS

G. N. R. Tripathi

Notre Dame Radiation Laboratory
Notre Dame, IN 46556

Email: Tripathi.1@nd.edu; tel: (574)631 5514; fax: (574)631 8068

Program Definition

This program aims to provide a molecular level understanding of the nature and role of solvent interactions in determining the molecular geometry, bond structure and chemical reactivity of prototype radical intermediates produced in radiation-induced reactions. Presently, an in-depth understanding of such interactions is lacking, in spite of their fundamental role in condensed phase chemistry. The structural studies of the solvent effects on short-lived radicals are being conducted using a variety of techniques, such as the Laboratory's unique pulse radiolysis time-resolved resonance Raman facility, transient absorption and electron spin resonance spectroscopy, and quantum chemical structure calculations. The information sought is valuable for gaining insight into the role of solvent interactions in directing the speed and course of reactions and making their useful applications to a wide variety of energy related chemical, industrial and biomedical processes, including electron transfer reactions relevant to energy conversion and storage devices. It is also of utmost importance for the development and testing of the appropriate theories for radical solvation.

Radical-solvent interactions can involve exchange between the unpaired electron on the radical and electron pairs on the solvent molecules. Therefore, these interactions can be very different in nature, strength and physicochemical effects from those in closely related closed-shell solute-solvent systems, including ions. Infrared studies on a few closed and open-shell ions clustered with water molecules have been performed recently in molecular beam experiments that aim to provide data for modeling the aqueous state.[1] In comparison, the structural studies on the interaction between transient radical intermediates and their chemical environment in liquid water are rare. The water molecules that comprise the first hydration shell of a chemical transient in liquid water are too few in number to be detected by infrared absorption. However, it is feasible to probe the solvent-solute coupling in aqueous radicals and radical ions by time-resolved resonance Raman spectroscopy.[2,3] Identification of the radical-solvent modes, without altering the strength of interaction, can be accomplished by replacing light water by heavy water. The interaction between the radical and its hydration shell can be gradually modified by associating ions with water molecules, converting the water structure from wet to 'dry' liquid state. These experimental strategies allow examination of the hydration shell effects even on charge-neutral radicals that may not interact with their aqueous environment as strongly as radical ions. Prototype radicals containing hydrogen bonding moieties whose resonance Raman and ESR spectra are well characterized, such as *p*-aminophenoxyl and *p*-phenylenediamine cation radicals, offer appropriate model probes.

Recent Progress

A dynamic solvation effect, not known previously, has been observed on ionic perturbation of the hydration shell structure of an amine radical.[4] It has been found that the association of ions (Li^+/Na^+, Cl^-) with water molecules hydrogen-bonded to an aromatic amine radical (*p*-$H_2NPhO^\bullet$) greatly enhances the dynamic coupling between the amine scissors and the ring stretching vibrations observed by time-resolved resonance Raman spectroscopy. The enhanced coupling is an indicator of a change in the amine group orientation and radical geometry towards planarity. These results are extremely important in view of the recent claim that the hydrogen bonding properties of water molecules are hardly affected by association with ions.[5]

The effects of hydrogen bonding and solvent reaction field on the aqueous radical (*p*-$H_2NPhO^\bullet$) have been calculated using ab initio and density functional theories and simple models of solvation.[6] The dipole moment of the radical in its ground electronic state ($^2B_1$) is predicted to increase by ~8 D and the difference between the CN and CO bond lengths to decrease by 0.05 Å from gas phase to aqueous solution. This profound hydration effect converts the structure and chemical properties of the radical from a substituted phenoxyl radical ($XPhO^\bullet$) in the gas phase to a semiquinone-like radical in water. The experimental and theoretical results have been combined to estimate the CO and CN bond lengths in *p*-$H_2NPhO^\bullet$ as 1.263 and 1.34 Å, respectively, in liquid water and 1.245 and 1.37 Å in the gas phase. The association of ions with the water molecules that are hydrogen bonded to the amine and oxygen sites in the radical enhances their structural effects. ESR studies provide definitive evidence of a shift in the unpaired electron density from the oxygen to the amine site in the presence of ions, consistent with the Raman observations.[7]

The ionic effect on molecular orientation has also been probed in heterogeneous aqueous systems, providing an insight into a chemical method of its control.[8] It has been established that 2-mercaptopyrimidine ($C_4H_3N_2SH$), a prototype of N-heterocyclic aromatic thiols, binds with 100-120 nm silver particles in aqueous solution in a radical-like ($C_4H_3N_2S$) state, rather than as an anion ($C_4H_3N_2S^-$). In the presence of chloride ions, the intensity profile of the Raman spectra changes dramatically, as the chloride ions cause reorientation of the molecule on the metal surface, from a vertical configuration of the ring to a slightly twisted horizontal configuration.

Quinones act as electron acceptors in natural photosynthesis. Artificial devices comprised of quinones are discussed in the literature for inducing light-driven electron transfer and charge separation, with the objective of converting solar energy into chemical energy.[9] The process of electron acceptance by quinones involves successive deactivation of the excited electronic states of their anion radicals in which the low lying weakly allowed or forbidden electronic states play a vital role. The energy location of these states, however, has been in question. The knowledge that the *p*-$H_2NPhO^\bullet$ radical acquires a semiquinone anion character due to solvent interactions in water has led to its use as a model for estimating the energy of the parity forbidden $^2B_{2g}$-$^2B_{1g}$ electronic transition in *p*-benzosemiquinone radical anion. The non-totally symmetric vibrations which couple a weakly allowed electronic transition with a close by strongly allowed transition are resonance enhanced in Raman by a non-Franck–Condon mechanism. The excitation wavelength for which the maximum enhancement occurs for such vibrations in the transient Raman spectra gives the energy of the weak transition. The transition energy for the $^2B_{1g}$ excited state of *p*-benzosemiquinone radical anion was determined as ~3.4 eV on that basis.[6]

It has been found that the chemical interaction between the aqueous silver clusters aggregated by the chloride ion and *p*-benzoquinone provides a rare observation of the transfer of electronic charge to the latter species, forming the radical anion on the metal surface.[10] The CO stretching frequency in the radical anion on the surface is ~10 cm^{-1} lower than in aqueous solution.

Future Plans

The effect of specific solvent interactions, e.g., hydrogen bonding, on prototype radicals containing strongly hydrogen-bonding moieties, such as NH_2 and O^-, and the role of long-range interactions such as solvent dielectric properties and viscosity on the radical structure will be investigated by transient absorption, Raman and ESR spectroscopy and quantum chemical calculations. These studies will involve ionic (e.g., Na^+, Li^+, Cl^-), isotopic and thermal modifications of the hydration shells. The effects of nonpolar as well as polar hydration shells in model radicals and radical ions with and without inversion symmetry will be examined. These studies will allow distinguishing between the pure hydrogen bonding effects and those combined with the effects of the solvent reaction field. For example, the enhanced dynamic coupling between the amine and the ring in *p*-$H_2NPhO^\bullet$ may be caused by one or both of these interactions. Their relative contributions remain to be determined. Isotopic substitutions in probe radicals will provide a means of changing the intrinsic coupling strength between the vibrations. Complementary studies in aprotic solvents will distinguish between the hydrogen-bond effects and bulk solvent effects such as viscosity and dielectric constant. We will also elucidate the early chemical steps in the radiation chemistry of saline aqueous solutions, relevant to amine radical formation in an ionic environment. The role of ions in making or breaking the hydrogen-bond structure in liquid water, which has been questioned recently, will be examined.

Elementary reactions involving hydrated electron and charged water species such as hydronium ion (H_3O^+) will be investigated by transient absorption and ESR spectroscopy in wet to dry liquid water produced by ionic perturbation, with the objective of understanding the structure and reaction rates of electron when an adequate number of free water molecules are not available for solvating the charged species. The experiments will be performed at ion concentrations much above the range within which the usual ionic strength effects are operative. These studies are hoped to provide new experimental data for modeling the nature of the hydrated electron.

Acknowledgement

The research described herein was supported by the Office of Basic Energy Sciences of the Department of Energy.

References

(1) Robertson W. H.; Johnson, M. A. *Annu. Rev. Phys. Chem.* **2003**, *54*, 173.

(2) Tripathi, G. N. R. In *Time-resolved Spectroscopy*, Clark, R. J. H., Hester, R. E., Eds.; Advances in Spectroscopy, Vol. 18; Wiley: New York, **1989**; pp 157-218.

(3) Su, Y.; Tripathi, G. N. R. *Chem. Phys. Lett*. **1992**, *188*, 388.

(4) Tripathi, G. N. R. *J. Phys. Chem. A* **2004**, *108*, 5139.

(5) Omta, A. W.; Kropman, M. F.; Woutersen, S.; Bakker, H. J. *Science* **2003**, *301*, 347;

J. Chem. Phys. **2003**, *119*, 12457

(6) Tripathi, G. N. R. *J. Chem. Phys.* **2003**, *118*, 1378.

(7) Tripathi, G. N. R.; Hug, G. H.; Schuler, R. H., *Work in Progress*.

(8) Tripathi, G. N. R.; Clements, M. *J. Phys. Chem. B* **2003**, *107*, 11125.

(9) Cook, A. R.; Curtiss, L. A.; Miller, J. R. *J. Am. Chem. Soc*. **1997**, *119*, 5729 and references therein

(10) Tripathi, G. N. R. *J. Am. Chem. Soc.* **2003**, *125*, 1179.

Publications of the DOE sponsored research (2002-2004)

Effect of Ionic Modification of the Hydration Shell of a Charge-Neutral Radical on its Resonance Raman Spectrum
G. N. R. Tripathi, J. Phys. Chem. A **2004**, *108*, 5139.

The Origin of Base Catalysis in the OH Oxidation of Phenols in Water
G. N. R. Tripathi & Y. Su, J. Phys. Chem. A **2004,** *108,* 3478-3484

Electronic Structure of para Aminophenoxyl Radical in Water
G. N. R. Tripathi, J. Chem. Phys. **2003**, *118*, 1378.,

p-Benzosemiquinone Radical Anion on Silver Nanoparticles in Water
G. N. R. Tripathi, J. Am. Chem. Soc. **2003**, *125*, 1179.

Adsorption of 2-Mercaptopyrimidine on Silver Nanoparticles in Water
G. N. R. Tripathi & M. Clements, J. Phys. Chem. B **2003**, *107*, 11125.

Structure and Proton Reactivity of the Semiquinone Anion and Dianion of Biphenol In Water
G. N. R. Tripathi & D. M. Chipman, J. Phys. Chem. A **2002**, *106*, 8908.

Chemical Kinetics and Dynamics at Interfaces

Gas Phase Investigation of Condensed Phase Phenomena [1]

Lai-Sheng Wang (PI)
Department of Physics, Washington State University, 2710 University Drive, Richland, WA, 99354 and the Chemical Sciences Division, Pacific Northwest National Laboratory,
P.O. Box 999, Mail Stop K8-88, Richland, WA 99354. E-mail: ls.wang@pnl.gov

Program Scope

This program is aimed at obtaining a microscopic understanding of environmental materials and solution chemistry in the gas phase using a variety of cluster models. Our primary experimental technique is photoelectron spectroscopy (PES) coupled with electrospray ionization (ESI), which is used to produce solvated clusters from solution samples. Experimental and ab initio calculations are combined to

- obtain a molecular-level understanding of the solvation and stabilization of singly and multiply charged anions important in the condensed phases
- understand the molecular processes and initial steps of dissolution of salt molecules by polar solvents
- probe the structure and dynamics of solution and air/solution interface.

Multiply charged anions are ubiquitous in nature, often found in solutions and solids. However, few multiply charged anions have been studied in the gas phase due to the difficulty in generating them and their intrinsic instability as a result of strong intramolecular Coulomb repulsion. Microscopic information on the solvation and stabilization of these anions is important for the understanding of solution chemistry and properties of inorganic materials or atmospheric aerosols involving these species. Gas phase studies with controlled solvent numbers and molecular specificity are ideal to provide such microscopic information. We have developed a new experimental technique to investigate multiply charged anions and solvated species directly from solution samples and probe their electronic structures, intramolecular Coulomb repulsion, stability, and energetics using electrospray and PES, as shown in our recent invited review article (6). A central theme of this research program lies at obtaining a fundamental understanding of environmental materials and solution chemistry. These are important to waste storage, subsurface and atmospheric contaminant transport, and other primary DOE missions.

Recent Progress (2002-2004)

Observation of Solvent-Mediated Folding of a Linear Doubly Charged Anion: The dicarboxylate dianions provide an interesting set of systems with two well-separated and localized charges. Stepwise solvation of these anions by water is expected to lead to a competition between Coulomb repulsion and water-water interactions. In addition, carboxylate is an important negative charge carrier in proteins, present in the C-terminal of polypeptides and the side chains of aspartic and glutamic acids. Linear dicarboxylate dianions $^{-}O_2C\text{-}(CH_2)_n\text{-}CO_2^{-}$ have two distinct charged groups ($-CO_2^{-}$) linked by a flexible aliphatic chain and can be viewed as simple models for peptides. We studied the microsolvation of the suberate dianion, $^{-}O_2C\text{-}(CH_2)_6\text{-}CO_2^{-}$ by water and observed a solvent-mediated folding as a function of solvent number. We showed that water molecules solvate the two negative charges in the linear suberate alternately at the two ends, but not the middle hydrophobic aliphatic chain. As the solvent number increases, a folding occurs at about 16 waters, where the cooperative hydrogen bonding of water is large enough to overcome the Coulomb repulsion and pull the two negative charges closer through a water bridge. This conformation change, revealed both from the PES data and molecular dynamic simulation is

[1] Collaborators on these projects include X. B. Wang, J. B. Nicholas, E. R. Vorpagel, and P. Jungwirth.

a manifestation of the hydrophilic and hydrophobic forces at the molecular level. This work provides a simple and clean model system to study the hydrophilic and hydrophobic effects and may be relevant to understanding the hydration and conformation changes of biological molecules. We further expanded such study to a series dicarboxylate dianions with different aliphatic chain lengths and demonstrated systematically the delicate interplay between the hydrophilic and hydrophobic interaction and electrostatic interactions.

Solvation of the Azide Anion (N_3^-) in Water Clusters and Aqueous Interfaces: As a classical example of a strong nucleophile, the azide anion is of considerable importance in organic and inorganic chemistry. We obtained the PES spectra $N_3^-(H_2O)_n$ (n = 0-16) clusters and performed computational studies on the hydrated N_3^- clusters. PES spectra of the solvated azide anions were observed to consist of a single peak, similar to that of the bare N_3^-, but the spectral width was observed to broaden as a function of cluster size due to solvent relaxation upon electron detachment. The adiabatic and vertical electron detachment energies were measured as a function of solvent number. The measured electron binding energies indicate that the first four solvent molecules have much stronger interactions with the solute anion, forming the first solvation shell. The spectral width levels off at n = 7, suggesting that three waters in the second solvation shell are sufficient to capture the second shell effect in the solvent relaxation. Density functional calculations were carried out for N_3^- solvated by one to five waters and showed that the first four waters interact directly with N_3^- and form the first solvation shell on one side of the solute. The fifth water does not directly solvate N_3^- and begins the second solvation shell, consistent with the observed PES data. Molecular dynamics simulations on both solvated clusters and bulk interface revealed that the asymmetric solvation state in small clusters persist for larger systems and that N_3^- prefers interfacial solvation on water clusters and at the extended vacuum/water interface.

Photodetachment of Hydrated Oxalate Dianions in the Gas Phase, $C_2O_4^{2-}(H_2O)_n$ (n = 3-40) – From Solvated Clusters to Nano Droplet: We have carried out extensive studies on the solvation and solvent stabilization of the sulfate dianions (SO_4^{2-}). Similar to sulfate, oxalate ($C_2O_4^{2-}$) is another common dianion in the condensed phase, but is not electronically stable as an isolated species in the gas phase, owing to the strong intramolecular Coulomb repulsion. We observed hydrated oxalate clusters, $C_2O_4^{2-}(H_2O)_n$ for n = 3-40, using electrospray ionization of an oxalate salt solution and studied their energetics and stabilities using PES and theoretical calculations. We found that the smallest observable solvated cluster, $C_2O_4^{2-}(H_2O)_3$, has an adiabatic electron binding energy of ~0.0 eV, i.e., a minimum of three H_2O molecules is required to stabilize $C_2O_4^{2-}$ in the gas phase, similar to SO_4^{2-}, which also requires a minimum of three waters to be stabilized in the gas phase. Theoretical calculations show that the first four waters bind tightly to $C_2O_4^{2-}$, each forming two H-bonds with $C_2O_4^{2-}$ peripherally without inter-water H-bonding. The charges of the dianion were stabilized sufficiently that additional waters beyond n = 4 form only single H-bonds with $C_2O_4^{2-}$ and inter-water H-bonding was observed only starting at n = 5. The repulsive Coulomb barrier (RCB), characteristic of multiply-charged anions, was estimated from photon energy-dependent spectra for the smaller clusters and was found to decrease with increasing n. We observed that photoelectron intensities for features of the solute decreased as n increased, whereas detachment signals from the solvent became dominant for the large solvated clusters. This observation suggested that $C_2O_4^{2-}$ is situated in the center of the solvated clusters so that electrons detached from the solute were suppressed by the surrounding solvent layer in the nanometer-sized water droplet containing a single solute molecule.

Photodetachment of Hydrated Nitrate Anion (NO_3^-): Nitrate is a common inorganic anion in the solid, solution, and atmosphere. For chemical reactions involving negative anions in the atmosphere, hydration is particularly important because water is present in the atmosphere in relatively high concentration. Understanding the interactions of nitrate with a few waters is the first step in providing a molecular description of the structure and energetics of nitrate in aqueous solutions at the air/solution interface. We investigated free and water-solvated gas phase nitrate anions, $NO_3^-(H_2O)_n$ (n = 0-5) using PES and ab initio calculations. We obtained the electronic structure and electron binding energies of the free and

solvated NO_3^- from PES at three photon energies. The spectra of the solvated nitrate complexes are similar to that of the bare NO_3^-, but with increasing electron binding energies. The spectra of the solvated species are broadened due to the solvation effect. Surprisingly, the spectrum of $NO_3^-(H_2O)_3$ showed a resolved vibrational progression due to the N-O symmetric stretching (1000 cm^{-1}), suggesting the cluster possesses relatively high symmetry. We calculated the geometries, vibrational frequencies, and energetics for $NO_3^-(H_2O)_n$ (n = 0-6) and showed that $NO_3^-(H_2O)_n$ with n = 1-3 are all planar with $NO_3^-(H_2O)_3$ forming a high symmetry C_{3h} structure. The next three waters form the second solvation shell, without direct contact with NO_3^-.

Future Plans

The main thrust of our BES program will continue to focus on cluster model studies of condensed phase phenomena in the gas phase. The experimental capabilities developed provide us with the opportunities to examine fundamental chemical physics issues in complex anion solvation and solution chemistry. The work planned for the Chemical Physics Program for the immediate future is briefly outlined here.

Development of a Second Generation ESI-PES Apparatus: Controlling the Cluster Temperatures: The electrospray photodetachment apparatus developed in our laboratory has proven to be a powerful technique to study multiply charged anions and solvated species. It has allowed a wide range of solution-phase species to be investigated in the gas phase. Over the past several years, we have gained considerable experience in operating this apparatus and recognize several of its limitations. A critical feature of this apparatus is its ability to trap ions and accumulate number density from the continuous electrospray source for subsequent time-of-flight mass analysis. The current trap is operated at room temperature. A second generation ESI-PES apparatus, which is aimed at controlling the cluster temperatures, is being developed in our laboratory. A cryogenic ion trap is being constructed to produce cold anions, which will be essential to suppress thermal broadening in the PES spectra. Furthermore, the current ion trap stores all incoming ions, which reduces the trapping efficiency due to space charge effect. A quadrupole mass filter will be added to pre-select the ions of interest for storage and accumulation. This is particularly important for large clusters and weakly populated species. The third improvement involves the construction of a high-resolution reflectron time-of-flight mass spectrometer, which will allow chemical reactions, photoexcitations, and fragmentations to be performed for the stored ions. We started the design work in 2002, and begun construction in 2003. Construction has been finished; testing and tuning are underway. Full operation of the new apparatus is expected to take place at the end of 2004.

Confirmation Change vs. Temperature: the Effect of Entropy: We anticipate that this second generation ESI-PES apparatus will significantly expand our capability and flexibility to study solvated species in the gas phase. A good example is to reexamine the microsolvation of dicarboxylate dianions, discussed above. The previous experiment on solvated dicarboxylate was done at room temperature, but the real temperature of the cluster was unknown. However, theoretical calculations indicate that the folding transition is not only dependent on the solvent number, but also on the cluster temperature due to the effect of entropy. In the new apparatus, the ion trap temperature can be controlled and varied from 17 K to 400 K. Systematical studies of the folding conformation change as function of temperature will be performed and compared with MD simulations.

Gas Phase Studies of Free and Solvated Oligonucleotides: The ionization of nucleotides plays very important roles in the chemistry of DNA. Induced by electrophiles or ionizing radiation, the electron deficient site (hole) on the nucleotide and its migration directly leads to DNA damages. In most cases, the initial oxidation site or the electron-loss center ultimately moves via the DNA π stack to end up at a guanine base, resulting in a guanine cation. This is attributed to the low ionization potential of guanine relative to the other DNA bases. Thus the electronic structure of nucleotides and their ionization properties are essential for understanding the mechanism of DNA damages. Gas phase PES studies probe

the intrinsic electronic properties of the nucleotides and provide important experimental data to compare with and verify theoretical methods. We plan to use PES to study nucleotide anions in the gas phase. One interesting question is whether we can observe a well-defined ionization peak at low binding energies for guanine-containing nucleotides, since guanine is the most susceptible to oxidation to give the guanine cation in DNA damages. We also plan to study the gas phase formation of the Watson-Crick base pairs, as well as solvent and counter-ion stabilization on the structure and energetics of DNA nucleotides in the gas phase.

References to Publications of DOE Sponsored Research (FY 2002-2004)

1. "Bulk-Like Features in the Photoemission Spectra of Hydrated Doubly-Charged Anion Clusters" (X. B. Wang, X. Yang, J. B. Nicholas, and L. S. Wang), *Science* **294**, 1322-1325 (2001).
2. "Experimental and Theoretical Investigations of the Stability, Energetics, and Structures of $H_2PO_4^-$, $H_2P_2O_7^{2-}$, and $H_3P_3O_{10}^{2-}$ in the Gas Phase" (X. B. Wang, E. R. Vorpagel, X. Yang, and L. S. Wang), *J. Phys. Chem. A* **105**, 10468-10474 (2001).
3. "Photodetachment and Theoretical Study of Free and Water-Solvated Nitrate Anions, $NO_3^-(H_2O)_n$ (n = 0-6)" (X. B. Wang, X. Yang, L. S. Wang, and J. B. Nicholas), *J. Chem. Phys*. **116**, 561-570 (2002).
4. "Photodetachment of Hydrated Sulfate Doubly Charged Anions: $SO_4^{2-}(H_2O)_n$ (n = 4-40)" (X. Yang, X. B. Wang, and L. S. Wang), *J. Phys. Chem. A* **106**, 7607-7616 (2002).
5. "Probing Solution Phase Species and Chemistry in the Gas Phase" (X. B. Wang, X. Yang, and L. S. Wang), *Int. Rev. Phys. Chem*., in press (2002). (**invited review**)
6. "Photodetachment of Hydrated Oxalate Dianions in the Gas Phase, $C_2O_4^{2-}(H_2O)_n$ (n = 3-40) – From Solvated Clusters to Nano Droplet" (X. B. Wang, X. Yang, J. B. Nicholas, and L. S. Wang), *J. Chem. Phys*. **119**, 3631-3640 (2003).
7. "Solvent-Mediated Folding of A Doubly Charged Anion" (X. Yang, Y. J. Fu, X. B. Wang, P. Slavicek, M. Mucha, P. Jungwirth, and L. S. Wang), *J. Am. Chem. Soc*. **126**, 876-883 (2004).
8. "Solvation of the Azide Anion (N_3^-) in Water Clusters and Aqueous Interfaces: A Combined Investigation by Photoelectron Spectroscopy, Density Functional Calculations, and Molecular Dynamics Simulations" (X. Yang, B. Kiran, X. B. Wang, L. S. Wang, M. Mucha, and P. Jungwirth), J. Phys. Chem. A, in press (2004).
9. "Bulk vs. Interfacial Aqueous Solvation of Dicarboxylate Dianions" (B. Minofar, M. Mucha, P. Jungwirth, X. Yang, Y. J. Fu, X. B. Wang, and L. S. Wang), J. Am. Chem. Soc., in press (2004).

Surface Chemical Dynamics

M. G. White, R. J. Beuhler, N. Camillone III, and A. L. Harris

Chemistry Department, Brookhaven National Laboratory, Upton, NY 11973

(mgwhite@bnl.gov, beuhler@bnl.gov, nicholas@bnl.gov, alexh@bnl.gov)

1. Project Scope

Thermal and photo-induced reactions on metal surfaces are being investigated with the aim of understanding the dynamics, energetics and morphology-dependence of elementary surface reactions that play key roles in energy-related catalysis. State- and energy-resolved measurements of the gas-phase products resulting from photo-initiated and thermal reactions on metal and metal oxide surfaces are used to infer the dynamics of product formation and desorption and to understand the surface-bound transition state(s). Thermal oxidation and atom-atom recombination reactions important in energy-related catalysis are also being studied with the goal of obtaining a microscopic description of the surface reaction dynamics. Future expansion of these efforts includes time-resolved studies of dynamics at surfaces utilizing ultrafast laser pulses to initiate and probe electronic and nuclear motion with femtosecond resolution. Initial ultrafast studies will focus on photoinitiated chemical transformations on single crystal metals and oxides, as well as supported metal nanoparticles. These experiments will serve as a point of entry for future ultrafast studies of electronic relaxation and adsorbate vibrational relaxation in these systems.

2. Recent Progress

Dynamics of O_2 interactions with transition metal surfaces. Measurements of the final state properties of desorbing O_2 molecules (translational, ro-vibronic and spatial distributions) are being used to investigate the dynamics of adsorption, desorption and dissociation of oxygen on metal and metal oxide surfaces. These processes are not well understood at a microscopic level, yet they are crucial in establishing the role that adsorbed molecular and atomic oxygen play in thermal and photo-induced oxidation reactions on solid surfaces. Our recent studies on the recombinative desorption of O-atoms on a polycrystalline Ag surface highlight the utility of state-resolved methods for exploring the nature of the low energy barrier(s) to adsorption and subsequent dissociation to surface O atoms [1]. We are currently extending these studies to single crystal Ag(111) and O/Ag(110) surfaces, whose well-defined structures offer the possibility of theoretical modeling. With the addition of a new O-atom beam source (thermal cracker), we have been able to prepare O-covered Ag(111) and Ag(110) with well-defined adlayer structures and coverages. With increasing coverage, thermal desorption measurements show that it is possible to produce surface O-atoms only (0.25 monolayers), surface and sub-surface species (0.25-0.4M), and at higher coverages, all three O-atom species (surface, sub-surface and bulk). Such well-characterized O/Ag surfaces are key to delineating the role of chemically-distinct surface and sub-surface O-atom species in current reaction studies involving O-atom recombination and oxidation of simple molecules (e.g., ethylene, methanol, ammonia).

Recent experiments have yielded the angular distributions of molecular oxygen resulting from recombinative desorption of O-atoms from the Ag(110) surface. The angular distributions along the $[1\bar{1}0]$ and [100] directions are different and suggest a larger barrier to adsorption for molecules approaching the surface perpendicular to the rows of surface Ag atoms. These results are consistent with

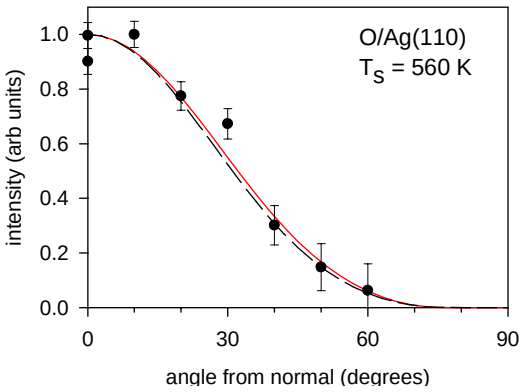

Angular distribution of O_2 desorbed from O/Ag(110) at 560K along the $[1\bar{1}0]$ direction. The solid and dashed curves are semi-empirical calculations based on the unimolecular rate theory of reference [3].

differences in energy scaling for dissociative sticking along the $[1\bar{1}0]$ and [100] directions as observed by molecular beam scattering [2]. In principle, sticking and recombinative desorption (e.g., angular distributions) can be connected via detailed balance and quantitative comparison is being attempted using a unimolecular (statistical) rate theory developed by Harrison and coworkers [3]. A comparison of the observed and predicted angular distribution for O_2 desorbing along the $[1\bar{1}0]$ direction is shown in the accompanying figure using parameters constrained to reproduce the dissociative sticking curve scaled to normal energy [2]. We are also pursuing measurements of the O_2 velocity distributions which provide further insight into the desorption dynamics and test the validity of the theoretical modeling. The latter experiments will be performed by simple heating or laser-induced transient heating of the O/Ag(110) surface and gas-phase detection using (2+1) REMPI [1] or one-photon VUV ionization of the desorbed molecular oxygen. Ultimately, these experiments can lead to a complete description of the energy and state dependence of O_2 sticking on low index Ag surfaces which should provide new information on the surface structure dependence of the O_2-Ag interaction potential.

Transition metal compound cluster formation and deposition: We have recently constructed a cluster deposition apparatus which employs a magnetron sputtering source for generating gas-phase cation clusters of pure metals and metallic compounds. The focus is on generating nanoparticle clusters of the early transition metal compounds (carbides, nitrides, sulfides, phosphides), which are known in their bulk form to be active catalysts for a wide range of heterogeneous reactions, such as hydrodesulfurization, and hydrocarbon isomerization and dehydrogenation. Our goal is to deposit mass-selected nanoparticles onto a substrate, e.g., graphite or TiO_2, and thereby prepare a model catalyst system whose particle size distribution is precisely known. Using the magnetron soure and high-mass quadrupole filter, we have demonstrated the ability to form a wide range of bare metal, metal carbide and metal sulfide cluster ions with resolvable masses up to 10,000 amu, e.g., Mo_{105}. Transition metals studied include Ti, V, Zr, Nb and Mo. Of significant interest is the observation of well-known "magic number" Metcar clusters (M_8C_{12}, M≡Ti, Zr), as well the observation of nearly stoichiometric niobium carbide nanocrystallites, *e.g.*, $Nb_xC_{x\pm1}$. For molybdenum sulfide, we observe a particulary stable cation cluster corresponding to Mo_3S_9 using the magnetron source whereas the most prominent peak in the neutral cluster distribution from laser ablation corresponds to Mo_6S_4 [4]. The Mo_3S_9 cluster has been identified as the structural building block in an amorphous phase of molybdenum sulfide which is particularly active for hydrodesurfurization [5]. Density functional calculations of the structures of the major Mo sulfide and oxide clusters are currently in progress.

3. Future Plans

Future experiments will incorporate existing and recently developed capabilities, as well as involve the development of new capabilities, to make state-, energy-, angular- and time-resolved measurements of the photoinduced surface chemical dynamics of O_2 and CO on TiO_2 and metal nanoparticles supported on TiO_2. In the near term, experiments on TiO_2 will focus on the dynamics of electron transfer in the single electron excitation regime, and those on the nanoparticles will involve multiple electronic transitions and

related excitations. Both types of experiments seek to explore structure-dependent dynamics and involve techniques that in the longer term will be mixed and matched to provide new insight into questions involving the relationships between structure and function.

Photo-induced desorption and reaction of O_2 on TiO_2 surfaces. Future studies will use spectroscopic tools developed in our on-going O_2/metal studies to investigate the interaction of O_2 with well-characterized TiO_2(110) surfaces. The goals of this work are to characterize molecular adsorption/desorption and surface bonding and to delineate the role of surface oxygen species in thermal and photoinduced oxidation reactions. This work bears on the important role that molecular oxygen plays in heterogeneous photoxidation of organic pollutants on titania surfaces, which are completely inactive in the absence of gas-phase oxygen [6].

Of particular interest is elucidating the photo-induced charge and energy transfer processes that give rise to desorption and reaction with co-adsorbates. The accepted mechanism for O_2 photodesorption involves electron-hole pair formation in the TiO_2 substrate and capture of the hole by adsorbed oxygen. Recent theoretical calculations suggest, however, that a direct, vertical transition between the ground state to a repulsive excited state of the O_2/TiO_2 surface bound complex may be a better description [7]. The desorption mechanism will be probed by experiments that measure the polarization dependence of the yield and final state properties of desorbed O_2 following UV laser photoexcitation above the band gap of TiO_2 (~3.1 eV). Detection of the desorbed O_2 will be performed by (2+1) REMPI [1] or one-photon photoionization using coherent VUV radiation. Photoions will be detected by time-of-flight mass spectrometry for mass and velocity analysis. Angular distributions of the desorbed O_2 molecules will also be attempted using ion optics recently developed for velocity map imaging from surfaces. The state-, energy- and spatially-resolved properties of O_2 molecules photodesorbed from the TiO_2(110) surface will provide a means of uncovering the desorption mechanism and distinguish desorption channels associated with chemically distinct surface bound O_2 species, i.e., α-O_2 or β-O_2, observed in previous studies [8].

Time-Resolved Photoinduced Chemical Dynamics at Nanoparticle Surfaces. Our goal in these experiments is to bring together the ultra-fast and the ultra-small to understand the chemical dynamics behind the chemistry of nanostructured materials. Towards this end we aim to apply time-resolved techniques developed to probe dynamics on 2-D planar surfaces [9-13] to the study of the chemistry of molecules adsorbed on supported nanoparticles. There are several aspects of nanoscale systems that we expect to lead to significant changes in their photochemical reactivity and dynamics. For example, spatial confinement of ballistic electrons, size-dependent electronic structure [14] and the sensitivity of electron-phonon coupling to surface thermal vibrations [15] can significantly extend hot electron lifetimes in small nanoparticles. Our plan is to explore the size-dependence of the photoinduced chemical dynamics as the nanoparticle size is varied through the regime spanning the non-metal to metal transition.

Our studies will involve a two-pulse correlation method wherein the excitation pulse (800 nm, ~ 100 fs, ~ 1 mJ/cm^2) is split into two pulses and directed to impinge upon the surface separated in time by a variable delay. The photoinduced desorption yield is measured by a mass spectrometer. Because the relaxation times of the electronic temperature and the lattice temperature differ by an order of magnitude, the time delay dependence of the yield depends upon the desorption mechanism. For example, when *electronic* coupling dominates, the desorption yield correlation width approximates the relaxation time of the electronic temperature, showing a sub-picosecond to picosecond response. For a *phonon*-mediated process, desorption remains efficient for much longer delay times and shows a much longer (~ 20 ps) correlation width [12].

Given the correlation between reactivity and electronic structure proposed to explain the size-dependent reactivity of metal nanoparticles supported on TiO_2 [14], our initial experiments will focus on probing the photoinduced desorption dynamics of O_2 and CO from Pd_n or Au_n/TiO_2. CO and O_2 adsorption and activation on Au_n/TiO_2 are necessary for catalytic oxidation to occur in these systems. By pumping the electrons of the CO– or O_2–(or O–)nanoparticle complex and monitoring the desorption event in real time, we will probe the coupling between the adsorbates and the nanoparticle electrons and phonons in these catalytically relevant systems.

References

1. R. J. Beuhler and M. G. White, *J. Chem. Phys*. **120**, 2445 (2004).
2. L. Vattuone, M. Rocca, C. Borangoand U. Valbussa, J. Chem. Phys. 101, 713 (1994); A. Raukema, D. A. Butler and A. W. Kleyn, *J. Phys: Condens. Matter* **8**, 1147 (1996).
3. V. A. Ukraintsev and I. Harrison, *J. Chem. Phys*. **101**, 1564 (1994); A. Bukoski, D. Blumling, I. Harrison, *J. Chem. Phys*. **118**, 843 (2002).
4. J. M. Lightstone, H. Mann, M. Wu, P. M. Johnson, and M. G. White, *J Phys. Chem*. **B107,** 10359-10366 (2003).
5. Th. Weber, J. C. Muijsers and J. W. Niemantsverdriet, *J. Phys. Chem*. **99**, 9194 (1995).
6. A. Heller, *Acc. Chem. Res*. **28**, 503 (1995).
7. M. P. de Laura-Castells and J. L. Krause, *J. Chem. Phys*. **118**, 5098 (2003).
8. C. N. Russu and J. T. Yates, *Langmuir* **13**, 4311 (1997); C. L. Perkins and M. A. Henderson, *J. Phys. Chem*. **105**, 3856 (2001).
9. F. Budde, T. F. Heinz, M. M. T. Loy, et al., *Phys. Rev. Lett*. **66**, 3024 (1991).
10. J. A. Misewich, A. Kalamarides, T. F. Heinz, et al., *J. Chem. Phys*. **100**, 736 (1993).
11. D. G. Busch, S. Gao, R. A. Pelak, et al., *Phys. Rev. Lett*. **75**, 673 (1995).
12. M. Bonn, S. Funk, C. Hess, et al., *Science* **285**, 1042 (1999).
13. C. Hess, S. Funk, M. Bonn, et al., *Appl. Phys*. A **71**, 477 (2000).
14. M. Valden, X. Lai, and D. W. Goodman, *Science* **281**, 1647 (1998).
15. T. Valla, M. Kralj, A. Šiber, et al., *J. Phys.: Condens. Matter* **12**, L477 (2000).

Publications 2002-2004

1. Gas-Phase Production of Molybdenum Carbide, Nitride and Sulfide Clusters and Nanocrystallites, J. M. Lightstone, H. Mann, M. Wu, P. M. Johnson, and M. G. White, *J Phys. Chem*. **B107,** 10359-10366 (2003).
2. State-Resolved Dynamics of Oxygen Atom Recombination on Polycrystalline Ag, R. J. Beuhler and M. G. White, *J. Chem. Phys*. **120**, 2445 (2004).
3. Reactivity Studies with Gold-Supported Molybdenum Nanoparticles, D. V. Potapenko, J. M. Horn, R. J. Beuhler, Z. Song and M. G. White, *Surf. Sci.* submitted.

Ionic Liquids: Radiation Chemistry, Solvation Dynamics and Reactivity Patterns

James F. Wishart, Alison M. Funston, and Tomasz Szreder
Chemistry Department, Brookhaven National Laboratory, Upton, NY 11973-5000
wishart@bnl.gov

Program Definition

Ionic liquids (ILs) are a rapidly expanding family of condensed-phase media with important applications in energy production, nuclear fuel and waste processing, improving the efficiency and safety of industrial chemical processes, and pollution prevention. ILs are nonvolatile, noncombustible, highly conductive, recyclable and capable of dissolving a wide variety of materials. They are finding new uses in chemical synthesis, catalysis, separations chemistry, electrochemistry and other areas. Ionic liquids have dramatically different properties compared to conventional molecular solvents, and they provide a new and unusual environment to test our theoretical understanding of charge transfer and other reactions. We are interested in how IL properties influence physical and dynamical processes that determine the stability and lifetimes of reactive intermediates and thereby affect the courses of chemical reactions and product distributions.

Successful use of ionic liquids in radiation-filled environments, where their safety advantages could be significant, requires an understanding of ionic liquid radiation chemistry. For example, characterizing the primary steps of IL radiolysis will reveal radiolytic degradation pathways and suggest ways to prevent them or mitigate their effects on the properties of the material. An understanding of ionic liquid radiation chemistry will also facilitate pulse radiolysis studies of general chemical reactivity in ILs, which will aid in the development of applications listed above. Very early in our radiolysis studies it became evident that slow solvation dynamics of the excess electron in ILs (which vary over a wide viscosity range) increases the importance of pre-solvated electron reactivity and consequently alters product distributions. Parallel studies of IL solvation phenomena using coumarin-153 dynamic Stokes shifts and polarization anisotropy decay rates are done to compare with electron solvation studies and to evaluate the influence of ILs on charge transport processes.

Methods. Picosecond pulse radiolysis studies at BNL's Laser-Electron Accelerator Facility (LEAF) are used to identify reactive species in ionic liquids and measure their solvation and reaction rates. IL solvation and rotational dynamics are measured by TCSPC and fluorescence upconversion measurements in the laboratory of E. W. Castner at Rutgers Univ. Diffusion rates are obtained by PGSE NMR in S. Greenbaum's lab at Hunter College, CUNY. We and our collaborators R. Engel and S. Lall-Ramnarine at Queens College, CUNY develop and characterize new ionic liquids specifically designed for our radiolysis and solvation dynamics studies.

Recent Progress

Solvated Electrons. Experiments performed at LEAF demonstrated for the first time that radiolysis of $[R_4N][NTf_2]$ $[R_4N][N(CN)_2]$, and $[R_4P][N(CN)_2]$ ionic liquids produces solvated electrons that absorb over a broad range in the near infrared and persisting for hundreds of nanoseconds [1,3,5]. The e_{solv}^- spectra of NTf_2^- salts of the *N*-methyl,*N*-butylpyrrolidinium (P_{14}^+) and hexyltributylammonium ($HxBu_3N^+$) cations are shown at right. (Each spectrum is representative of four examples of liquids with similar structures.) The differences in band shape and position indicate different distributions of electron solvation cavity sizes and shapes as a function of cation structure, the nature of which may be revealed by future MD simulations.

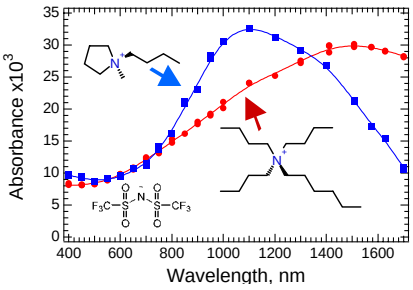

Pre-solvated electron reactivity and solvation dynamics in ILs. In the course of kinetic measurements described below it was found that relatively low scavenger concentrations substantially reduced the initial yield of solvated electrons [1]. Direct scavenging of pre-solvated ("dry") electrons competes effectively with the slower electron solvation processes in ionic liquids. For example, a pyrene concentration of only 63 mM reduces the solvated electron yield to 37% of the scavenger-free value. This finding has major implications for processing of radioactive materials, where seemingly innocuous quantities of solutes may scavenge electrons very effectively. Conversely, dry electron scavenging facilitates the use of pulse radiolysis in electron transfer studies by providing a

way to circumvent diffusion-limited precursor formation rates. Measurements of excess electron solvation processes and emission dynamics (Stokes shift and polarization anisotropy decay) of solvatochromic coumarin-153 show that the reorganization dynamics of ionic liquids occur on much longer timescales (nanoseconds) than in conventional polar solvents (picoseconds). The slow solvation dynamics would also be expected to significantly alter transition state dynamics and provide a potential means to control product distribution. This becomes particularly important for transition states with a very different polarity from the reactants and/or products.

To look at electron solvation with higher time resolution, we developed novel ionic liquids with lower melting points and viscosities, based on ether-substituted pyrrolidinium cations [5]. The new liquids have RT viscosities low enough (~66 cP) to flow through the picosecond pulse-probe transient absorption system at LEAF, which requires sample exchange to avoid cumulative radiation effects. Consequently, the electron solvation process was directly observed in *N*-methyl,*N*-ethoxyethyl-pyrrolidinium NTf_2^- by monitoring the decay of pre-solvated electrons at 1400 nm (to yield a solvated electron spectrum similar to the blue curve for P_{14}^+ above). The electron solvation lifetime is 300 ps (See plot at right), while $<\tau_{solv}>$ obtained from coumarin 153 Stokes shift measurements is 500 ps.

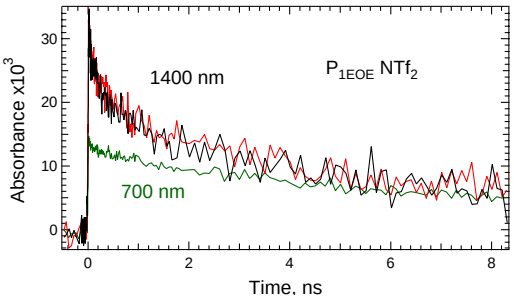

Even slower solvation processes were observed in pulse radiolysis studies of ionic liquids containing ether-, alcohol- and alkyl-functionalized quaternary ammonium dications $(CH_3)_2(R)N^+(CH_2)_nN^+(R)(CH_3)_2\ (NTf_2^-)_2$, where R = $(CH_2)_3OH$, $(CH_2)_2OCH_2CH_3$, or $(CH_2)_3CH_3$ and n = 3–8. Spectra on nanosecond timescales revealed that solvation of the excess electron is particularly slow in the case of the alcohol-derivatized ionic liquids. The blue shift of the electron spectrum to the customary 650 nm peak takes 25-40 nanoseconds at RT (viscosities ~4500-6800 cP). Comparison with the ~1 ns electron solvation time observed in similarly viscous 1,2,6-trihydroxyhexane (2500 cP) reveals the hindering effect of the ionic liquid lattice on hydroxypropyl side chain reorientation [4].

Reaction rates. Electron reactions with several aromatic acceptors, acids, and oxygen were measured in $(MeBu_3N^+)(NTf_2^-)$. Rate constants for solvated electron capture by benzophenone, pyrene and phenanthrene were on the order of $1.6 \times 10^8\ M^{-1}\ s^{-1}$, typically 100 times slower than observed in conventional polar solvents [1]. The reactions of hydrogen atoms with several of the same reactants were measured in the same ionic liquid. H-atoms react very rapidly with pyrene and phenanthrene ($\sim 3 \times 10^9\ L\ mol^{-1}\ s^{-1}$) to form H-adduct radicals [2]. The H-atom rate constants are similar to the values measured or estimated for the same reactions in aqueous solutions. The H-atom reactions with the aromatic hydrocarbons must be diffusion-controlled. but are faster than diffusion-controlled reactions for solvated electrons in the same ionic liquid.

The results indicate that the diffusion rate for the solvated electron in ionic liquids can be significantly lower than those of small neutral molecules or radicals such as the H-atom, in contrast to the situation in molecular solvents. These results support the contention that the diffusion constants of charged and neutral reactants differ considerably in ionic liquids, which could lead to a means of controlling reactivity and transport phenomena through rational selection of ionic liquid properties.

Future Plans

Electron solvation and reactivity. The validity of proposed pre-solvated electron scavenging mechanisms will be tested by exploring the competition between the electron solvation and electron capture processes in ionic liquids. Electron solvation dynamics in several families of low-viscosity ILs will be measured by pulse-probe radiolysis. Subsequently, scavengers will be added to measure the kinetics of pre-solvated electron capture. It is well known from work in molecular solvents that many scavengers, for example SeO_4^{2-}, have widely different reactivity profiles towards pre-solvated and solvated electrons. By quantitative measurement of the scavenging profiles of many reactants, we hope to explain such conundrums mechanistically.

Many ionic liquids with slow electron solvation rates are too viscous to be flowed for pulse-probe experiments. Detailed studies of electron solvation in these ILs will be possible upon installation of the “ultrafast single-shot” detection system at LEAF. In the meantime, C-153 solvation dynamics studies will serve as proxies for the electron

results to aid the study of pre-solvated electron scavenging mechanisms as measured by "time-zero" radiolytic product yields.

Charge transport in ionic liquids. Pulse radiolysis will be used to study how ionic liquids affect charge-transport reactions related to solar energy photoconversion systems, where their characteristics may prove valuable. IL-based photoelectrochemical cells have already been reported. Focus areas will be the combined effects of ionic solvation and slow solvent relaxation on the energy landscape of charge transport, and the influence of the lattice-like structure of ionic liquids on the distance dependence of electron transport reactions.

Non-classical diffusion in ionic liquids. Ionic liquids contain considerable void space due to the poor packing that makes them liquids instead of solids. The combination of voids and the ionic lattice result in unusual diffusion rate trends reported in the literature. Kinetic and high-pressure pulsed-gradient spin echo NMR studies of diffusion rates of charged and neutral species will examine how ionic liquids modulate diffusion as a function of size and charge.

Publications on ionic liquids

1. *Spectrum and Reactivity of the Solvated Electron in the Ionic Liquid Methyltributylammonium Bis(trifluoromethylsulfonyl)imide* J. F. Wishart and P. Neta *J. Phys. Chem. B* **107,** 7261-7267 (2003)
2. *Pulse Radiolysis Study of the Reactions of Hydrogen Atoms in the Ionic Liquid Methyltributylammonium Bis(trifluoromethylsulfonyl)imide* J. Grodkowski, P. Neta and J. F. Wishart *J. Phys. Chem. A*, **107,** 9794-9799 (2003).
3. *Radiation Chemistry of Ionic Liquids: Reactivity of Primary Species* J. F. Wishart in "Ionic Liquids as Green Solvents: Progress and Prospects" Rogers, R. D. and Seddon, K. R., Eds.; *ACS Symp. Ser*. **856**, Ch. 31, pp. 381-396, American Chemical Society, Washington, DC, 2003.
4. *Effects of Functional Group Substitution on Electron Spectra and Solvation Dynamics in a Family of Ionic Liquids* J. F. Wishart, S. I. Lall-Ramnarine, R. Raju, A. Scumpia, S. Bellevue, R. Ragbir, and R. Engel *Radiat. Phys. Chem.* in press.
5. *Dynamics of Fast Reactions in Ionic Liquids* A. M. Funston and J. F. Wishart in "Ionic Liquids: Progress and Prospects" Rogers, R. D. and Seddon, K. R., Eds.; *ACS Symp. Ser.* in press.

Publications on radiation chemistry, electron transfer and reaction mechanisms

6. *Mechanistic Information from Pressure Acceleration of Hydride Formation via Proton Binding to a Cobalt(I) Macrocycle* E. Fujita, J. F. Wishart and R. van Eldik *Inorg. Chem.* **41,** 1579-1583 (2002)
7. *A Dendrimer-Based Electron Antenna: Paired Electron Transfer Reactions in Dendrimers with a 4,4'-bipyridine Core and Naphthalene Peripheral Groups* T. H. Ghaddar, J. F. Wishart, D. W. Thompson, J. K. Whitesell, and M. A. Fox *J. Am. Chem. Soc.* **124,** 8285-8289 (2002)
8. *Reactions of Charged Species in Supercritical Xenon as Studied by Pulse Radiolysis* R. A. Holroyd, J. F. Wishart, M. Nishikawa, and K. Itoh *J. Phys. Chem. B* **107,** 7281-7287 (2003)
9. *Do Main Chain Hydrogen Bonds Create Dominant Electron Transfer Pathways? An Investigation in Designed Proteins* Y. Zheng, M. A. Case, J. F. Wishart, and G. L. McLendon *J. Phys. Chem. B* **107,** 7288-7292 (2003)
10. *Radiation Chemistry of Methyl*-tert-*Butyl Ether (MTBE) in Aqueous Solution* S. P. Mezyk, J. Jones, W. J. Cooper, T. Tobien, M. G. Nickelsen, J. W. Adams, K. E. O'Shea, D. M. Bartels, J. F. Wishart, P. M. Tornatore, K. S. Newman, K. Gregoire, and D. J. Weidman *Envir. Sci. Tech.*, **38**, 3994-4001 (2004).
11. *Long-Range Electron Transfer across Peptide Bridges: the Mechanistic Transition from Superexchange to Hopping* R. Abdel Malak, Z. Gao, J. F. Wishart, and S. S. Isied, *J. Am. Chem. Soc.* in press.
12. *Convergence of Spectroscopic and Kinetic Electron Transfer Parameters for Mixed-Valence Binuclear Dipyridylamide Ruthenium Ammine Complexes* A. J. Distefano, J. F. Wishart, and S. S. Isied *Coord. Chem. Rev.*, in press.

Ultrafast Pulse Radiolysis at BNL's Laser-Electron Accelerator Facility (LEAF)

James F. Wishart, Andrew R. Cook, Richard A. Holroyd, Sergei V. Lymar and John R Miller
Chemistry Department, Brookhaven National Laboratory, Upton, NY 11973-5000
wishart@bnl.gov, acook@bnl.gov, holroyd@bnl.gov, lymar@bnl.gov, jrmiller@bnl.gov

The BNL Laser-Electron Accelerator Facility (LEAF) is a pioneering facility for the study of fast radiation-induced reactions. LEAF uses a laser-pulsed photocathode, radio-frequency electron gun to generate 7-picosecond pulses of 8.7 MeV electrons for pulse radiolysis experiments. The compact and operationally simple accelerator system includes synchronized laser pulses that can be used to probe or excite the electron-pulsed samples to examine the dynamics and reactivity of chemical species on the picosecond timescale.

Two experimental stations are in operation at LEAF. A pulse-probe transient absorption station uses femtosecond Ti:S fundamental (800 nm), second harmonic (400 nm) or optical parametric amplifier probe pulses. The present detection range is 200 – 1700 nm with a 10 ns time range. A digitizer-based transient absorption station has up to ~120 ps time resolution in the visible and nanosecond resolution in the NIR.

LEAF's pulse-probe system was used to observe the formation of Xe_2* excimers in irradiated supercritical xenon (scXe) and rates of electron attachment to C_6F_6 in scXe and subsequent electron transfer to benzoquinone were measured using the digitizer station [16]. LEAF has also been used to investigate fast electron transfer reactions in dendrimers [7] and molecular wires [17], measure solvated electron spectra and reaction kinetics of solvated and pre-solvated electrons and of H-atoms in ionic liquids [1,2], and examine picosecond dissociation of aryl-halide molecules upon electron attachment [18]. Other LEAF experiments showed that addition of arenes such as benzene or toluene increased the yield of radical cations in irradiated dichloroethane[19]. Ongoing studies include geminate recombination and electron-hole pair distribution in aliphatic and aromatic non-polar solvents, "dry" electron capture, and further work on ionic liquids, molecular wires, electron transfer and nanoscience applications.

Future plans include the development of ultrafast single-shot absorbance detection methods for faster kinetic measurements on precious or viscous samples (unsuitable for the pulse-probe flow system) and a femtosecond pulse-pump-probe experimental system for studying excited states of radical ions.

Access to the LEAF facility by users outside of BNL is encouraged, either through user-facility arrangements or collaboration with BNL staff. Please contact the authors above or the general user facility address (crcr@bnl.gov) for more information.

Publications on the Laser-Electron Accelerator Facility (LEAF)

13. *Accelerators for Ultrafast Phenomena* J. F. Wishart, in "Radiation Chemistry: Present Status and Future Trends" C. D. Jonah, B. S. M. Rao, Eds.; *Studies in Physical and Theoretical Chemistry, Vol. 87*, Ch. 2, Elsevier Science, (2001), pp. 21-35.
14. *Radiolysis with RF Photoinjectors: Supercritical Xenon Chemistry* J. F. Wishart in "Femtosecond Beam Science" Uesaka, M., Ed.; Imperial College Press, London, in press.
15. *The LEAF Picosecond Pulse Radiolysis Facility at Brookhaven National Laboratory* J. F. Wishart, A. R. Cook, and J. R. Miller *Rev. Sci. Inst.*, in press.

Publications since 2002 on work done at LEAF (Six additional publications were published before 2002.)
Publications 1-5, 7, 8, 11 and 12 from the previous abstract, plus:

16. Density Inhomogeneities and Electron Mobility in Supercritical Xenon, R. A. Holroyd, K. Itoh and M. Nishikawa, *J. Chem. Phys.* **118,** 706-710 (2003).
17. Charge Transfer through Terthiophene End-Capped Poly(arylene ethynylene)s A. M. Funston, E. E. Silverman, J. R. Miller, and K. S. Schanze *J. Phys. Chem. B* **108,** 1544-1555 (2004).
18. Faster Dissociation: Measured Rates and Computed Effects on Barriers in Aryl Halide Radical Anions, N. Takeda, P. V. Poliakov, A. R. Cook, and J. R. Miller, *J. Am. Chem. Soc*., **126,** 4301-4309 (2004).
19. Increased Yields of Radical Cations by Arene Addition to Irradiated 1,2-Dichloroethane, A. M. Funston and J. R. Miller, *Radiat. Phys. Chem.*, in press.
20. Electron Attachment to C_{60} in Nonpolar Solvents, R. A. Holroyd, *Radiat. Phys. Chem.* (in press).

Title: Electronically non-adiabatic interactions in molecule metal-surface scattering: Can we trust the Born-Oppenheimer approximation in surface chemistry?

Principal Investigators: Alec M. Wodtke, Department of Chemistry and Biochemistry, University of California Santa Barbara, Santa Barbara, CA 93106 (wodtke@chem.ucsb.edu) and Daniel J. Auerbach. Hitachi Global Storage Technologies, 650 Harry Road, San Jose, California 95120 (Daniel.Auerbach@hgst.com)

Program Scope and Definitions: When molecules with low levels of vibrational excitation collide with metal surfaces, vibrational coupling to electron-hole pairs is not found to be strong unless incidence energies are high. However, there is accumulating evidence that coupling of large amplitude molecular vibration to metallic-electron degrees-of-freedom can be much stronger even at the lowest accessible incidence energies. As reaching a chemical transition-state also involves large amplitude vibrational motion, we pose the basic question: are electronically non-adiabatic couplings important at transition-states of reactions at metal surfaces? We have indirect evidence in at least one example that the dynamics and rates of chemical reactions at metal surfaces may be strongly influenced by electronically non-adiabatic coupling. This implies that theoretical approaches relying on the Born-Oppenheimer approximation may not accurately reflect the nature of transition-state traversal in reactions of catalytic importance. Developing a predictive understanding of surface reactivity beyond the Born-Oppenheimer approximation represents one of the most important challenges to current research in chemical dynamics. We are developing a new instrument to investigate the interactions of vibrationally excited HCl(v) on gold. Overtone excitation may be used to populate states up to v=7, where at the outer turning point electron-transfer from the metal is more energetically favorable than near the molecule's equilibrium bond-length. Electron mediated vibrational energy transfer as well as dissociative adsorption will be studied with state-to-state molecular beam methods. With this grant we will work to produce a comprehensive set of data characterizing: vibrational-state-specific survival probabilities, state-to-state vibrational energy transfer and vibrational promotion of dissociative adsorption for HCl(v) on gold. We will compare our data to results of theoretical approaches within as well as beyond the Born-Oppenheimer approximation, allowing us to evaluate the importance of electronically non-adiabatic coupling in this model system. This work promises to provide perhaps the best characterized example of electronic non-adiabaticity in surface reactivity.

Recent Progress: The majority of the last year has been devoted to the design and machine-shop construction of a new apparatus for use with two-color overtone-overton pumping of MH bonds in small molecules. A schematic diagram is shown in Figure 1. This machine is outfitted with a cryo-static pump on the source chamber that is optimal for producing the molecular beams of HCl intended for this work. With this arrangement we achieve much higher pumping speeds for lower cost than with either conventional diffusion pumps or turbo-molecular pumps. The differential pumping chambers have been so-constructed to minimize the distance from the beam source to the surface. This provides a substantial improvement in beam intensities over our previous experimental apparatus. In addition, we intend to install in the next year an additional feature, a quadrupolar focusing element for state selective focusing of HCl. We anticipate this will provide between one and two orders of magnitude additional beam intensity. The apparatus is also equipped with a brand new long travel manipulator, provided by the generosity of Dan Auerbach and IBM. Also, Auger Electron Spectroscopy, Argon Ion Sputtering and temperature control of the surface will be features of the apparatus.

We have also set up a tunable dye laser system with frequency doubling for HCl REMPI detection at 235 nm. A new laser system has just been installed that will soon be configured with difference frequency generation to produce light at ~1.7-1.3 μm to pump v=0→2,3 transitions in

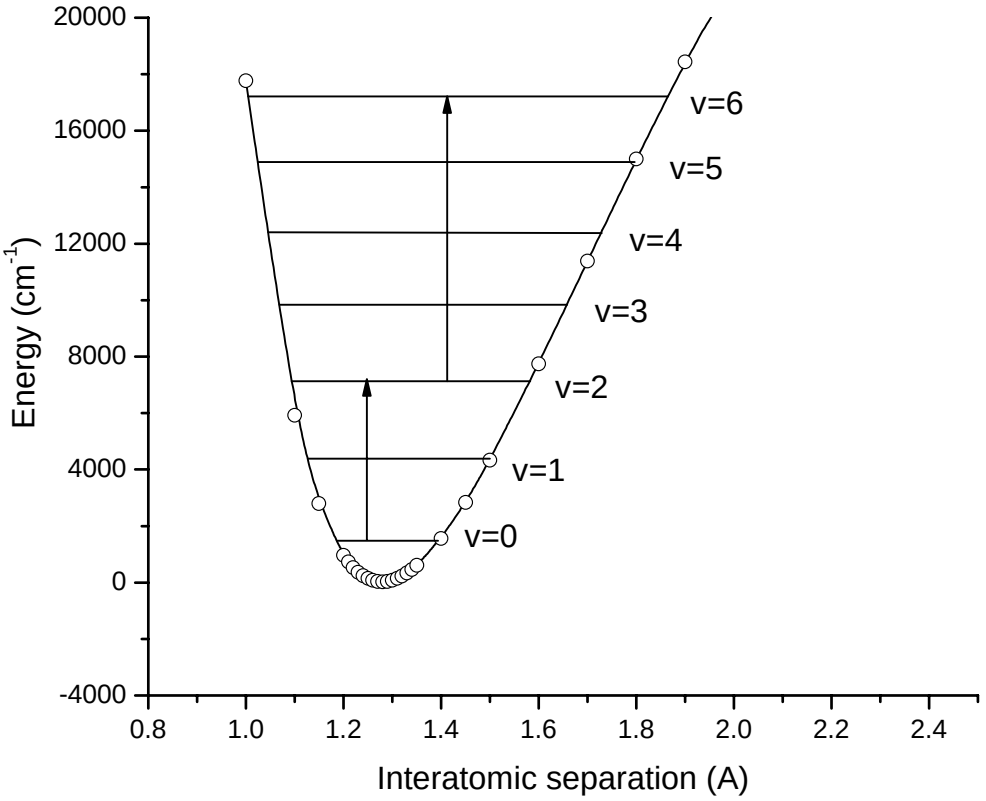

Figure 1: "PUMP and PUMP" excitation of HCl(v=6). Excitation of the 2-0 transition requires only small pulse energies at 1.7 mm. The proposed laser light source is strong enough subsequently to saturate the 6-2 transition.

HCl and later in other molecules for example H_2O. At the end of September, we will receive delivery of a third dye laser to be set up with an existing YAG for Raman shifting Red dye laser light to ~1 μm. This will allow pumping HCl 2-6 and 3-7 transitions. The overall optical pumping scheme is shown in Fig. 1.

In work related to the goals of this grant, we have prepared highly vibrationally excited NO(v=0-18) and investigated the propensity for electron ejection on low work function surfaces. We observe electron emission with high quantum efficiency (~0.02) when highly vibrationally excited nitric oxide molecules are scattered from a low work function (~1.3-1.6 eV) metal surface. The observed efficiency is $\sim 10^4$ larger than previous reports of exoelectron emission from surfaces with similar work functions. These observations give direct evidence that molecules experiencing large amplitude intramolecular nuclear motion can interact with metal surfaces in such a way as to promote strong non-adiabatic coupling to excited electronic states of the metal. Due to the very interesting nature of these results we have also modified the design of the new apparatus to allow for easy preparation of low work function surfaces, we anticipate that this will be a critical part of the ongoing effort.

Future Plans: We intend to carry out experiments in the near future that will attempt to observe the surface temperature dependence and incidence energy dependence of vibrational excitation of H(D)Cl(v=0→1), which is known to be a sensitive probe of the coupling of electrons to vibrational motion in surface collisions. The seminal observations on NO/Ag(111)[1] have yet to be

confirmed for another molecule. These experiments seek to generalize previous results and examine differences. Due to their simplicity, these experiments will be pursued first. Infrared excitation of HCl v=2 and 3 will then be undertaken on simple metal surfaces. Survival probabilities will be obtained as a function of incidence energy ^{2}. These experiments will lead inexorably to the two-color overtone-overtone pump and pump excitation of HCl to v=6 and 7. Survival probabilities will be determined as a function of incidence energy. Experiments on low work function surfaces will be carried out to investigate vibrational promotion of electron emission to the gas phase.

A List of Publications related to this grant

1. *Interaction of NO(v=12) with LiF(001): Anomalously large vibrational relaxation rates*, Alec M. Wodtke and Yuhui Huang, Daniel J. Auerbach, Journal of Chemical Physics **118**(17) 8033-41 (2003)

List of public presentations of work related to this grant

1. Invited Talk "Nonadiabatic Effects in Molecular Interactions with Metal Surfaces", Daniel Auerbach, Jason White, Daniel Matsiev, Jun Chen, and Alec Wodtke, Gordon Research Conference on Dynamics at Surfaces, Andover NH, Aug 10-15 2003.

2. Gordon Conference on Dynamics at Surfaces, Andover NH, Aug 10-15 2003, Poster presentation

3. Invited Lecture, University of California Santa Barbara Department of Chemistry and Biochemistry, "Electronically Non-Adiabatic Interactions In Molecule Metal-Surface Scattering: Do We Know How To Think About Surface Chemistry?" , Oct. 20, 2003

4. Invited post deadline paper "Direct Observation of Nonadiabatic Coupling in Molecular Interactions with Surfaces", Daniel Auerbach, Jason White, Daniel Matsiev, Jun Chen, and Alec Wodtke, AVS annual meeting, Baltimore MD, Nov 6, 2003.

5. Invited Lecture, Emory University Department of Chemistry, "Electronically Non-Adiabatic Interactions In Molecule Metal-Surface Scattering: Do We Know How To Think About Surface Chemistry?" , Dec. 3, 2003

6. Invited Talk "Nonadiabatic Effects in Molecular Interactions with Metal Surfaces", Daniel Auerbach, Jason White, Daniel Matsiev, Jun Chen, and Alec Wodtke, Ein Gedi International Symposium on Nonadiabatic Processes on Surfaces, Ein Gedi, Israel, January 11-15, 2004.

7. Invited lecture. Symposium on Atomic, Cluster and Surface Physics (SASP), La Thuile (Aosta) Italy, Invited lecture. "Electronically non-adiabatic interactions in molecule metal-surface scattering: Can we trust the Born-Oppenheimer approximation in surface chemistry?", February 1-6 2004

8. Invited lecture. Free University of Berlin, "Electronically non-adiabatic interactions in molecule metal-surface scattering: Can we trust the Born-Oppenheimer approximation in surface chemistry?", February 9 2004

9. Invited Lecture. University of Göttingen, "Electronically non-adiabatic interactions in molecule metal-surface scattering: Can we trust the Born-Oppenheimer approximation in surface chemistry?", February 10, 2004.

10. Invited Lecture. University of Marburg, "Electronically non-adiabatic interactions in molecule metal-surface scattering: Can we trust the Born-Oppenheimer approximation in surface

chemistry?", February 11, 2004.

11. Invited Lecture. University of Münster, "Electronically non-adiabatic interactions in molecule metal-surface scattering: Can we trust the Born-Oppenheimer approximation in surface chemistry?", February 12, 2004.

12. Invited Lecture. American Physical Society March Meeting, "Observation of electron emission from a metal surface due to collisions of vibrationally excited Molecules", March 26th 2004.

13. Invited Lecture. Emory University – Atlanta Georgia, "Do we know how to think about surface chemistry? Electronically non-adiabatic interactions in molecule metal-surface scattering", April 5 2004.

14. Invited Lecture. University of North Carolina - Chapel Hill, "Do we know how to think about surface chemistry? Electronically non-adiabatic interactions in molecule metal-surface scattering", April 7 2004.

15. Invited Lecture. Dalian Institute of Chemical Physics, "Do we know how to think about surface chemistry? Electronically non-adiabatic interactions in molecule metal-surface scattering", June 20 2004.

16. Invited Lecture, International Symposium on Gas Kinetics, University of Bristol, UK August 7-12 2004

17. Plenary Lecture, MOLEC XV, Sept. 5-10 2004.

References

1. Rettner, C. T., Fabre, F., Kimman, J. & Auerbach, D. J. Observation of direct vibrational excitation in gas-surface collisions: NO on Ag(111). *Phys. Rev. Lett.* **55**, 1904-7 (1985).

2. Huang, Y., Wodtke, A. M., Hou, H., Rettner, C. T. & Auerbach, D. J. Observation of vibrational excitation and de-excitation for NO(v=2) scattering from Au(111): Evidence for electron-hole pair mediated energy transfer. *Phys. Rev. Lett.* **84**, 2985-8 (2000).

Participants

Scott Anderson
University of Utah
Chemistry / 315 S. 1400 E. Rm 2020
Salt Lake City, UT 84112
Email: anderson@chem.utah.edu
Phone: 801-585-7289

Paul Barbara
The University of Texas at Austin
1 University Station, A5300
Austin, TX 78712
Email: p.barbara@mail.utexas.edu
Phone: 512.471.2356

Nicholas Camillone
Brookhaven National Laboratory
Chemistry Department, Bldg 555
Upton, NY 11973
Email: nicholas@bnl.gov
Phone: 631-344-4412

A. Welford Castleman, Jr.
Penn State University
104 Chemistry Building
University Park, PA 16802
Email: awc@psu.edu
Phone: 814-865-7242

Daniel Chipman
Notre Dame Radiation Laboratory
303B Radiation Laboratory
Notre Dame, IN 46556
Email: chipman.1@nd.edu
Phone: 574-631-5562

James Cowin
Pacific Northwest National Labs
EMSL K8-88
Richland, WA 99354
Email: jp.cowin@pnl.gov
Phone: 509 376 6330

Michael Duncan
University of Georgia
Department of Chemistry
Athens, Georgia 30602
Email: maduncan@uga.edu
Phone: 706-542-1998

Barney Ellison
University of Colorado at Boulder
Department of Chemistry & Biochemistry
Boulder, CO 80309
Email: barney@jila.colorado.edu
Phone: 303-492-8603

Michael Fayer
Stanford University
Department of Chemisry, Stanford University
Stanford, CA 94305
Email: fayer@stanford.edu
Phone: 650 723-4446

Mark Gordon
Iowa State University
201C Spedding Hall
Ames, Iowa 50011
Email: mark@si.fi.ameslab.gov
Phone: 515-294-2327

Peter Armentrout
Chemistry Dept, University of Utah
315 S. 1400 E. Rm 2020
Salt Lake City, UT 84112
Email: armentrout@chem.utah.edu
Phone: 801-581-7885

David Bartels
Notre Dame University
Radiation Laboratory
Notre Dame, IN 46556
Email: bartels.5@nd.edu
Phone: 574 631 5561

Ian Carmichael
Notre Dame Radiation Laboratory
Notre Dame University
Notre Dame, IN 46556
Email: carmichael.1@nd.edu
Phone: 574-631-4502

David Chandler
University of California, Berkeley
Department of Chemisty, 210 Gilman Hall
Berkeley, CA 94720
Email: chandler@cchem.berkeley.edu
Phone: 510-643-6821

Steven Colson
Pacific Northwest National Laboratory
PO Box 999 - MSN K9-80
Richland, WA 99352
Email: Steve.Colson@pnl.gov
Phone: 509-375-2288

Robert Crowell
Argonne National Laboratory
Chemistry Division
Argonne, IL 60439
Email: rob_crowell@anl.gov
Phone: 630-252-8089

Michel Dupuis
Pacific Northwest National Laboratory
K1-83 Battelle blvd PO Box 999
Richland, WA 99352
Email: michel.dupuis@pnl.gov
Phone: 509-3752617

Mostafa El-Sayed
Georgia Institute of Technology
School of Chemistry & Biochemistry
Atlanta, GA 30332
Email: mostafa.el-sayed@chemistry.gatech.edu
Phone: 404-894-0292

Bruce Garrett
Pacific Northwest National Laboratory
P.O. Box 999, MS: K1-83
Richland, WA 99352
Email: bruce.garrett@pnl.gov
Phone: 509-372-6344

David Gosztola
Argonne National Laboratory
9700 S. Cass Ave.
Argonne, IL 60439
Email: gosztola@anl.gov
Phone: 630-252-3541

Krishnan Balasubramanian
University of California, Davis
661 East Gate Dr., Hertz Hall
Livermore, CA 94550
Email: kbala@ucdavis.edu
Phone: 925-422-4984

Elliot Bernstein
Colorado State University
Department of Chemistry
Fort Collins, CO 80523
Email: erb@lamar.colostate.edu
Phone: 970-491-6347

Emily Carter
Princeton University
Mechanical & Aerospace Engineering
Princeton, NJ 8544
Email: eac@chem.ucla.edu
Phone: 609-258-6490

James Chelikowsky
University of Minnesota
421 Washington Avenue SE
Minneapolis, MN 55455
Email: jrc@msi.umn.edu
Phone: 612 625 4837

L. Rene Corrales
Pacific Northwest National Lab
P.O. Box 999
Richland, WA 99352
Email: Rene.Corrales@pnl.gov
Phone: 509-375-2404

Liem Dang
Pacific Northwest National Lab
P.O. Box 999
Richland, WA 99352
Email: Liem.Dang@pnl.gov
Phone: 509-375-2557

Kenneth Eisenthal
Columbia University
116th Street and Broadway
New York, NY 10027
Email: eisenth@chem.columbia.edu
Phone: 212-854-3175

Jim Evans
Ames Laboratory
315 Wilhelm Hall, Iowa State University
Ames, Iowa 50011
Email: evans@ameslab.gov
Phone: 515-294-1638

Evelyn Goldfield
Department of Chemistry, Wayne State University
Wayne State University
Detroit, MI 48202
Email: evi@sun.science.wayne.edu
Phone: 313-577-2580

Stephen Gray
Argonne National Laboratory
Chemistry Division, Argonne National Laboratory
Argonne, IL 60439
Email: gray@tcg.anl.gov
Phone: 630-252-3594

Mary Gress
U.S. Department of Energy/Office of Basic Energy Sciences
SC-14/Germantown Building, 1000 Independence Ave.
Washington, DC 20504
Email: mary.gress@science.doe.gov

Ian Harrison
University of Virginia
Dept of Chemistry, P.O. Box 400319
Charlottesville, VA 22904
Email: harrison@virginia.edu
Phone: 434-924-3639

Richard Hilderbrandt
U.S. Department of Energy/Office of Basic Energy Sciences
SC-14/Germantown Building, 1000 Independence Ave.
Washington, DC 20585
Email: richard.hilderbrandt@science.doe.gov

Bret Jackson
Dept. of Chemistry, UMass, Amherst
Dept. of Chemistry, University of Massachusetts
Amherst, MA 1003
Email: jackson@chem.umass.edu
Phone: 413-545-2583

Kenneth Jordan
University of Pittsburgh
Dept. of Chemistry
Pittsburgh, PA 15260
Email: jordan@pitt.edu
Phone: 412-624-8694

Greg Kimmel
Pacific Northwest National Laboratory
MSIN K8 - 88, PO Box 999
Richland, WA 99352
Email: gregory.kimmel@pnl.gov
Phone: 509-376-2501

Edward Lim
The University of Akron
Department of Chemistry
Akron, OH 44325
Email: elim@uakron.edu
Phone: 330 972-5297

Mark Maroncelli
Penn State University
104 Chemistry Building
University Park, PA 16802
Email: mpm@chem.psu.edu
Phone: 814-865-0898

Juan Meza
Lawrence Berkeley National Lab
Mail Stop 50B-2239
Berkeley, CA 94720
Email: JCMeza@lbl.gov
Phone: 510 486-7684

Lukas Novotny
University of Rochester
The Institute of Optics
Rochester, NY 14627
Email: novotny@optics.rochester.edu
Phone: 585 2755767

Charles Harris
Lawrence Berkeley National Lab
Chemical Sciences Division
Berkeley, CA 94720
Email: harris@socrates.berkeley.edu
Phone: 510-6422814

Carl Hayden
Combustion Research Facility, Sandia National Lab
PO Box 969, MS 9051
Livermore, CA 94551
Email: cchayde@sandia.gov
Phone: 925-294-2298

Wilson Ho
University of California, Irvine
2162 Frederick Reines Hall
Irvine, CA 92697
Email: wilsonho@uci.edu
Phone: (949)824-5234

Julius Jellinek
Argonne National Laboratory
9700 S. Cass Ave.
Argonne, Illinois 60439
Email: jellinek@anl.gov
Phone: (630)252-3463

Shawn Kathmann
Pacific Northwest National Lab
P.O. Box 999
Richland, WA 99352
Email: Shawn.Kathmann@pnl.gov
Phone: 509-375-2870

Branka Ladanyi
Colorado State University
Department of Chemistry, Colorado State University
Fort Collins, CO 80523
Email: bl@lamar.colostate.edu
Phone: 970-491-5196

Steven G. Louie
LBNL and UC Berkeley
Department of Physics
Berkeley, California 94720
Email: sglouie@berkeley.edu
Phone: 510-642-1709

William McCurdy
Lawrence Berkeley National Laboratory
One Cyclotron Road, MS-50B-4230
Berkeley, CA 94720
Email: cwmccurdy@lbl.gov
Phone: 510/486-4283

John Miller
U.S. Department of Energy/Office of Basic Energy Sciences
SC-14/Germantown Building, 1000 Independence Ave.
Washington, DC 20585
Email: john.miller@science.doe.gov

Thomas Orlando
Georgia Institute of Technology
School of Chemistry and Biochemistry, 770 State Street
Atlanta, GA 30332
Email: thomas.orlando@chemistry.gatech.edu
Phone: 404-894-8222

Alex Harris
Chemistry Dept, Brookhaven National Lab
Building 555, P.O. Box 5000
Upton, NY 11973
Email: alexh@bnl.gov
Phone: 631-344-4301

Wayne Hess
Pacific Northwest National Lab
MS K8-88
Richland, WA 99352
Email: wayne.hess@pnl.gov
Phone: 509-376-9907

Koblar Jackson
Central Michigan University
Physics Dept/CMU
Mt. Pleasant, MI 48859
Email: jackson@phy.cmich.edu
Phone: 989 774 3310

Mark Johnson
Yale University Chemistry Department
P.O. Box 208107
New Haven, CT 6520
Email: mark.johnson@yale.edu
Phone: 203 432 5226

Bruce Kay
Pacific Northwes National Laboratory
EMSL K8-88 PO Box 999
Richland, WA 99352
Email: bruce.kay@pnl.gov
Phone: 509-376-0026

Nancy Levinger
Colorado State University
Department of Chemistry, Colorado State University
Fort Collins, CO 80523
Email: levinger@lamar.colostate.edu
Phone: 970 491-1331

H. Peter Lu
Pacific Northwest National Lab
P.O.Box 999
Richland, WA 99352
Email: peter.lu@pnl.gov
Phone: 509-376-3897

Dan Meisel
University of Notre Dame
Radiation Laboratory
Notre Dame, IN 46556
Email: dani@nd.edu
Phone: 574 631-5457

Michael Morse
University of Utah, Department of Chemistry
315 S. 1400 East, Room 2020
Salt Lake City, UT 84112
Email: Morse@chem.utah.edu
Phone: (801) 581-8319

Richard Osgood
Columbia University
530 West 120th Street
New York, NY 10027
Email: osgood@columbia.edu
Phone: 212-854-4462

Hrvoje Petek
University of Pittsburgh
Department of Physics and Astrnomy, 3941 O'hara St.
Pittsburgh, PA 15260
Email: Petek@pitt.edu
Phone: 412 624-3599

Douglas Ray
Pacific Northwest National Laboratory
PO Box 999, MSIN: K9-90
Richland, WA 99352
Email: doug.ray@pnl.gov
Phone: 509-375-2500

Greg Schenter
Pacific Northwest National Lab
P.O. Box 999
Richland, WA 99352
Email: Greg.Schenter@pnl.gov
Phone: 509-375-4334

Timothy Steimle
Arizona State University
Dept. of Chemistry and BioChemistry
Tempe, AZ 85287
Email: TSteimle@asu.edu
Phone: (480)965-3265

Ward Thompson
University of Kansas
Department of Chemistry
Lawrence, KS 66045
Email: wthompson@ku.edu
Phone: (785) 864-3980

Frank Tully
U.S. Department of Energy/Office of Basic Energy Sciences
SC-14/Germantown Building, 1000 Independence Ave.
Washington, DC 20585
Email: frank.tully@science.doe.gov

Lai-Sheng Wang
Washington State University
2710 University Drive
Richland, WA 99352
Email: ls.wang@pnl.gov
Phone: (509) 376-8709

Alec Wodtke
University of California Santa Barbara
5548 Somerset Dr.
Goleta, CA 93111
Email: wodtke@chem.ucsb.edu
Phone: 805-893-8085

Simon Pimblott
University of Notre Dame
304C Radiation Laboratory
Notre Dame, IN 46556
Email: simon.m.pimblott.1@nd.edu
Phone: 574.631.7151

Eric Rohlfing
U.S. Department of Energy/Office of Basic Energy Sciences
SC-14/Germantown Building, 1000 Independence Ave.
Washington, DC 20585
Email: eric.rohlfing@science.doe.gov

Ilya Shkrob
Chemistry Division, Argonne National Laboratory
9700 S. Cass Ave
Argonne, IL 60439
Email: shkrob@anl.gov
Phone: 630-2529516

Walter Stevens
U.S. Department of Energy/Office of Basic Energy Sciences
SC-14/Germantown Building, 1000 Independence Ave.
Washington, DC 20585
Email: Walter.Stevens@science.doe.gov

Andrei Tokmakoff
MIT Department of Chemistry
Room 6-225, 77 Massachusetts Ave.
Cambridge, MA 2139
Email: tokmakof@mit.edu
Phone: 617-253-4503

Stefan Vajda
Argonne National Laboratory
Chemistry Division, 9700 South Cass Ave
Argonne, IL 60439
Email: vajda@anl.gov
Phone: (630)-252-8123

Michael White
Brookhaven National Laboratory
Chemistry Department
Upton, NY 11973
Email: mgwhite@bnl.gov
Phone: 631 344 4345

Sotiris Xantheas
Pacific Northwest National Lab
P.O. Box 999
Richland, WA 99352
Email: Sotiris.Xantheas@pnl.gov
Phone: 509-375-3684

Tijana Rajh
Argonne National Laboratory
9700 S. Cass Ave
Argonne, IL 60439
Email: rajh@anl.gov
Phone: 630.252.3542

Richard Saykally
Univeristy of California/Lawrence Berkeley National Labs
Department of Chemistry
Berkeley, CA 94720
Email: saykally@berkeley.edu
Phone: 510 642-8269

Steven Sibener
University of Chicago
5640 South Ellis Avenue
Chicago, IL 60637
Email: s-sibener@uchicago.edu
Phone: 773-702-7193

Mark Stockman
Georgia State University
University PLaza
Atlanta, GA 30303
Email: mstockman@gsu.edu
Phone: 404-651-2779

G. N. R. Tripathi
Notre Dame Radiation Laboratory
University of Notre Dame
Notre Dame, IN 46556
Email: tripathi.1@nd.edu
Phone: (574) 631 5514

Albert Wagner
Argonne National Laboratory - Chemistry Division
9700 S. Cass Avenue, Bldg. 200
Argonne, IL 60439
Email: wagner@tcg.anl.gov
Phone: 630-252-3570

James Wishart
Brookhaven National Laboratory
Chemistry Department
Upton, NY 11973
Email: wishart@bnl.gov
Phone: 631 344-4327

Sunney Xie
Harvard University
Department of Chemistry, 12 Oxford Street
Cambridge, MA 2138
Email: xie@chemistry.harvard.edu
Phone: 617-496-9925

Author Index